Intercalation mechanism of polycarboxylate-based superplasticizers into montmorillonite clays

DOCTORAL THESIS

Thesis by publications

Doctoral Thesis by:

Pere Borralleras Mas

Directed by:

Antonio Aguado de Cea

Ignacio Segura Pérez

Barcelona, September 2019

Universitat Politècnica de Catalunya

Departament d'Enginyeria Civil i Ambiental

Curso académico: 2018 - 2019

Acta de calificación de tesis doctoral

Nombre y apellidos	PERE BORRALLERAS MAS
Programa de doctorado	INGENIERÍA DE LA CONSTRUCCIÓN
Unidad estructural responsable del programa	DEPARTAMENTO DE INGENIERÍA CIVIL Y AMBIENTAL

Resolución del Tribunal

Reunido el Tribunal designado a tal efecto, el doctorando / la doctoranda expone el tema de su tesis doctoral titulada

"*Intercalation mechanism of polycarboxylate-based superplasticizers into montmorillonite clays*".

Acabada la lectura y después de dar respuesta a las cuestiones formuladas por los miembros titulares del tribunal, éste otorga la calificación:

☐ NO APTO ☐ APROBADO ☐ NOTABLE ☐ SOBRESALIENTE

(Nombre, apellidos y firma) Presidente/a	(Nombre, apellidos y firma) Secretario/a	
(Nombre, apellidos y firma) Vocal	(Nombre, apellidos y firma) Vocal	(Nombre, apellidos y firma) Vocal

_____, _____ de _____ de _____.

El resultado del escrutinio de los votos emitidos por los miembros titulares del tribunal, efectuado por la Escuela de Doctorado, a instancia de la Comisión de Doctorado de la UPC, otorga la MENCIÓN CUM LAUDE:

☐ SÍ ☐ NO

(Nombre, apellidos y firma) Presidente de la Comisión Permanente de la Escuela de Doctorado	(Nombre, apellidos y firma) Secretario de la Comisión Permanente de la Escuela de Doctorado

Barcelona, a _____ de _____ de _____.

“*First you have to learn the rules of the game,*

and then play better than anyone else”

Albert Einstein

ACKNOWLEDGMENTS

Although these are the first sentences of this thesis for the reader, I´m writing them at the time when all the work is already concluded. And at this point of time, it is inevitable to look at it with a kind of somewhat more human and less scientific perspective, that undoubtedly, it confirms to me that the most precious thing that I take has been what the people who have been accompanying me all this time have given me.

Without going into self-assessments about the contribution that this work may have, my first and greatest personal satisfaction is simply having done it. And those persons responsible for making it happen are my thesis directors, Prof. Antonio Aguado and Dr. Ignacio Segura, from UPC – Polytechnical University of Catalunya and Smart Engineering Consulting, to whom I want to show my most honest gratitude for the time they have dedicated me, as well as their patience, their support, their encouragement and all the unpayable learnings that will help me do a little better in both my professional career and my personal life.

The other person to whom I want to show my deepest gratitude is Prof. Miguel A. G. Aranda from Scientific Director of ALBA Synchrotron and professor at Málaga University. Infinite thanks for all the help given in a disinterested way and for the high-quality of his scientific contribution, without which this work would have been not possible. Without any doubt, Miguel Ángel has been the greatest “discovery” of this thesis.

I would not like to forget all my fellow workers who, at some point and in some way or another, have lent me their time and their disinterested support. Thousand thanks to Andrés Fernández, Joan Pujol, Esther Hernández, Miriam Bretones, Juanjo Jurado, José Mª Sacido, David Osuna, Adrián Muñoz, Sergio Parra and Jorge Caballero. And to many others.

The words to thank Neus cannot be written because they have not yet been invented.

AGRADECIMIENTOS

Aunque para el lector estas sean las primeras frases de esta tesis, las estoy escribiendo cuando todo el trabajo ya está concluido. Y en este momento, resulta inevitable mirarlo con un tipo de perspectiva un tanto más humana y menos científica que, indudablemente, me confirma que lo más preciado que me llevo ha sido lo que la gente que ha estado acompañándome todo este tiempo me ha dado.

Sin entrar en autovaloraciones acerca de la aportación que podrá tener este trabajo, mi primera y mayor satisfacción personal es simplemente el haberlo hecho. Y los responsables de que haya acabado siendo así son mis directores de tesis, Prof. Antonio Aguado y Dr. Ignacio Segura, de la UPC – Universidad Politécnica de Catalunya y Smart Engineering Consulting, a quienes quiero agradecer todo el tiempo que me han dedicado, así como su paciencia, su empuje, sus ánimos y el aprendizaje de unos conocimientos impagables que me servirán para hacer las cosas un poco mejor, tanto en mi carrera profesional como en mi vida personal.

La otra persona a quien quiero mostrar mi más profundo agradecimiento es Prof. Miguel A. G. Aranda, Director Científico del Sincrotrón ALBA y profesor de la Universidad de Málaga. Infinitas gracias por toda su ayuda prestada de forma desinteresada y por la calidad de su contribución científica, sin la cual este trabajo no hubiera sido posible. Sin duda, Miguel Ángel ha sido el mayor “descubrimiento” de mi tesis.

No quisiera olvidarme los todos los compañeros de trabajo que de alguna u otra manera me han prestado su tiempo y su apoyo desinteresado en algún momento. Mil gracias a Andrés Fernández, Joan Pujol, Esther Hernández, Miriam Bretones, Juanjo Jurado, José Mª Sacido, David Osuna, Adrián Muñoz, Sergio Parra y Jorge Caballero. Y a otros tantos.

Las palabras de agradecimiento para Neus no soy capaz de escribirlas porque aún no han sido inventadas.

ABSTRACT

The presence of clays in the sands used for concrete production interferes with the development of the fluidity of concrete, producing an instantaneous slump loss just after batching and the premature loss of fluidity. This interference occurs with all types of additives and clays but is especially problematic when combining sands containing expansive clays such as montmorillonites with new-generation high water-reducer/superplasticizer admixtures based on polycarboxylate polymers (PCE).

Water-reducers based on PCE polymers offer much better performance than traditional superplasticizers based on sulfonated naphthalene polymers (BNS) and sulfonated melamine polymers (MNS), making great advances in concrete technology, both from the technical and economical point of view as in reducing the environmental impact associated to concrete. However, these advantages are inhibited when sands contain clays of the expansive type in their composition.

All the preventive or corrective measures to mitigate the harmful effect of clays contained in sands result in increases of production costs and in greater environmental impact. For this reason, during the last years it has been tried to develop polymeric structures that offer the same benefits than polymers PCE but with improved tolerance against clays of the expansive type, such as montmorillonite clays, but without getting to reach solutions with guarantees of success, due to the complexity of the interaction process between PCE polymers and montmorillonite clays.

This doctoral thesis aims to deepen knowledge about the mechanism of interaction between PCE polymers and montmorillonite clays, assuming that the deep understanding of the interaction mechanism is the essential previous step to finally develop high-performance, clay-insensitive superplasticizers for concrete. For this, the research is structured in three parts, motivated by the discrepancies that the current model of interaction proposed shows with the experimental results of sorption and fluidity loss.

In the first part, it is intended to develop a test method that allows to observe the real expansion profiles of the clays in such a way that the mentioned discrepancies can be clarified.

Secondly, with the proposed test method, it is intended to identify how the structure of PCE polymers, as well as the dosage used, influences on the expansion of montmorillonite clays produced by the absorption of polymer. And, thirdly, to identify how the properties of clay affect the interaction process.

The first phase of the research campaign has made it possible to propose an improved test method for the d-spacing determination that revealed the real intercalation behavior, by which the number of PCE side chains intercalated into the interlaminar space of montmorillonite clays is up to ten times higher than that deducted from the traditional analytical method. And from the new test method proposed it has been possible to clarify the role of the different structures of PCE polymers and the properties of montmorillonite clays in the intercalation mechanism, in agreement with the experimental results of fluidity loss and of sorption behavior.

Based on the mentioned achievements, an extended model for the intercalation mechanism has been proposed, whereby montmorillonite clays inhibit the dispersing capacity of PCE polymers, being able to identify the parts and properties of both the clay and the PCE polymers that control this process.

With this contribution, the knowledge of the intercalation mechanism is extended to understand how the interaction between PCE polymers and montmorillonite clays is developed, which is the main objective of this research.

RESUMEN

La presencia de arcillas en las arenas empleadas para producir hormigón interfiere en el desarrollo de la fluidez de los hormigones, produciendo una pérdida de cono instantánea tras el amasado y la pérdida prematura de fluidez. Esta interferencia se produce con todos los tipos de aditivos y de arcillas, pero es especialmente problemática cuando se combinan arenas que contienen arcillas expansivas del tipo montmorillonita con aditivos superplastificantes de nueva generación basados en polímeros de policarboxilato (PCE).

Este tipo de aditivos superplastificantes basados en polímeros de PCE ofrecen prestaciones muy superiores a las de los superplastificantes tradicionales basados en polímeros de naftalensulfonatos (BNS) y melaminas sulfonadas (MNS), aportando grandes mejoras en la tecnología del hormigón, tanto desde el punto de vista técnico y económico como en la reducción del impacto ambiental asociado al hormigón. Sin embargo, estas ventajas quedan inhibidas cuando las arenas contienen arcillas del tipo expansivo en su composición.

Todas las medidas preventivas o correctivas aplicadas para mitigar el efecto dañino de las arcillas contenidas en las arenas acarrean incrementos de coste de producción y mayor impacto ambiental. Por este motivo, durante los últimos años se ha intentado desarrollar estructuras poliméricas que ofrezcan las mismas prestaciones que los polímeros de PCE pero con mayor tolerancia frente a arcillas del tipo expansivo, como por ejemplo las montmorillonitas, pero sin llegar a alcanzar soluciones con garantías de éxito, debido a la complejidad del proceso de interacción entre los polímeros de PCE y las arcillas montmorillonitas.

Esta tesis doctoral pretende profundizar en el conocimiento en torno al mecanismo de interacción entre los polímeros de PCE y las arcillas montmorillonita, entendiéndose que la comprensión del mecanismo de interacción es la etapa previa esencial para lograr, finalmente, desarrollar aditivos superplastificantes de altas prestaciones e insensibles a las arcillas. Para ello, la investigación se estructura en tres partes, motivado por las discrepancias que el actual modelo de interacción propuesto muestra con los resultados experimentales de sorción y de pérdida de fluidez.

En primer lugar, se pretende desarrollar un método de ensayo que permita observar el perfil de expansión de la arcilla real de tal modo que las discrepancias mencionadas puedan ser clarificadas.

En segundo lugar, con el método de ensayos propuesto, se pretende identificar como influye la estructura del polímero de PCE, así como su dosificación, en la expansión de la arcilla producida por la absorción de polímero. Y, en tercer lugar, identificar como influyen las propiedades de la arcilla en el proceso de interacción.

La primera fase de investigación ha permitido proponer un método de ensayo para el factor de expansión d-spacing que vislumbra que el número de cadenas laterales del polímero de PCE intercaladas dentro del espacio interlaminar de las montmorillonitas es hasta más de diez veces superior al deducido con el método analítico tradicional. Y a partir del nuevo método de ensayo ha sido posible clarificar el rol de las diferentes estructuras de los polímeros de PCE y de las propiedades de la arcilla en el mecanismo de intercalación, en consonancia con los resultados de fluidez y de sorción.

A partir de los logros mencionados, se ha propuesto un modelo extendido del mecanismo de intercalación por el cual las arcillas montmorillonitas inhiben el efecto dispersante de los polímeros de PCE, pudiendo identificar cuáles son las partes y propiedades tanto de la arcilla como de los polímeros de PCE que controlan este proceso.

Con esta aportación, se amplía el conocimiento para comprender como se desarrolla la interacción entre los polímeros de PCE y las arcillas montmorillonitas, que es el objetivo principal de esta investigación.

TABLE OF CONTENTS

LIST OF FIGURES

LIST OF TABLES

Chapter 1
GENERAL INTRODUCTION

This chapter describes the current framework for the use of sands with contaminated with clays for concrete production by presenting the affectation on concrete performances, environmental impact and economical. Moreover, Chapter 1 presents the state of the art of the understanding on the interaction mechanism between water-reducers and clays and highlights the points of disagreement between the models and the experimental evidences.

Contents

1.1. PREFACE

From the introduction of the first commercial water-reducer admixtures for concrete, around the year 1950, the greatest advances in the technological development of concrete have always been the consequence of the innovation in the design of new concrete admixtures with superior performance [1]. The introduction of the first *water reducer/plasticizer* admixture, based on hardly refined lignosulfonates (LS) as by-products from paper industry, allowed the production of concrete with S2 consistency class that replaced the typical concretes used at those times of S0-S1 consistency class and produced with high w/c (water-to-cement) mass ratio, usually above 0,70 [2].

In the year 1970, the chemistry of sulfonated naphthalene (BNS) and sulfonated melamine (MNS) was developed. With this new chemistry, the first high-water reducer/superplasticizer admixtures (known as *traditional superplasticizers*) were introduced to the concrete market. These polymers, still used today, are obtained from chemical synthesis processes and not from by-products as in the case of the first plasticizers. In this way, the undesired side-effect on the setting delay caused by impurities were controlled. With the superplasticizer admixtures based on BNS and MNS polymers appeared the fluid concrete with S3 and S4 consistency class and with moderate w/c, which opened in the development of high-strength and easy-to-place concretes [1].

Concrete technology made a breakthrough with the introduction of polycarboxylate based superplasticizers (PCE) at the end of the 90´s [3,4], commonly names as *new-generation superplasticizers*. In the same way as for BNS and MNS, PCE polymers are obtained from chemical synthesis. However, and conversely to BNS or MNS production, the synthesis of PCE polymers allows to adapt and modulate the structure of polymers to obtain a wide range of performances. Therefore, it is possible to design tailored high-performance superplasticizers of adjusted compatibility with cements and to modulate the properties of concrete according to the intended application, such as extended slump retention or early development of concrete strength [5].

Because of this synthesis versatility, the overall performances offered by the PCE based superplasticizers are largely superior than those of the traditional superplasticizers based on BNS and MNS condensates, to the point that nowadays, the new-generation superplasticizers are the most widely used type of admixtures for concrete. In this way, the technology split (expressed as per quantities) for water-reducers in 2017 European market is presented in Figure 1.1(a), observing that PCE technology means more than 50% of total water-reducers market.

In comparison to the traditional superplasticizers, the most improved property by PCE based superplasticizers is the water reduction capacity. Figure 1.1(b) compares the water reduction capacity as per gram of active solid of lignosulfonate (LS), naphtalensulfonate condensate (BNS) and polycarboxylate polymer (PCE) at the common working dosages, referenced to the reduction of water content from the reference concrete at equivalent slump but produced without any water-reducer admixture.

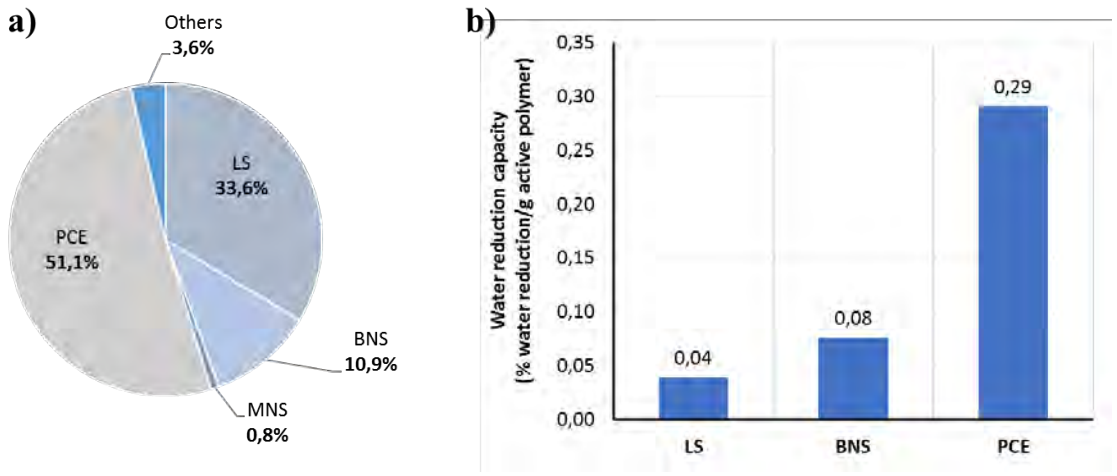

Figure 1.1. a) Technology split in volume of water-reducer admixtures in Europe in 2017 (courtesy of BASF C.C. Market Intelligence); b) Water reduction capacity of LS, BNS and PCE per active gram of polymer (adapted from [6,7])

From Figure 1.1(b) it is noticed that, meanwhile the water reduction capacity of BNS based traditional superplasticizers increases by double compared to that of LS based plasticizers, the water reduction capacity of PCE based new generation superplasticizers is by 3-4 times higher than of BNS technology. It is due to the different dispersing mechanism of PCE polymers, based on the steric repulsion created by the side chains rather than on electrostatic repulsion as for BNS, MNS and LS based dispersants [5].

Thanks to the high-water reduction capacity of PCE based superplasticizers, with this technology it is possible to design and produce advanced concretes with improved properties impossible to be achieved with the predecessor water-reducer admixtures.

The advances made by PCE technology have been such to the point that new concrete types like high-strength concrete, self-compacting concrete and more recently ultra-high-performance concrete [8] are possible nowadays, offering the possibility to cast structures with extended durability and designed with thin sections while allows faster and safer execution of concrete in a friendlier work environment.

PCE based admixtures are also used in the daily production of standard low-strength concrete such as C25/30. Here, the most remarkable benefit achieved with the new generation superplasticizers is the positive contribution to sustainability. By using PCE based admixtures, the amount of cement per cubic meter of concrete can be optimized, both by reducing the total quantity or by using more-sustainable cement types with larger amounts of SCM [1].

Whatever the case, the optimization of cement content has a direct, positive contribution in the reduction of CO_2 footprint, water consumption and other environmental parameters, making the concrete production more sustainable and environmentally friendly.

Figure 1.2 presents the relative average reduction of the most relevant environmental parameters for concrete achieved by each of the water-reducers technologies. The contributions are calculated from the typical mix design optimizations affordable by each technology and on the basis of a mix design for a C25/30 concrete class.

The environmental impact of the single ingredients required for the calculation is taken from the published EPDs for CEM II cement type [9], crushed aggregates [10] and for the different water-reducer admixtures [11]. All EPDs used are properly certified by notified bodies according to ISO 14025 and EN 15804 standards.

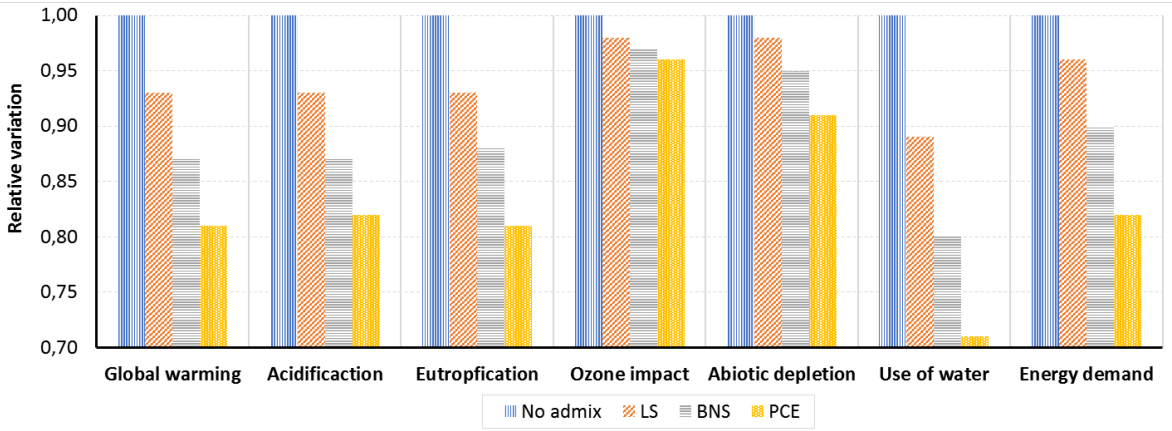

Figure 1.2. Calculated relative average variation of the environmental impact parameters for concrete as per the type of water-reducer admixture used

Figure 1.2 supports that every new-technology development for water-reducer admixtures further contributes in reducing the environmental impact of concrete. For all the environmental parameters presented, PCE technology contributes with the greatest improvements, with especial emphasis on the reduction of global warming (CO_2 footprint) and of net use of water.

Despite all the positive contributions made by the PCE based superplasticizers for concrete, there is a point pending of improvement for this technology related to their compatibility with sands of limited quality. It is well known that sands contaminated with small quantities of some specific types of clays severally affect the performance of the PCE based superplasticizers [12].

The type of clays able to almost totally inhibit the dispersing capacity of PCE polymers are those that have swelling properties and, in particular, the clays belonging to the smectite-montmorillonite group [13-15].

When sands with clay contamination are used for concrete production, all the benefits achieved by using PCE based superplasticizers are severally restricted or even completely annulled, thus limiting the environmental, economic and technological benefits provided.

This thesis is a research work addressed to better understand the interaction process between PCE polymers and montmorillonite clays.

The objective of this investigation is to enlarge the knowledge of the interference process by which the performance of PCE polymers is altered, as well as to identify the most determining factors that control the intercalation mechanism. Therefore, the final aim is to generate new knowledge useful for the development of clay-resistant PCE polymers to fully exploit the benefits of this technology even when sands of poor quality are used for concrete production.

1.2. UNDESIRED EFFECTS OF SANDS CONTAMINATED WITH CLAYS ON CONCRETE PERFORMANCE

The main undesired negative impacts on the performances of concrete caused by sands with clay contamination are produced in the fresh state [16]. In short, sands of poor quality increase the water demand of concrete. Thus, higher quantity of water is required to achieve a specific concrete slump, forcing to an increase of the w/c (water-to-cement) ratio.

Figure 1.3(a) shows the water demand for a C30 and C60 concrete class at constant slump as the amount of clay contamination in sand increases (expressed as per the methylene blue value - MBV). For the same variations of MBV, Figure 1.3(b) displays the amount of BNS-based traditional superplasticizer required to achieve the same initial concrete slump as the clay contamination of the sand increases.

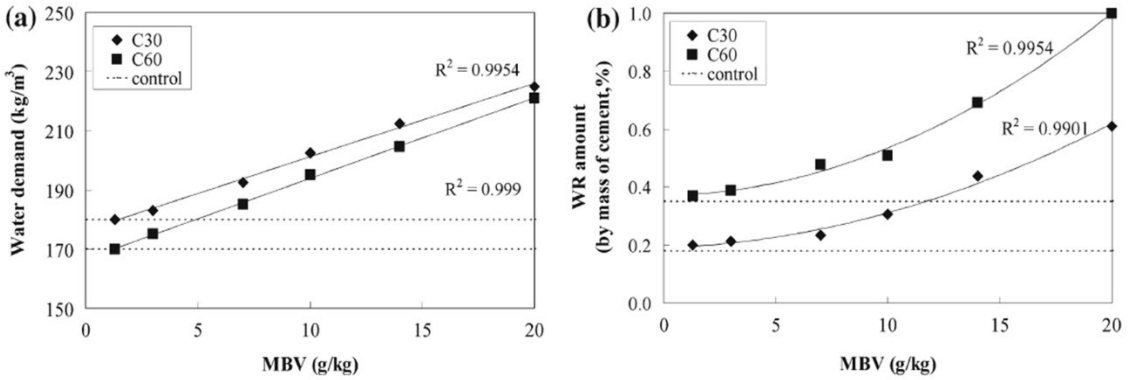

Figure 1.3. Impact on the fluidity behaviour of concrete as the MBV of sand increases [17]; a) Increase of water demand; b) Increase of water-reducer (WR) dosage

As Figure 1.3(a) shows, the water demand of concrete increases linearly as the MBV of the sand increases, so when the contamination by clays increase. It is observed that the increase of MBV of the sand impacts almost equally in the water demand for both C30 and C60 concrete, despite the cement content for high-strength concretes such as C60 is significantly higher than for C30 concrete.

Differently than for the increase of water demand, Figure 1.3(b) reveals that the demand of superplasticizer increases exponentially as the MBV of sand increases. Here, the impact is more pronounced for the C60 concrete, probably because the more relevant role of water-reducers on the slump than for the case of concretes of higher w/c ratio. In any case, the exponential evolution observed in Figure 1.3(b) denotes that by increasing the dosage of water-reducer admixture is not a cost-effective measure to overcome the increase of water demand caused by sands contaminated with clays.

The increase of water demand generates a reduction of concrete slump at initial time just after batching, demanding higher quantity of mixing water to achieve the expected concrete slump, so forcing to an increase of the w/c ratio [18]. Therefore, by increasing the w/c ratio, severe reductions of mechanical strengths and durability are unavoidable if corrective actions are not applied.

In addition to the instant slump loss observed just after batching, sands contaminated with clays cause an additional, undesired problem in the premature loss of slump during transport of fresh concrete or during concrete placing at the jobsite. It is due to the fact that the total water uptake by sands contaminated with clays is not fully satisfied just after mixing and so progresses over the time [19].

Concrete with reduced slump is of complex execution, delaying the placing time, making pumping more difficult, requiring extended vibration to achieve the appropriate compaction and leading to surface finish of bad quality.

The greatest risk of executing structures with too low concrete slump is when the steel reinforcement bars remain exposed due to an insufficient coating thickness. In this situation, the exposed reinforcement promotes the early corrosion of the structure thus reducing the durability and the expected service life. The images presented in Figure 1.4 shows the exposed reinforcement as consequence of casting with concrete of too low, inadequate slump.

Figure 1.4. Exposed reinforcement caused by casting with concrete of inadequate slump

To prevent the additional complexity in the casting operations when concrete slump is prematurely lost before completing the execution, there is the risk of uncontrolled water addition at site with the aim to restore the slump lost over time. This is known as retempering of concrete and leads to a damage of concrete performance in both mechanical and durability properties.

In the typical levels of clay contamination, the negative effects observed in most of the properties of hardened concrete such as mechanical strength and durability are just a consequence of the retempering of concrete by uncontrolled water addition.

Figure 1.5(a) displays the progressive slump loss over time for a concrete with 190 mm initial Abrams slump and the amount of retempering water needed to restore the initial target slump. The relationship between the amount of added water for retempering and the relative reduction of compressive strengths at 28 days is presented in Figure 1.5(b).

Additionally, Figure 1.5(c) shows the relative reduction of compressive strength for concretes of equal slump but produced with sands containing variable amounts of clays. In this case, the increase of water demand from the worsen quality of sand is mitigated by increasing the amount of water.

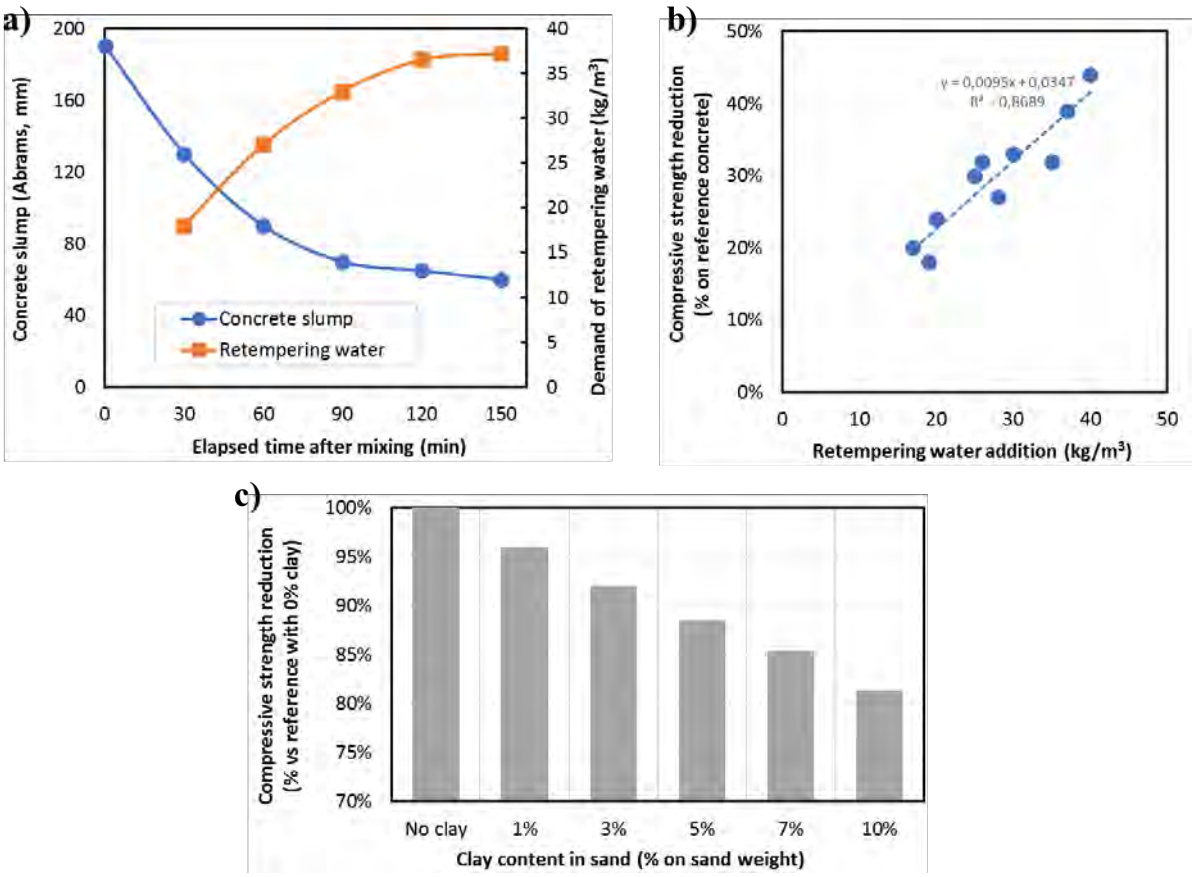

Figure 1.5. a) Reduction of concrete slump over time and amount of retempering water required to restore the initial slump [20]; b) Impact of retempering water on the reduction of compressive strength at 28 days [20]; c) Relative reduction of compressive strength as per the clay amount in sand increases [21]

From both Figure 1.5(a) and 1.5(b) it is deducted that there is a direct relationship between the slump loss, the demand of retempering water and the reduction of compressive strengths. Figure 1.5(b) displays that by adding 20 kg/m^3 of retempering water, compressive strength is reduced by 20%, and by adding 40 kg/m^3, the reduction of strength jumps up to 45%. Therefore, it supports the statement that the negative impact on concrete strength caused by sands of poor quality is mainly a consequence of the addition of retempering water.

Similar conclusions are extracted from Figure 1.5(c), where the slump loss of concretes produced with sands with increased amounts of clay is adjusted by increasing the w/c ratio. It

can be observed that as clay content in sand increases, the compressive strength at 28 days is being reduced linearly.

Figure 1.6 presents the reduction of compressive strength for a C30 concrete at the age of 3 days and 28 days as the MBV of sand increases. Figure 1.6(a) shows the reduction of compressive strengths when the initial slump of fresh concrete is adjusted by increasing the water content, while Figure 1.6(b) shows the impact on compressive strength when the slump loss is mitigated by increasing the dosage of water-reducer, so without modifying the w/c ratio.

Meanwhile Figure 1.6(a) confirms that any increase of w/c ratio means a reduction of compressive strength at all ages, Figure 1.6(b) shows that no reduction of compressive strength is produced when the slump loss is restored by increasing the dosage of water-reducer admixture. Despite the correction by increasing the dosage of admixture is not a cost-effective measure (due to the exponential increase of the dosage demand presented in Figure 1.3(b)), this confirms another time that the reduction of mechanical strengths promoted by sands of poor quality is just a direct consequence of concrete retempering by uncontrolled water addition.

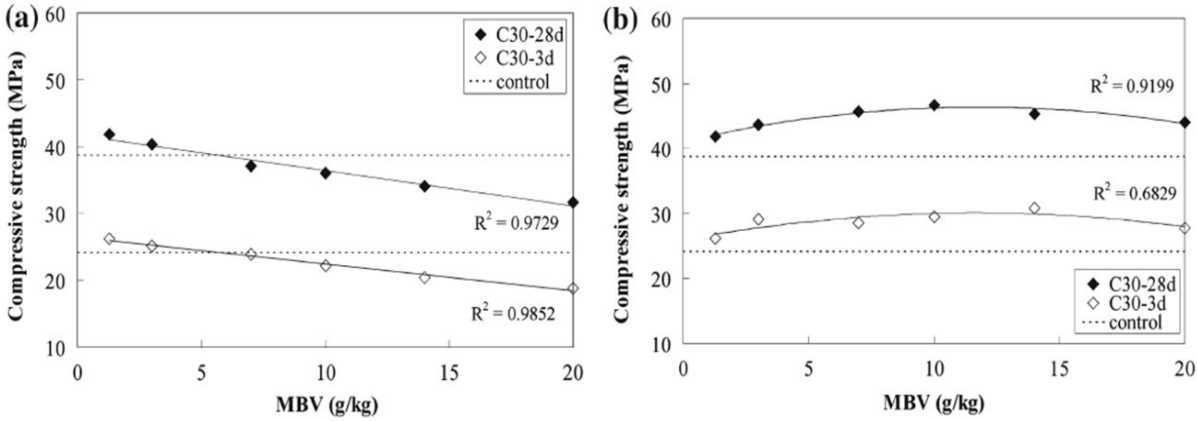

Figure 1.6. Reduction of compressive strength at equivalent concrete slump as MBV of sand increases [17]; a) By increasing the mixing water content; b) By increasing the dosage of water-reducer admixture

Simultaneously to the reduction of mechanical strengths, other properties of hardened concrete are negatively affected by the increase of water demand promoted by sands with clay contamination. Figure 1.7(a) and 1.7(b) shows respectively how concrete shrinkage and chloride-ion permeability evolves as the MBV of sand increases when the slump loss is restored by increasing the w/c ratio.

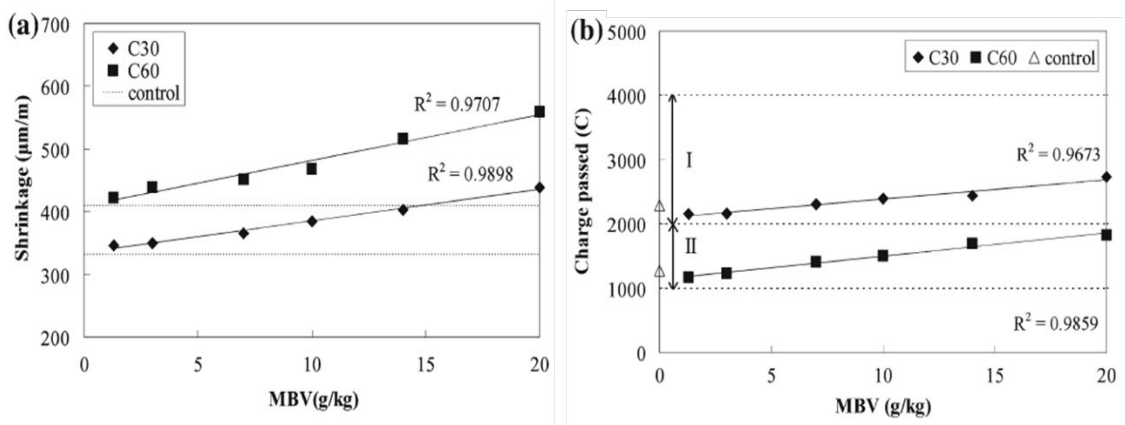

Figure 1.7. Impact on the properties of concrete as the MBV of sand increases [17]; a) Increase of concrete shrinkage at 120 days; b) Increase of chloride-ion permeability

The increase of shrinkage observed in Figure 1.7(a) promotes cracking of concrete thus facilitating the ingress of aggressive agents. Therefore, it can be stated that the poorer quality of sands leads to a reduced durability of the structures.

The same conclusion is extracted from Figure 1.7(b), since the increase of charge passing is associated to an easier diffusion of chloride ions into concrete, thus making the structure more sensitive to damages by corrosion [22].

As summary, sands contaminated with clays promotes the reduction of initial slump of fresh concrete and the premature slump loss, but most of the affectations on the properties of hardened concrete such as mechanical strength and durability are mainly collateral consequences of concrete retempering by additional of further water amounts with the aim to restore the slump target to allow casting the concrete in the proper conditions for execution.

1.3. QUALITY OF SANDS USED FOR CONCRETE MANUFACTURING

Because sand is the major ingredient of concrete, the quality of sand is one of the most critical factors in the industrial production of concrete, both in ready-mix concrete and in precast. Inadequate quality of sands entails negative effects on the properties of concrete, both in fresh state and hardened state, which may compromise the expected performances and durability of concrete structures.

To prevent the problems caused by sands of poor-quality and to ensure that concrete structures meet the established mechanical requirements and the expected service life, the vast majority of standards and regulations aimed at concrete production includes minimum quality

requirements for sands. Much of these requirements are intended to limit the amount of clays in sands since clays are the most problematic of the usual unwanted components typically found in sands.

1.3.1. Structure and properties of clays

Clays are minerals that belong to the group of phyllosilicates, which are characterized by an extreme fineness and a very high surface area [23]. They are formed by laminar structures that can be described as a succession of stacked plates forming the pristine clay particle, such that there is a space between each superposed plate that is named interlaminar space [24,25].

Figure 1.8 illustrates the particular structure of clay particles, which can be clearly recognized in the real SEM images of natural occurring clay minerals presented in the next Figure 1.9.

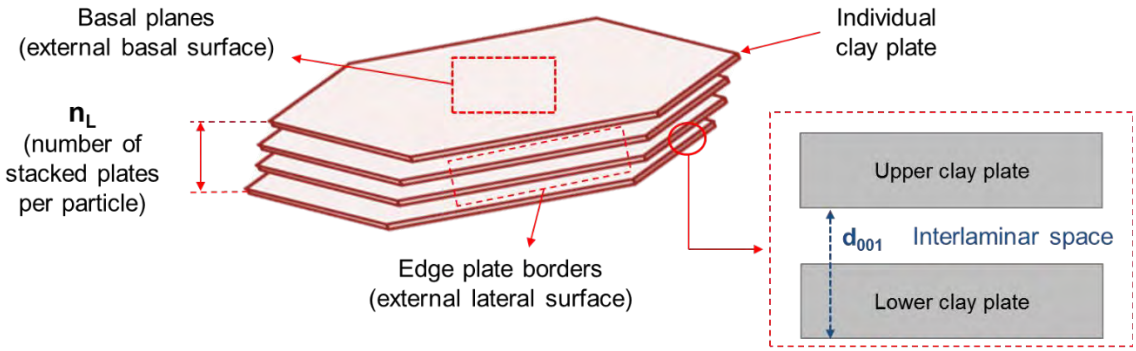

Figure 1.8. Structure of clay particles

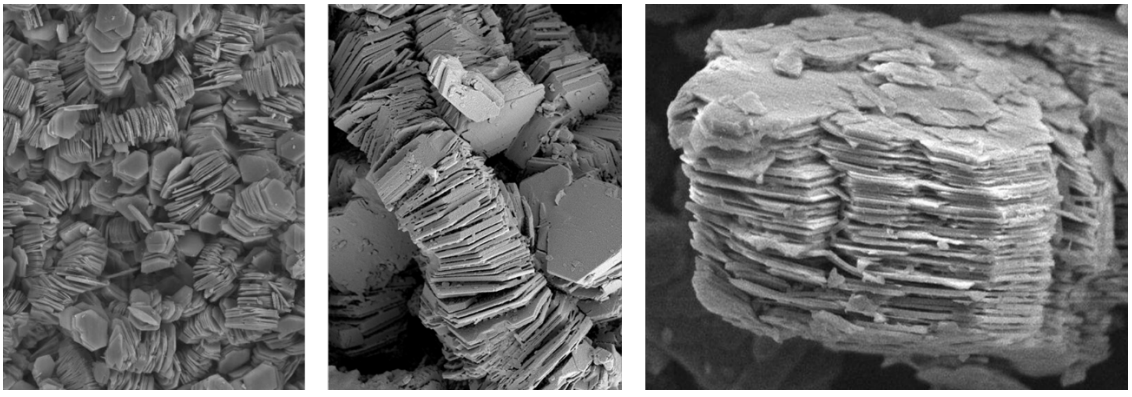

Figure 1.9. Real SEM images of natural occurring clay minerals [26]

Both Figure 1.8 and Figure 1.9 shows that the morphology of clay particles is based on a succession of stacked thin, lazy plates of semi-hexagonal shape and characterized by a very large aspect ratio, so of high proportion between width (defined by the area of the basal planes) and thickness (defined by the number of stacked plates per particle, n_L) [25].

The external, exposed surface of clay particles is composed by the lateral (edge) surface (S_{edge}) and by the basal surface (S_{basal}). The lateral surface corresponds to the area of the plate borders and it is defined by the particle thickness, so by the number of stacked plates. The basal surface is equivalent to the area of the exposed basal planes of the end-plates sandwiching the rest of stacked plates forming the clay particle. In general, due to the typical high aspect ratio of clay particles, basal surface means up to 98% of total surface and therefore most of the exposed clay surface is basal surface [24,25].

Individual clay plates are formed by tetrahedral silicate layers (T layer) and octahedral aluminate layers (O layer) covalently bonded through the oxygen atoms of the vertices. Depending on the sequence disposition of the silicate and aluminate layers, two different clay structures are defined [27]. T-O clays are based on clay plates formed by one silicate tetrahedral layer and one aluminate octahedral layer. This is the typical structure of *kaolinites*. In parallel, T-O-T plates are formed by one aluminate octahedral layer in between two silicate tetrahedral layers. *Micas*, *chlorites* and *smectites* are based on T-O-T structures [28].

The open space in between the stacked plates forming the clay particle referred as interlaminar space. The interlaminar space defines the total internal surface area of clay particles, which means the sum of the surface of all the interior basal planes. Therefore, the internal surface is only accessible through the interlaminar space [29]. The opening of the interlaminar space and its accessibility is particular for each clay mineral and its thickness is characterized by the interlayer d-spacing (d_{001}). As indicated in the previous Figure 1.8, the d-spacing (d_{001}) value does not refer directly to the opening length in between two plates but to the total length including one clay plate and the opening of the interlaminar space, since it is the repetitive unit which compose the entire structure of the clay particles [30].

There are different types of clays with very variable properties and behaviour among them. Clay groups are defined from the differences in the chemical composition and in the stacking structure of the individual clay plates [30] (being a direct consequence of their chemical composition). Figure 1.10 presents the classification criteria of clays and clay minerals as function of the stacking structure of the individual clay plates (T-layer of tetrahedral silicate and O-layer of octahedral aluminate). Two clay groups are recognized according this classification criteria: T-O clays and T-O-T clays (also named as 2-1 and 2-1-2 clays).

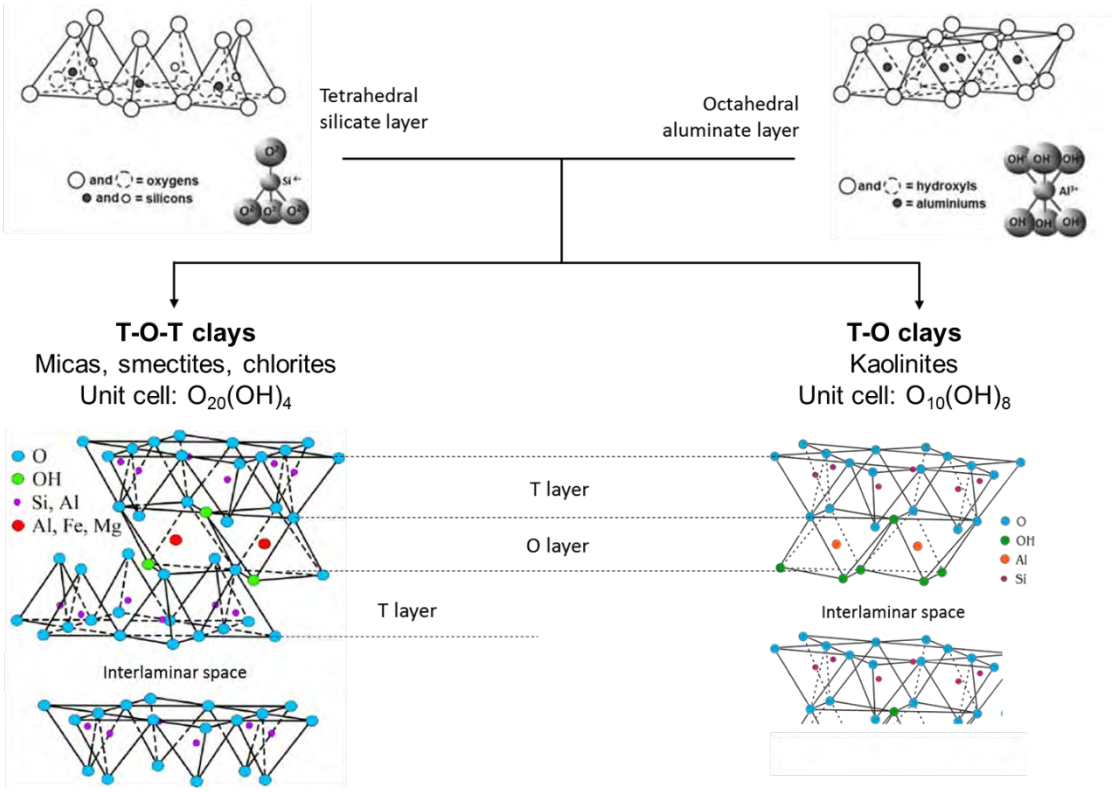

Figure 1.10. Clay groups as function of the structure of the individual plates (T-O-T and T-O clays)

In addition to the structure of plates, another key-factor differentiating the clay groups is the isomorphic substitution, which means the partial replacement of Si atoms in the T layer and/or of Al atoms in the O layer by cations of equivalent size but with lower charge [25]. Many properties of clay minerals such as the accessibility of the interlaminar space are defined by the type and amount of isomorphic substitution.

Isomorphic substitution generates a charge deficiency in the clay structure, accumulating residual charges in the clay plates (named as layer charge, ξ) that need to be balanced. Generally, T-O clays do not experience isomorphic substitution and it is more typical in T-O-T clays. *Pyrophyllite* and *talc*, with formula unit $Al_2Si_4O_{10}(OH)_2$ and $Mg_3Si_4O_{10}(OH)_2$ respectively, are the T-O-T clays without isomorphic substitution so their structures are electrically neutral [30]. Thus, pyrophyllite and talc represent to the ideal dioctahedral and trioctahedral smectites and so they do not have any swelling properties.

When Si atoms (formerly as Si^{4+}) from the tetrahedral layer are replaced by Al^{3+} or Fe^{3+} cations, a residual charge of -1.0 per half-cell unit is generated in the T layer (tetrahedral layer charge, ξ_{tet}). This is the typical structure of *mica* clays and *illites*. Since the tetrahedral layers

means the external surface of clay plates, the residual charge of -1.0 can be efficiently balanced by monovalent cations in perfect stoichiometry. Typically, potassium K^+ is the cation balancing the residual charges generated by tetrahedral substitution because it fits almost perfectly in the spaces in between the oxygen vertices of the substituted tetrahedrons [28]. Therefore, tetrahedral layer charges balanced by potassium cations lead to very stable clay structures with restricted accessibility of the interlaminar space to the point that micas are not expandable clays.

When Al^{3+} cations forming the octahedral layer are replaced by divalent cations such as Mg^{2+}, Fe^{2+}, Ti^{2+} or other metallic divalent cations of comparable size, a non-stochiometric charge of -0.33 per cell unit is generated in the O layer (octahedral layer charge, ξ_{oct}). The cumulated total layer charge generated by octahedral isomorphic substitution distinguishes diverse types of clays within the smectite-group. For *montmorillonite* clays, the total layer charge per half-cell unit is defined for the value range $0.2< \xi <0.6$, while for *vermiculites* is $0.6< \xi <0.9$ [30,31].

Contrary to tetrahedral substitution, the charge deficiency created by the octahedral substitution cannot be balanced with the same efficiency because it is not stoichiometric and because it is located in the inner, inaccessible region of the clay plate. Therefore, these residual charges can be compensated only by soluble cations arranged in the interlaminar space, typically Na^+, Ca^{2+} and K^+. As consequence, the resulting structures are not as stable as micas because there is a natural electrostatic repulsion between the individual clay plates [25]. For this reason, the interlaminar space of these clays is easily accessible, allowing the soluble cations to be exchanged by other cations (*cation exchange capacity* - CIC) or by polar molecules, thus giving the clay expansive and swelling properties [32].

Smectite clays with octahedral isomorphic substitution typically owns some substitution in the tetrahedral layer at the same time. From the corresponding formula unit $M^{(+)}_{(x+y)}(Al_{(2-y)},Mg_y)(Si_{(4-x)}Al_x)O_{10}(OH)_2$ of smectites, *x* represents the tetrahedral substitution and *y* the octahedral substitution, while $M^{(+)}$ means the interlayer soluble monovalent cations balancing both residual layer charges *(x+y)*. In this respect, $y > x$ for montmorillonite clays while $y < x$ for *beidellite* clays [25,30].

Chlorites are the clay types owning both tetrahedral and octahedral isomorphic substitution at the same time. These structures are possible because the interlaminar space is occupied by a hydroxide layer named *brucite-like layer* which owns electropositive behaviour to compensate the negative residual charges cumulated in the clay plates [33]. Brucite-like layer of chlorites is composed by mixed aluminium, ferric hydroxides and $M(OH)_2$ hydroxides, typically magnesium and ferrous but also others such as nickel or manganese, and in practical terms, it makes the interlaminar space non-accessible. Thus, chlorite clays do not own accessible interlaminar space.

For some of the clay minerals belonging to different clay groups, Table 1.1 summarizes the structure of the individual clay plates, the typical values of d-spacing (d_{001}) referred to the thickness of the interlaminar space and the expansion behavior, which is related to the accessibility of the interlaminar space and to the swelling properties of clay minerals. It can be seen that the substituted smectites are the swelling clays, and within them, montmorillonites are those that show the greatest expansion capacity.

Clay group	Clay mineral	Structure of plates	d-spacing d_{001} (Å)	Expandable Swelling properties
Kaolinites	Kaolin Halloysite	T-O	7.2 10.1	Non-expandable
Micas	Muscovite Biotite Illite	T-O-T	10	Non-expandable
Chlorites	Clinochlore Ripidolite Chamosite Nimite	T-O-T	14 including interlayer brucite	Non-expandable
Smectites	Pyrophyllite	T-O-T	9.2	Non-expandable
	Talc		9.2	Non-expandable
	Montmorillonite		12.3 – 18.5	Highly expandable
	Vermiculite		12.1 - 14.8	Moderate expandable
	Beidellite		12.5 - 14.9	Moderate expandable
	Nontronite		13.5 - 15.6	Moderate expandable
	Hectorite		12.4 - 15	Moderate expandable
	Saponite		12.3 - 15.2	Moderate expandable

Table 1.1. Plate structure, interlaminar d-spacing (d001) and expandable behavior for some clay minerals [25,31,34]

All the clay minerals present an intrinsic capacity to interfere in the fluidity of concrete. It is related to the water demand from the large exposed surface area. But in addition to this, swelling clays with expansion capacity can absorb water and other polar molecules inside their easily accessible interlaminar space, thus multiplying the affectation on the slump loss. Therefore, the higher the expansion capacity of the clay, the higher the impact on the affectation in the properties of fresh concrete.

In this sense, according to Table 1.1, clays can be divided in two large groups considering the potential affectation: that of the *non-swelling clays* characterized by having an inaccessible interlaminar space; and that of *swelling clays*, which includes the smectite clays owning isomorphic substitution. Kaolinites, micas, chlorites and the smectites pyrophyllite and talc without isomorphic substitution are non-swelling clays, meanwhile vermiculites, saponites, beidellites, hectorites, nontronites and, in particular, montmorillonites are clay minerals with swelling capacity.

1.3.2. Clay contamination in sands

Clay minerals are formed from the natural weathering of rocks and minerals. Depending on the type of rocks and on the exposition conditions during their alteration process, the different types of clays are formed [35]. Despite clay sediments can be transported from the original location where they were formed, in general, the natural occurrence of specific clay reservoirs is found in the same geological environment than the original rocks from they are formed.

It means that for each particular type of rock used to produce aggregates, some of the specific clays are more likely to be present than others. Nevertheless, in natural conditions clay minerals rarely occurs isolated and the clay reservoirs contain mixes of different clay minerals, although one of the types is occurring as the majority.

Therefore, from the mineralogy of the aggregates it is possible to propose the clay minerals commonly occurring. Table 1.2 shows which are the most usual clays contained in aggregates of different mineralogy and origin. It is proposed from the clay formation conditions and environment but also supported by experimental identification of clays in sands of different mineralogy and origin [36].

Mineralogy of sands	Extraction áreas Rock reservoirs	Typical clays identified
Siliceous	Riverbeds, sedimentary deposits	Montmorillonite
Limestone	Calcareous rocks	Muscovite, other micas
Dolomite	Dolomite rocks	Muscovite, other micas
Basaltic	Volcanic lava deposits	Montmorillonite, chlorite
Granitic	Granite rocks	Chlorite, muscovite, illite

Table 1.2. Typical clays identified in sands of diverse origins (adapted from [36])

Since montmorillonite are the most problematic clays for concrete, from Table 1.2 it can be deducted that natural siliceous sands are potentially the most conflictive, to the point that the finest fraction of natural siliceous sands containing the clays is usually removed by washing processes to meet the minimum quality required for concrete production. Conversely, clays contained in the finest fraction of limestone-based sands is not as critical as of the siliceous sands, since the most frequent clays are not of the expansive/swelling type. For this reason, in many concrete standards the limitation for <0.063mm fines content is more restrictive for siliceous sands than for limestone sands [37].

1.3.3. Identification of clays in sands with the methylene blue test (MBV)

The most widely used test to advice on the clay content of sands for concrete is the *methylene blue (MB) test*. It is a standardized test whose procedure is described by the standard EN 933-9 [38], and by which the minimum requirements for the quality of sands are set, limiting the maximum MB value (MBV) allowed for sands used for the production of concrete [37,39].

The MB test is based on a volumetric titration where the indicator is used for the detection of the point of equivalence, by observing how the color of the sample evolves, as shown in Figure 1.11.

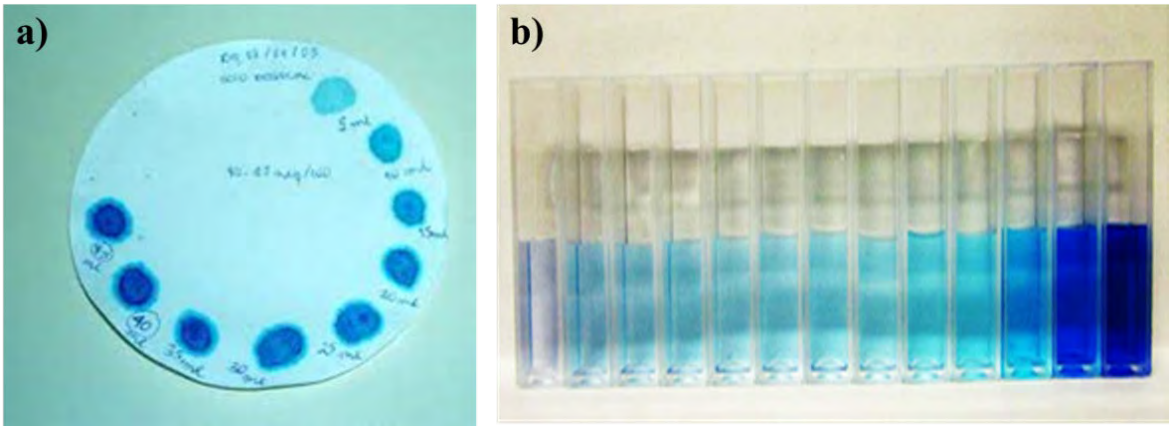

Figure 1.11. Color grading in the titration of sands with methylene blue dye

Methylene blue test is performed on the <2mm fraction of the sand and consists of determining the amount of methylene blue necessary to coat the total surface of the solid with a mono-molecular film of dye. Therefore, the identification of the point of equivalence and thus of the result of MBV in the standardized method is based on the visual criteria of the operator.

The operator should note that the liquid phase of the sample treated with methylene blue, deposited on a white filter paper, creates a stable, light blue halo around the central reservoir of blue colored solid material, as it can be observed in Figure 1.11(a). At this time, the titration is considered as concluded, and the volume consumed corresponds to the result of the methylene blue (MB) test.

Since the detection of the point of equivalence is based on visual observation, the subjectivity in the criterion of the operator can influence on the repeatability and representability of the results.

To improve these aspects, the point of equivalence of the titration can be determined by spectroscopic methods [36,40], requiring previous calibration lines prepared from the color gradings shown in Figure 11(b).

The correlation between the MBV of sands and the clay activity has been largely proved by many publications but also by practical experiences [36,41,42]. Figure 1.12(a) shows how the MBV changes when different amounts of three clays (A, B, C) are added on a reference sand having an initial MBV of 0,4 g/kg. To compare the impact of non-clay fines on the MBV, Figure 1.12(b) displays the MBV evolution as the content of limestone fines (<0.063 mm) content increases in sand.

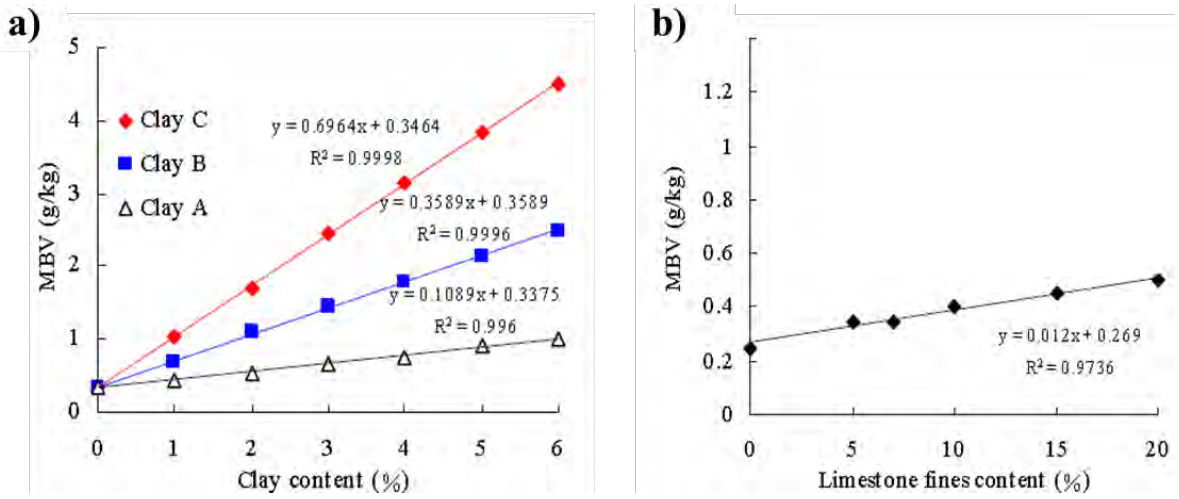

Figure 1.12. a) MBV for sands with diverse amounts of clays added [41]; b) MBV for sands with different amount of limestone fines [41]

By comparing the evolution of MBV from both Figure 1.12(a) and 1.12(b), it is observed that the response to the MB test of clays is much higher than of the limestone fines. Thus, MB test is sensitive to clays but almost insensitive to non-clay fines. Nevertheless, Figure 1.12(a) confirms that the influence on the MB values is not the same for sands containing clays of different properties.

Complementing Figure 1.12(a), Figure 1.13 presents the response to MB value produced by the addition of different types and amounts of clays on a limestone-based reference sand with a residual MBV of 0,4 g/100gr, including montmorillonite (MNT) clays of different properties and diverse types of non-swelling clays.

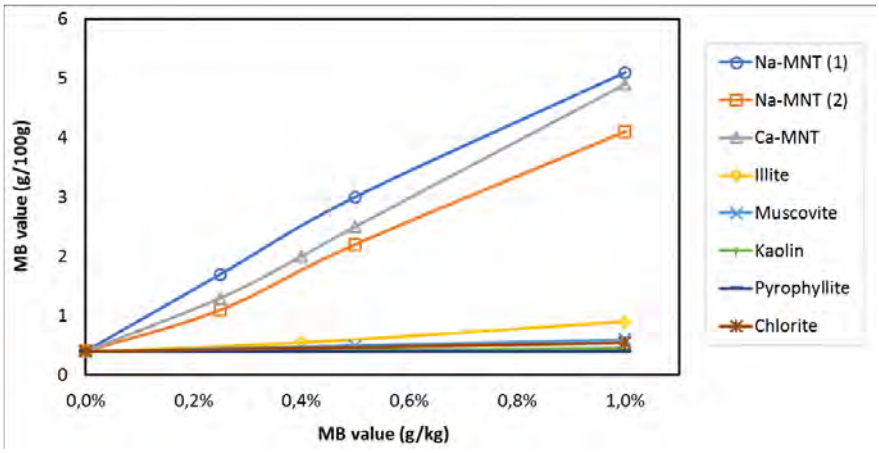

Figure 1.13. Changes in the MB value of sand produced by the addition of clays on a reference limestone sand [36]

According to the changes on MBV observed in Figure 1.13, MB test is sensitive enough to advice on the presence of swelling clays in sands, such as montmorillonites, but it does not allow to advice the presence of non-swelling clays in sands because almost no variation in the MB value is recorded despite increasing the amount of these clays in the reference sand.

Although Figure 1.13 shows that the non-swelling clays generate a low response to the MBV, Figure 1.14 advices that some of the non-swelling clays can produce significant reductions of paste flow. Here, the reduction of paste flow in cement pastes containing 2% bcw of clay is reported for pastes prepared with PCE based water-reducer and for pastes without admixture but with increased w/c to equalize the same paste flow.

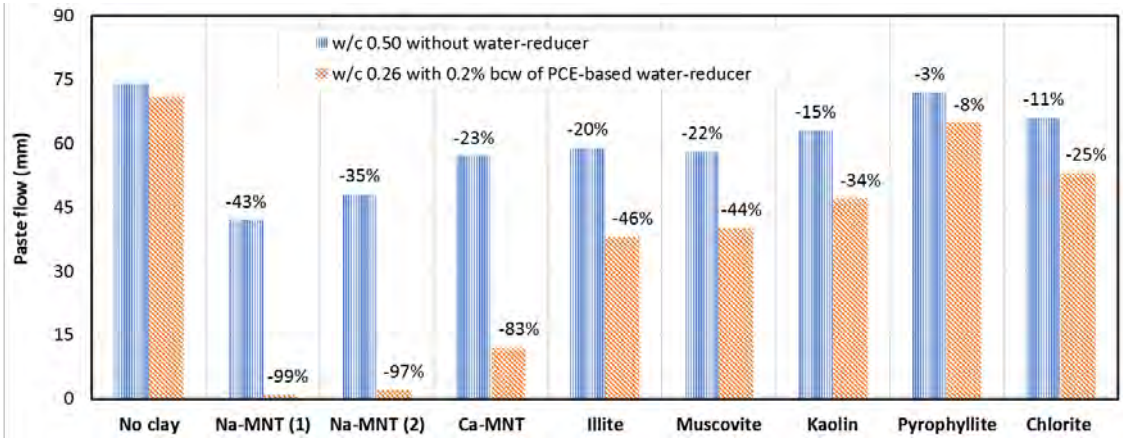

Figure 1.14. Paste flow loss in cement pastes produced with and without PCE based admixture (adapted from [36])

Figure 1.14 reveals that montmorillonite clays cause the highest reduction of paste flow. It is aligned with the MB values reported for these clays in the previous Figure 1.13. However,

within the three montmorillonites presented, the reduction of paste flow is substantially higher for Na-MNT (1) and Na-MNT (2) than for Ca-MNT, despite the changes produced by this clay in the MBV are of similar magnitude than by Na-MNT (1) and ever higher than by Na-MNT (2). Therefore, it denotes some dealignments between the MB values and the effective reduction of fluidity experienced.

In the same way, for most of the non-swelling clays, the values of MB displayed in Figure 1.13 are not aligned with the paste flow reductions presented in Figure 1.14, since minor reductions of paste flow should be expected for the non-swelling clays as per their small changes in MBV as the clay content increases. Only for the case of pyrophyllite there is a clear alignment between the MBV and the paste flow reduction, since this clay almost does not interfere on the fluidity of the pastes.

Therefore, in general terms, the estimation of the potential affectation on the fluidity of fresh cementitious systems deducted from the MBV seems to be reliable for sands contaminated with swelling clays, but the MB test has limitations for detecting non-swelling clays contained in sands.

Figure 1.14 also notices that the reduction of paste flow is higher for the pastes with low w/c containing PCE based water-reducers than for the pastes with higher w/c and without water-reducer. This trend is replicated by all the clays presented. Therefore, this suggests that water-reducer admixtures distortions the MB values in such a way that same values of MB lead to higher reduction of fluidity when water-reducer admixtures are used than when not used. This limitation of the MB test has been already reported in [41,42] by testing with mortars produced with sand contaminated by clays. The evolution of the relative reduction of mortar flow is presented in Figure 1.15(a) for mortars without water-reducer and for mortars containing PCE based superplasticizer.

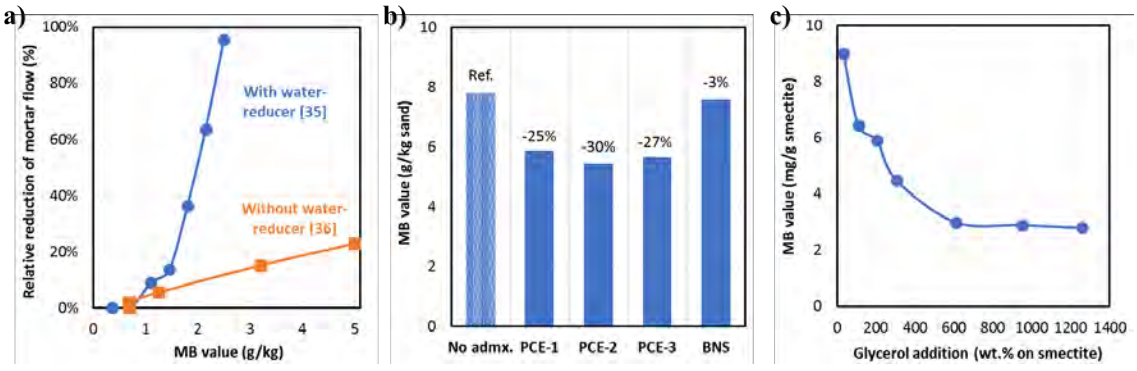

Figure 1.15. a) Relative reduction of flow for mortars produced with sands of different MBV [41,42]; b) MBV for sands treated with BNS and PCE polymers [43]; c) MBV measured on a smectite clay treated with glycerol [44]

The relationship presented in Figure 1.15(a) confirms that when PCE based superplasticizers are used, equivalent increases of MBV imply higher fluidity loss than when admixture is not used. In an extended way, Figure 1.15(b) shows that the distortion on the MBV is not homogeneous within the different types of water-reducer polymers. Meanwhile BNS polymers almost do not show any deviation with the MBV, PCE based superplasticizers reduce the MBV by 25-20%.

This particular behavior of PCE polymers to distortion the MB test results is supported by Figure 1.15(c), where the MBV recorded in smectite clay samples treated with glycerol is displayed. It can be observed that higher the amount of glycerol, the lower the MBV, until reaching a stationary value where no further reduction is observed despite increasing the glycerol content. Therefore, in the same way than for PCE polymers, glycerol alters the MBV since it is a polyol of comparable chemistry than of the side chains of PCE.

1.4. MEASURES TO OVERCOME THE NEGATIVE EFFECTS OF SANDS CONTAMINATED WITH CLAYS

To mitigate the undesired effects on concrete slump when sands contaminated with clays are used, it is required to apply some preventive and corrective measures to ensure that the expected concrete performances are met. The most common measures to overcome the negative effects of clays contained in sands can be synthetized in two: the corrective measures applied during the production of concrete and the preventive measures applied during the manufacture of sands.

1.4.1. Corrective measures at concrete plant: increase of cement content

When sands contaminated with clays are used for the industrial production of concrete at batching plants, it is required to provide an additional amount of mixing water to mitigate the negative impact on concrete slump and on the slump retention derived from the increase of water demand by sands of poor quality. Because any increase of w/c ratio leads to a reduction of mechanical strengths and of durability, the additional amount of mixing water must be balanced by increasing the amount of cement to continue fulfilling the demanded and expected concrete performances.

Since any increase of cement content increases the environmental impact associated to concrete, Figure 1.16 displays how the individual environmental parameters are worsened by increasing the cement amount per cubic metre by 10% and 20% in a C25-30 reference mix

designed with 275 kg/m^3 of cement. The relative increase is calculated from the EPDs of the single ingredients [9,10,11].

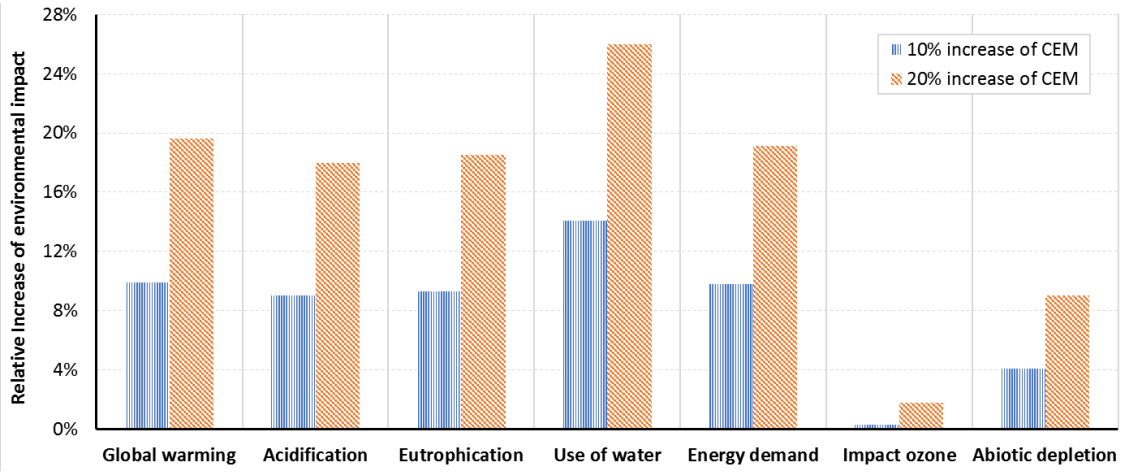

Figure 1.16. Relative increase of the environmental impact of concrete by increasing cement content by 10% and 20% in a C25-30 concrete class

According to Figure 1.16, the most damaged environmental parameters by increasing the cement content are the global warming (related to the CO_2 footprint) and the net use of water, worsened by 10% and 14% respectively when cement content is increased by 10% and up to 20% and 26% when cement content is increased by 20%.

The common increase of cement content to overcome the undesired effects of sands contaminated with clays typically varies from 5% to 25%, depending on the amount of clays in sands and on the punctual requirements of strength, durability, slump retention, etc. Whatever the case, the corrective measure based on increasing cement has a direct impact on rising the cost of concrete cubic meter up to 15%, in addition to other production costs. Therefore, this corrective measure is not the most convenient for both economic and environmental aspects.

1.4.2. Preventive measures at sand production facilities: sand washing

The washing process of sands is widely used in the manufacturing process of sands for concrete. The purpose of sand washing is to reduce the amount of clays contained in the raw sand (extracted lands) by removing the finest fraction, which is where the clays are contained. The washing process consist in exposing the extracted raw sand to a flow of water that drags most of the fine and light particles, thus allowing to separate the clay fraction from the sand.

Sand washing is common in natural siliceous sands obtained by sieving and classification of raw lands directly extracted from riverbeds or sedimentary reservoirs. This is because the high amount of montmorillonite clays naturally occurring in these environments, which are presented in Figure 1.17(a,b), respectively.

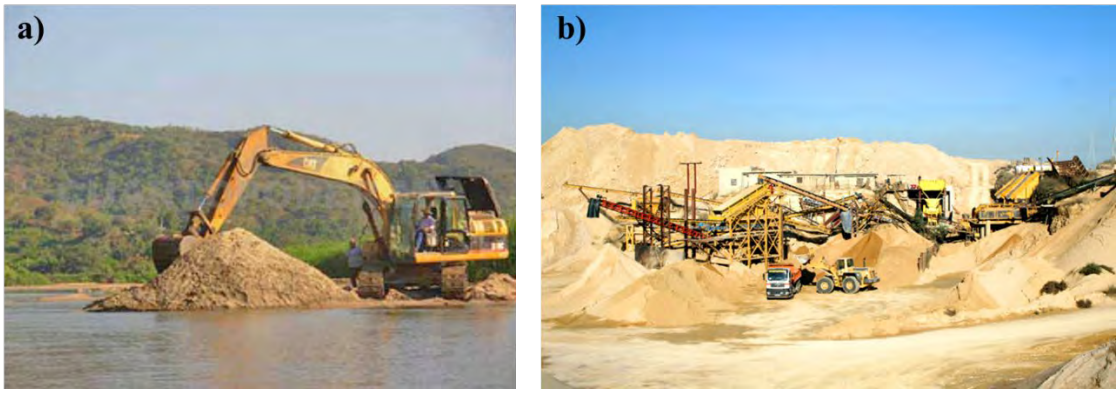

Figure 1.17. Extraction of raw lands to produce natural siliceous sands: a) From riverbeds; b) From sedimentary deposits

In such conditions of extraction, sand washing is mandatory to obtain sands in compliance with the maximum methylene blue values allowed and of enough quality to be used for concrete production. Conversely, sand washing in crushed sands obtained from the demolition of solid rock deposits is not as common as for natural siliceous sands. On the one hand, the clays occurring in limestone, dolomite and granite reservoirs nor are usually of the swelling types such as montmorillonite and, therefore, less problematic. And on the other hand, the limitations on the maximum content of fines <0,063mm and on the methylene blue value are less restrictive in crushed sands than in natural sands [37].

Nevertheless, sand washing reduces the business profitability for both the sand and the concrete producers and increases the environmental impact of sands due to the increase of water consumption and the generation of solid wastes. From the economical perspective, the increase of production costs is caused by the net increase of water consumption and by the operative costs of the washing plant, including the initial investment, the maintenance costs and the cost of the operators. Sand washing also reduces the production output of the facilities and cuts the cost of opportunity because all the extracted volume of material cannot be transformed into commercial sand.

The ratio of material lost damaging the ratio between the total extracted volume and the final volume of commercial sand produced is related to the amount of material removed in the washing process. Therefore, in addition to damaging the productivity, the removed material by washing has to be managed as a solid waste.

The typical scheme of a sand washing plant is shown in Figure 1.18, including all the process steps and the machinery and equipment involved. Figure 1.18 also presents the productivity rates at each step of the treatment, considering a plant yield of 100% for an example with a processing capacity of 100 Tn/h.

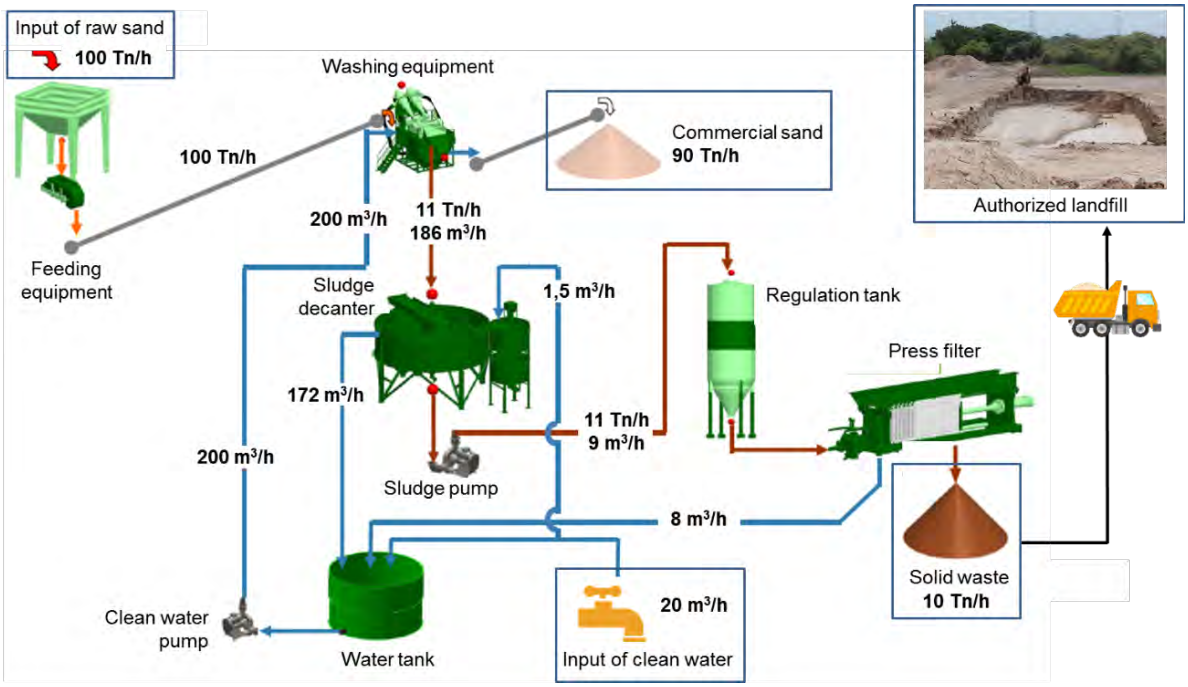

Figure 1.18. Typical scheme and output rates for a washing plant for natural sands (adapted from [45])

In the normal operating conditions of washing plants, the volume of washing water used to produce 1 Tn of commercial sand is 2,5 – 4 m^3, despite Figure 1.18 shows that only 2,2 m^3 of water are required per Tn of commercial sand because it is estimated assuming the washing plant processing at full capacity and at maximum efficiency. However, it is shown in Figure 1.18 that up to 90-91% of the total water volume is supplied by the water recovery equipment (86% from the sludge decanter and 4% from the press filters), thus optimizing the net increase of consumption of clean water. Nevertheless, despite the recovered water, washing of sands in highly efficient facilities requires a constant input of clean water by 10%, being increased up to 30% in washing plants of lower efficiency.

In the same way, according to Figure 1.18 the amount of raw material lost by washing is 10%. It means that, per 1 Tn of finished commercial sand, the ratio of solid waste generated is 11%. This ratio is exclusively referred to the dry-solid fraction of waste generated by the washing equipment, since the total waste amount is enlarged as the residual moisture increases. The sludge decanter and the press filters contribute in removing the water content of the solid waste

generated by washing. Therefore, when the efficiency of the water recovery equipment is not the optimal, the ratio of waste generation per Tn of commercial sand produced increases.

Of course, the production rates presented in Figure 1.18 for both the water consumption and the generation of solid waste are very variable as per the amount of clay to be removed, the efficiency of the washing equipment and the recovery capacity of the sludge decanter and of the press filters. Whatever the case, sand washing always implies additional net use of water, increased consumption of energy, generation of solid waste and reduction of productivity and of profitability.

From the input and output rates displayed in the example from Figure 1.18, Table 1.3 resumes the overall balance for the sand washing process as per 1 Tn of commercial sand produced.

Sand washing process balance per 1 Tn of commercial sand produced		
Productivity loss	Net use of clean water	Solid waste generation
10%	0,11 m^3/Tn	0,17 Tn/Tn

Table 1.3. Productivity rate, net use of clean water and solid waste generation of washing process as per 1 Tn of commercial sand produced (calculated from Figure 1.18)

Apart from the cost increase linked to the consumption of water, maintenance and operativity of the washing plant as well as the side-costs related to the lowered productivity rate due to the removed material by washing, the global costing balance for sand production must include all the costs for managing the solid waste generated. It includes the processing costs at the washing plant, the transport costs to the authorized landfill, the cost for the disposal and the taxes related to the generation of wastes.

Another setback from the washing of sands is caused by to the lack of fines typical of washed sands, since sand washing removes all the fine particles in addition to clays. Thus, washed sands commonly owns very low content of <0,063 mm fines (always below 3-5% but even 0%), leading to technical problems in concrete. The low fines content of washed sands generates a lack of paste volume in the concrete mix. Therefore, for concrete types produced with low amount of cement (<300 kg/m^3, typically for C25/30) and washed sands with almost no fines, the fresh concrete lacks stability and becomes more prompt to segregation [46].

Figure 1.19(a) shows the typical problem of concrete surface delamination in concrete floors produced by segregation of fresh concrete. Delamination of concrete surface lowers the resistance against abrasion [47], thus limiting the expected service life of concrete floors.

However, segregation of fresh concrete is more critical in vertical applications such as walls or pillars, leading to surface finish of bad aesthetics quality or even compromising the minimum reinforcement coating thickness [48], as shown in Figure 1.19(b) and 1.19(c), respectively.

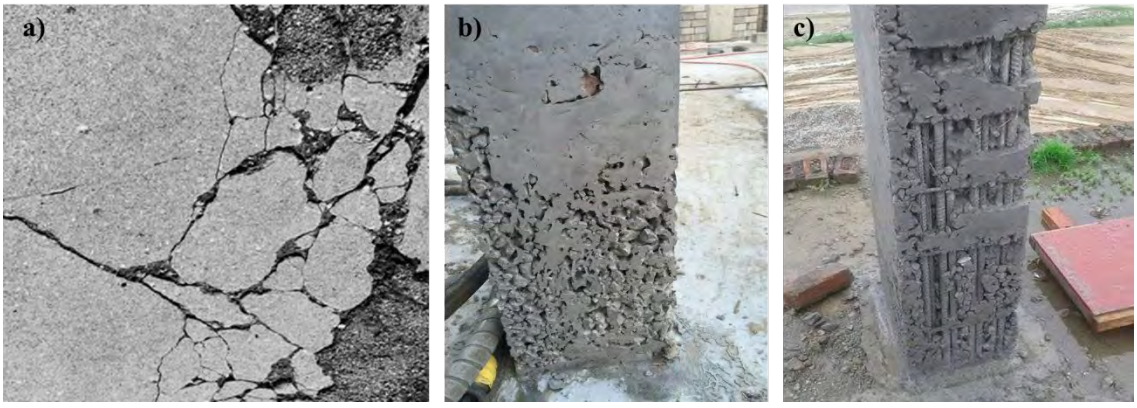

Figure 1.19. Typical damages generated by segregation of fresh concrete; a) delamination of concrete floors surface; b) aesthetics deficiencies in vertical applications; c) exposed reinforcement in pillars

To respect the minimum thickness for the reinforcement coating is imperative to keep the steel rebars passivated against corrosion since steel reinforcement exposed to atmospheric oxygen, CO_2 or chloride makes the structure more prompt to be affected by early corrosion. Thus, the consequences from concrete segregation are critical for the durability and service life of reinforced concrete structures [22], meaning additional costs for repairing.

To prevent the risk of segregation of fresh concrete promoted by using washed sands, it is needed to provide additional fines to restore the stability of fresh concrete by [46], either by using corrective sand of by increasing the cement content.

Corrective sands are sands with high content of fines partially replacing washed sands in concrete mix designs to balance the lack of fines. Therefore, the fine fraction of corrective sands must be of high quality, with low MBV and free of clays, and for this reason corrective sands are more expensive than washed sands. Moreover, additional storing and dispensing equipment are required in the concrete plant for their handling, resulting in increased production cost for the concrete producer.

The other alternative to prevent segregation of concrete is to restore the total fines content by increasing the cement amount, despite not being necessary for the mechanical and durability demands. Of course, this measure also rises the cost of concrete and increases the environmental impact associated.

1.5. INTERFERENCE MECHANISMS OF CLAYS PROMOTING THE SLUMP LOSS OF FRESH CONCRETE

The interference on the fluidity behaviour of fresh concrete generated by clays contained in sands is promoted by two different mechanisms of interaction: the first mechanism is based on the water uptake capacity of clays promoting the increase of the water demand, and the second is based on the reduction of the dosage efficiency of water-reducer admixtures. Both mechanisms progress simultaneously, contributing at the same time to the reduction of concrete slump and to the premature fluidity loss.

1.5.1. Increase of water demand: water uptake capacity of clays

The first undesired effect produced by clays contaminating sands is the increase of the *water demand* of concrete promoted by the water uptake capacity of clays. When a dry-powder of hydrophilic behavior gets in contact with water, the exposed surface is wetted by surface hydration.

Since the water demand is defined as the amount of water required to fully hydrate the exposed surface of any dry-powder when it is dispersed in water, the water uptake of clays means the net amount of free-water stolen by surface adsorption to hydrate all the clay surface accessible to water. Thus, in practical terms, the increase of water demand reduces the slump of concrete is the same way than by reducing the net amount of mixing water.

Since it is a surface process, the water uptake of clays increases as the surface are in direct contact with water increases. In this way, clays with high specific surface are prompt to generate higher slump loss. However, the activity of the hydrated surface of clay colloids defined by the degree of ionization [32], also modulates the water uptake capacity of clays, in addition to the surface area.

Table 1.4 presents the typical ranges of average particle size and BET specific surface for some clay minerals, which belongs to different clay groups. These values are compared against the most typical fine-powders used in concrete, including the cement, various types of SCM (supplementary cementitious materials) and the sands (including typical limestone crushed sands and natural washed siliceous sands).

Fine-powder raw materials		D_{50} particle diameter	BET specific surface (m^2/g)
Cement	CEM I	5 – 20 µm	0,9 – 1,6
	CEM II	10 – 30 µm	0,6 – 1,2
SCM	Microsilica	0.5 – 3 µm	3 – 17
	Blast furnace slag	6 – 10 µm	1 – 5
	Fly ash	5 – 18 µm	1 – 5
	Natural puzzolan	7 – 20 µm	2 – 5
	Limestone filler	3 – 30 µm	<1 – 4
Sand	Natural washed sand	10 – 20 mm	--
	Crushed sand	5 – 20 mm	--
Clays	Kaolin	0,5 – 5 µm	8 – 16
	Muscovite	1 – 10 µm	3 – 13
	Chlorite	2 – 15 µm	4 – 12
	Montmorillonite	0,5 – 2 µm	15 – 60

Table 1.4. Comparison of typical particle diameter by laser granulometry and specific BET surface for some clay minerals, cements, SCMs and sands (adapted from [24,25,34,36,49-54])

By observing the differences in D_{50} and specific BET surface between the powder materials displayed in Table 4.1, it can be seen that the surface area of clays is systematically higher despite some of the clays own comparable particle diameters than SCMs and cement. This is a consequence to the typical morphology of the clay particles, which can be visualized in Figure 1.20.

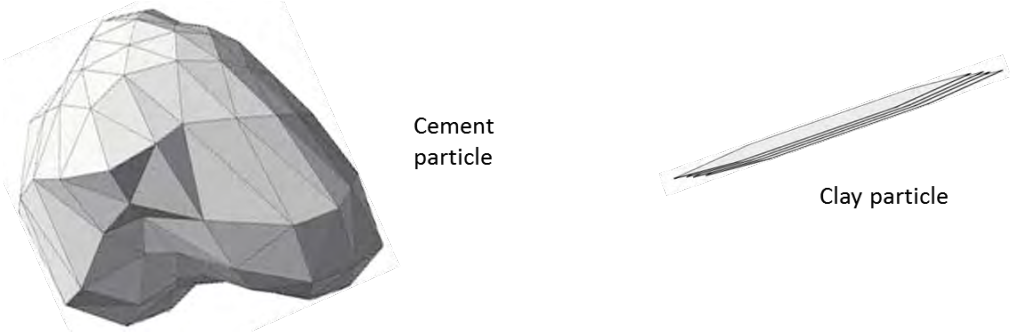

Figure 1.20. Comparison between the typical morphology of clay and cement particles

As Figure 1.20 shows, the typical morphology of clay particles is based on thin, lazy plates of semi-hexagonal shape, with a very high proportion between width (basal surface of basal planes) and thickness (edge surface of plate borders), to the point that clay particles can be considered almost as two-dimensional particles [51-53]. Conversely, cement particles are more spherical, therefore exposing less surface area at equivalent weight.

Due to the high surface area of clay particles, just small amounts of clay in sands are enough to cause significant increases in the water demand, which inevitably force to increase the total mixing water in concrete to achieve the expected slump target. However, Figure 1.21(a) shows that not all the clays generate the same impact on the fluidity loss, since the water uptake capacity is defined by the total exposed surface area but also by the ionic activity of the hydrated clay [36]. Complementary, Figure 1.21(b) displays the reduction of slump at initial time just after batching and after 60 minutes measured in concretes produced with sands containing 2wt.% of clay addition.

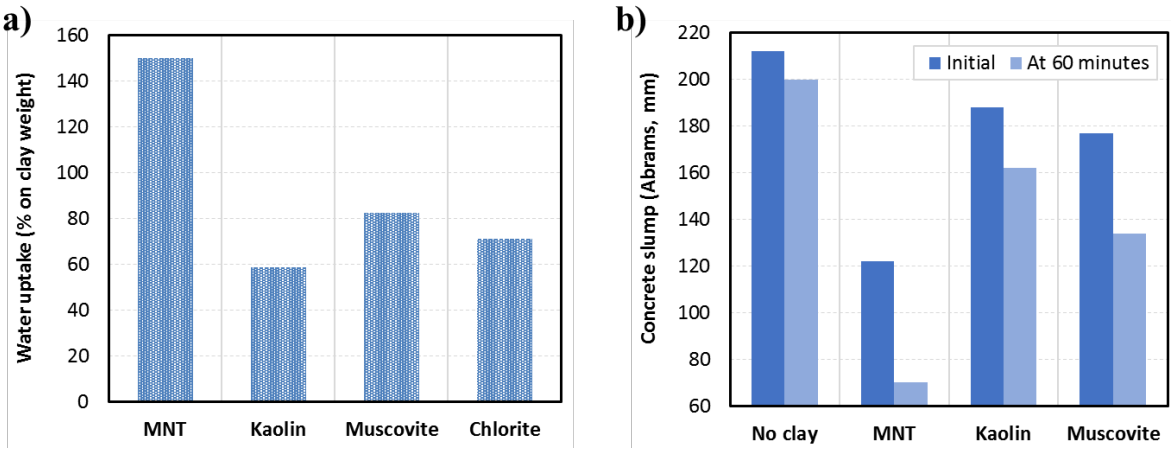

Figure 1.21. a) Water uptake of clays belonging to different clay groups [55]; b) Impact on the initial slump and after 60 minutes by addition of 2 wt.% of clay on sand [55]

Figure 1.21 evidences that the higher the water uptake of clay, the larger the slump loss. In this respect, swelling clays such as montmorillonites own the highest water uptake capacity (being almost the double than of the non-swelling clays), which is always linked to the highest reduction of slump.

The slump loss measured after 60 minutes follows the same pattern than the initial reduction of slump but denoting higher reductions than the observed just after batching. And in the same way than for the initial slump loss, the highest reductions are produced by montmorillonite clays. Therefore, the higher the water uptake capacity of clays, the higher initial slump loss and the shorter the slump retention.

The higher water uptake capacity and the more pronounced reduction of slump flow of montmorillonite clays is due to the additional water uptake produced by the interlaminar space of the expandable clays, which is complementary to the water uptake promoted by the hydration of the exposed clay surface [56].

Therefore, and differently than for the non-swelling clays kaolin and muscovite, the two sorption mechanisms are actively contributing in the water uptake capacity of montmorillonite clays: the first one is the described for the non-swelling clays, based on surface adsorption; and the second one is based on the absorption of the active interlaminar space, which is not produced in non-swelling clays with inaccessible interlaminar space[15,57].

The swelling mechanism proposed in [56] by which montmorillonite clays absorb water into the interlaminar space is presented in Figure 1.22.

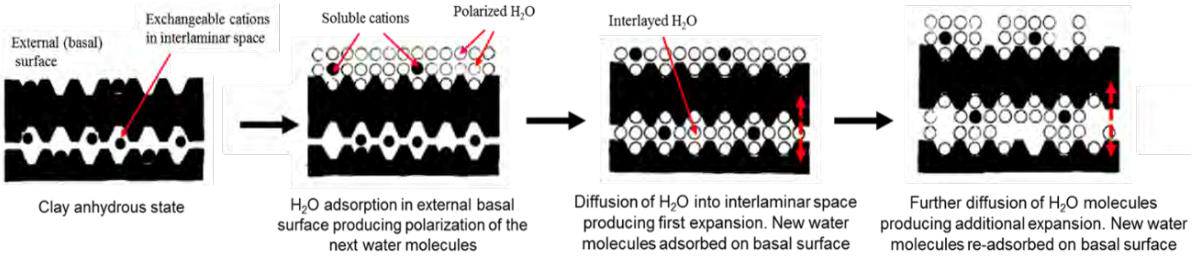

Figure 1.22. Swelling mechanism of montmorillonite clays (adapted from [56])

According to the swelling mechanism represented in Figure 1.22, the expansion of montmorillonite clays is produced by the amount of absorbed water into the interlaminar space [57-60]. Therefore, the higher the accessibility of the interlaminar space, the higher the water uptake of the clay.

Moreover, for both mechanisms responsible for the water uptake, the polarization of the already adsorbed water molecules on the external clay surface is key for the enlargement of the Stern and of the diffuse layer of water and cations surrounding the charged clay colloids, allowing new water layers to be further adsorbed in an overlapped arrangement [56,61], as Figure 1.22 shows, thus increasing the interference on the fluidity behavior by enhancing the water uptake on clay surface.

The water uptake of clays promoted by surface adsorption is boosted by clay exfoliation [62]. The exfoliation of clay particles is illustrated in Figure 1.23 and consists on the progressive delamination of the stacked plates forming the pristine particle. The delamination of clays is commonly produced when clays are dispersed in polar solvents such as water and increases by mechanical share and as the clay expands.

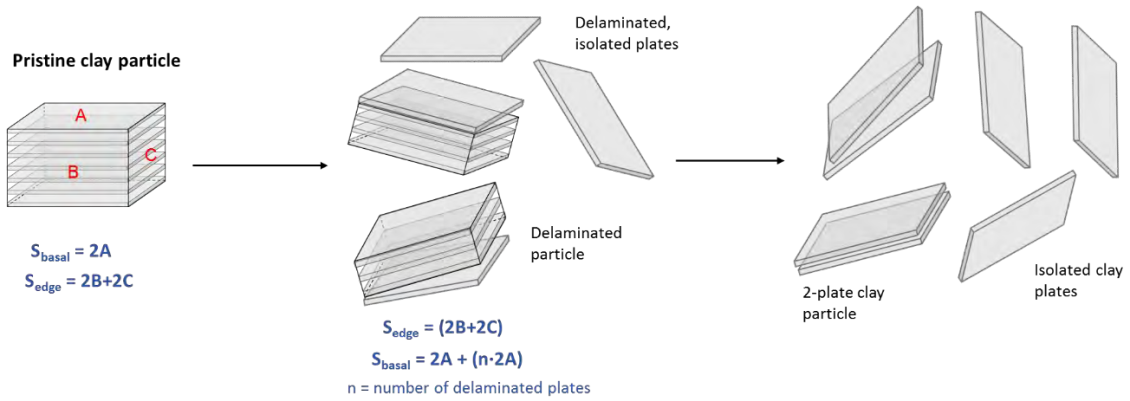

Figure 1.23. Exfoliation process of clay particles and consequences in the total exposed basal and edge surface

Figure 1.23 shows that the exfoliation of the pristine clay particles releases new clay specimens with reduced number of stacked plates [63,64]. The delamination of clay particles can progress until fragmenting the original particle in simple clay units formed only by two stacked plates (this is the minimum configuration for clays to absorb water) or even resulting in single isolated plates [65].

According to Figure 1.23, per each plate delaminated from the pristine clay particle, exfoliation produces a theoretical increase of basal surface equivalent to the double of the original. Thus, due to the high aspect ratio typical of clay particles, exfoliation generates huge increase of the total exposed clay surface ready for adsorption [23-25]. For this reason, exfoliation of clay particles boosts the water uptake capacity of clays and further increases the water demand. In this way, for clays of similar nature, the higher the tendency to exfoliate, the bigger the increase of the water demand, resulting in the more pronounced slump loss of fresh concrete.

1.5.2. Interference on the dispersing capacity of water-reducer admixtures

Clays contained in sands used for concrete interfere in the performance of water-reducer admixtures by reducing or even by totally inhibiting their effective dispersing capacity. However, there are two different mechanism of interaction depending on the type of polymer and on the type of clay [15,67]. The two models of interaction between water-reducer polymers and clays are illustrated in Figure 1.24.

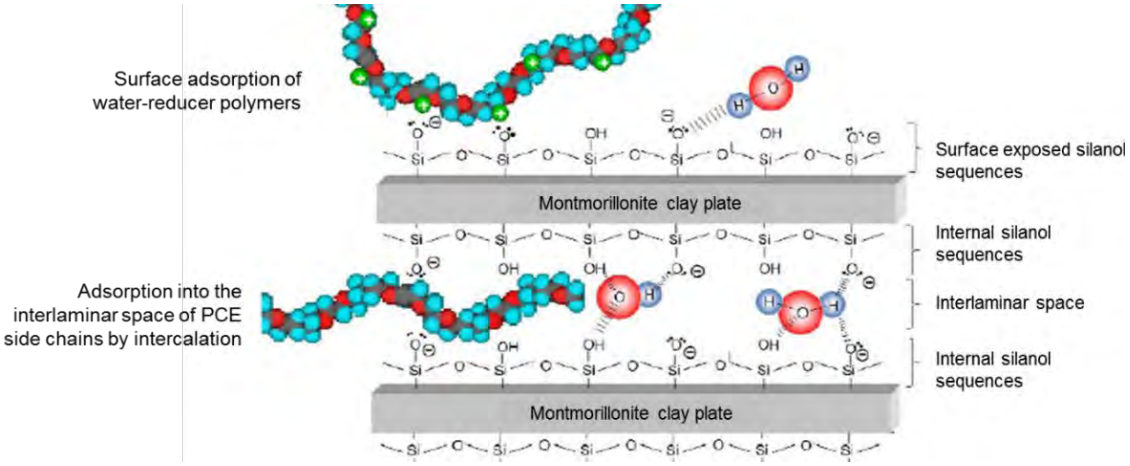

Figure 1.24. Adsorption and absorption arrangements of water-reducers interacting with clays (adapted from [66])

In the same way than clays interact with water, the interaction between water-reducer and clay particles is based on the adsorption of polymer on the external clay surface (both on basal and lateral surface), and on the absorption of polymer into the interlaminar space, being the last exclusive for swelling clays [15,68,69]. Complementing Figure 1.24, the interaction mechanisms experienced by each of the combinations between the types of water-reducer polymer and the types of clays (in regards the swelling behavior) is summarized in Table 1.5 [15,66-69].

Water-reducer polymer	Non-swelling clays	Swelling clays
Lignosulfonate (LS)	Surface adsorption	Surface adsorption
B-Naphtalenne sulfonate (BNS) Melamine sulfonate (MNS)	Surface adsorption	Surface adsorption
Polycarboxylate ether/ester (PCE)	Surface adsorption	Surface adsorption Absorption by intercalation

Table 1.5. Interaction models between water-reducers and clays

According to Table 1.5, all clays and all polymers interact at least by surface adsorption, but only the swelling clays can interact by absorption processes. Nevertheless, there are additional restrictions from the structure of the water-reducer polymers for being absorbed into the interlaminar space of swelling clays, since LS, BNS and MNS polymers cannot be absorbed by swelling clays such as montmorillonites because the sulfonic terminals and the non-polar sequences [15] of these polymers. Thus, the interaction mechanism based on absorption is exclusive for PCE polymers interacting with swelling clays [15,69].

The interference on the dispersing performance of water-reducer admixtures which impacts on the fluidity loss behavior is not of equal magnitude for each of the combinations listed

in Table 1.5. In this way, Figure 1.25(a,b) presents the paste flow loss and the reduction of the dosage efficiency of water-reducers (the dosage demanded to produce the equivalent paste flow) recorded in cement pastes containing some of the combinations between water-reducer polymers and clays.

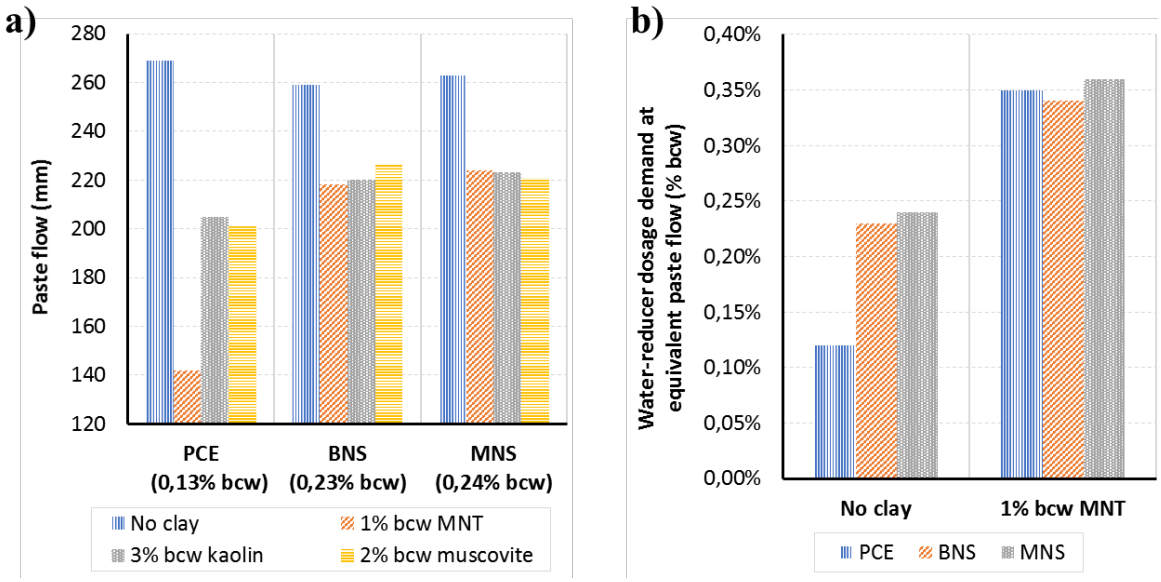

Figure 1.25. a) Paste flow of cement pastes with different water-reducers and clays (adapted from [15]); b) Dosage efficiency of water-reducers (adapted from [15,70])

Figure 1.25(a) confirms that the combination montmorillonite clays - PCE based superplasticizers is the most critical for both the paste flow loss and the reduction of the dosage efficiency. Nevertheless, the impact on paste flow reduction produced by kaolin and muscovite cannot be neglected despite being not as high as of montmorillonite clay.

The impact on fluidity loss for the pastes containing kaolin and muscovite is of lower magnitude than of montmorillonite whatever the water-reducer used, although the larger reduction is produced by the PCE polymer. Similar results than of the pastes containing kaolin and muscovite are observed with pastes containing montmorillonite clay and water-reducers based on BNS or MNS polymers. Conversely, the cement paste produced with PCE polymer and montmorillonite shows the most drastic reduction of paste flow, being up to four times larger than all the other combinations.

The impact on the dosage efficiency of water-reducers presented in Figure 1.25(b) reproduces the same behavior than Figure 1.25(a). In the reference paste without clay, the dispersing capacity of PCE polymers is largely superior than of BNS and MNS, requiring less than the half of the dosage to achieve the same paste flow. However, in the presence of small

amounts of montmorillonite clay, the dosage efficiency of PCE polymer is worsen by 300% while for BNS and BNS is worsen only by 50%, to the point that no further differences are observed in the dispersing capacity within the three water-reducers.

From the observed behavior, it is proposed that the interaction mechanism based on surface adsorption just reduces partially the dispersing capacity of all water-reducers, but the interaction based on absorption into the interlaminar space almost totally inhibits the dispersing capacity of PCE polymers [15].

The exposed surface of all clays owns active sites for the adsorption of water and other polar or ionic molecules such as the water-reducer polymers. Since the dispersing mechanism requires the polymer to be adsorbed on the colloid surface, all the exposed clay surface is competing against the cement surface for the adsorption of polymer [71]. The phenomenon of competitive adsorption of water-reducers polymers generated by the presence of clays is represented in Figure 1.26.

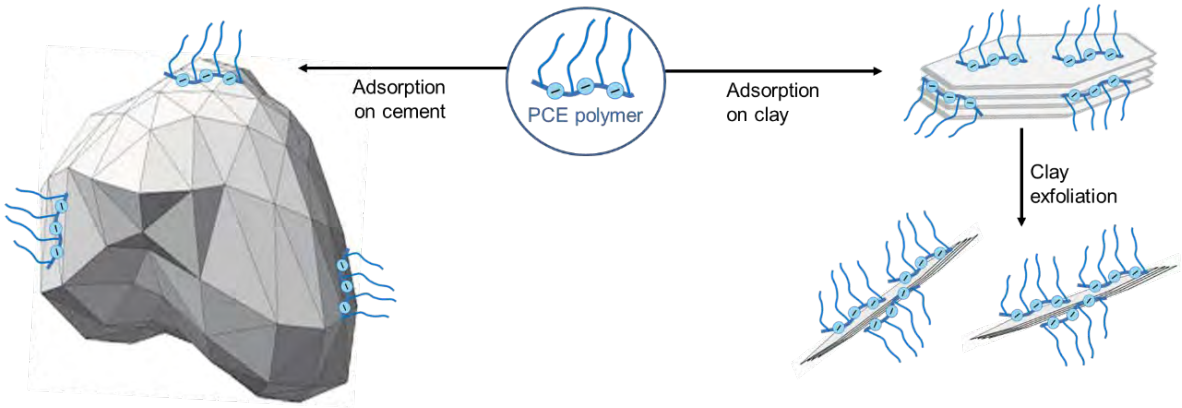

Figure 1.26. Competitive adsorption of water-reducer PCE-based polymers between cement particles and clay particles (adapted from [36])

Since all the clay typologies owns active external surface, the competition for the adsorption of the water-reducer polymers represented in Figure 1.26 is common property of all clays, regardless of whether they have an accessible interlaminar space or not, affecting to all types of water-reducer polymers. However, water-reducer polymers adsorbed on the external surface of clay particles can continue to develop their plasticizing effect, since the polymer can acquire the required arrangement to generate efficient dispersion of the colloids in the same way than when adsorbed on cement [15]. Nevertheless, the efficiency of the water-reducer polymers for dispersing clay particles of lazy shape is lower than for dispersing spherical-like particles such as cement [72,73].

Therefore, the particle morphology of clays reduces the dosage efficiency of water-reducers. Consequently, clays demand bigger quantity of water-reducer polymers than cement to produce the same dispersion degree (so, the same level of fluidity, expressed as paste flow or slump). In this way, the greater the affinity of the water-reducer polymer for being adsorbed on the external clay surface in comparison to the affinity for adsorption on the cement, the greater the competition balance and the higher the interference on the dispersing capacity, thus producing larger impact on the fluidity loss and on the premature loss of fluidity over time [15,36].

In addition to the lazy shape of clay particles, which results in large exposed basal planes able for adsorption of the polymer units, from Figure 1.26 it is possible to deduct that the exfoliation of the clay particles also boosts the total adsorption of polymers on clay surface, as it happens with the water uptake too. As it is represented, the exfoliation of the pristine clay particles increases the total exposed clay surface by releasing new additional and accessible basal surface. The new released basal surface adsorbs further amounts of water-reducer polymer, being comparable, in practical terms, to a net increase of the clay content. Thus, the total net adsorption of the water-reducer polymer on the exposed, external clay surface increases as the particle delamination progresses. Nevertheless, the direct consequences of clay exfoliation on the interference with the performance of superplasticizer are different for each type of clay.

Figure 1.27(a,b) presents the evolution of the net sorption measured by TOC analysis of a PCE-based superplasticizer and of a BNS-based water-reducer, respectively, on montmorillonite, muscovite and kaolin pastes, as the dosage of polymer increases. Since this analytical method reports the total amount of organic polymer adjoined to the particles, the results of sorption reported include both the polymer adjoined by adsorption on the external clay surface and by absorption into the interlaminar space (in those clays having accessible interlaminar space).

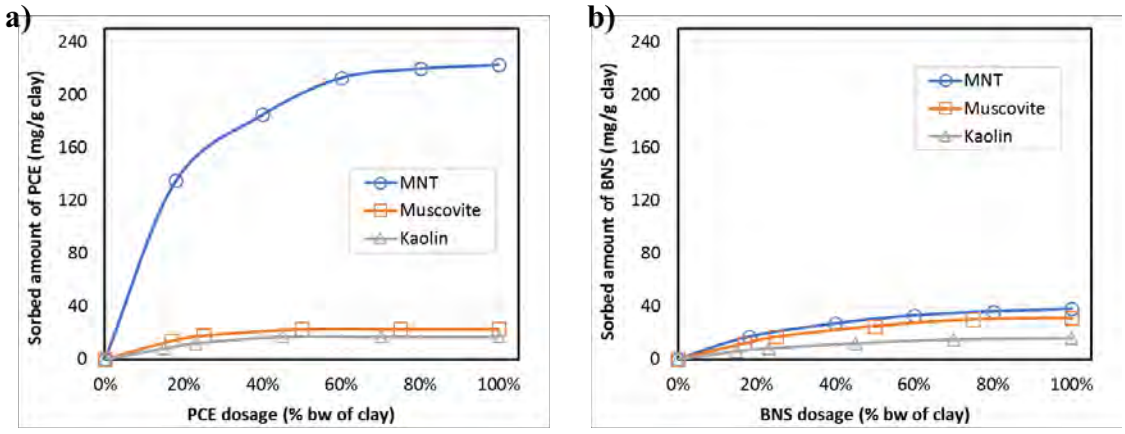

Figure 1.27. Sorption of polymer on different clays (adapted from [15]); a) For PCE polymer; b) For BNS polymer

Figure 1.27(a) confirms that the sorbed amount of PCE polymer on montmorillonite clays is up to 10 times bigger than the sorption on muscovite and on kaolin. In addition to the differences of specific surface between these clays, the bigger sorption in montmorillonite clays is basically promoted by to the additional amount of polymer absorbed into the interlaminar space of montmorillonites, which is not produced in muscovite and kaolin [15].

Conversely, the evolution of the net sorbed amount of BNS polymer presented in Figure 1.27(b) shows almost no differences between the montmorillonite clay and the non-swelling clays muscovite and kaolin. It is because BNS polymers interact with clays exclusively by surface adsorption, so they are never absorbed regardless of whether clay owns accessible interlaminar space or not [15].

The mechanism by which PCE polymers are absorbed into montmorillonite is based on the intercalation of the PEG/PEO side chains of PCE polymers into the interlaminar space. In the same way that water, the intercalation of the side chains produces the expansion of montmorillonite clays.

The expansion of montmorillonite clay is denoted by an increase of the d-spacing (d_{001}) value, which is determined by XRPD analysis performed on the dried powder samples obtained from the drying of the solid phase of fresh clay pastes containing PCE-based superplasticizers, previously centrifugated or filtrated to separate the liquid phase form the solid fraction.

Figure 1.28(a,b,c) shows the XRPD patterns obtained from dried clay pastes containing diverse water-reducer polymers. All the clay pastes are prepared by dispersing the powder clays muscovite, kaolin and montmorillonite, respectively, in synthetic cement pore solution, followed by the addition of some water-reducer superplasticizers of different chemistry.

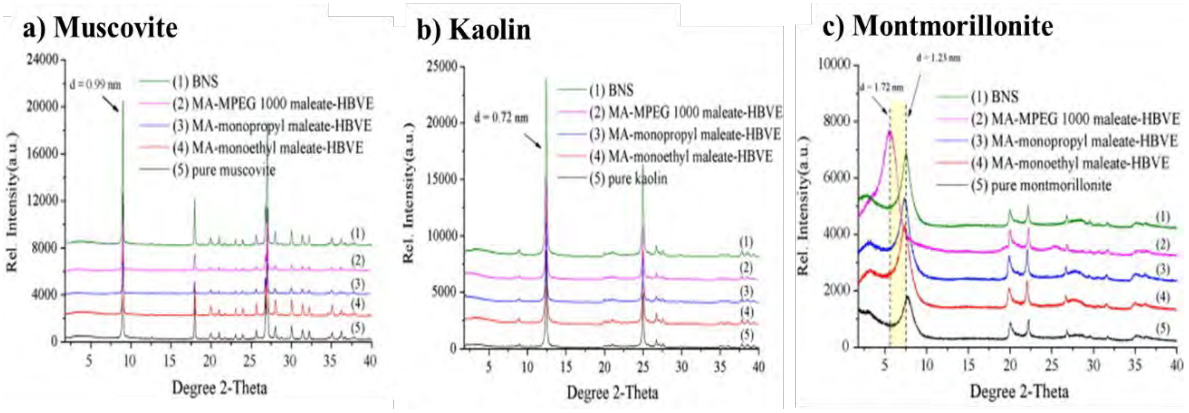

Figure 1.28. XRPD patterns on dried pastes for different water-reducers; a) Muscovite; b) Kaolin; c) Montmorillonite (adapted from [15])

The XRPD patterns obtained from the muscovite and kaolin pastes presented in Figure 1.28(a) and 1.28(b) confirm that any displacement of the 2θ position is produced regardless the type of water-reducer used, thus keeping the same position that of the pure clay paste without water-reducer.

However, Figure 1.28(c) denotes that there is a switch to lower angles in the XRPD pattern obtained from the montmorillonite clay paste, by which the d-spacing expands to 1,72 nm from the initial 1,23 nm measured in the montmorillonite paste without water-reducer. Moreover, the expansion observed in the montmorillonite clay paste containing PCE polymer (referred as MA-MPEG 1100 in Figure 1.28) is not observed when BNS polymer is used, confirming that there is no absorption of BNS into montmorillonite.

From the interpretation of the interlayer d-spacing enlargements recorded by XRPD analysis performed on dried clay pastes according to the analytical procedure described, the absorption mechanism based on the intercalation of PCE side chains into the interlaminar space of montmorillonites is proposed [68-69].

The proposal currently accepted for the intercalation mechanism is presented in Figure 1.29. It shows that the intercalation of PEG/PEO based side chains produces the expansion of the clay in an average thickness of 5,4Å [67-69], according to the results of d-spacing measured. Therefore, from the net expansion of the interlaminar space it is deducted that only one single monolayer of PCE side chains is intercalated, together with two monolayers of water molecules. The water molecules are arranged to coordinate the electronegative oxygen atoms of the PEG/PEO side chain of the PCE polymer and of the internal siloxane sequences of the montmorillonite clay plates through their electronegative hydrogen atoms.

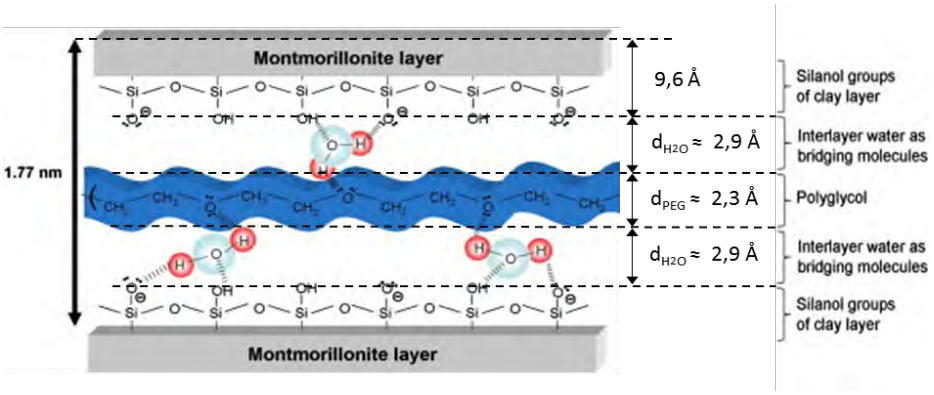

Figure 1.29. Arrangement of the intercalation of PEG/PEO side chains into montmorillonite clay (adapted from [69])

According to Figure 1.29, the monolayer of side chains is intercalated in a zig-zag planar arrangement in between the two water monolayers coordinating the oxygen atoms of the -CH_2-

O-CH_2- sequences of the side chain by hydrogen bonds. This is the configuration that fits with the net expansion of the clay measured with the current analytical method. Therefore, since the thickness of the intercalated water molecules is known, as well as the thickness for the single montmorillonite plates [23,74-76], from the net expansion calculated it is possible to estimate the thickness of one monolayer of side chains intercalated, resulting in 2,3-2,4 Å [67].

1.5.3. PCE polymeric structures with improved clay tolerance

Since the absorption mechanism by the intercalation of PCE side chains into the interlaminar space of montmorillonite clays was understood, the researchers are working to develop water-reducer admixtures with the same dispersing capacity than of standard PCE based superplasticizers but with improved clay tolerance. This commitment is mainly approached from two different angles: the design of new polymeric structures with reduced sensitivity and the use of sacrificial agents to prevent the absorption of the active dispersing agent into the clay.

- Polymeric structures with improved clay tolerance:

From the polymer point of view, most of the development of tailored polymers is focused on preventing the intercalation of side chains. Of course, by removing the side chains from the polymeric structure there is no intercalation possible, but since the side chains are the promoters of the steric repulsion mechanism, the dispersing capacity and the dosage efficiency is worsening among the number and length of side chains is reduced [78].

Figure 1.30(a,b,c) presents some of the most promising polymer modifications available in the literature to improve the clay tolerance of high-performance water-reducers.

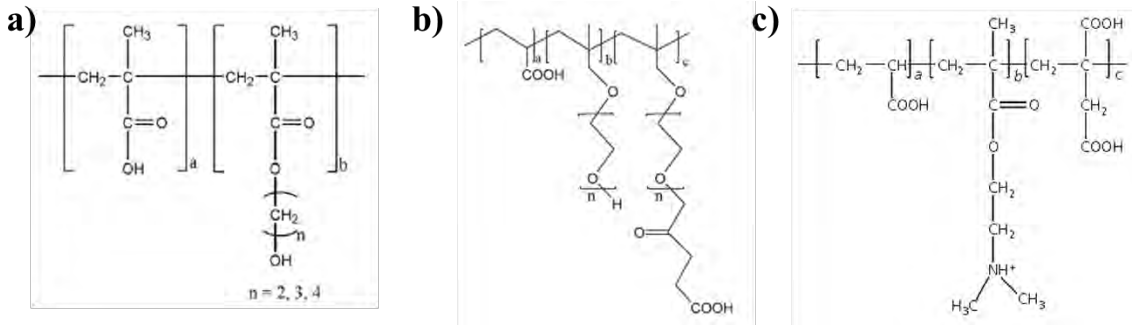

Figure 1.30. a) Vinyl ether-based polycarboxylate (from [7,70]); b) PCE with anionic carboxylic-ended side chains [79]; c) PCE with cationic-ended amide side chains [43,80,81]

The polymer proposed in [7,70] and presented in Figure 1.30(a) is based on esterified alkyl, hydroxyl-ended side chains of very short length produced by the polymerization of a

reduced number of vinyl monomers ($n \leq 4$) and attached to a typical poly-methacrylic backbone. Thus, it is almost a linear polymer.

This type of polymer is not intercalated into montmorillonites due to the short length of their hydrophobic side chains. Nevertheless, the very short side chains of this polymer suggest that its water reduction capacity must be of lower order than of standard PCE structures and, due to the similarities in the structures, comparable to linear poly-acrylates, poly-methacrylates and BNS polymers.

The PCE polymer presented in Figure 1.30(b) is proposed in [79]. This polymer combines standard neutral hydroxyl-ended IPEG side chains and anionic carboxylic-ended PEG side chains, attached on an acrylic backbone. The anionic-ended side chains, synthetized by condensing succinic anhydride and polyethoxylated isoprenol, owns an electronegative character by which the modified side chains are repelled from the interlaminar space because it owns the same electronegative character.

The experimental results presented in [79] show no intercalation of the modified polymers and promising performances compared to conventional PCE polymers. However, further confirmations are needed to asses that the standard IPEG side chains contained in the polymer are not intercalated by the clay. In this situation, despite the partial intercalation of the side chains of the polymer, it is expected that almost the same interference than of conventional PCE polymers can be produced. Additionally, it must be proved that the anionic termination of the modified side chains does not produce flocculation, which is the opposite behavior than intended.

Finally, the structure presented in Figure 1.30(c) is a PCE polymer based on an acrylic and methacrylic acid backbone grafting standard PEG side chains partially replaced by short alkylamide side chains with a cationic quaternary amine-based end-terminal. Despite the experimental results reported in [43,80,81] shows that this amide-modified polymer is not intercalated into montmorillonites, some discrepancies are denoted within the three publications cited in regards of the efficiency of these amino-modified PCE structures. But in addition, the lack of intercalation reported seems to be contradictory with the well-known affinity of organic quaternary amines for being intercalated into montmorillonites [81,82].

Thus, in the same way as for the previous polymer modifications, further evaluations are required since there is no impediment expected for the intercalation of the standard PEO/PEG based side chains of the polymer, as well as the expected potential flocculation through the ionic terminations of the amide-based side chains.

For all the PCE-modified polymers presented in Figure 1.30, because the number of references is too limited, further research is needed to confirm that these proposals can be a path-forward for the development of PCE polymers with improved clay tolerance. Therefore, to proof the robustness of these new developments, the testing conditions must be extended, including montmorillonite clays and cements of different properties.

Finally, since the studies with all the polymers presented are limited to cement and clay pastes, it is pending to evaluate their efficiency in the real conditions of use, so in concrete and at real scale in concrete plants. Therefore, nowadays the candidate solutions presented in Figure 1.30 are still far from being commercially available. However, they can be a promising starting point for the development of clay-insensitive water-reducer polymers with high water reduction capacity as of conventional new-generation superplasticizers based on PCE polymers.

- Use of sacrificial agents to prevent the absorption of the active dispersing polymer:

Since the main reason for the inhibition of the dispersing capacity of PCE polymers is the intercalation of their PEO/PEG based side chains into the interlaminar space of montmorillonites, another way to reduce this problematic is to formulate sacrificial agents together with the active dispersing polymer to prevent its intercalation.

The technical approach assumes that the sacrificial agent is absorbed faster (so before) than the PCE polymer such that the amount of polymer inhibited for dispersing is being minimized. This implies that the affinity for absorption must be greater than that of the PCE polymer itself.

Some of the most typical sacrificial agents studied are the lineal polyglycols, emulating the side chains of the PCE [77], and some linear polysaccharides able to be absorbed [78]. Nevertheless, the use of sacrificial agents is not delivering the level of improvement to overcome the interference in an effective way since the amount of sacrificial agent required to prevent the absorption of the active dispersing polymer is generally too high, making these formulated superplasticizers not cost-effective or carrying critical non-desired, secondary effects such as strong retardation.

Therefore, the use of sacrificial agents is far from being a suitable way to manage the interference generated by clays and their implications in the premature slump loss of concrete, due to the lack of robustness, limited effectives and retardation effects produces and by not being a cost-effective solution.

1.6. DISAGREEMENTS BETWEEN THE EXPERIMENTAL EVIDENCES AND THE INTERCALATION MECHANISM PROPOSAL

The model of the arrangement for the intercalated side chains of PCE polymers into the interlaminar space of the montmorillonite clays presented in the previous Figure 1.29 is deducted from the d-spacing enlargement obtained by XRPD measurements performed on dried powders. The analytical method consists on preparing clay pastes with cement pore solution and admixture in which the solid phase is isolated from the liquid phase by filtration of centrifugation and posteriorly dried at temperatures below 80 ºC to completely remove the moisture [67-70].

From the interpretation of the XRPD patterns, the conformation of absorption is always the same, by which one single monolayer of PEG/PEO side chains is intercalated together with two monolayers of coordination water molecules. Therefore, this statement leads to the conclusion that there is one unique intercalation arrangement independently of the structure of the PCE polymer and of the properties of the clay.

However, this appointment is contradictory with the experimental evidences supporting that the interference on the fluidity and on the sorption behavior is clearly variable within PCE polymers of different structure and within diverse montmorillonite clays.

Therefore, the conclusions extracted from the d-spacing measurements seem to be contradictory with the evidences and conclusions extracted from other simpler tests such as paste flow measurements.

1.6.1. Influence of the PCE polymer structure on the intercalation behaviour

Figure 1.31(a) presents the experimental results of paste flow reported in [69] for plain cement pastes and cement pastes with 1% bcw of montmorillonite clay treated with two PCE polymers of different structure. The polymeric structure for both PCE is described in Figure 1.31, denoting large differences in anionic charge and in grafting ratio of side chains.

Complementing the paste flow tests, Figure 1.31(b) shows the percental fraction of sorbed polymer on cement and on clay for both PCE structures at equivalent dosage, and Figure 1.31(c) displays the d-spacing value obtained by XRPD measurements performed on dried clay pastes according the traditional method for the references clay paste without PCE polymer and for the clay pastes containing the two different types of PCE polymers used at equivalent dosage.

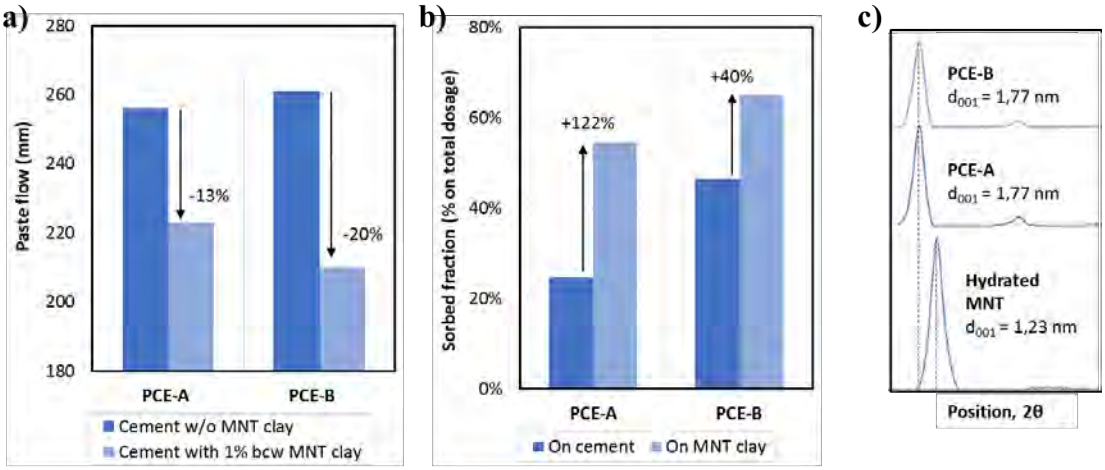

	PCE-A	PCE-B
Anionic charge (µeq/g)	175	1100
Grafting ratio	1,5 : 1	6,0 : 1

Figure 1.31. a) Paste flow lectures for PCE-A and PCE-B in cement pastes without clay and with 1% bcw of montmorillonite; b) Sorbed fraction of PCE on cement and on montmorillonite; c) d-spacing by XRPD on dried clay pastes (adapted from [69])

Figure 1.31(a) and 1.31(b) confirms that the two different PCE structures used present different affectation in both the fluidity and the sorption behavior. Nevertheless, from Figure 1.31(c) it is deducted that both PCE polymers generate an equivalent expansion of the montmorillonite clay because the d-spacing values are identical for both structures.

Therefore, the intercalation model previously presented in Figure 1.29 deducted from the d-spacing variations is not in agreement with the reported results of paste flow loss and of sorption evolution.

Another example illustrating the same disagreements is identified in [85]. In this publication, four PCE polymers with same side chain length but with different grafting ratios are used. Figure 1.32(a) displays the dosage demand of PCE polymer to achieve the same paste flow in cement pastes without clay and in cement pastes containing 1,5% bcw of montmorillonite clay, and Figure 1.32(b) reports the net sorbed amount of each PCE polymer on clay, measured in clay pastes by TOC.

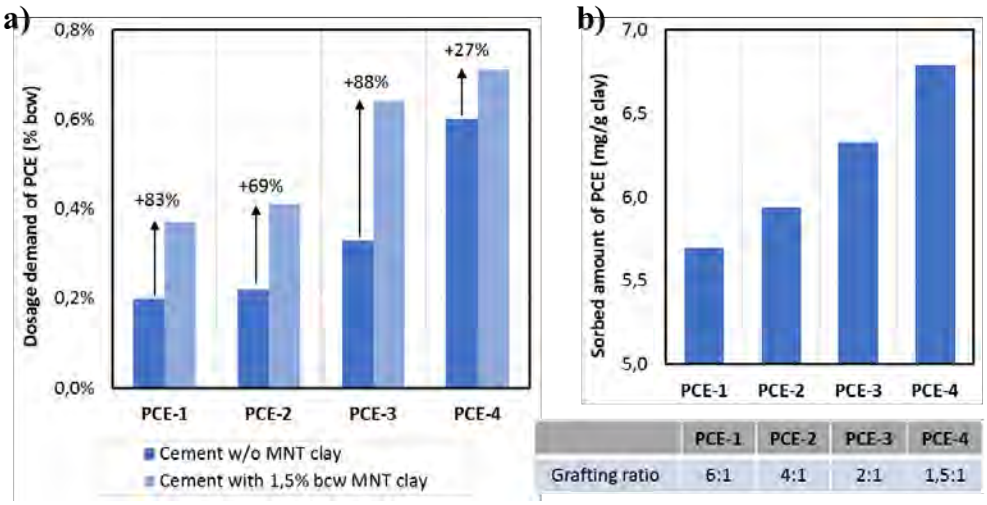

Figure 1.32. a) Dosage demand of PCE for equivalent paste flow in cement pastes without clay and containing 1,5% bcw of montmorillonite; b) Sorbed fraction of PCE measured on montmorillonite pastes (adapted from [85])

In the same way than in the previous example, relevant differences in both the fluidity loss behavior and in the net sorption of polymer can be observed within the four different PCE structures used. However, it is not reproduced in the XRPD patterns and in the d-spacing values presented in Figure 1.33(a), obtained from dried clay pastes.

To further highlight the evidence of the disagreements, the increase of the interlayer d-spacing produced by the intercalation of the PCE polymers used in [85] and the PCE polymers used in [69] is jointly represented in Figure 1.33(b). This plot also represents the calculated d-spacing for montmorillonites expanded by water absorption for each of the number of water monolayers (W) absorbed into the interlaminar space [76].

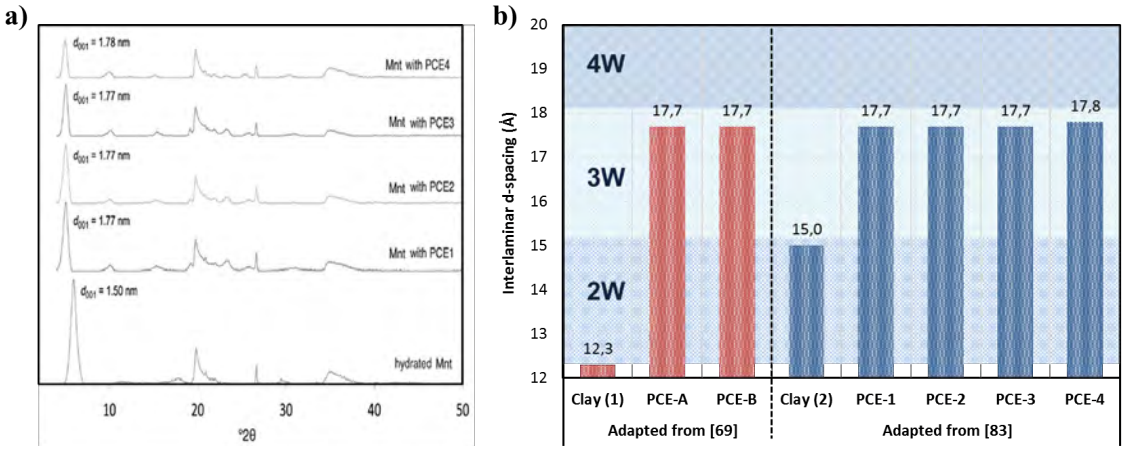

Figure 1.33. a) d-spacing values by XRPD on dried montmorillonite pastes (adapted from [85]); b) Comparison of d-spacing recordings from [69] and [85].

Again, the d-spacing measured for each PCE polymer shows almost identical values, in the range of 1,77 nm, matching with the d-spacing results from the previous example, as observed in Figure 1.33(b). On the one hand, it is observed that despite different PCE polymers and different montmorillonite clays are used, the expansion by intercalation always results in the same conformation, by which one monolayer of side chains is coordinated by two monolayers of water. And on the other hand, the recorded expansion of the clay at 17,7Å d-spacing produced by the intercalation of PCE side chains is even lower than the expansion at 18-19Å d-spacing produced by the absorption of 3 monolayers of water into the interlaminar space of montmorillonites dispersed in alkaline aqueous media [34].

The same disagreement between d-spacing measurements on dried clay pastes and other experimental evidences is observed in the intercalation of linear polyglycols (PEG) of different molecular weight into montmorillonites. Linear PEGs are of identical composition that the side chains of PCE and therefore, they are absorbed into the interlaminar space of montmorillonite clays by intercalation in the same way than PCE polymers are doing.

The experimental results reported in [86] for the net sorption of three linear PEG having molecular weight of 400, 1100 and 6000 g/mol and for a conventional PCE polymer are presented in Figure 1.34(a). The changes of d-spacing measured for each linear PEG and for the PCE are presented in Figure 1.34(b), including the range of d-spacing values calculated for absorbed water monolayers just for comparison purpose.

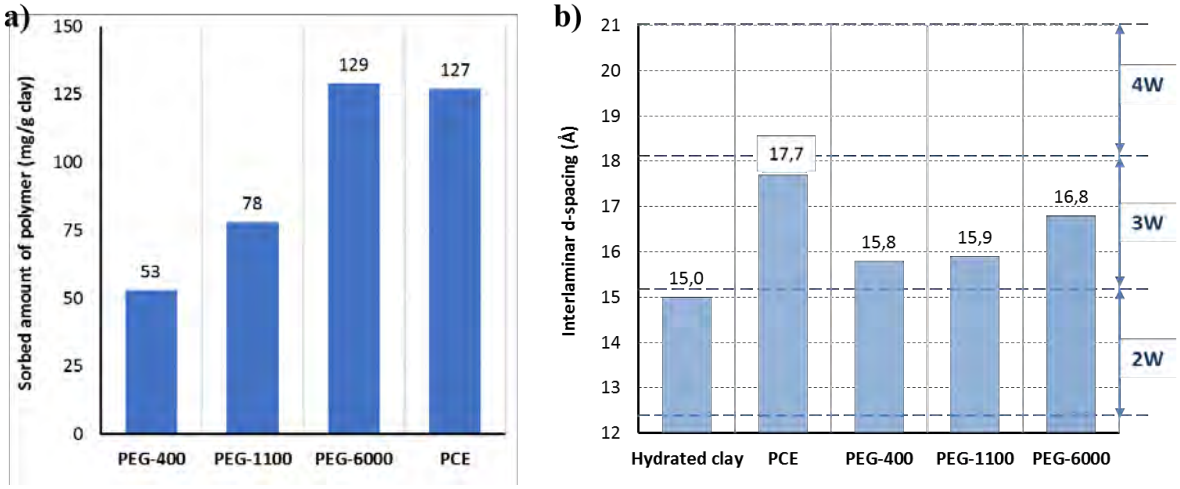

Figure 1.34. a) Net sorbed amounts of PEG on montmorillonite clay; b) d-spacing by XRPD on dried clay pastes containing linear PEG (adapted from [86])

Comparing Figure 1.34(a) and Figure 1.34(b), it is observed that the profiles of sorption do not stablish any direct relationship with the interlaminar d-spacing measured. Despite the

expansion produced by the linear PEGs is lower than the produced by the PCE, it can be observed in Figure 1.34(b) that the difference is smaller than 2,9 Å in all cases, which is the size corresponding to one water layer intercalated. In addition, for both the PCE and all the linear PEG of different length, the d-spacing measured is always compressed in the same range than for three water layers absorbed, reproducing the same behavior than for the cases presented in the previous Figure 1.33(b).

1.6.2. Influence of the properties of montmorillonite clay on the intercalation behaviour

The examples displayed in the previously presented Figure 1.33(b) (since different clays are used in each publications) already denote that no relevant differences are identified in the d-spacing results despite using montmorillonite clays of different properties.

Thus, from the perspective of the clay, the measurement of d-spacing are still reflecting the same disagreement between the fluidity and sorption behavior and the corresponding expansion of the clay produced by the intercalation of side chains.

One example confirming the influence of the properties of montmorillonites clays on the intercalation behavior of PCE side chains is extracted from [67] and presented in Figure 1.35, 1.36 and 1.37. Here, in addition to three PCE polymers of different structures, three montmorillonite clays owning different exchangeable cations are used: sodium salt (Na-MNT), magnesium salt (Mg-MNT) and calcium salt (Ca-MNT).

The polymeric structure for each PCE polymer is presented in Figure 1.35(a), together with their sorption isotherms on each montmorillonite clay. In the same way than in the previous examples, it can be observed that each of the PCE polymers generates different sorption isotherms, but also each of the montmorillonite clays presents different patterns of sorption.

From the clay perspective, the highest sorption rates are produced on the sodium montmorillonite. However, despite there are relevant differences in the net amounts of sorbed polymer between the three clays, it is noticed that each montmorillonite reproduces a common profile of sorption isotherms in regards of the diverse PCE polymers.

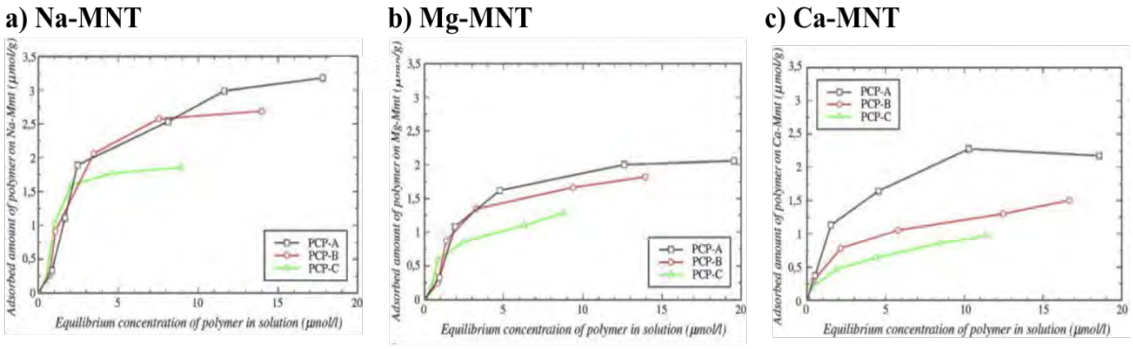

	PCP-A	PCP-B	PCP-C
Side chain length (mol EO)	45	31	114
Grafting ratio	4 : 1	3 : 2	4 : 1

Figure 1.35. Net sorbed amounts of PCE polymers (A,B,C) on montmorillonites with different exchangeable cations; a) Na-MNT; b) Mg-MNT; c) Ca-MNT (adapted from [67])

The XRPD patterns obtained from dried clay pastes of each montmorillonite clay and for the three PCE polymers are shown in Figure 1.36(a,b,c). Complementing Figure 1.36, the corresponding values of d-spacing are presented in Figure 1.37, deducted from the XRPD patterns presented.

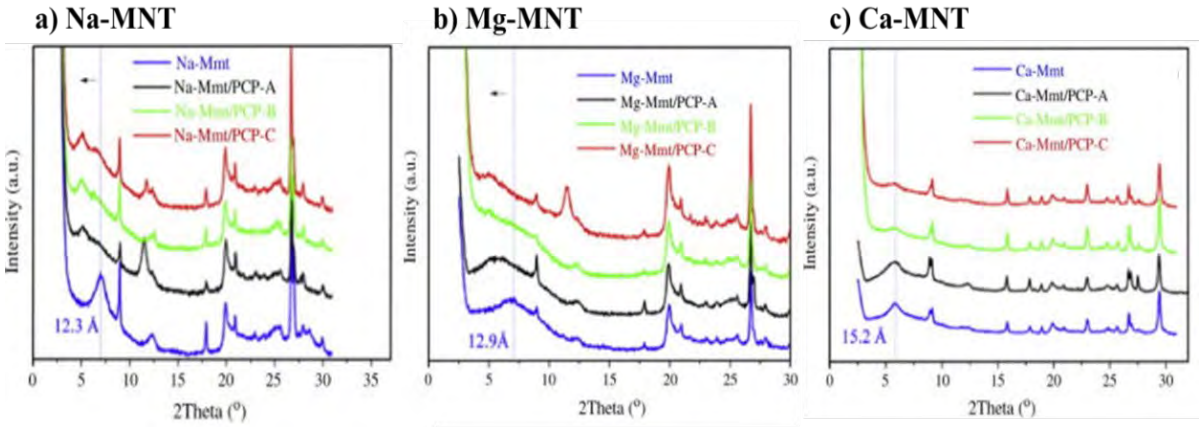

Figure 1.36. XRPD patterns from dried clay pastes for each PCE polymer (A,B,C) and for each montmorillonite clay owning different exchangeable cations; a) Na-MNT; b) Mg-MNT; c) Ca-MNT (adapted from [67])

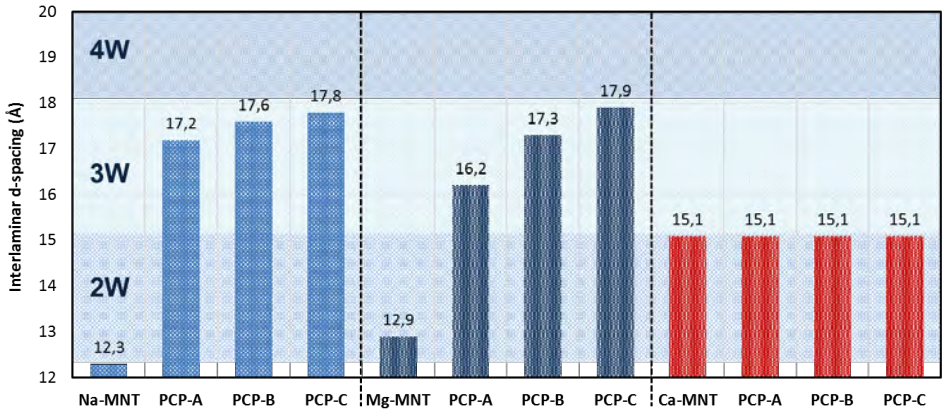

Figure 1.37. d-spacing for each of the combinations between PCE polymers (A,B,C) and montmorillonite clays owning different exchangeable cations (adapted from [67])

Once again, the intercalation into the sodium Na-MNT and the magnesium Mg-MNT reports comparable d-spacing for all the PCE polymers despite having different structure and despite being intercalated into montmorillonites of different properties. For all these cases, the expansion of the clay by the PCE polymers is compressed in the same range than for 3 water layers absorbed.

Therefore, the same disagreement is found in between the homogeneity of the d-spacing values and the different behaviors noticed in the sorption isotherms, but for this example, the disagreement is extended to the differences in the properties of the montmorillonite clays, in addition to the differences in the structure of the PCE polymers.

For the case of the pastes produced with calcium montmorillonite (Ca-MNT) and the three PCE polymers, no expansion is observed thus no intercalation is assumed despite the sorbed amounts of PCE observed in Figure 1.35(c) are relevant and with comparable results than of magnesium montmorillonite (Mg-MNT). It happens for calcium montmorillonites with very low layer charge, which shows almost no expansion and very reduced cation exchange capacity [35].

1.6.3. Disagreements identified by theoretical simulations

Some disagreements identified by theoretical simulations are extracted from [69]. In this investigation, the experimental sorption isotherms of PCE polymers are compared against de theoretical sorption isotherms calculated from the sorption isotherms of the individual side chains (by sorption measurements of linear polyethylene glycols (PEG) of equivalent molecular weight than of the side chains) and from the sorption isotherms of the methacrylic backbone (by sorption measurements of a linear poly-methacrylate polymer).

Figure 1.38 (a,b) compares the experimental sorption results for two PCE polymers and for the corresponding linear PEG of equivalent molecular weight against the theoretical sorption isotherms for the PCE polymers calculated from the sorption behavior of the linear PEG, respectively. Figure 1.38 (c,d) shows the same comparison but against the theoretical PCE sorption isotherms calculated from the sorption behavior of a linear poly-methacrylate simulating the structure of the PCE backbone.

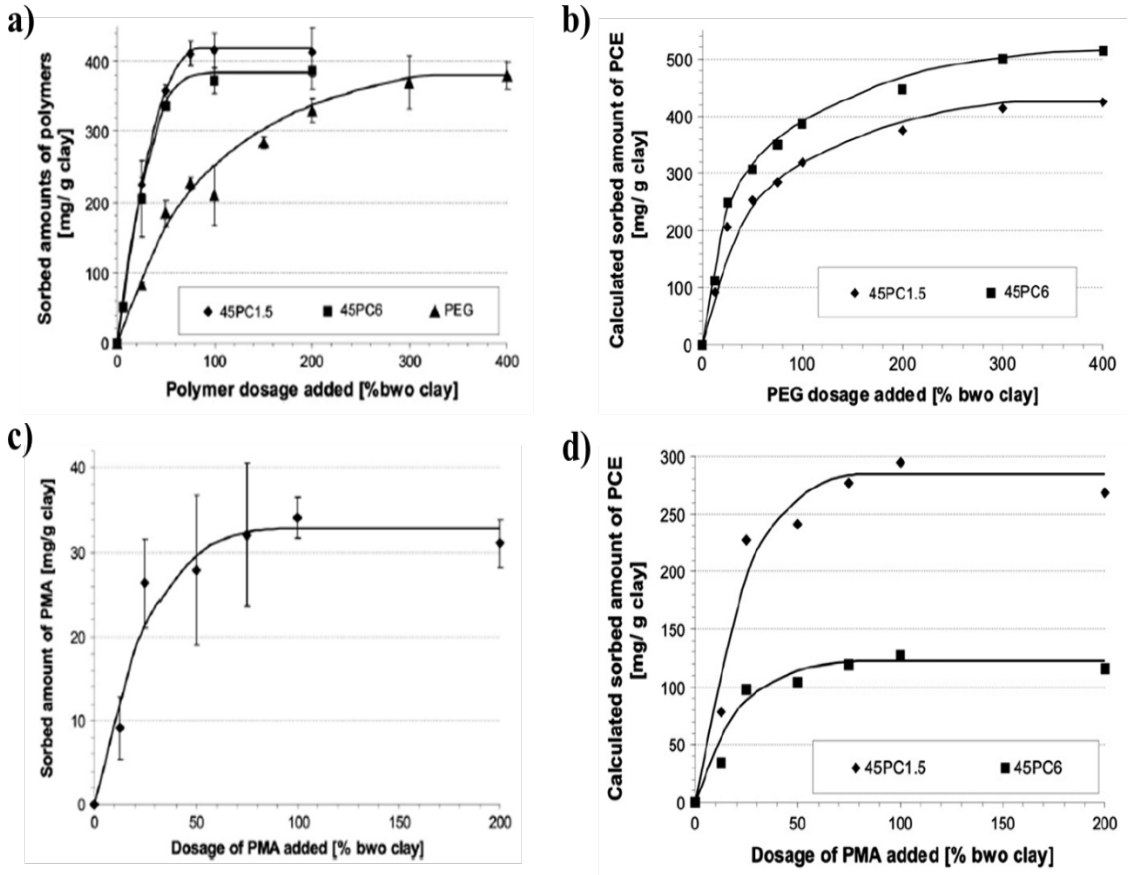

Figure 1.38. a) Experimental sorption isotherms for PCE polymers and for linear PEG of equivalent molecular weight; b) Calculated sorption isotherms for PCE polymers from the sorption behavior of linear PEG; c) Experimental sorption isotherms for linear poly-methacrylate; d) Calculated sorption isotherms for PCE polymers from the sorption behavior of linear poly-methacrylate (adapted from [69])

It can be observed relevant discrepancies between the experimental results and the theoretical calculations, for both the maximum sorbed amount and the progression of the sorption rate as the polymer dosage increases, by which the author concludes that there must be other factors participating in the intercalation mechanism, such as clay exfoliation.

All the examples reported confirms that the experimental results of fluidity loss, dosage efficiency of PCE polymers and of sorption behavior are not in agreement with the intercalation mechanism deducted from the XRPD measurements performed on dried clay pastes according to the traditional analytical method.

Since all these dealignments identified are evidently noticeable with the differences in the structure of PCE polymers but also with the differences in the properties of montmorillonite clays, it is feasible to consider that the d-spacing results obtained with the traditional method based on XRPD measurements performed on dried clay pastes are not representative of the real intercalation behavior experienced.

1.7. CURRENT AND FUTURE PERSPECTIVES OF AGGREGATES DEMAND

Aggregates represent the second raw material most consumed by man after water [87]. For 2019, the forecast for aggregates consumption is estimated by 52000 million tons [88], which is equivalent to 20000 million cubic meters of extraction. This current consumption represents a net increase of 7% respect to the consumption data of 2015, being close to an annual increase of +2% per year.

In Spain, the consumption of aggregates from natural extraction for construction uses stood at 110.5 million tons in 2017, equivalent to a consumption per capita of 2.3 kg/year per inhabitant. This represents an increase of +10.5% over the previous year. The forecast figures presented by ANEFA (National Association of Aggregates Manufacturers) indicate a similar increase for both 2018 and 2019, linked to the forecasts of the construction sector [87].

Figure 1.39(a,b) displays the total worldwide aggregate consumption for the period 2005-2020 (being forecast for 2019 and 2020). It can be observed that from 2005, the consumption of aggregates has been practically doubled, and although it is estimated a moderation in the demand for the period 2015-2020, it is expected that the consumption of aggregates will continue to grow according to the current construction practices and the forecast of demand from both developed countries and especially from the emerging economies of some Asian countries.

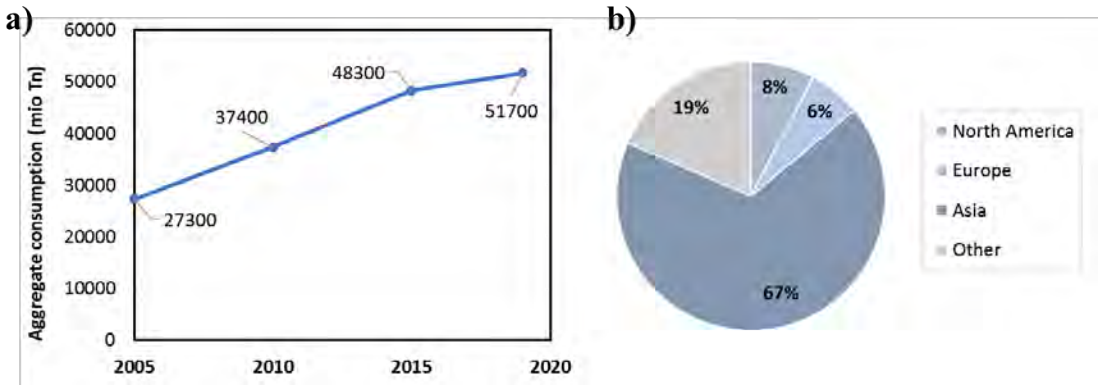

Figure 1.39. a) History and forecast of global worldwide consumption of aggregates; b) Distribution of consumption by regions (adapted from [88])

Natural aggregates are used as raw material in various sectors, as shown in Figure 1.40(a). And since construction sector is the largest consumer, Figure 1.40(b) shows the split of natural aggregates consumption by the main applications within construction activities.

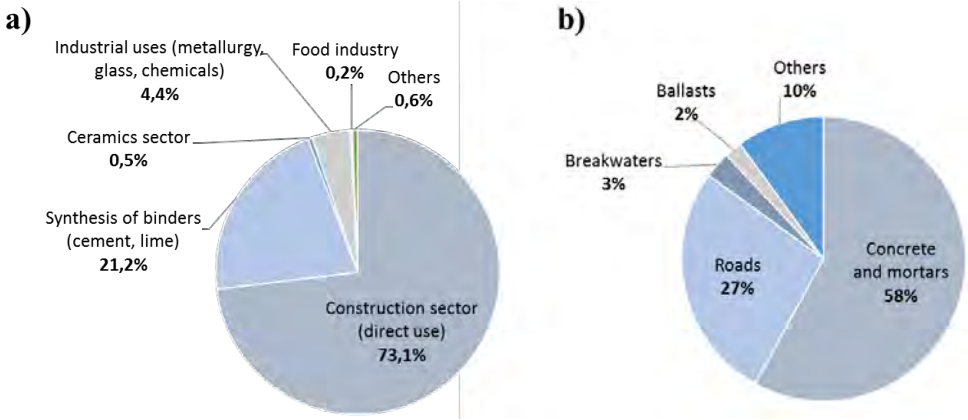

Figure 1.40. a) Distribution of the aggregates consumption by industry sectors; b) Consumption of aggregates in construction sector as per main uses [87]

Figure 1.40(a) denotes the relevance of the construction sector in the aggregate consumption statistic, which represents 73% of total consumption. To this 73%, the contribution of the cement and lime manufacturing industry, which represents 21% of the total, should be added, since the demand of these inorganic binders is directly linked to the construction activity.

In summary, accounting for direct and indirect contributions, the construction activity in global means 94% of the total consumption of natural aggregates. Regarding the use of aggregates for construction purposes, from Figure 1.40(b) it can be observed the relevant weight of concrete and mortar production, which represents 58% of total consumption of aggregates in construction sector.

1.7.1. Aggregates demand from construction sector

The figures presented in the previous Figure 1.40 reflecting the importance of the construction sector in the total consumption of aggregates are explained by the relevance of aggregates in the composition of the most common materials used in construction projects. In this respect, Figure 1.41(a) displays the weight percentage of aggregates in the composition of asphalt conglomerates, road fillings and concrete. It can be noted that for each of the three construction materials presented, aggregates mean more than 80% of their total composition.

Complementary, since reinforced concrete is the most used construction material in the world and therefore the main consumer of natural aggregates, Figure 1.41(b) shows the composition split for the typical raw materials used in concrete mixes, as per weight and as per volume, detailing the aggregate fractions as per sand and coarse aggregate.

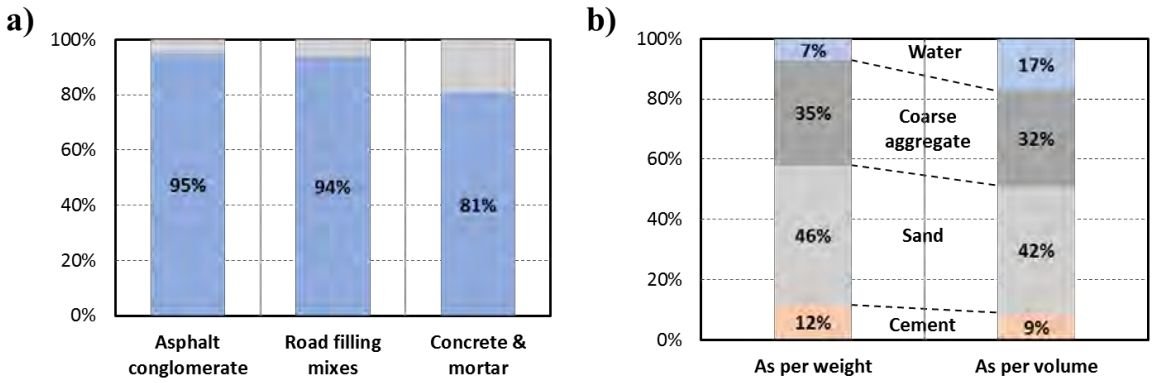

Figure 1.41. a) Percentage of aggregates in the composition of the most common building materials [85]; b) Share of concrete composition ingredients, by weight and volume [46]

From Figure 1.41(b) and Figure 1.41(b) it can be deduced that most of the aggregate demand in construction activities corresponds to the use of sands for concrete manufacturing. This fraction of aggregate, with particle size typically compressed between 0-6 mm, represents up to 40-50% of the composition of a C-25/30 concrete class, which is the most used concrete type in conventional constructions.

1.7.2. Outlook for sand extraction and consumption

The UNEP-United Nations Environment Programme launched an official report in March 2014 [89] advising on the huge current impact from sand extraction and alerting on the future outlook for this natural resource since sands are being extracted at a rate far greater than their renewal. Sands are mainly extracted in land quarries and riverbeds. However, a shift to marine

and coastal aggregates mining is occurring due to the decline of inland resources and the increasing demand.

The extraction of sands from both inland and marine reservoirs has a big impact on the environment. The pictures presented in Figure 1.42(a-d) reveal the most evident impact from the inland extraction of aggregates. It is the impact on the landscape derived from the huge land areas of extraction required to satisfy the current demands.

Figure 1.42. Impact on landscape caused by the inland extraction of sands; a) From quarries; b) From sedimentary reservoirs; c) From riverbeds

Apart from the visual impacts shown in Figure 1.42, there are far more impacts on the environment derived from the extraction of sands. Table 1.6 summarizes the main impacts reported by the UNEP in regards of the extraction of natural aggregates and sands.

Impacts on	Description of impacts
Biodiversity	Direct impacts on ecosystems
Land losses	Both inland and coastal through erosion
Hydrological	Change in water flows, flood regulation and marine currents
Water supply	Through lowering of the water table and pollution
Infrastructures	Damage to bridges, river embankments and coastal infrastructures
Climate	Directly through transport emissions, indirectly through cement production
Landscape	Coastal erosion, changes in deltaic structures, quarries, pollution of rivers
Extreme events	Decline of protection against extreme events (flood, drought, storm surge)

Table 1.6. Summary of the main consequences of extraction of aggregates and sands [89]

As consequence of the environmental impacts presented in Table 1.6 and attending to the increasing demand of sands, the UNEP report includes some recommendations to ensure the sustainable future use of sands, with especial focus on the demand of sands from the construction sector, and to protect the environment against the extraction activities. These recommendations are:

- Reduction of consumption of natural sands
- Use of artificial sands from recycled aggregates or demolished concrete
- Use of by-products as sand replacers
- Use of extraction waste from aggregate extraction as sand replacer
- Shift to other construction materials than concrete of earlier renewal such as wood
- Reduction of the negative consequences of extraction by regulations
- Tax on aggregates extraction to create incentives on alternatives
- Direct control and regulation on extraction activities and persecution of illegal extraction

The use of recycled aggregates and sands obtained from demolished concrete is considered as the longest-term sustainable alternative. However, the higher cost of recycled sands, the technical limitations due to its high absorption and the lack of incentives to promote their use makes that, at present, the share of use of recycled sands is practically insignificant in relation to the total consumption [90-94]. Moreover, most of the local concrete regulations restrict the use of recycles sands to very limited quantities or directly prohibit their use [37].

The use of by-products such as ashes from incineration of urban wastes has been already evaluated as a replacement for sands in concrete. But unfortunately, most of the technical properties of concrete are damaged, resulting in reduced durability and reduced mechanical properties [95].

The use of wastes from the extraction of aggregates, such as the solid waste produced in the washing of sands or the dust materials generated in quarries, is in the scope of this work. In these terms, in addition to the optimization of sand consumption, this measure will contribute in other side benefits such as reduction of water consumption, better use of natural resources and extended service life of the extraction sites. Therefore, one of the ways to achieve this goal is through the development of upgraded water-reducer admixtures to allow these residues to be used in concrete in a sustainable way and without penalizing their properties.

1.8. CONCLUSIONS

The future perspective to satisfy the increasing demand of sands for concrete production is not optimistic due to the huge environmental impacts associated to the aggregate's extraction activities and due to the finite availability of this natural resource. Therefore, measures with short to mid-term contribution seems to urge to guarantee the sustainable development of the structures built with reinforced concrete.

One of the improvement measures identified is based on the opportunity to use sands of lower quality without penalizing any of the properties of concrete and the durability of the structures, in such a way that the global environmental impact of concrete can be reduced. By this measure, the efficiency of the sand extraction process can be maximized in a cost-effective way by a more efficient use of the natural resources and by reducing, or even avoiding, the economic and environmental impact of the side operations for sand processing such as the sand washing.

In the same way than the technological development of PCE based superplasticizers/water-reducer admixtures for concrete has contributed to reduce the environmental impact of concrete by optimizing the use of cements, the same concept can be addressed to the sand management. However, this technology appears to be extremely sensitive to the quality of sands and, specifically, to the clay content, by worsening or even inhibiting their water reduction capacity and so their dosage efficiency.

Due to the complexity of the interaction process between PCE polymers and clays and, particularly, with swelling clays, a deep understanding of the interaction mechanism is needed to finally develop efficient, robust and cost-effective water-reducers with comparable performance than of the conventional PCE polymers and with improved clay tolerance.

Despite many progresses have been made in the understanding of the interaction process between PCE polymers and montmorillonite clays, some disagreements are noticed between some experimental evidences and the intercalation mechanism deducted from d-spacing measurements, thus suggesting that the current model proposed is not reflecting the real process by which PCE polymers are intercalated into montmorillonite clays.

REFERENCES

[1] P.C. Aïtchin, R.J. Flatt, Science and technology of concrete admixtures, ISBN 978-0-08-100693-1 (2016).

[2] P. Borralleras, Superplastificantes basados en la tecnología PAE de BASF, Cemento Hormigón 980 (2017), 32-35.

[3] E. Sakai, A. Ishida, A. Ohta, New trends in the development of chemical admixtures in Japan, Proceedings Journal of Advanced Concrete Technology 4 (2006) 211-223.

[4] F. Puertas, H. Santos, M. Palacios, S. Martínez-Ramírez, Polycarboxylate superplasticizers admixtures: effect on hydration, microstructure and rheological behaviour in cement pastes, Advances in Cement Research 17 (2005) 77-89.

[5] G. Gelardi, S. Mantellato, D. Marchon, M. Palacios, A.B. Eberhardt, R.J. Flatt, Chemistry of chemical admixtures - Science and technology of concrete admixtures, ISBN 978-0-08-100693-1 (2016).

[6] M.M. Alonso, R. Martínez-Gaitero, S. Gismera-Diez, F. Puertas, PCE and BNS admixture adsorption in sands with different composition and particle size distribution, Materiales de Construcción 67 (2017), 326.

[7] L. Lei, J. Plank, Synthesis and properties of a vinyl ether-based polycarboxylate superplasticizer for concrete possessing clay tolerance, Industrial & Engineering Chemistry Research 53 (2014) 1048-1055.

[8] J. Plank, C. Schroefl, M. Gruber, M. Lesti, R. Sieber, Effectiveness of polycarboxylate superplasticizers in ultra-high strength concrete: the importance of PCE compatibility with silica fume, Journal of Advanced Concrete Technology 7 (2009) 5-12.

[9] IECA, Declaración ambiental de producto – cemento CEM II, AENOR (2014), https://www.ieca.es/wp-content/uploads/2017/10/GlobalEPD_003_002_ESP.pdf.

[10] Aggregate Industries, EPD for concrete aggregates 000206 (2018), https://www.aggregate.com/sites/aiuk/files/atoms/files/bardon_hill_epd.pdf

[11] EFCA, Environmental product declaration for concrete admixtures, Institut Bauen und Umwelt e.V. (2015), http://www.efca.info/efca-publications/environmental/.

[12] D. Atarashi, Interaction between superplasticizers and clay minerals, Japan Cement Association (2005) 287-292.

[13] D. Atarashi, K. Yamada, A. Ito, M. Miyauchi, E. Sakai, Interaction between montmorillonite and chemical admixture, Journal of Advanced Concrete Technology 13 (2015) 325-331.

[14] L. Xoing, G. Zheng, Y. Bi, C. Fu, Effect of typical clay upon the dispersion performance of polycarboxylate superplasticizer, Proceedings International Conference on Materials, Environmental and Biological Engineering (2015) 226-229.

[15] L. Lei, J. Plank, A study on the impact of different clay minerals on the dispersing force of conventional and modified vinyl ether based polycarboxylate superplasticizers, Cement and Concrete Research 60 (2014) 1-10.

[16] V.A. Fernandes, P. Purnell, G.T. Still, T.H. Thomas, The effect of clay content in sands used for cementitious materials in developing countries, Cement and Cocnrete Research 37 (2007) 751-758.

[17] Z. Liu, Properties of low- and high-strength concrete incorporating clay-contaminated microfines, Arabian Journal for Science and Engineering (2005) 15-23.

[18] J.E. Ujhelvy, Water demand of concrete mixtures, Periodica Polytechnica 41 (1997) 199-225.

[19] N.S. Klein, A. Aguado, B.M. Toralles-Carbonari, L.V. Real, Prediction of the water absorption by aggregates over time: Modelling through the use of value function and experimental validation, Construction and Building Materials 69 (2014) 213-220.

[20] T.Y. Sai, M. Sambasivarao, Retempering of concrete, International Journal of Current Enginnering and Scientific Research 2 (2015) 63-69.

[21] T.J. Désire, M. Léopold, Impact of clay particles on concrete compressive strenght, expoedededInternational Research Journal on Engineering 1 (2013) 49-56.

[22] Various, Corrosion of steel in cocrete structures, Wooldhead Publishing, Ed. Amir Poursaee (2016).

[23] N. Güven, Smectites – Hydrous phyllosilicates, Reviews in Mineralogy 19 (1988) 497-560.

[24] P.H. Nadeau, The physical dimensions of fundamental clay particles, Clay Minerals 20 (1985) 499-514.

[25] M.J. Wilson, Sheet silicates: clay minerals, ISBN 978-1-86239-359-2, The Geological Society Publishing House, Second edition (2013).

[26] The Clay Minerals Society, http://www.clays.org/.

[27] I. Bibi, J. Icenhower, N. K. Naz, M. Shahid, S. Bashir, Clay Minerals: Structure, Chemistry, and Significance in Contaminated Environments and Geological CO2 Sequestration, Environmental Materials and Waste (2016) 543-567.

[28] A.T. Serstevens, P.G. Rouxhet, A.J. Herbillon, Alteration of mica surfaces by water and solutions, Clay Minerals 13 (1978) 401-410.

[29] Y.H. Shen, Estimation of surface area of montmorillonite by ethylene oxide chain adsorption, Chemosphere 48 (2002) 1075-1079.

[30] R.T. Martin, Report of the clay mineral society nomeclature committee: revised classification of clay minerals, Clays and Clay Minerals 39 (1991) 333-335.

[31] S. Hillier, Clay Mineralogy, Encyclopaedia of sediments and sedimentary rocks: Kluwer Academic Publishers (2003) 139-142

[32] T. Preocanin, A. Abdelmonem, G. Montavon, J. Luetzenkirchen, Charging behavior of clays and clay minerals in aqueous electrolyte solutions. Experimental methods for measuring the charge and interpreting the results – Clays, clay minerals and ceramic materials based on clay minerals, ISBN 978-953-51-2259-3 (2016).

[33] A.A. Jones, Charges on the surfaces of two chlorites, Clay Minerals 16 (1981) 347-359.

[34] M. Matusewicz, K. Pirkkalainen, J.P. Suuronen, A. Root, A. Muurinen, R. Serimaa, M. Olin, Microstrcutural investigation of calcium montmorillonite, Clay Minerals 48 (2013) 267-276.

[35] M.J. Wilson, L. Wilson, I. Patey, The influence of individual clay minerals on formation damage of reservoir sandstones: acritical review with some new insigthts, Clay Minerals 49 (2014) 147-164.

[36] P. Borralleras, Arenas con arcillas y sus problemáticas en la producción de hormigón. Interferencia con los aditivos superplastificanes basados en PCE, Proceedings of the V Congreso Nacional de Áridos - Spain (2018), Area A, 27-53.

[37] Various, EHE-08: Instrucción de Hormigón Estructural, Ministerio de Fomento. Gobierno de España (2008).

[38] Various, EN 933-9:2009+A1 – Tests for geometrical properties of aggregates – Part9: Assesment of fines – Methylene blue test, CEN-European Committee for Standarization (2013).

[39] J.L. Ramírez, J.M. Barcena, J.I. Urreta, Proposal for limitation and control of fines in calcareous sands based on upon their influence in some concrete properties, Materials and Structures 23 (1990) 277-288.

[40] M.A. Hossain, M.M. Ali, T.S.A. Islam, Comparative adsorption of methylene blue on different low cost adsorbents by continuous column process, International Letters of Chemistry, Physics and Astronomy 77 (2018) 26-34.

[41] B. Li, M. Zhou, J. Wang, Effect of the Methylene Blue of manufactured sand on performances of concrete, Journal of Advanced Concrete Technology 9 (2011) 127-132.

[42] L. Courard, F. Michel, J. Pierard, Influence of clay in limestone fillers for self-compacting cement based composites, Construction and Building Materials 25 (2011) 1356-1361.

[43] G. Xing, W. Wang, G. Fang, Cement dispersion performance of superplasticizers in the presence of clay and interaction between superplasticizers and clay, Advances in Cement Research 29 (2017) 194-205.

[44] A.I.G. Yool, T.P. Lees, A. Fried, Improvements of the methylene blue dye test for harmful clay in aggregates for concrete and mortar, Cement and Concrete Research, 28 (1998) 1417-1428.

[45] Produc Specs – Non-mobile washing plant for natural, rounded aggregates (41 Tn/h), Triman Minerals website (2018), http://www.triman.es/instalaciones/fabricacion-aridos/instalacion-fija-canto-rodado-lavado-150tnh-fcrl-150-a/.

[46] M.F. Cánovas, Hormigón, Ed. Garceta, ISBN 9788415452508 (2013).

[47] C. Birnel, Is delamination really a mystery?, Concrete International 20 (1998) 29-34.

[48] Various, Guide to formed concrete surfaces 347.5 R-13, Technical Committee 347, ACI – American Concrete Institute (2014).

[49] N.M. Alderete, Y.A. Villagrán Zaccardi, G.S. Coelho Dos Santos, Particle size distribution and specific surface area of SCM´s compared through experimental techniques, Proceedings of the International RILEM Conference on Materials, Systems and Structures in Civil Engineering, Denmark (2016) 61-71.

[50] E.C. Arvaniti, M.C.G. Juenger, S.A. Bernal, J. Duchesne, L. Courard, S. Leroy, J.L. Provis, A. Klemm, N. de Belie, Determination of particle size, surface area and shape of supplementary cementitious materials by different techniques, Materials and Structures (2015) 3687-3701.

[51] A. Kahn, Studies on the size and shape of clay particles in aqueous suspension, Clays and Clay Minerals 6 (1959) 220-236.

[52] D.P. Veghte, M.A. Freedman, Facile method for determining the aspect ratios of mineral dust aerosol by electron microscopy, Aerosol Science and Technology 48 (2014) 715-724.

[53] C. Weber, M. Heuser, H. Stanjek, A collection of aspect ratios of common clay minerals determined from conductometric titrations, Clay Minerals 49 (2014) 495-498.

[54] F. Macht, K. Eusterhues, G.J. Pronk, K.U. Totsche, Specific surface area of clay minerals: comparison between force microscopy measurements and bulk-N2 gas (BET) and bulk-liquid (EGME) absorption methods, Applied Clay Science 53 (2011) 20-26.

[55] X. Liu, J. Guan, G. Lai, Y. Zheng, Z. Wang, S. Cui, M. Lan, H. Li, Novel design of polycarboxylate superplasticizers for improving resistance in clay-contaminated concrete, Journal of Industry and Engineering Chemistry (2014) 213-220.

[56] I. Barshad, Absorptive and swelling properties of clay-water system, Clays and Clay Technology 169 (1950) 70-77.

[57] W.A. White, E. Pichler, Water-sorption characteristics of clay minerals, Division of the Illinois state geological survey, Circular 266 (1959).

[58] A. Maes, M.S. Stul, A. Cremers, Layer charge-cation exchange capacity relationships in montmorillonite, Clays and Clay Minerals 27 (1979) 387-392.

[59] A. Seppala, E. Puhakka, M Olin, Effect of layer charge on the crystalline swelling of Na+, K+ and Ca2+ montmorillonites: DFT and molecular dynamics studies, Clay Minerals 51 (2016) 197-211.

[60] L. Ammann, Cation exchange and adsorption of clays and clay minerals, Doctoral dissertation, Christian-Albrechts University of Kiel (2003).

[61] E. Tombácz, M. Szekeres, Colloidal behavior of aqueous montmorillonite suspensions: the specific role of pH in the presence of indifferent electrolytes, Applied Clay Science 27 (2004) 75-94.

[62] M.A. González-Ortega, S.H.P. Cavalaro, A. Aguado, Influence of barite aggregate friability on mixing process and mechanical properties of concrete, Construction and Building Materials 74 (2015) 169-175.

[63] R. F. Geise, The electrostatic interlayer forces of layer structure minerals, Clay and Clay Minerals 26 (1978) 51-57.

[64] H. Li, Y. Zhao, S. Song, Y. Hu, Y. Nahmad, Delamination of Na-montmorillonite particles in aqueous solutions and isopropanol under shear forces, Journal of Dispersion Science and Technology 38 (2017) 1117-1123

[65] R. Tettenhorst, H. E. Roberson, X-Ray diffraction aspects of montmorillonite, American Mineralogist 58 (1973) 73-80.

[66] Moratti, Nascimben, Rocchegiani, Borghettho, Clay contamination: how to deal with problematic sands, 2nd BASF Construction Chemicals Connectivity Symposium, Germany (2017) Poster session.

[67] R. Ait-Akbour, P. Boustingorry, F. Leroux, F. Leising, C. Taviot-Guého, Adsorption of polycarboxylate poly(ehtylene glycol) (PCP) esters on montmorillonite (MNT): Effect of exchangeable cations (Na+, Mg2+ and Ca2+) and PCP molecular structure, Journal of Colloid and Interface Science 437 (2015) 227-234.

[68] H. Tan, B. Gu, B. Ma, X. Li, C. Lin, Mechanism of intercalation of polycarboxylate superplasticizer into montmorillonite, Applied Clay Science 129 (2016) 40-46.

[69] S. Ng, J. Plank, Interaction mechanisms between Na-montmorillonite clay and MPEG-based polycarboxylate superplasticizers, Cement and Concrete Research 42 (2012) 847-854.

[70] L. Lei, J. Plank, A concept for a polycarboxylate superplasticizer possessing enhanced clay tolerance, Cement and Concrete Research 42 (2012) 1299-1306.

[71] R.J. Flatt, I. Schober, E. Raphael, C. Plassard, E. Lesniewska, Conformation of adsorbed com polymers dispersants, Langmiur 25 (2009) 845-855.

[72] G. Skripkiunas, M. Dauksys, A. Stuopys, R. Levinskas, The influence of cement particles shape and concentration on the rheological properties of cement slurry, Materials Science 11 (2005) 150-158.

[73] I. Mehdipour, K.H. Khayat, Effect of the particle-size distribution and specific surface area of different binder systems on packing density and flow characteristics of cement paste, Cement and Concrete Composites 78 (2017) 120-131.

[74] D. Senich, T. Demirel, R.L. Handy, X-Ray diffraction and adsorption isotherm studies of the calcium montmorillonite-H2O system, Highway Research Record 209, 46th Annual meeting of Physico-Chemical Phenomena in Soils (1956) 23-54.

[75] P.F. Low, J.L. White, Hydrogen bonding and polywater in clay-water systems, Clays and Clay Minerals 18 (1970) 63-66.

[76] M. Szczerba, Z. Klapyta, A. Kalinichez, Ethylene glycol intercalation in smectites. Molecular dynamics simulation studies, Applied Clay Science 91 (2014) 87-97.

[77] A. Jeknavorian, E. Koehler, Use of chemical admixtures to modify rheological behavious of cementitious systems containing manufactured aggregates, Proceedings of the International Concrete Sustainability Conference, Qatar (2011).

[78] H. Tan, F. Zou, B. Ma, Y. Guo, Effect of competitive adsoprtion between sodium gluconate and polybarboxylate superplasticizer on rheology of cement paste, Construction and Building Materials 144 (2017) 338-346.

[79] R. Qianping, X. Wang, X. Shu, J. Liu, Effects of sequence structure of polycarboxylate superplasticizers on the dispersion behavior of cement paste, Journal of Dispersion Science and Technology 37 (2016) 431-441.

[80] G. Chen, J. Lei, Y. Du, X. Du, X. Chen, A poycarboxylate as a superplasticizer for montmorillonite clay in cement: adsoprtion and tolerance studies, Arabian Jorunal of Chemistry – article in press (2017) 1-8.

[81] G. Xing, W. Wang, J. Xu, Grafting tertiary amine groups into the molecular structures of polycarboxylate superplasticizers lowers their clay sensitivity, RSC Advances 6 (2016) 106921-106927.

[82] C. Sun, H. Zhou, X. Li, S. Wang, J. Xing, The clay-tolerance of amide-modified polycarboxylate superplasticizers and its performance with clay-bearing aggregates, MEBE - International Conference on Materials, Environment and Biological Engineering (2015) 237-241.

[83] Y. Li, L. Zeng, Y. Zhou, T. Wang, Y. Zang, Preparation and characterization of montmorillonite intercalation compounds with quaternary ammonium surfactant: adsoprtion effect of zaeralenone, Journal of Nanomaterials (2014) 1-7.

[84] E.B. Kinter, S. Diamond, Characterization of montmorillonite saturated with short-chain amine cations: interlayer surface coverage by the amine cations, Proceedings of the 10th National Conference on Clays and Clay Minerals USA (1961) 174-190.

[85] H. Tan, Xin Li, M. Liu, B. Ma, B. Gu, X. Li, Tolerance of cement for clay minerals: effect of side-chain density in polyethylene oxide (PEO) superplasticizers additives, Clay and Clay Minerals 64-6 (2016) 732-742.

[86] H. Tan, B. Gu, Y. Guo, B. Ma, J. Huang, J. Ren, F. Zou, Improvement in compatibility of polycarboxylate superplasticizers with poor-quality aggregate conatining montmorillonite by incorporating polymeric ferric sulfate, Construction and Building Materials 162 (2018) 566-575.

[87] C. Luades Frades, El sector de los áridos español en 2017 y perspectivas 2018-2020, Proceedings of the V Congreso Nacional de Áridos - España (2018), Area E, 49-70.

[88] Various, World Construction Aggregates - Industry market research: Demand and sales forecast, market share, market size, market leaders. The Freedonia Group Inc. (2016).

[89] Various, Sand, rarer than one thinks, UNEP Global Environmental Alert Service (GEAS) report (2014).

[90] M. Sanchez de Juan, P. Alaejos, Study on the influence of attached mortar content on the properties of recycled concrete aggregate, Construction and Building Materials 23 (2009) 872-877.

[91] E. Fernández-Ledesma, J.R. Jiménez, J. Ayuso, V. Corinaldesi, F.J. Iglesias-Godino, A proposal for the maximum use of recycled concrete sand in masonry mortar design, Materiales de Construcción 66 (2016)

[92] C.S. Poon, Z.H. Shui, L. Lam, H. Fok, S.C. Kou, Influence of moisture states of natural and recycled aggregates on the slump and compressive strength of concrete, Cement and Concrete Research 34 (2004) 31–36.

[93] W.Y Tam, X.F. Gao, C.M. Tam, Microstructural analysis of recycled aggregateconcrete produced from two-stage mixing approach, Cement and Concrete Research 35 (2005), 1195– 1203.

[94] W.Y Tam, X.F. Gao, C.M. Tam, Comparing performance of modified two-stage mixing approach for producing recycled aggregate concrete, Magazine of Concrete Research 58 (2006), 477–484.

[95] J. Pera, J. Ambroise, L. Coutaz, M. Chababbet, Use of incinerator bottom ash in concrete, Cement and Concrete Research 27 (1997), 1–5.

Chapter 2
OBJECTIVES, METHODOLOGY, STRUCTURE AND PUBLICATIONS

This chapter outlines the general and specific objectives of this thesis, formulated from the discussion presented in Chapter 1, as well as the main tasks of the methodology followed to accomplish them. Additionally, Chapter 2 includes the structure of the document and the list of publications derived from this work.

Contents

2.1. GENERAL OBJECTIVE

The main objective of this work is to provide new insights of the intercalation mechanism of PCE side chains into the interlaminar space of montmorillonite clays because it is the process by which the dispersing performance of PCE polymers is inhibited when sands for concrete are contaminated with montmorillonite clays.

The contributions from this investigation can be used to complement, validate or question the current proposed model for the intercalation mechanism based on the single intercalation of side chains (monolayer model). This model of intercalation mechanism is deducted from the experimental results of d-spacing obtained by performing XRPD measurements on dried clay pastes.

In this way, the objective of the thesis is not to develop water-reducers polymers with improved tolerance to clays. During the last years, all the attempts to develop efficient, robust, cost-effective and environmentally friendly solutions have not fully succeeded due to the complexity of the interaction mechanism, the large number of variables involved and the for the lack of complete understanding of the process. Hence, it is suggested that it is not possible to achieve this goal without a deeper understanding of the interaction mechanism.

2.2. AREAS OF CONTRIBUTION AND SPECIFIC OBJECTIVES

Due to the abstractive of the *general objective*, the accomplishment of the general objective is stablished on the basis of the three areas of contribution recognized by which this thesis is structured.

These areas of contribution define the *specific objectives*. Therefore, the general objective is considered as reached by the accomplishment of the three specific objectives presented in Table 2.1, where the expected outcome for the accomplishment of each specific objective is described.

Areas of contribution Specific objectives	Expected outcome for the accomplishment of the specific objectives
1- To improve the analytical method for measuring d-spacing enlargement of swelling clays by PCE side-chain intercalation	a) To identify the potential limitations of the current analytical method and to understand the disagreements between the d-spacing results obtained and the fluidity and sorption experimental evidences with pastes b) To propose an improved testing methodology to reveal the real intercalation behavior not in contradiction with fluidity and sorption results
2- To identify the influence of the structure of PCE polymers in the affinity for intercalation and to propose absorption conformations	c) To understand the clay affinity of PCE polymers from the differences in the structure of the polymers in coherence with the experimental results of fluidity loss and sorption behavior recorded in cement pastes d) To propose models of arrangement for the intercalation process, named as absorption conformations
3- Identification of the influence of the properties of montmorillonite clays in the affinity for intercalation	e) To understand the role of the main properties of montmorillonite clays in the intercalation behavior in agreement with the experimental results of fluidity loss and sorption f) To clarify the relative importance of clay properties and PCE polymer structure controlling the interaction process and conditioning the dispersing inhibition effect

Table 2.1. List of specific objectives and expected outcome for their accomplishment

2.3. OVERVIEW OF THE RESEARCH METHODOLOGY

The research methodology guides the course of activities to be undertaken during the research. Therefore, the methodology planned to accomplish each of the individual specific objectives is conditioned to the outcome of the experimental campaign of the previous objectives.

The basic structure of the methodology followed is summarized in Figure 2.1, structured on the basis of the expected outcome at the conclusion of the experimental programs planned for each step.

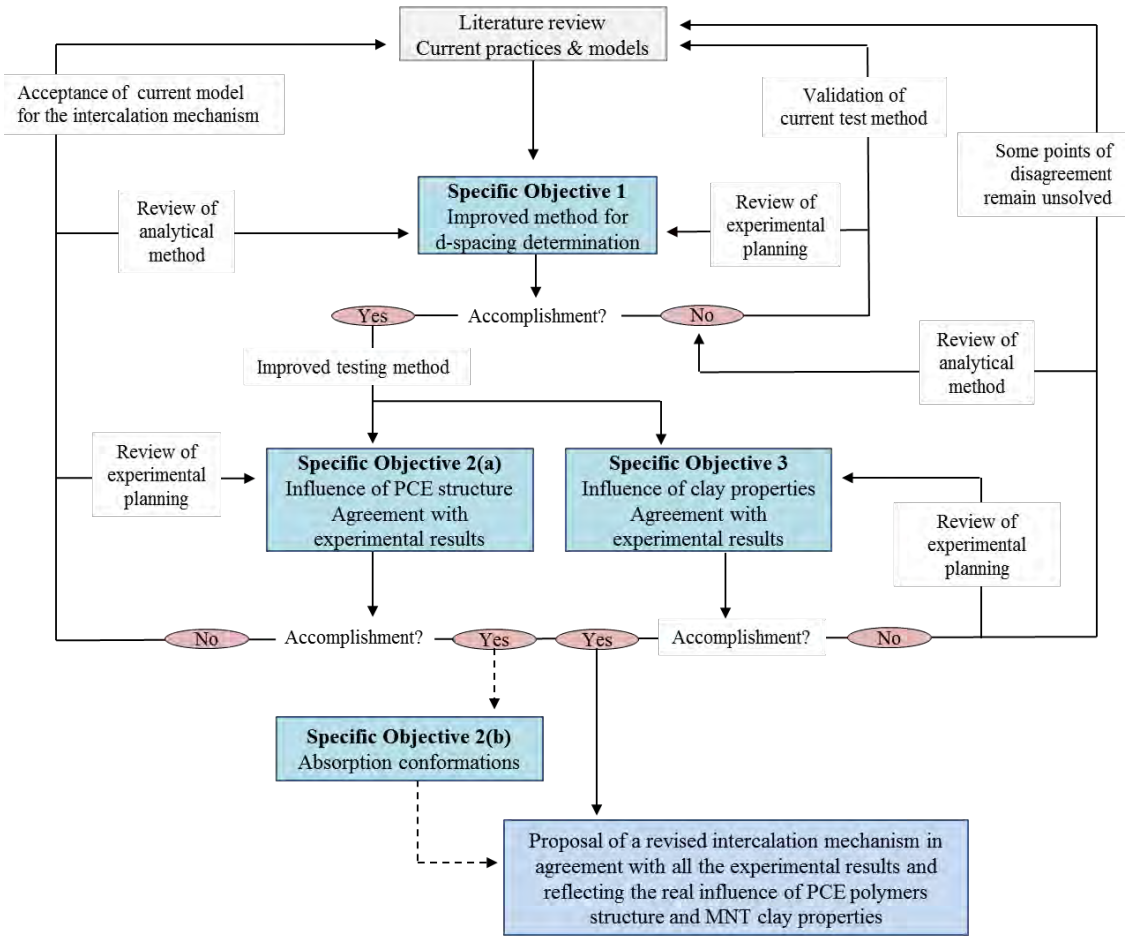

Figure 2.1. Structure and path-forward of the research methodology

The dissertation starts with a literature review to contextualize the current state of the art in the understanding of the interaction between clays and superplasticizers, by which the main points for discussion are identified. This review as well as the extracted conclusions are presented in the *General Introduction* constituting Chapter 1.

The specific objectives are covered by the published papers, including the experimental procedure and tests executed and the conclusions presented from the interpretation of the results obtained. Most of the analytical tests used are performed on cement and clay pastes, by properly adjusting the involved variables according to the specific objectives to be achieved. Finally, the new insights of the intercalation mechanism deducted from the jointly interpretation of the specific objectives are proposed in Chapter 5, which presents the main conclusions of the thesis.

2.3.1. Specific objective 1

The first phase of the experimental program is intended to accomplish the *specific objective 1*, which is focused on the test method currently used for the determination of the changes in d-spacing produced by the intercalation of PCE side chains into montmorillonites (referred as traditional methed). Based on the disagreements between d-spacing results and experimental evidences, the first specific objective assumes the hypothesis that the current test method performed on dried clay pastes does not reflect the real intercalation behavior. Therefore, the specific objective 1 is aimed to propose and improved testing methodology for the d-spacing measurements. The main tasks planned to assess it are the following:

- **Task 1:** To test the influence of the separation method and of the sample drying used in the current, traditional testing methodology for d-spacing determination
- **Task 2:** To evaluate the feasibility of performing XRPD measurements directly on fresh, unaltered clay pastes (named as *in-situ* XRPD) by using synchrotron light for optimal resulution
- **Task 3:** To investigate the influence of different PCE dosage on the results of d-spacing enlargement by using the new-modified analytical method based on *in-situ* XRPD measurements.
- **Task 4:** To prove the reproducibility and the repeatability of the new-improved testing methodology for d-spacing determination in a Cu Kα standard lab-diffractometer.

If the hypothesis is validated and a new-improved testing method for d-spacing measurement can be proposed, the specific objective 1 is accomplished and the next specific objectives 2 and 3 can be approached. Conversely, if the specific objective 1 cannot be accomplished, a review of the experimental planning is required.

If all the new proposals of alternative analytical methods report the same d-spacing results than the current traditional methodology, there are no evidences to question the proposed mechanism based on the intercalation of monolayers of side chains. Therefore, there is no opportunity to clarify the disagreements between the expansion of montmorillonites and the experimental evidences from fluidity and sorption tests. In this case, the general objective cannot be reached in any case.

2.3.2. Specific objective 2

Currently, according to the d-spacing results obtained with the traditional analytical method, the differences in the structure of PCE polymers do not produce any significant variations in the expansion profile of MNT clays by the intercalation of PCE side chains. Conversely, the results of fluidity loss and sorption rates in pastes report clear differences in performance between PCE polymers of different structure, hence, making it impossible to correlate the d-spacing changes with the fluidity and sorption behavior. In consequence, the

specific objective 2 is based on the hypothesis that the structure of PCE polymers have a direct and relevant influence on the intercalation process but it cannot be observed with the traditional analytical method for d-spacing measurements.

The specific objective 2 is divided in two sub-objectives, 2(a) and 2(b). The first one -2(a)- is focused on the influence of the structure of PCE polymers in the expansion profile of montmorillonite clays promoted by the intercalation of side chains. The second sub-objective -2(b)- is aimed to interpret the spatial arrangements taken by the PCE polymers interacting with clays and promoting the intercalation phenomenon. These arrangements are named as *absorption conformations* of PCE polymers. Since both sub-objectives 2(a) and 2(b) are focused on the role of the structure of PCE polymers, the experimental program for the specific sub-objective 2(b) is planned considering the outcome from the previous specific sub-objective 2(a). In these terms, the specific objective 2 is structured from the following tasks:

-Specific objective 2(a):

- **Task 1:** To characterize the polymeric structures of different PCE samples as well as their dispersing ability and their base performances
- **Task 2:** To perform measurements of d-spacing with the new-improved analytical method by using PCE polymers of different structure and at different dosages
- **Task 3:** To analysis the concordance between the experimental results of d-spacing obtained by *in-situ* XRPD measurements and the results of fluidity and sorption obtained in pastes
- **Task 4:** To identify the most important key structural parameters of PCE polymers controlling the interaction process and the affinity for intercalation

-Specific objective 2(b):

- **Task 1:** To deduct the intercalation arrangements taken by PCE polymers during the intercalation into montmorillonites (absorption conformations) from the interpretation of known absorption conformations taken by some non-ionic polymers and their fluidity and sorption behavior observed in cement and clay pastes
- **Task 2:** To identify key-parameters of PCE conditioning the absorption conformation taken

Despite accomplishing the specific objective 1, if the proposed new-improved testing method for d-spacing measurement does not allow to clarify the role of the structural differences of PCE polymers in the expansion behavior of the clay and, complementary, if the d-spacing results obtained remain in disagreement with the experimental results of fluidity and sorption, the specific objective 2 cannot be accomplished. In this situation, the second phase of the experimental campaign must by re-planned and/or the alternative test method proposed in the previous phase requires further improvements. Nevertheless, if no new insights are found, the general objective cannot be reached.

2.3.3. Specific objective 3

The *specific objective 3* is a replica of the specific objective 2(a) but from the clay properties perspective. Therefore, the experimental campaign of this phase is planned independently of the outcome of the previous specific objective 2 and it is exclusively conditioned by the conclusions of the specific objective 1. The development of the specific objective 3 is structured from the following main tasks:

- **Task 1:** To characterize the main properties of different montmorillonite clay samples and their capacity to inhibit the dispersing performances of PCE polymers
- **Task 2:** To perform measurements of d-spacing with the new-improved analytical method by using montmorillonite clays of different properties
- **Task 3:** To analysis the concordance between the experimental results of d-spacing obtained by *in-situ* XRPD measurements and the results of fluidity and sorption obtained in pastes
- **Task 4:** To identify the key-properties of montmorillonite clays controlling the interaction process and promoting the interference of the dispersing capacity of PCE polymers

If the experimental results supporting the specific sub-objective 3 do not reveal any clear influence of the clay properties in the intercalation behavior, the experimental campaign needs to be reviewed because there is an inconsistency with the achievements from the accomplished specific sub-objective 2 and especially with the empirical results of fluidity loss and sorption rates observed in cement pastes containing just small amounts of montmorillonite clays of different properties. In this case, the general objective is only partially achieved and some of the disagreements between the intercalation mechanism and the experimental evidences will remain unsolved.

Since the accomplishment of the specific objectives 2 and 3 allows to clarify how the the structure of PCE polymers and the properties of montmorillonite clays condition the intercalation process, at this point it is feasible to propose a new-revised model for the intercalation mechanism. It can be deducted from the global and jointly interpretation of the conclusions extracted in each of the individual specific objectives. Whatever the case, to consider that the general objective has been fully accomplished it is mandatory that the new proposal for the intercalation mechanism keeps fully alignment with all the other experimental results.

2.4. STRUCTURE OF THE DOCUMENT

Since this is an article-based thesis consisting of a set of papers as part of the research program, this document aims to present and discuss the contributions derived from the

compilation of all the papers written. The content of this document is divided in 5 chapters, and the content of each one is summarized below:

- **Chapter 1** displays the technical barriers related to the quality of sands for concrete production, with specific focus on the presence of clays and its implications in the quality of concrete structures and introduces the problem of the extraction and processing of sands used for concrete production and the consequences for the sustainable development of aggregates and concrete industry. This chapter also collects the conclusions from the previous studies addressed to understand the interference produced by clays on the fluidity behavior of cementitious systems, by which it is not possible to fully exploit all the advantages of the new-generation superplasticizers based on PCE polymers. From the currently proposed model for the interaction mechanism deducted from the d-spacing results, the disagreements identified between this current model and other experimental evidences are emphasized.
- **Chapter 2** describes the general and specific objectives of the thesis. Additionally, a summarized overview of the methodology is presented, as well as the structure of the document. Finally, the list of publications derived is displayed, indicating the areas of contribution of each paper according to the specific objectives described.
- **Chapter 3** collects the full version of the published publications, including journal papers and conference papers.
- **Chapter 4** includes the full version of the submitted papers pending for publication or under revision and the conference abstracts accepted for future presentation at congress.
- **Chapter 5** presents the general discussion and the main contributions resulting from the research done. The discussion is structured by following the specific objectives defined in this chapter to finally present a new-revised model for the intercalation mechanism by a jointly interpretation. Moreover, based on the limitations of the experimental program, this chapter proposes relevant areas and topics for further research in order to complement the achievements and to enlarge the understanding of the interaction process between PCE based water-reducers and montmorillonite clays.

A separate list of references is included for Chapter 1 and for Chapter 5. Each paper included in Chapter 3 and Chapter 4 follows its own numbering of sections, figures, equations and references.

2.5. LIST OF PUBLICATIONS

The publications derived from this thesis are listed below, grouped into published and submitted papers and including journal papers and conference papers. The journal papers published are corresponded to each of the specific objectives defined, being properly indicated, while the conference papers are not explicitly focused on any specific objective.

Published Journal papers

JOURNAL PAPER I

"Influence of experimental procedure on d-spacing measurement by XRD of montmorillonite clay pastes containing PCE-based superplasticizers", P. Borralleras, I. Segura, M.A. García Aranda, A. Aguado, Cement and Concrete Research 116 (February 2019) 266-272.
https://doi.org/10.1016/j.cemconres.2018.11.015
Impact factor: 5.6; Q1

This paper covers the specific objective 1.

JOURNAL PAPER II

"Influence of the polymer structure of polycarboxylate-based superplasticizers on the intercalation behaviour in montmorillonite clays", P. Borralleras, I. Segura, M.A. García Aranda, A. Aguado, Construction and Building Materials 220 (June 2019) 285-296.
https://doi.org/10.1016/j.conbuildmat.2019.06.014
Impact factor: 4.1; Q1

This paper covers the specific objective 2(a).

JOURNAL PAPER III

"Absorption conformations in the intercalation process of polycarboxylate ether-based superplasticizers", P. Borralleras, I. Segura, M.A. García Aranda, A. Aguado, Construction and Building Materials (August 2019) 116657.
https://doi.org/10.1016/j.conbuildmat.2019.08.038
Impact factor: 4.1; Q1

This paper covers the specific objective 2(b).

Published Conference papers

CONFERENCE PAPER I

"Modelización del mecanismo de pérdida de consistencia provocado por arcillas en pastas de cemento con superplastificantes base policarboxilato", P. Borralleras, I. Segura, A. Aguado, Proceeding of the HAC2018 – Congreso Iberiamericano de Hormigón Autocompactante y Hormigones Especiales, Valencia, Spain (March 2018) 279-289. ISBN: 978-84-9048-591-0 doi:10.4995/HAC2018.2018.5634

Other published papers

OTHER PUBLICATIONS I

"Luz sincrotrón para iluminar el desarrollo de aditivos superplastificantes de altas prestaciones insensibles a las arcillas" P. Borralleras, I. Segura, M.A. García Aranda, A. Aguado, Cemento Hormigón 993 (July 2019) 52-55.
ISSN: 0008-8919

Non-technical paper to divulgate the achievements of the analytical method to measure clay d-spacing by PCE intercalation and its implications on the interpretation of the interaction mechanism, addressed to the concrete and aggregate producers' community.

Submitted Journal papers

JOURNAL PAPER IV

"Influence of the properties of montmorillonite clays in the performance of PCE-based superplasticizers", P. Borralleras, I. Segura, M.A. García Aranda, A. Aguado
Submitted to Building and Construction Materials (under second revision)

Journal Paper IV covers the specific objective 3.

Accepted Conference papers

11th ACI/RILEM International Conference on Cementitous Materials and Alternative Binders for Sustainable Concrete, to be held in Toulouse, France, 29th June – 1st July 2020:

- "Improved analytical methodology for measuring interlayer d-spacing of montmorillonite clays expanded by intercalation of PCE polymers", P. Borralleras, I. Segura, A. Aguado.
- "Influence of the structure of PCE polymers and of the properties of montmorillonite clays in the intercalation mechanism producing fluidity loss of cementitious systems", P. Borralleras, I. Segura, A. Aguado.
- "Interpretation of the mechanism and key-parameters controlling the interaction between PCE based-superplasticizers and montmorillonite clays", P. Borralleras, I. Segura, A. Aguado.

Chapter 3
PUBLICATIONS: PUBLISHED PAPERS

This chapter reproduces the published journal and conference papers derived from this thesis. Each paper follows its own numbering of sections, figures, equations and references.

Contents

3.1. JOURNAL PAPER I

INFLUENCE OF EXPERIMENTAL PROCEDURE ON D-SPACING MEASUREMENT BY XRD OF MONTMORILLONITE CLAY PASTES CONTAINING PCE-BASED SUPERPLASTICIZERS

Published in Cement and Concrete Research 116 (February 2019) 266-272.

Pere Borralleras[a], Ignacio Segura[b, c,*], Miguel A. G. Aranda[d] and Antonio Aguado[b]

[a] BASF Construction Chemicals Iberia, Ctra del Mig 219, E-08907 Hospitalet de Llobregat, Barcelona, Spain

[b] Department of Environmental and Civil Engineering, Universitat Politècnica de Catalunya-Barcelona Tech, Jordi Girona 1-3, C1, E-08034 Barcelona, Spain

[c] Smart Engineering Ltd, Jordi Girona 1-3, ParcUPC–K2M, E-08034 Barcelona, Spain

[d] ALBA Synchrotron, Carrer de la Llum 2-26, E-08290, Cerdanyola del Vallès, Barcelona, Spain

* Corresponding author: Ignacio Segura, Department of Environmental and Civil Engineering, Universitat Politècnica de Catalunya-Barcelona Tech, Jordi Girona 1-3, C1, E-08034 Barcelona, Spain. Email address: ignacio.segura@upc.edu Tel: +34 93 4054684

Abstract

This study investigates the influence of the experimental procedure on determining the d-space enlargement of montmorillonite clay (MNT) produced by the absorption of polycarboxylate (PCE) based superplasticizers. d-spacing alterations registered by in situ X-ray Diffraction (XRD) analysis on fresh clay pastes have been compared against the results obtained when clay pastes are previously centrifuged and dried (reference methodology reported in bibliography). Data from experiments show relevant differences between the two methodologies. While MNT clay d-spacing present limited expansion when recorded on samples previously separated and dried, direct XRD for fresh clay pastes shows much larger expansion of inter-laminar space. Clay expansion evolves with the increase of PCE dosage up to 3 times larger than typical data recorded when samples previously dried. The results shown here indicates that information collected following the typical experimental procedure based on sample drying could not be representative of MNT clay interference on dispersion mechanism of PCE superplasticizers.

Keywords: XRD, Polycarboxylate, Clay, d-spacing, Portland cement, Intercalation

1. INTRODUCTION

The capacity of montmorillonite clays (MNT) to inhibit the dispersing capacity of PCE-based superplasticizers for concrete is well known [1]. The interference mechanism is based on the preferential intercalation of polyethylene oxide/polyethylene glycol (PEO/PEG) side-chains of the PCE polymer in the MNT interlaminar space. From an initial d-spacing of 12.3–12.6 Å or 15.0–15.5 Å (depending on the degree of clay hydration) when no admixture is present [2, 3], PCE intercalation produces a d-spacing expansion of up to 17–18 Å when a PCE-based superplasticizer is used. This enlargement has been reported to correspond to one single intercalated poly-glycol chain in MNT clay, coordinated with water molecules [4-8]. All available studies in the literature address the interaction of clays with PCE-based superplasticizers via the same experimental procedure [1,4,8]. PCE-clay pastes are centrifuged, and the solid residue is extracted. Subsequently, this residue is dried at temperatures between 40–80 ºC in all cases.

Other studies [8,9] have reported similar MNT d-spacing expansions by following the same experimental process, as shown in Fig 1. Nevertheless, other authors [10] reported experiments where the observed d-spacing expansions of MNT clays were not homogeneous and varied depending on the structure of the PCE polymer and the nature of MNT clay. In general, they reported expansions in the range of 4.9–5.5 Å.

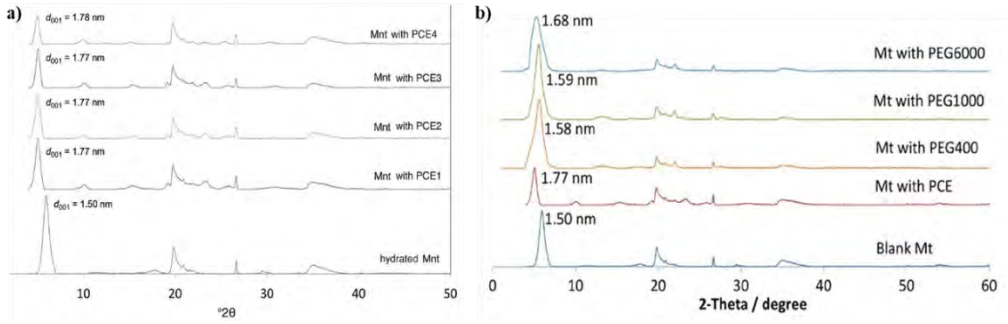

Fig. 1. a) Laboratory XRD patterns for centrifuge-dried MNT samples with different PCE-based superplasticizers (adapted from [5]); b) Laboratory XRD patterns for centrifuge-dried MNT samples with PCE- and PEG-based superplasticizers (adapted from [9])

The main objective of our study is to identify the influence of the sample preparation procedure on the d-spacing expansion of clay-PCE pastes as measured by XRD techniques, since clay interference with PCE superplasticizer dispersion capacity is an exclusive effect of fresh state systems. Moreover, superplasticizer admixtures that can be more resilient to the negative effect of clay in aggregates have been very recently highlighted as a research priority [11], and can only be attained with a well-established, robust, methodology.

In this investigation, XRD patterns were recorded directly from fresh pastes of MNT clay, including different dosages of a PCE-based admixture without any phase separation or drying process. To provide a frame of comparison, clay pastes having identical composition were prepared according to the standard procedure described in the literature [1] and powder XRD patterns were recorded. To extend the assessment of the influence of the experimental methodology on the final clay d-spacing and to confirm the reproducibility of the results obtained when testing fresh samples directly, *in situ* XRD measurements were performed with two different X-ray diffractometers at two different facilities: standard laboratory XRD (Cu X-ray tube) and X-ray synchrotron radiation analyses. It should be noted that synchrotron radiation techniques are especially suited for carrying out *in situ* studies on unaltered cement pastes [12].

2. MATERIALS

The materials used for the preparation of pastes were sodium montmorillonite powder and pure non-formulated PCE polymer. The liquid phase used to produce the pastes was always a synthetic cement pore solution as a simulant of the liquid phase formed during the early-age hydration of Portland cement.

2.1. Sodium montmorillonite clay (Na-MNT)

The clay sample used was a sodium montmorillonite (Na-MNT) clay powder. Oxide composition by XRF is shown in Table 1, expressed in oxide wt.%. Measured BET specific surface was 49.5 m^2/g (average of two measurements: 46.1 m^2/g and 52.8 m^2/g). The crystalline composition of Na-MNT clay was obtained by laboratory powder XRD analysis (see Fig 2).

SiO_2	TiO_2	Al_2O_3	Fe_2O_3	MgO	MnO	NiO	CaO	K_2O	Na_2O	LOI	Total
63.12	0.01	19.88	1.37	2.33	0.04	0.06	2.24	0.44	3.43	5.97	98.89

Table 1. Oxide composition in wt.% by XRF for Na-MNT clay sample

The clay presents basal displacement d_{001} of 12.3 Å deduced from its 2θ position at 7.2º. This value is typical for Na-MNT clays with one H_2O molecule layer inside the interlaminar space [3] [11]. 4.8 wt.% of quartz and 3.3 wt.% of calcite were identified as minor impurities, so the last explains the LOI value observed. Both quartz and calcite impurities cannot intercalate polycarboxylate side chains thus not influencing in the interpretation of the experimental results [9].

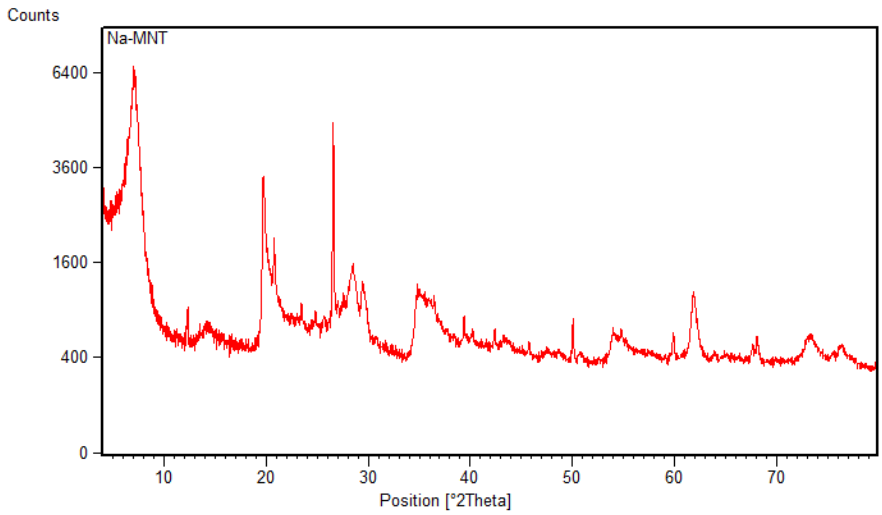

Fig. 2. Laboratory XRD pattern for raw Na-MNT used in this study

2.2 Polycarboxylate superplasticizer

Pure PCE polymer based on poly(ethylene glycol) ether on polyacrylate backbone from BASF Construction Chemicals was used. It is available in water-solution at 51 wt. %

concentration. Basic PCE characteristics are given in Table 2. Dosages of the PCE admixture are always referred to percentage of PCE active solids by weight of clay (expressed as % bwc).

Parameter	Value
Side-chain length	1.100 g/mol (25 mol EO)
Total carboxylic (by titration)	95 mg KOH/g PCE
Polymer type	PEG side chain on acrylic backbone

Table 2. Chemical structure and characterization of PCE polymer

2.3 Synthetic cement pore solution

All clay pastes were produced using synthetic cement pore solution as the liquid phase. This solution is prepared by dissolving 14.3 g of Na_2SO_4, 3.05 g of NaOH and 3.00 g of $Ca(OH)_2$ in 1 litre of distilled freshly-boiled water (equivalent to 0.157 mol/l of OH^-, 0.278 mol/l of Na^+, 0.100 mol/l of SO_4^{2-} and 0.040 mol/l of Ca^{2+} concentration). Synthetic cement pore solution used here was always recently prepared to avoid minimize carbonation.

3. EXPERIMENTAL METHODS

3.1. Preparation of clay pastes

Mixing procedures are reported to affect the admixtures' performances [13]. Therefore, the same mixing procedure is always carried out here. Clay pastes were prepared at 22 ºC by dispersing 10 g of powder clay in 50 g of synthetic cement pore solution to produce a 16.7 wt. % paste concentration. The mixing process was done with a vertical shaft mixer equipped with a helical head, at 1200 rpm. The total mixing time was three minutes. The admixture was incorporated at the required dosage at the one-minute mixing time.

3.2 *In situ* XRD of fresh clay pastes with synchrotron X-ray source

XRD patterns for six clay pastes were performed, including the reference paste at 16.7 wt. % concentration without the admixture and pastes with 13%, 50%, 100%, 220% and 325% bwc active solids of PCE polymer. Each fresh clay paste was introduced into a thin glass capillary of 1.5 mm diameter just after mixing. Capillaries filled with fresh clay pastes were mounted on a capillary rack, as shown in Fig. 3.

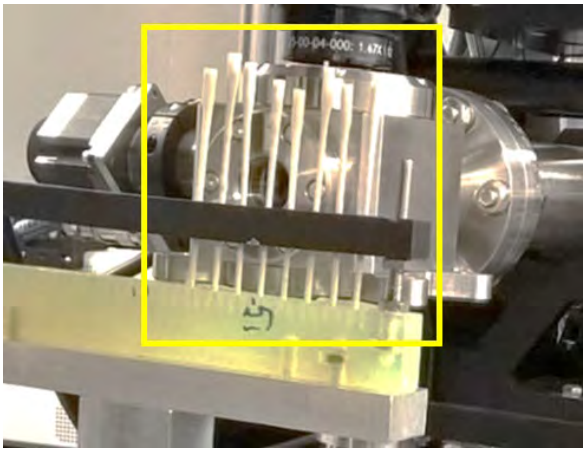

Fig. 3. Capillaries containing the fresh pastes mounted on the rack for synchrotron XRD data collection

Samples were measured on the BL11-NCD device of ALBA Synchrotron (Barcelona). Small angle X-ray scattering (SAXS) and wide angle X-ray scattering (WAXS) patterns were simultaneously recorded at 12.4 keV. The sample detector distances were 2.450 m and 0.170 m for SAXS and WAXS respectively. The WAXS detector was tilted by 27° along the horizontal axis perpendicular to the beam path. The beam stop was located on the top left corner of the SAXS detector and the data acquisition time was five seconds.

3.3 *In situ* XRD patterns of fresh pastes with standard Cu Kα lab diffractometer

XRD patterns for clay pastes without the admixture and clay pastes including different dosages of PCE were recorded at the CCiT facilities of the University of Barcelona using a laboratory X-ray powder diffractometer. Fresh pastes were sandwiched between two polyester films (thickness of 3.6 μm) and locked by two metallic rings as shown in Fig. 4.

A PANalytical X'Pert PRO MPD diffractometer of 240 mm of radius was used, in a configuration of convergent beam with a focalizing mirror and a transmission geometry with flat samples sandwiched between low absorbing films. Cu Kα radiation (λ = 1.5418 Å) was produced by an X-ray tube operating at 45 kV–40 mA and measured by a PIXcel detector with active length = 3.347 º. The incident beam slits defining a beam height were 0.4 mm for wide-angle and 0.05 mm for small-angle. Two 2θ/θ scans were recorded: i) SAXS data from 0.3 to 12 º2θ with a step size of 0.013 º2θ and a measuring time of 647 seconds per step; and ii) WAXS data from 2 to 30 º2θ with a step size of 0.026 º2θ and a measuring time of 148 seconds per step.

Fig. 4. Holder containing the fresh pastes, sandwiched between thin polyester films, for Cu Kα laboratory XRD data collection

3.4 Powder XRD patterns of separated-dried clay pastes

Clay pastes were also prepared following the same mixing process and transferred into a centrifuge tube. Samples were centrifuged at 10,000 rpm for 12 minutes. As an alternative approach to the centrifugation method for phase separation, some clay pastes were separated by filtration using a Buchner funnel powered by suction. The solids were collected, washed and dried at 40 ºC for seven days. Subsequently, the solid deposits were collected and dried at 40 ºC for seven days.

Powder XRD patterns of the dried solid fractions were collected by using the same PANalytical X'Pert PRO MPD Cu Kα laboratory diffractometer at the CCiT facilities of the University of Barcelona. The incident beam slits defining a beam height were 0.4 mm for wide-angle and 0.05 mm for small-angle. The 2θ/θ scan conditions were: i) SAXS data from 0.2 to 6 º2θ with a step size of 0.013 º2θ and a measuring time of 800 seconds per step; ii) WAXS data from 2 to 60 º2θ with a step size of 0.026 º2θ and a measuring time of 298 seconds per step.

4. RESULTS AND DISCUSSION

4.1 Influence of separation method on d-spacing of dried clay pastes

Prior to evaluating the possible impact of sample drying process on d-spacing measurement, the influence of separation method on XRD results of dried clay pastes was investigated.

XRD patterns collected from dried clay pastes containing 13% bwc of PCE are shown in Fig. 5, where it is compared with the patterns for the samples separated using both centrifugation and filtration methods.

From Fig. 5, it can be stated that both clay d-spacing results of 18.6 Å and 19.1 Å do not differ significantly from the literature values, using the same sample preparation approaches [3-5].

The difference in d-spacing observed in Fig. 5 between centrifugation and filtration separation methods (≈ 0.5 Å) is not very significant. Thus, it can be deduced that separation method has a minor influence on d-spacing measurements on dried clay pastes.

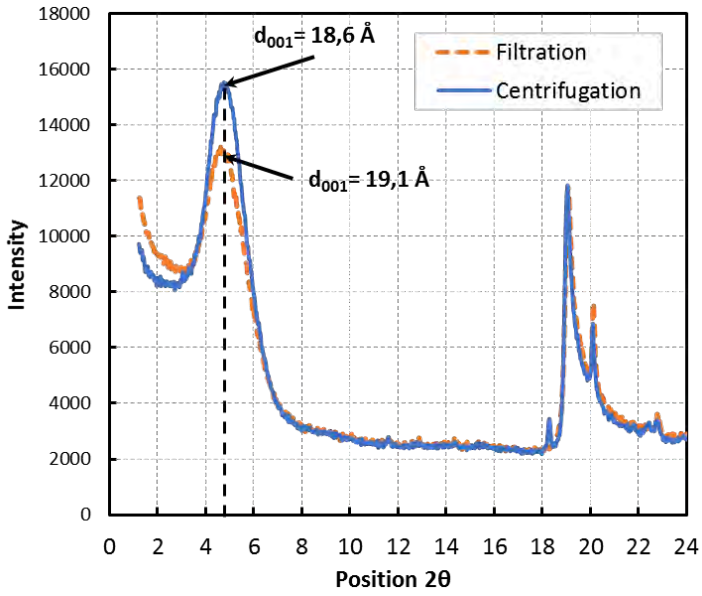

Fig. 5. Laboratory XRD patterns for dried clay pastes by using two different separation methods

4.2 Influence of clay paste drying process on d-spacing measurements

Figure 6 displays the XRD patterns obtained with the non-separated, non-dried fresh clay paste series, as prepared without the admixture, with 13% bwc and with 50% bwc of PCE polymer. Synchrotron XRD patterns from fresh pastes collected at ALBA and laboratory XRD data are shown in Fig. 6(a) and Fig. 6(b) respectively.

For the sake of comparison, Fig. 6(c) displays the laboratory XRD patterns for the same samples but after centrifugation and drying processes.

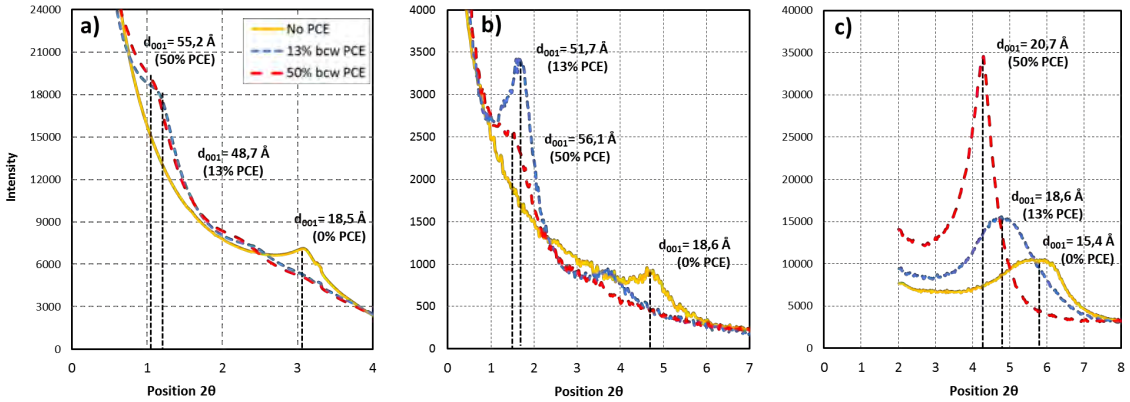

Fig. 6. XRD patterns for Na-MNT pastes with increasing PCE content for: a) fresh pastes collected with synchrotron radiation; b) fresh pastes collected with a Cu Kα diffractometer; c) centrifuged and dried pastes collected with a Cu Kα diffractometer

The d_{001} spacing obtained from the XRD patterns shown in Fig. 6 are listed in Table 3. This value provides the basal spacing or layer stacking in a phyllosilicate. Despite using different equipment, the values presented in Table 3 are similar for the *in situ* analyses of fresh pastes at the three tested dosages. Conversely, the basal spacing obtained from powder XRD analyses are undeniably much lower at all PCE dosages.

For clay pastes containing PCE polymer, the basal spacing measured from powder XRD analyses are compatible with d-spacing's observed in MNT clay pastes with a single intercalated monolayer of PEO/PEG side-chains [16]. These experimental results are in agreement with values obtained under similar conditions by other authors [4, 5, 7, 9, 10].

Sample	d_{001} spacing (Å)		
	In situ XRD (fresh pastes)		Powder XRD (dried pastes)
	Synchrotron	Cu Kα	Cu Kα
0% PCE	18.5	18.6	15.4
13% PCE	48.7	51.7	18.6
50% PCE	55.2	56.1	20.7

Table 3. Basal spacing (d001) obtained from XRD measurements of clay-PCE pastes

Chiefly, when comparing *in situ* XRD patterns of fresh pastes with powder XRD patterns of dried pastes, major differences in d-spacing values are observed. This direct experimental result clearly indicates that some intercalated PCE side-chains and water molecules are lost during the drying process, thereby causing a reduction in the measured

expansion. Therefore, we are forced to conclude that the final d-spacing recorded is critical on sample treatment by drying and it can be misleading as correlations should be established in the fresh paste state.

XRD measurements for clay-PCE dried samples suggest intercalation of one single monolayer of PEG/PEO side-chains with two water molecules. However, *in situ* XRD data for similar samples but recorded in fresh pastes could be indicative of a mechanism based on multiple intercalated layers of side-chains. To the best of our knowledge, there are no references reporting diffraction data in these experimental conditions. Therefore, more studies by independent laboratories are needed to firmly establish this behavior.

d_{001} d-spacing values corresponding to fresh clay pastes without admixture (see Table 3), are compatible with MNT clay with three water molecules in the interlayer region, typical in calcium alkaline media [2, 3]. When clay pastes without admixture are dried, the original d_{001} spacing of 12.3 Å of raw-powder clay increases to 15.4 Å. This basal spacing value is referred to in publications as characteristic of calcium montmorillonite with two water molecules in the interlayer region [2, 3, 5].

This observation indicates that not all absorbed water is lost during the drying process (even considering that the tested sample was dried for 7 days at 40 ºC). The results also suggest that some cation exchange could take place, sodium by calcium, while the clay is dispersed in the cement pore solution.

4.3 Impact of PCE dosage on Na-MNT d-spacing expansion

To further investigate the influence of PCE dosage on the expansion of Na-MNT interlaminar space, an additional XRD study was performed. Fig. 7 reports the d-spacing values, obtained from synchrotron and laboratory XRD patterns, for clay pastes prepared with increasing dosage of PCE admixture.

Firstly, laboratory XRD data for corresponding dried samples show much smaller d-spacing values as shown in Fig. 7. Secondly, d-spacing variations recorded in dried clay pastes containing PCE from 13% bwc to 160% bwc show no significant difference. Maximum d-spacing of 20.7 Å is observed at PCE dosage of 50% bwc, which is identical, within the errors, to that of 160% bwc. For all dried samples, the obtained results are compatible with one single monolayer of intercalated PEO/PEG side-chain in a zig-zag planar disposition coordinated by two water molecules [7, 10]. Thirdly, for the fresh paste samples, changes in d-spacing values are observed with increasing PCE dosage, with both diffraction equipment set-ups.

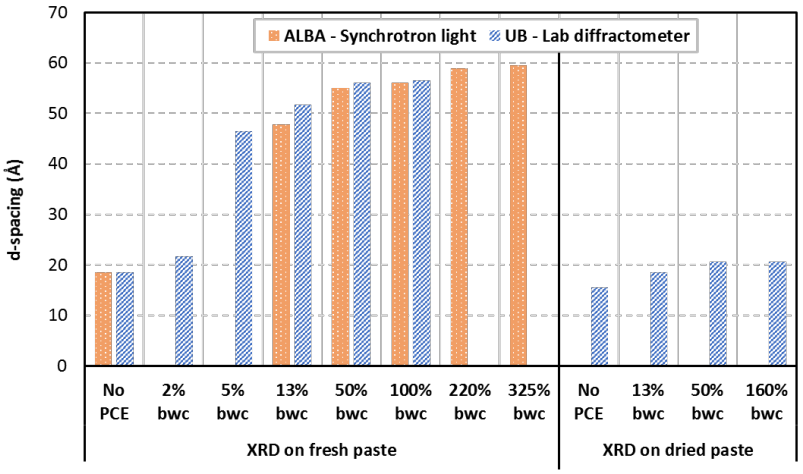

Fig. 7. d-spacing of clay pastes with different PCE dosages and different XRD diffraction measurement conditions

The largest observed d-spacing is close to 60 Å, being three times the maximum value obtained for dried clay pastes. From this observation, it can again be concluded that dried pastes do not reproduce the real impact on interlaminar expansion generated by PCE dosages, as observed in XRD patterns for fresh clay pastes (see Fig. 7). The large d-spacings (layer expansion) observed upon PCE intercalation has been assigned to regular side chains intercalation between the clay layers. At this stage, it is not possible to rule out irregular side chain intercalation each few clay layers. This will be studied in a future research, but it does not affect the main findings of this work: the previously reported sample preparation for XRD yielded misleading results. Finally, d-spacing expansions recorded on fresh pastes by using synchrotron and laboratory XRD sources are quite similar for all PCE tested dosages. Therefore, we infer that the experimental conditions used for the diffraction experiments do not affect the results.

5. HYPOTHESIS FOR PCE INTERCALATION MODEL IN MNT CLAY

Based on the observed d-spacing expansion, a hypothesis for the PCE intercalation model on MNT clay can be proposed. The theoretical thickness of one monolayer of water molecules within the interlaminar space can be estimated by assuming a thickness of 9.6 Å for the T-O-T layer structure of MNT clay [17]. Thus, inter-layer space can be deduced by subtracting this value from the experimental d-spacing values.

Table 4 presents some reported d-spacing data from various references as well as from proposed coordination models, which allows for the derivation of the theoretical H_2O

monolayer thickness. As can be seen, almost all values are between 2.7 Å and 2.9 Å. The resulting average value of 2.81 Å would correspond to the thickness of one single H_2O monolayer within the MNT interlaminar space. This result is in agreement with hydrogen bonding lengths in similar structures [19].

Data source		Sample state	d-spacing (Å)	Coord. H_2O layers	Calc. length of H_2O monolayer (Å)
[18]		dried	12.6	1	3.0
[4]			12.3	1	2.7
[3]		fresh	19.1	3	3.17
[10]		dried	15.2	2	2.8
[2]		simulation	12.3–21.0	1–4	2.7–2.85
[5]		dried	15.0	2	2.7
This study	Cu Kα	raw	12.3	1	2.7
		dried	15.4	2	2.9
		fresh	18.6	3	2.99
	Synchrotron		18.5	3	2.97

Table 4. d-spacing data for MNT clay without PCE admixture

To theoretically estimate the thickness of one single PEG/PEO side-chain, intercalated into the MNT interlaminar space, Table 5 presents d-spacing results from references for MNT pastes treated with PCE polymers.

Reference	Sample state	d-spacing (Å)	H_2O:PEO coordination	Calculated length of PEO monolayer (Å)
[4]	dried	17.7	2:1	2.3
[5, 7, 9]	dried	17.8	2:1	2.4
		17.7		2.3
[20]	simulation	17.9	2:1	2.5
[1, 8]	dried	17.2	2:1	2.0
[10]	dried	17.6	2:1	2.2
		17.8		2.4
		17.9		2.5

Table 5. d-spacing data for MNT clay with PCE admixture

Assuming an intercalation model where PEG/PEO side-chain is coordinated with two water molecules by hydrogen bonding [9], arranged in a zig-zag planar disposition [7], the equivalent thickness of one single PEO monolayer can be deduced from the proposed configuration, as presented in Table 5. The result of the simple calculation is 2.48 Å.

Considering a thickness of 2.81 Å for H_2O monolayer and 2.48 Å thickness for PEG/PEO side-chain monolayer and by accepting the intercalation model proposed, it is possible to calculate the number of H_2O and PEO unit layers intercalated in fresh clay pastes. The number of intercalated layers calculated from d-spacing results obtained from synchrotron XRD source are given in Table 6.

PCE dosage (% bwc)	d-spacing (Å)	H_2O layers coordinated	PEO layers coordinated	Error (Å)
13%	48.7	8	7	-0.7
50%	55.2	9	8	0.5
100%	56.1	9	8	1.4
220%	58.9	10	9	-1.1
325%	59.5	10	9	-0.5

Table 6. Calculated H2O and PEO layers intercalated into MNT clay

By comparing intercalated units of PEG/PEO side-chains from XRD patterns of fresh clay pastes (Table 6) with the intercalation number deduced from XRD patterns of dried clay pastes (Table 5), it is possible to conclude that the degree of intercalation of PCE side-chains is up to nine times larger and increases with PCE dosage.

The error calculated as the difference between theoretical (simplified) calculations and experimental d-spacing are also reported in Table 6. The maximum observed error, 1.4 Å, can be considered low and within the errors and approximations. Therefore, it would be possible to validate the model of multiple intercalation based on PEG/PEO side-chains coordinated with H_2O molecules by H-bonding. This means that the theoretical thickness deducted for one H_2O-PEO layer corresponds to 5.3 Å, which fits with most reported data [1, 7, 10] while being in agreement with the experimental results reported here.

A scheme of the multiple intercalation model is displayed in Fig. 8(b), derived from an initial configuration of three H_2O layers where no PCE admixture is present, as shown in Fig. 8(a). When PCE polymer is added, Fig. 8(b) proposes an intercalation model based on

repetitive sequences of H_2O-PEO layers (LH_2O-PEO) ended by a single H_2O monolayer bonded to internal MNT clay surface by H-bonding.

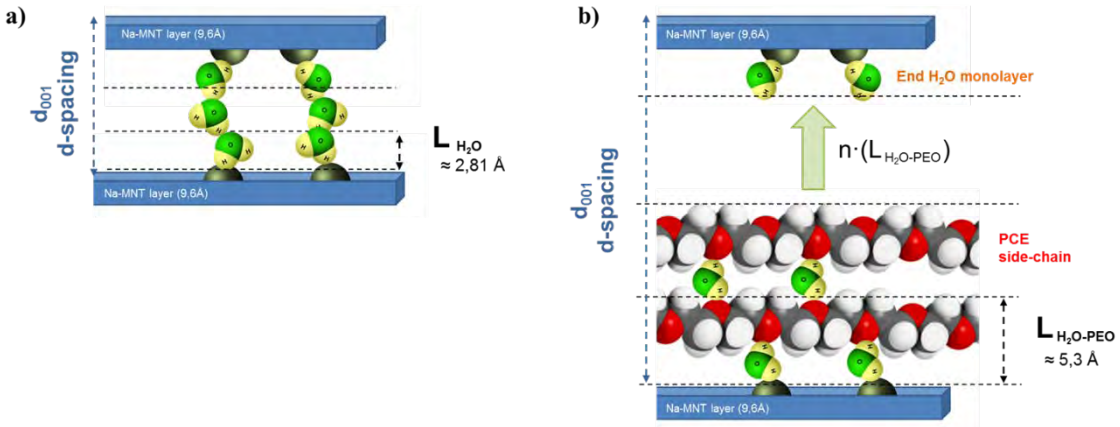

Fig. 8. Intercalation models in MNT clay; a) without PCE polymer added; b) with PCE based admixture added

In situ XRD data from fresh clay pastes indicate that up to nine PEG/PEO side-chains of PCE polymer can be intercalated in a single interlaminar space of MNT clay. This value is much larger than the intercalation numbers deduced from powder XRD patterns for dried clay samples.

Considering the potential steric repulsion derived from the concentration of a large number of long PEG/PEO side-chains in a limited space, it is possible to propose that all side-chains intercalated in a single unit of dispersed MNT clay particle belongs to a restricted number of polymer units or even to a unique PCE molecule adsorbed on the clay surface.

The multiple intercalation model proposed is not in contradiction with the mechanisms proposed by Ng & Plank [4] Tan et al. [7]. In fact, the assumed molecular interaction is the same as that proposed by the aforementioned authors, but data from *in situ* XRD patterns obtained on fresh clay pastes allow for an extension of the initial PEG/PEO monolayer model of intercalation to a multiple-chain intercalation model, where many PCE side-chains can be absorbed at the same time into interlaminar space of MNT clay.

6. CONCLUSIONS

An undesired influence of the drying process of clay pastes on d-spacing determination by XRD has been identified. Changes in d-spacing due to the intercalation of PCE side-chains

measured in dried clay pastes by powder XRD are systematically much lower than the changes observed by *in situ* XRD recorded for fresh pastes. Absolute d-spacing values, when the PCE admixture is used, are altered by the drying process, and up to nine times lower number of intercalated PEG/PEO side-chains are observed. Furthermore, the dried sample XRD data does not reproduce the true degree of intercalation as the dosage of PCE admixture increases.

The behavior of fresh paste analysis has been confirmed by performing *in situ* measurements with two different sets of equipment, a synchrotron and a laboratory diffractometer, which yielded comparable results. Based on these observations, a multiple intercalation model of PCE side-chains has been proposed, based on a sequence of overlapping H_2O-PEO layers ending with a H_2O monolayer.

Acknowledgments

Mr. Borralleras is grateful for all the support given by BASF Construction Chemicals to the development of this work. Dr. I. Segura is supported by the postdoctoral Torres Quevedo program of the Spanish Ministry of Economy and Competitiveness.

References

[1] L. Lei, J. Plank, A concept for a polycarboxylate superplasticizer possessing enhanced clay tolerance, Cement and Concrete Research 42 (2012) 1299-1306.

[2] S. Karaborni, B. Smit, W. Heidug, J. Urai. E. van Oort, The swelling clays: molecular simulations of the hydration of montmorillonite, Science 271 (1996) 1102-1104.

[3] M. Matusewicz, K. Pirkkalainen, J.P. Suuronen, A. Root, A. Muurinen, R. Serimaa, M. Olin, Microstructural investigation of calcium montmorillonite, Clay Minerals 48 (2013) 267-276.

[4] S. Ng, J. Plank, Interaction mechanisms between Na-montmorillonite clay and MPEG-based polycarboxylate superplasticizers, Cement and Concrete Research 42 (2012) 847-854.

[5] H. Tan, Xin Li, M. Liu, B. Ma, B. Gu, X. Li, Tolerance of cement for clay minerals: effect of side-chain density in polyethylene oxide (PEO) superplasticizers additives, Clay and Clay Minerals 64-6 (2016) 732-742

[6] G. Xing, W. Wang, G. Fang, Cement dispersion performance of superplasticizers in the presence of clay and interaction between superplasticizers and clay, Advances in Cement Research 29 (2017) 194-205.

[7] H. Tan, B. Gu, B. Ma, X. Li, C. Lin, Mechanism of intercalation of polycarboxylate superplasticizer into montmorillonite, Applied Clay Science 129 (2016) 40-46.

[8] L. Lei, J. Plank, A study on the impact of different clay minerals on the dispersing force of conventional and modified vinyl ether based polycarboxylate superplasticizers, Cement and Concrete Research 60 (2014) 1-10.

[9] H. Tan, B. Gu, S. Jian, B. Ma, Y. Guo, Z. Zhi, Improvement of polyethylene glycol in compatibility with polycarboxylate superplasticizer and poor-quality aggregates containing montmorillonite, Journal of Materials in Civil Eng. 29-9 (2017).

[10] R. Ait-Akbour, P. Boustingorry, F. Leroux, F. Leising, C. Taviot-Guého, Adsorption of polycarboxylate poly(ethylene glycol) (PCP) esters on montmorillonite (MNT): Effect of exchangeable cations (Na^+, Mg^{2+} and Ca^{2+}) and PCP molecular structure, Journal of Colloid and Interface Science 437 (2015) 227-234.

[11] J. Cheung, L. Roberts, J. Liu, Admixtures and sustainability, Cement and Concrete Research, *in press*.

[12] M.A.G. Aranda, Recent studies of cements and concretes by synchrotron radiation crystallographic and cognate methods, Crystallography Reviews 22 (2016), 150-196.

[13] F. Winnefeld, Influence of cement ageing and addition time on the performance of superplasticizers, ZKG International 61 (2008), 68–77,

[14] R.L. Parfitt, D.J. Greenland, The adsorption of poly(ethylene glycols) on clay minerals, Clay Minerals 8 (1970) 305.

[15] R.A. Schoonheydt, C.Y. Johnston, The surface properties of clay minerals, EMU Notes in Mineralogy 11-10 (2011) 337-373.

[16] D. Senich, T. Demirel, R.L. Handy, X-Ray diffraction and adsorption isotherm studies of the calcium montmorillonite-H_2O system, Highway Research Record 209, 46th Annual meeting of Physico-Chemical Phenomena in Soils (1956) 23-54.

[17] P.F. Low, J.L. White, Hydrogen bonding and polywater in clay-water systems, Clays and Clay Minerals 18 (1970) 63-66.

[18] M. Szczerba, Z. Klapyta, A. Kalinichez, Ethylene glycol intercalation in smectites. Molecular dynamics simulation studies, Applied Clay Science 91 (2014) 87-97.

3.2. JOURNAL PAPER II

INFLUENCE OF THE POLYMER STRUCTURE OF POLYCARBOXYLATE-BASED SUPERPLASTICIZERS ON THE INTERCALATION BEHAVIOR IN MONTMORILLONITE CLAYS

Published in Construction and Building Materials 220 (June 2019) 285-296.

Pere Borralleras[a], Ignacio Segura[b, c,*], Miguel A. G. Aranda[d] and Antonio Aguado[b]

[a] BASF Construction Chemicals Iberia, Ctra del Mig 219, E-08907 Hospitalet de Llobregat, Barcelona, Spain

[b] Department of Environmental and Civil Engineering, Universitat Politècnica de Catalunya-Barcelona Tech, Jordi Girona 1-3, C1, E-08034 Barcelona, Spain

[c] Smart Engineering Ltd, Jordi Girona 1-3, ParcUPC–K2M, E-08034 Barcelona, Spain

[d] ALBA Synchrotron, Carrer de la Llum 2-26, E-08290, Cerdanyola del Vallès, Barcelona, Spain

* Corresponding author: Ignacio Segura, Department of Environmental and Civil Engineering, Universitat Politècnica de Catalunya-Barcelona Tech, Jordi Girona 1-3, C1, E-08034 Barcelona, Spain. Email address: ignacio.segura@upc.edu Tel: +34 93 4054684

Abstract

The influence of polymeric structure of polycarboxylate-ether (PCE) based superplasticizers on the intercalation behavior in sodium montmorillonite clay (Na-MNT) is investigated by performing *in-situ* X-ray diffraction (XRPD) on fresh, unaltered clay pastes. The use of this technique reveals the real influence of the PCE structure and of the PCE/clay dosage ratio on the expansion profile of the clay. This is not observed with the traditional XRPD methodology performed on dried clay pastes, which shows the same values of d-spacing despite using polymers of diverse structures. It is observed that PCE polymers with long side chains and high side chain density result in larger expansion. Additionally, polymers with a high anionic charge saturate the interlaminar space of montmorillonite at a lower dosage. The experimental results also indicate that clay exfoliation is critical in the intercalation process and the exfoliation tendency of the clay is influenced by the structure of PCE polymers.

Keywords: XRD, Polycarboxylate, Clay, d-spacing, Synchrotron radiation, Intercalation, exfoliation

1. INTRODUCTION

The dispersing capacity and water reduction efficiency of polycarboxylate-ether (PCE) based superplasticizers is severally affected by the presence of montmorillonite clays (MNT) in the sands used for concrete production. This type of clays has the ability to absorb large quantities of PCE polymers through an intercalation mechanism of the PEG/PEO (poly-ethylene glycol/poly-ethylene oxide) side chains of the polymer [1,2], which is responsible for the partial or total loss of their dispersing capacity.

The absorption behaviour of PCE-based superplasticizers on MNT clay has already been investigated by different authors using XRPD analysis on centrifuged and dried clay pastes [1,2]. These studies show almost no influence on the d-spacing of MNT clay when different structures of PCE polymers are used since the maximum clay expansion value always remains in the range of 18-21 Å and, in all cases, the average differences of d_{001} values within PCE polymers of diverse structures does not exceed 3 Å (the distance equivalent to one water molecule arranged in the interlayer of MNT clays).

The intercalation level associated with the d-spacing measured by traditional XRPD on dried pastes corresponds to one monolayer of PEG/PEO (poly-ethylene glycol/poly-ethylene oxide) side chains intercalated into the interlaminar space of MNT clay with two coordination water molecules [2-5]. Since the net expansion of 3 Å is equivalent to a one single water

molecule layer or to a one single monolayer of PEG/PEO side chain intercalated into the interlaminar space of MNT clay [6], it indicates that the same intercalation degree of side chains is inferred by applying the traditional analytical technique. Thus, this methodology does not allow to determine whether the structure of the PCE polymers influence in the expansion behaviour of MNT clay that induced by the intercalation of side chains.

Therefore, by relying on the experimental results from XRPD analysis performed on centrifuged and dried clay pastes, it should be concluded that there is almost no influence of the structure of PCE polymers in the has intercalation degree of side chains. Nevertheless, fluidity tests for cement pastes containing MNT clay and PCE based superplasticizers shows significant differences in the paste flow loss for different PCE structures [2, 7, 8].

These experimental results confirm that the structure of PCE polymer has a more relevant role in the interaction process with the clay versus the conclusions deducted from the XRPD analysis on centrifuged and dried clay pastes.

The objective of this study is to identify the influence of the polymer structure of PCE-based superplasticizers in the interaction process with MNT clays by performing *in situ* XRPD analysis on fresh, unaltered clay pastes. The authors previously demonstrated the methodology for *in-situ* XRPD characterization and the information that can be obtained for MNT clay expansion [6]. This allows researchers to identify increased intercalation degrees than those previously deducted by the traditional analytic methodology. It also demonstrates greater influence of PCE dosage on the d-spacing evolution.

2. RESEARCH SIGNIFICANCE

As far as the authors know, this is the first study using *in-situ* XRPD measurements on fresh, unaltered clay pastes to examine the intercalation mechanism of PCE-based superplasticizers in montmorillonite clays and the influence of the polymer structure in this process.

Several investigations have previously studied this process using traditional XRPD analysis on centrifuged and dried clay pastes [1-5]. However, the conclusions extracted from the experimental results did not offer a clear view on the influence of the PCE structure in the intercalation mechanism.

3. MATERIALS

3.1 Cement

Cement pastes are prepared with cement type CEM I 52.5R. Table 1 presents oxide and mineral phase composition of anhydrous cement (expressed in wt. %) determined by XRF (X-ray fluorescence). The Blaine value reported in cement specifications is 4750 cm^2/g. The measured BET-specific surface is 1.6 m^2/g and the particle size (D_{50}), determined by laser diffraction, is 10 μm. For the reproducibility of the experimental results obtained in this study, it should be stated that the amount of orthorhombic C_3A of cement is very low, while its sulphate content is high. This feature is important when conditioning the levels of adsorption of the admixtures [9].

Oxide composition (wt. %)		**Mineral phases (wt. %)**	
SiO_2	19.60	C_3S	58.9
Al_2O_3	5.38	C_2S	14.0
Fe_2O_3	2.41	C_3A total	9.4
CaO	65.29	C_3A ort/cub	99% cubic
Na_2O	0.05	$C_4(A,F)$	5.7
K_2O	0.84	$M_X(SO_4)$	5.5
MgO	0.82	Total	93.5
SO_3	3.34		
LOI	2.18		

Table 1. Oxide composition and mineral phases of anhydrous cement used

3.2 Sodium montmorillonite clay (Na-MNT)

The clay used in this investigation is a powder sodium montmorillonite (Na-MNT) sample. Oxide composition by XRF is shown in Table 2 (expressed in wt. %). The BET-specific surface is measured at 49.5 m^2/g (average of two measurements: 46.1 m^2/g and 52.8 m^2/g) and the average particle size (D_{50}), determined by laser diffraction, is 7.4 μm. A d_{001} value of 12.3 Å is deduced from its 2θ position at 7.2º in XRPD analysis on raw (dry) clay powder. This value is typical for Na-MNT clays with one H_2O molecule layer inside the interlaminar space [10]. Some impurities are identified: 4.8 wt.% of quartz and 3.3 wt.% of calcite, which explains the loss-on-ignition (LOI) value. The cation exchange capacity (CEC) value reported in product specifications is 105 mmol/100g, which agrees with the typical values for MNT clays [11].

Oxide composition of Na-MNT (wt. %)										
SiO_2	TiO_2	Al_2O_3	Fe_2O_3	MgO	MnO	NiO	CaO	K_2O	Na_2O	LOI
63.12	0.01	19.88	1.37	2.33	0.04	0.06	2.24	0.44	3.43	5.97

Table 2. Oxide composition of MNT clay used

3.3 Polycarboxylate-ether (PCE) polymers

Four different pure polycarboxylate-ether (PCE) polymers in aqueous solution are used (AA-1100, AA-2000, AA-3000 and AM-5800). The solid content and the structural characteristics of each PCE polymer are presented in Table 3. Complementary to the different PCE types, a superplasticizer based on calcium β-naftalensulfonate (Ca-BNS) is also used for comparison purposes. All admixtures are tested at an equal solid concentration of 20 wt.%, prepared by dilution with distilled water.

Parameter		AA-1100	AA-2000	AA-3000	AM-5800
Solid concentration (wt. %)		50.3%	40.2%	35.9%	46.4%
Side chains	Type	IPEG	TPEG	VPEG	VPEG
	mol EO/side chain	25	46	68	132
	Mw (g/mol)	1100	2000	3000	5800
Main monomer of the backbone		Acrylic	Acrylic	Acrylic	Maleic

Table 3. Chemical structure and composition of PCE polymers

3.4 Synthetic cement pore solution

All clay pastes are produced using synthetic cement pore solution as the liquid phase. The solution is prepared by dissolving 14.3 g of Na_2SO_4, 3.05 g of NaOH and 3.00 g of $Ca(OH)_2$ in 1 litre of distilled freshly-boiled water (equivalent to 0.157 mol/l of OH^-, 0.278 mol/l of Na^+, 0.100 mol/l of SO_4^{2-} and 0.040 mol/l of Ca^{2+} concentration). The synthetic cement pore solution is always freshly prepared to avoid carbonation.

4. EXPERIMENTAL METHODS

4.1. Determination of PCE anionic charge

Anionic charge of PCE polymers is measured by the titration of free carboxylic groups with 0.5 M KOH solution freshly standardized with sulfamic acid. Mettler-Toledo DL28

equipment is used for the titration process. 10 g of 20 wt.% PCE sample are diluted in 50 ml of distilled water and acidified with concentrated HCl, added drop by drop until a pH of 1.5 is reached.

Titration with KOH is performed on the acidified samples until final pH value of 12-13 is reached. After the titration, two inflexion points are observed that correspond to the points of equivalence. The first point is attributed to the HCl surplus and the second point (located close to pH 9) is attributed to the neutralization of PCE carboxylic groups. The points of equivalence are identified using the method of incremental ratios [12].

The total *PCE anionic charge* is calculated using the difference in the KOH volume corresponding to the first and the second inflexion points. The PCE anionic charge results are expressed as *mg KOH/g* or as *mol COOH/g PCE*.

4.2. Preparation of cement and clay pastes

Clay pastes are prepared at 22 ºC by dispersing powdered Na-MNT clay in the synthetic cement pore solution at 17 wt.% concentration. The mixing process is done using a vertical shaft mixer equipped with a helical head, moving at 600 rpm. The total mixing time is four minutes, during which the admixture is added at the required dosage after the one-minute mark. Cement pastes are prepared following the same procedure as clay pastes, using a water-to-cement (w/c) mass ratio of 0.26 and dispersing cement (and clay when used) with tap water at 22 ºC. For cement pastes containing clay, both powders are dry-mixed prior to the addition of water.

4.3. Measurements of paste fluidity

Fluidity of cement and clay pastes is determined by the measurement of paste flow in the mini-slump test. The test uses a metallic truncated mini-cone that is 55 mm high, with an upper diameter of 19 mm and a lower diameter of 38 mm. The mini-cone is arranged on a flat, clean glass surface. It is filled with fresh paste and then compacted with a crystal rebar to evacuate trapped air. The mini-cone is then lifted to let the paste to flow onto the glass surface until the paste reaches maximum spread.

The paste spread (paste flow, expressed in mm) is measured in two perpendicular directions and the average value is taken. This test is widely used to evaluate the fluidity of fresh cementitious pastes.

4.4 XRPD patterns of clay pastes

XRPD patterns for fresh and dried clay pastes are obtained following the experimental procedures previously described in [6]. In brief, *in-situ* XRPD analysis of fresh, unaltered clay pastes are performed using an MSPD diffractometer using synchrotron radiation at ALBA Synchrotron (Barcelona) and with a PANalytical X'Pert PRO MPD Cu Kα lab diffractometer (λ = 1.5418 Å). The XRPD analysis of clay pastes centrifuged and then dried for seven days at 40 ºC are performed with a Cu Kα lab diffractometer.

4.5 Sorption of PCE polymers

The sorbed fraction of PCE polymers is measured by determination of the total organic carbon (TOC) with Shimadzu testing equipment. Freshly prepared cement pastes containing PCE polymers are diluted with Milipore water and mixed for 30 seconds. The suspension is separated by centrifugation at 15000 rpm for 10 minutes and the obtained liquid phase is filtrated with a 0.45 µm syringe Nylon filter. The final filtrate is acidified with concentrated HCl to remove inorganic carbon and is then submitted for TOC analysis by combustion at 900 ºC. Same procedure is applied to measure PCE sorption in clay pastes prepared with synthetic cement pore solution.

Previously, calibration lines of each pure PCE polymer were prepared by recording the TOC value of three different concentrations of PCE [13]. The sorbed fraction of PCE is calculated by interpolation between the calibration lines from the difference of the total PCE dosage added and the non-sorbed fraction of PCE identified in the filtrate. Results are expressed as a percentage of sorption of the total PCE dosage and/or in sorbed mg of PCE per gram of cement or clay.

5. RESULTS AND DISCUSSION

5.1 Identification of PCE structural configuration

Table 4 shows the results of the PCE anionic charge obtained by titration. Considering an ideal structure in which the PCE backbone is exclusively composed of the main carboxylic monomer and knowing the molecular weight of the PEG/PEO side chains (reported in Table 3), the grafting ratio and the side chain frequency of each PCE is calculated from the measured anionic charge [14]. The calculated parameters are reported in Table 4.

	Parameter	AA-1100	AA-2000	AA-3000	AM-5800
Anionic charge	mg KOH/g PCE	99	41	127	44
	mmol COOH/g PCE	1.77	0.73	2.27	0.79
Calculated side chain structure	Grafting ratio (mol side chain/mol carboxylic monomers)	1 : 2.2 (0.45)	1 : 1.5 (0.65)	1 : 8.1 (0.12)	1 : 2.4 (0.42)
	Side chain frequency (mol side chain/total mol in the backbone)	0.31	0.39	0.11	0.29

Table 4. Anionic charge and deducted side chain structure of studied PCE polymers

The results presented in Table 3 indicate that the AA-2000 polymer is characterized by the highest grafting ratio, while AA-3000 possess the lowest content of side chains due to its highest anionic charge. At a comparable molecular weight, higher anionic charge values are attributed to a longer backbone length of the polymer [15]. Thus, AA-3000 and AA-1100 are polymers with presumably longer backbones than AA-2000 and AM-5800. AA-1100 and AM-5800 polymers present relevant differences in anionic charge, but their grafting ratios are similar. It is important to note that the AM-5800 polymer´s side chains are more than five times longer than the side chains of AA-1100, which means that there are significant differences in the structural configuration between both PCE polymers [16]. To account for the relationship between side chain length and side chain frequency, the parameter *side chain density* is defined as [*(mol EO side chain) x (side chain frequency)*]. The side chain density calculated for each PCE polymer is presented in Figure 1.

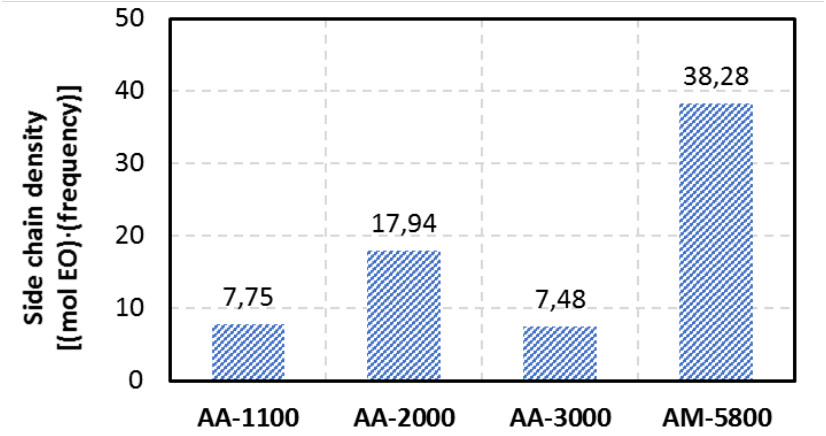

Figure 1. Side chain density values calculated for PCE polymers

The results shown in Figure 1 indicates that AM-5800 is the PCE with the highest density of side chains due to the longest side chain length, despite not exhibiting the highest grafting ratio. AA-2000 is the PCE with the second highest side chain density due to its highest grafting ratio, despite a shorter side chain length than AA-3000. For AM-5800 and AA-2000 polymers, it is expected that important steric repulsion will be key in determining their adsorption behaviour [17].

AA-1100 and AA-3000 polymers present the lowest side chain densities, so steric effects will be lessened. However, due to their high anionic charge, they are expected to have a higher affinity for adsorption when compared to the AA-2000 and AM-5800 polymers [18].

5.3 Dispersion ability of PCE polymers in cement pastes containing Na-MNT clay

The influence of the Na-MNT clay content on the fluidity of cement pastes is displayed in Figure 2. Paste flow loss is evaluated with cement pastes containing 0.3% by cement weight (bcw) of PCE active solids and increasing quantities of Na-MNT clay (0%, 0.14%, 0.3%, 0.6% and 1.0% bcw) are added to verify its influence in the fluidity of cement pastes.

Figure 2(a) presents the average values of the initial flow of cement pastes at each percentage of clay, including the standard deviation for each individual measurement. For comparison purpose, the Ca-BNS polymer is also tested at 1.2% bcw dosage (in order to balance paste fluidity at a comparable level to PCE).

To provide a better comparison on the impact of clay dosage on the paste flow loss, Figure 2(b) represents the *relative reduction of fluidity*, calculated by dividing the average paste flow loss at each clay dosage by the paste flow value of cement paste without Na-MNT clay. Therefore, a relative value of 1 corresponds to a total fluidity loss, while a relative value of 0 means no reduction of fluidity.

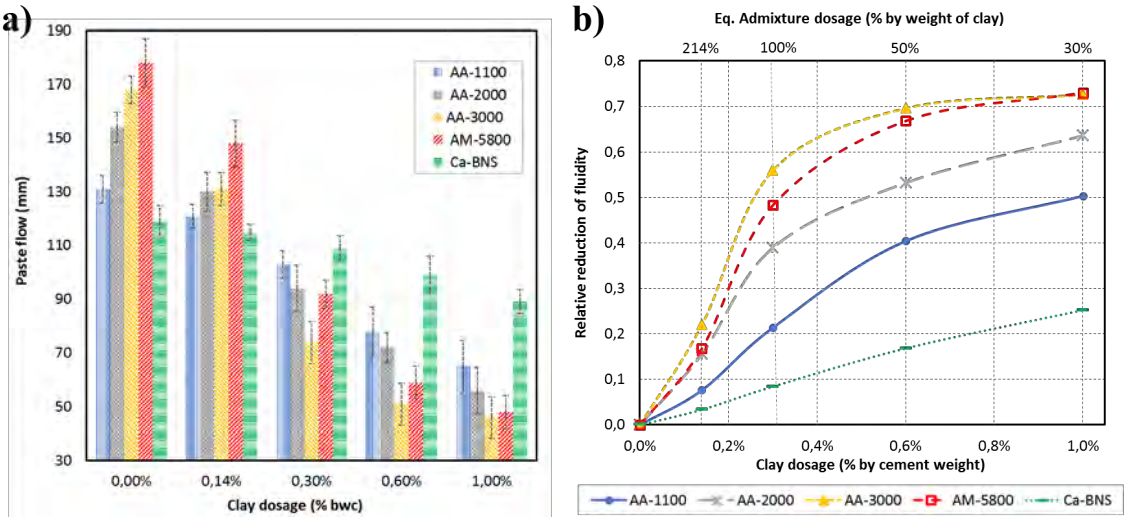

Figure 2. a) Paste flow results of cement pastes with different amounts of Na-MNT clay, with standard deviation; b) Relative paste flow loss at each clay dosage

The specific capability of each PCE polymer to disperse cement particles can be determined from the initial paste flow values shown in Figure 2(a) for cement paste samples without clay. AM-5800 has the highest cement dispersing capacity for the studied PCE polymers due to its longest side chains and highest side chain density [19]. AA-3000 shows similar performance to AM-5800 despite having shorter side chains and lower side chain density. This property can be attributed to AA-3000´s high anionic charge, which promotes a larger quantity of polymer adsorbed on the cement particles, generating effective dispersion. This approach is supported by the hypothesis proposed by [20], in which the global dispersing ability of PCE polymers is defined simultaneously by the dispersing capacity of PCE (as consequence of its polymeric structure) and by the total amount of polymer adsorbed on cement. The AA-2000 PCE polymer shows lower capacity for cement dispersion than AM-5800 and AA-3000, despite its high side chain density, while AA-1100 is the PCE polymer that demonstrates the lowest paste flow value. The initial fluidity of cement paste with Ca-BNS is lower than that of AA-1100, even after being dosed up to four times more.

When Na-MNT clay is added to the cement pastes, all samples present a significant decrease in their fluidity, with the reduction being most obvious in PCE polymers. The significant reduction of PCE dispersion ability can be observed in Figure 2(b) for all PCE polymers, even at the lowest clay dosage (up to 22% paste flow loss for AA-3000). Ca-BNS presents a totally different profile of paste flow loss. This observation is evidence that BNS condensates have much better tolerance to MNT clays than PCE polymers [18-21], and the described linear reduction of paste flow can be attributed simply to the increase of total water demand by the addition of clay.

The relative reduction of paste flow presented in Figure 2(b) also confirms and highlights that the impact on the dispersing capacity of PCE polymers produced at equivalent Na-MNT dosages is not homogeneous for the different polymer structures used. AM-5800 and AA-3000 presents the maximum paste flow loss at all clay dosages, but demonstrate a more relevant impact at low clay contents. AA-2000 shows a similar impact at a low dosage of clay, but the interference on its dispersing ability at a higher clay dosage is comparatively lower than that of AM-5800 and AA-3000.

The lowest relative reduction of paste flow observed in AA-1100 at all clay dosages suggests that this PCE structure has the most reduced clay sensitivity for all PCE polymers tested. Therefore, according to the experimental paste flow results, it can be firmly stated that different PCE polymeric structures result in relevant differences on the paste flow loss of cement pastes containing Na-MNT clay.

5.3 Sorption rate of PCE polymers on cement pastes containing Na-MNT clay

Figure 3 presents the results of PCE sorption measurements performed just after completing the mixing process. The net sorbed amount of PCE measured on cement pastes without clay are presented in Figure 3(a), including the percentage of sorbed PCE (on total PCE dosage). Figure 3(b) shows the evolution of sorption rate measured in cement pastes including MNT clay at increasing dosages, expressed in the net amount of sorbed PCE (mg PCE/g) and in the sorption percentage on the total PCE weight.

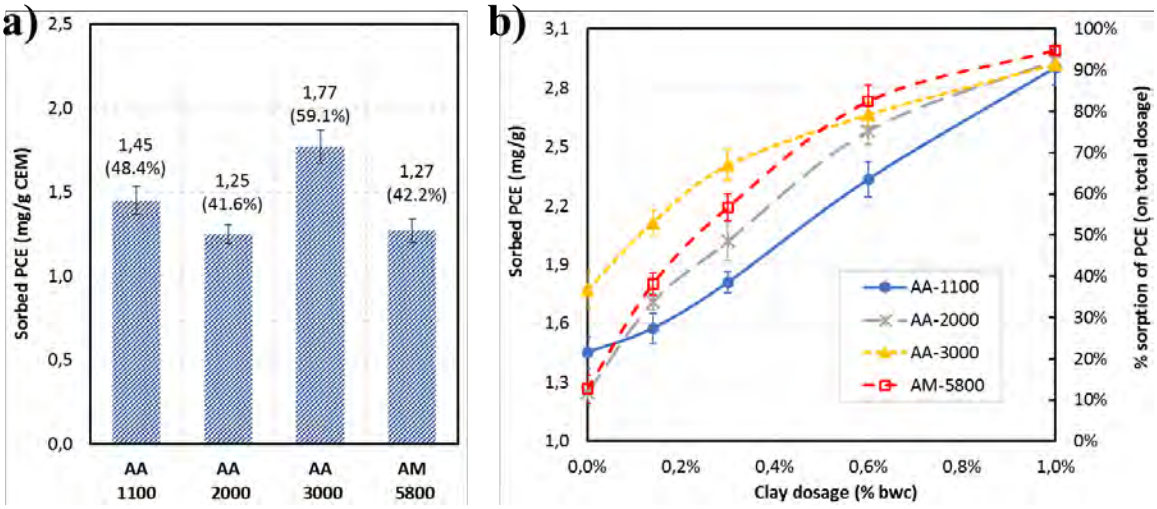

Figure 3. Net sorbed amount of PCE and percentage of sorption (including standard deviation) of; a) Cement pastes without clay; b) Cement pastes including different amounts of Na-MNT clay;

The natural sorption behaviour of each PCE polymer on cement can be deducted from Figure 3(a). AA-3000, followed by AA-1100, show the highest sorption rates, so they are the PCE polymers having the greatest affinity for the cement used. This is attributed to their high anionic charge, which promotes early adsorption on cement surface [17, 22].

As expected, PCE polymers AA-2000 and AM-5800 show the lowest net sorption of polymer, in agreement with the lower anionic charge. Therefore, it indicates that the effective dispersion is produced by a lower amount of polymer than the AA-1100 and AA-3000 PCE polymer.

When Na-MNT clay is added to the cement pastes, both net sorption of PCE and the sorption percentage increase. Using Figure 3(b), note that the progression of polymer sorption in cement pastes containing Na-MNT clay shows clear differences for the different PCE structures used and aligns with the paste flow results presented in Figure 2. At a low dosage of clay, AA-3000 is the PCE type presenting the highest sorption rate, which slows down from 0.3% bwc of clay upwards.

The AA-1100 polymer shows opposite behaviour when compared to that of AA-3000. AA-2000 and AM-5800 polymers present similar evolution of sorption rate, progressing between the levels of AA-1100 and AA-3000 up to a clay dosage level of 0.6% bwc. At this clay dosage, the sorption rate of AA-2000 and AM-5800 rises to AA-3000 values. At 1.0% clay dosage, AM-5800 shows the highest sorption within all the PCE polymers and AA-2000 and AA-1100 present similar values than that of AA-3000. In any case, at 1.0% bwc clay dosage all PCE polymers present comparable results of net sorption around 3.0 mg/g. It means that the sorbed fraction of PCE already reaches nearly 100%, as observed in Figure 3(b).

The level of sorbed fraction indicates that the PCE admixture is under clear stoichiometric limiting conditions, so that there is not enough polymer to interact with all the sorption sites available in both the cement and clay colloids. Thus, any possible differences between sorption rates of each PCE structure cannot be identified from this clay dosage.

5.4 Expansion of Na-MNT clay by *in-situ* XRPD analysis on fresh clay pastes

In-situ XRPD analysis on fresh, unaltered clay pastes evaluates the evolution of the interlaminar space dimension (d_{001}) for Na-MNT clay produced by different dosages of PCE polymers. XRPD patterns are recorded at 0%, 2%, 5%, 13%, 50%, 100% and 220% dosage of PCE polymer by weight of clay.

Table 5 displays the results of d-spacing (expressed in Å) corresponding to the main peaks identified by *in-situ* XRPD for each PCE polymer at each clay dosage tested (excluding equivalent peaks being second order reflections). Table 5 includes the results of d-spacing obtained by the traditional method of XRPD measurements.

Treatment method	PCE (wt.% clay)	Main peaks	PCE type			
			AA-1100	AA-2000	AA-3000	AM-5800
Fresh, unaltered clay pastes	0	Peak 3		18.5		
	2	Peak 1	21.6	21.7	21.6	21.6
	5	Peak 1	46.4	43.2	65.8	44.1
	13	Peak 1	48.7	47.6	66.9	51.5
		Peak 3	--	18.3	18.3	18.3
	50	Peak 1	55.2	61.5	67.0	64.4
		Peak 2	--	44.8	--	41.7
		Peak 3	--	18.3	18.3	18.3
	100	Peak 1	56.1	64.6	76.0	72.5
		Peak 2	--	45.2	42.1	45.7
		Peak 3	--	18.3	18.3	18.3
	220	Peak 1	58.9	69.7	80.9	78.5
		Peak 2	--	--	43.0	--
		Peak 3	--	18.3	18.3	18.3
Centrifuged and dried clay pastes	0	Peak 1		15.4		
	5	Peak 1	18.4	17.9	17.6	17.7
	13	Peak 1	18.6	18.4	18.7	17.9
	50	Peak 1	20.7	20.6	20.6	20.7
	100	Peak 1	20.8	20.7	20.7	20.8
	220	Peak 1	21.0	20.7	21.1	20.7

Table 5. Interlayer d-spacing (Å) from main peaks by *in situ* XRPD analysis; a) On fresh, unaltered clay pastes; b) On centrifuged and dried clay pastes

These results are displayed in Figure 4(a) as a function of PCE dosage. Figure 4(b) represents the d-spacing results obtained using the traditional testing methodology on centrifuged and dried clay pastes of equivalent composition.

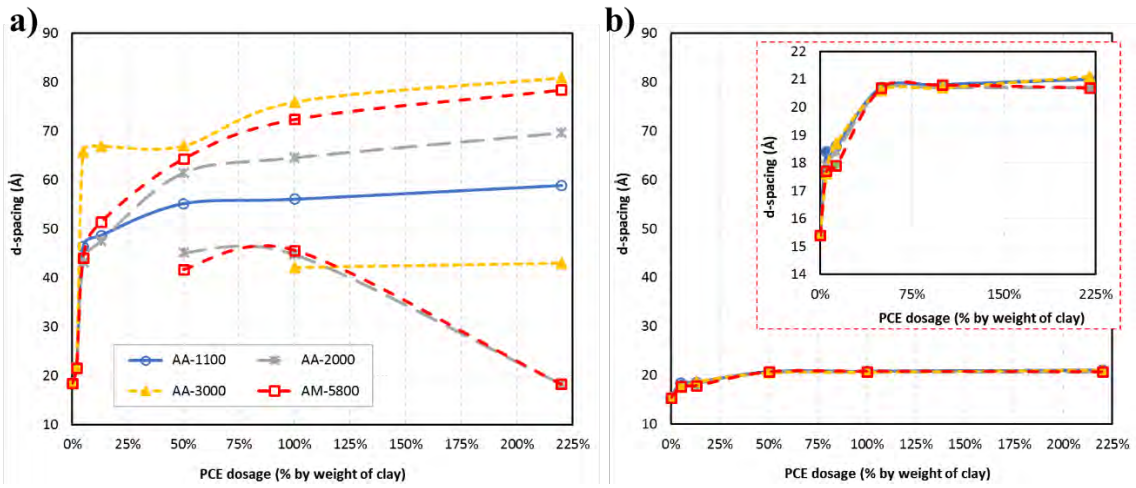

Figure 4. Expansion (d-spacing – d_{001} evolution) for Na-MNT clay from XRPD-SAXS patterns; a) On fresh clay pastes by *in-situ* XRPD; b) On centrifuged and dried clay pastes

Observed in Figure 4(a) that the measured d-spacing evolution for fresh pastes progresses to much larger values in comparison to the results presented in Figure 4(b), where XRPD measurements are performed on centrifuged and dried pastes. XRPD patterns obtained on dried clay pastes show maximum d-spacing value close to 21 Å for all PCE polymers tested, independent of their polymeric structure. These expansion rates are in agreement with results reported in other publications using the same experimental methodology [1-4]. In addition, there is no difference in d-spacing values for all PCE polymers upwards of the 50% dosage, where stationary state is reached.

The d-spacing variations measured using *in-situ* XRPD on fresh, unaltered clay pastes demonstrate a more complex absorption pattern (see Figure 4(a)). Larger d-spacing values are recorded, indicating that a higher degree of side-chain intercalation is possible. It also indicates clear dependence on the PCE dosage [6]. Furthermore, one can observe that the evolution of clay expansion progresses differently for each PCE polymer, indicating that the polymeric structure has a more relevant role in the intercalation process than that previously suggested by the results reported by XRPD analysis on dried pastes. Therefore, in agreement with our previous publication [6], it can be stated that this methodology, in which diffraction data is taken in the clay powder obtained from centrifuged and dried PCE-treated clay pastes, likely giving incorrect results. This conclusion is in agreement with [23], which used molecular dynamics simulation of ethylene glycol intercalation in montmorillonite clay.

Figure 4(a) describes a common model of d-spacing evolution for all the PCE polymers tested. The most significant changes in d-spacing are observed at a low dosage of PCE (from 2% to 13%). Despite describing all PCE types as a common profile of clay expansion, each

polymeric structure shows a particular evolution of d-spacing. When the PCE dosage is higher than 50%, d-spacing variations tend to converge towards a nearly constant value, thus describing a stationary state. Each structure also demonstrates unique behaviour at the PCE dosage required to reach the stationary state and at the maximum d-spacing value produced at the stationary state.

The AA-3000 polymer shows the maximum clay expansion at low PCE dosage and its d-spacing at stationary state is the largest for all PCE polymers tested, 80 Å. AM-5800 shows a d-spacing value at stationary state similar than that of AA-3000, but it is reached more progressively. The d-spacing evolution for AA-2000 at low PCE dosage progresses like AM-5800, but at a higher PCE dosage, it stabilizes earlier and on a lower value, 70 Å. AA-1100 is the polymer presenting the lowest d-spacing value, 60 Å, in the stationary state. Experimental results suggest that side chain length is controlling maximum d-spacing, so the higher expansion level affordable by the clay, which is larger for polymers with longer side chains. Nevertheless, no variation is observed between AA-3000 and AM-5800, presenting maximum d-spacings close to 80 Å. It is hypothesized that 80 Å is the maximum expansion that this clay can support to hold the integrity of the laminar structure, making further expansion impossible.

Figure 4(a) also reports the coexistence of various specimens with different degrees of side-chain intercalation, according the mechanism proposed by [6]. This phenomenon is only observed from 50% PCE dosage and higher and could be related to clay exfoliation. In any case, these specimens cannot be identified by XRPD analysis on dried clay pastes.

5.5 Exfoliation of Na-MNT induced by PCE polymers

Clay exfoliation is based on the progressive delamination of individual sheets forming the pristine clay particle and yields smaller clay particles with a reduced number of stacked plates [24]. The maximum level of exfoliation generates two-plates clay structures (the minimum configuration for clay nature) and even releases isolated plates [25]. For each layer delaminated from the primary clay particle, exfoliation produces a theoretical increase of the basal surface equivalent to double of the original. Therefore, due to the high ratio between the basal surface and edge surface that is typical of montmorillonite clays, exfoliation produces a huge increase in the total exposed clay surface available for adsorption [26-28].

When exfoliation occurs, one can hypothesize that it produces a reorganization of PCE units already absorbed into the interlaminar space. It looks coherent since the new active sites created on the new released basal surface of clay will demand further polymer for adsorption. Thus, PCE units already intercalated could be partially de-absorbed and migrate to occupy the vacant adsorption positions located in the new external basal surface created by exfoliation

[28]. Therefore, clay exfoliation distortions the ratio between PCE content and the total reactive clay surface. In stoichiometry terms, the reactant PCE is moved towards limiting conditions. This statement is consistent with the simultaneous occurrence of new clay specimens having lower intercalation degree than that of the main unexfoliated main clay specimen. Moreover, exfoliation is a dynamic process of known kinetics, so it takes time to attain the equilibrium configuration [29].

For the specific Na-MNT clay used in this study, it is noted that from 80 Å, the structure of clay based on stacked plates is almost lost and, in parallel, exfoliation only begins if the interlayer d-spacing exceeds 60 Å. This behaviour suggests that the electrostatic forces stabilizing the layered structure become too weak between layers from beginning at 60 Å and they are almost largely ineffective upwards of 80 Å [30, 31]. In between these two distances, delamination of the peripheral layers from the primary clay particle is produced and new, additional basal surface is released, according the schematic representation shown in Figure 5.

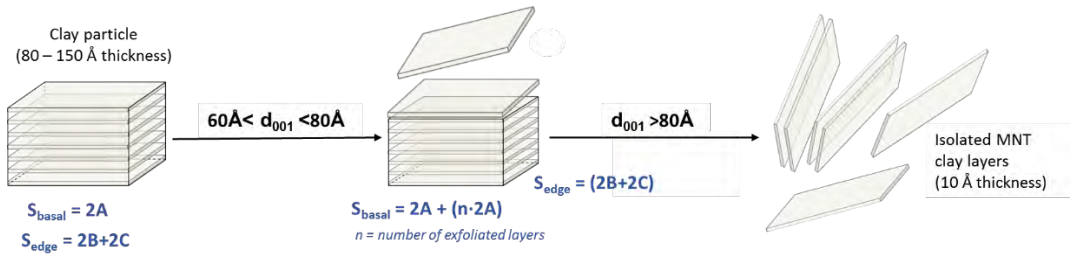

Figure 5. Representation of MNT clay exfoliation and impact on the exposed, accessible basal and edge surface (adapted from [26])

The simultaneous coexistence of clay specimens with different interlayer d-spacing is observed for all the PCE polymers except AA-1100. It is the polymer having the shortest side chain length and its d-spacing at the stationary state is lower than 60 Å, making it the smallest of all polymers tested. Thus, it is assumed that no relevant clay exfoliation is produced for AA-1100 (regardless of the release of isolated clay plates). Clay pastes with AA-2000 and AM-5800 polymers present the earliest exfoliation signature at 50% dosage, due to the highest side chain density. For both polymers, new released clay specimens with d-spacing values of 40-45 Å can be observed simultaneously to the main clay specimen having a larger d-spacing. For 220% dosage of AA-2000 and AM-5800, clay specimens with 40-45 Å d-spacing are no longer observed and only a specimen with 18.3 Å d-spacing coexists with the main clay specimen. With the AA-3000 polymer, clay exfoliation also produces new specimens with 42 Å interlayer d-spacing. Unlike AA-2000 and AM-5800, it is not observed until 100% dosage and it remains visible at 220% dosage, while the peak at 18.3 Å is not observed at any time. It is evident that

the clay exfoliation induced by AA-3000 progresses differently than that of AA-2000 and AM-5800 polymers.

Thus, the study concludes that PCE polymers with higher side chain density promote clay exfoliation more quickly and extensively than polymers such as AA-3000 that have large side chains but reduced side chain density. Nevertheless, for AA-1100, no exfoliation signatures can be observed despite having a higher side chain density than AA-3000. This result suggests that side chains of 1100 g/mol are not large enough to induce clay exfoliation. One could also propose that clay exfoliation not only depends on side chain density, but also on side chain length.

To support the interpretation of clay exfoliation and its consequences, Kratky plots from the *in-situ* XRPD patterns of AM-5800 polymer are presented in Figure 6(a). The diffraction patterns of AM-5800 obtained by *in-situ* XRPD analysis are presented in Figure 6(b).

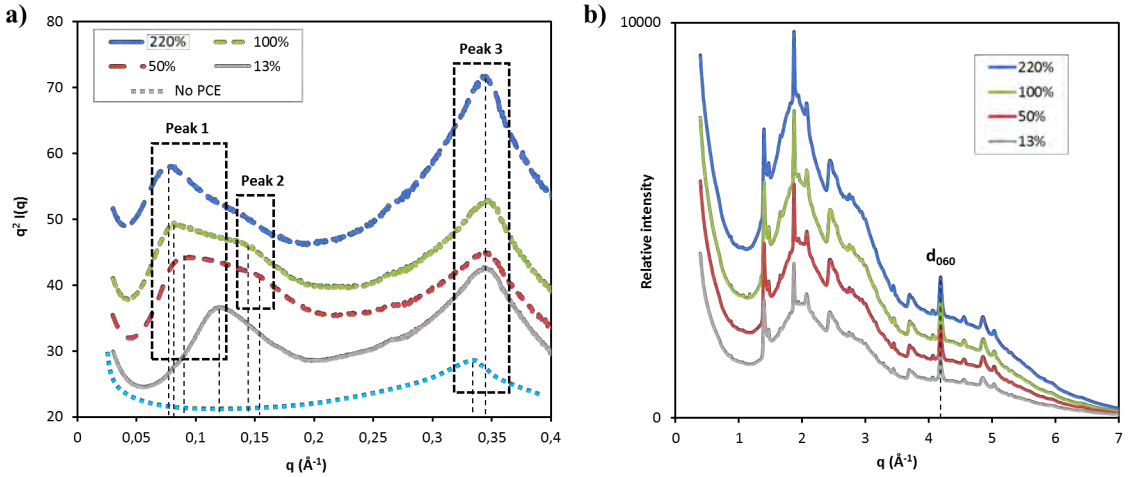

Figure 6. a) Kratky plot for AM-5800 patterns; b) *in-situ* XRPD patterns of clay pastes with AM-5800 polymer

The representation of Kratky plots for Na-MNT clay with an increasing dosage of AM-5800 polymer allows for the identification of up to three peaks corresponding to clay specimens with different degrees of intercalation. Peak 1 corresponds to the main clay specimen with the largest d-spacing, associated to a higher number of intercalated side chains [6]. It can be observed that Peak 1 is not present when clay paste does not contain any PCE and it is visible only in pastes containing a PCE polymer. Peak 1 is present at every PCE dosage but is being displaced as the polymer dosage increases. Peak 2 refers to clay specimens with 42-46 Å

interlayer d-spacing. This peak is not present in the clay pastes without a PCE polymer. Contrary to Peak 1, it is not fully recognized at the 13% PCE dosage.

Peak 2 becomes visible at the AM-5800 dosages of 50% and 100% and demonstrates higher intensity at 100% than at 50%. At 220% dosage Peak 2 becomes negligible, meaning that the corresponding clay specimens with 42-46 Å d-spacing are nearly absent, likely due to additional exfoliations. Peak 3 at 18.5 Å is characteristic of Na-MNT clay in calcium alkaline solution in the absence of PCE polymers. This d-spacing size is associated to three water molecules absorbed in the interlayer region [10].

Peak 3, originally at 18.5 Å, remains always visible but it is being displaced to 18.3 Å when clay pastes include a PCE polymer. This d-spacing size is compatible with two layers of water molecules surrounding one layer of PEG/PEO side chain intercalated [32]. This means the minimum configuration possible for PCE intercalation since only one single side chain is absorbed. As seen in Figure 6(a), the intensity of Peak 3 is similar at 13%, 50% and 100% dosage, but it increases at 220%.

This behaviour suggests that at a 220% dosage of AM-5800, the clay specimen with the minimum configuration of side chains intercalation is present in relevant amounts. This is a result of thinner clay particles that are produced by multiple delamination of the Na-MNT clay, which leads the PCE polymer to limiting stoichiometric balance against the enlarged clay surface.

One can observe that the shape of all peaks in the Kratky plots from Figure 6(a) becomes broader at an increased PCE dosage. This characteristic is observed in all the PCE polymers tested and is attributed to the increased content of structural defects including turbostratic disorder by layer stacking [4]. This phenomenon is represented in Figure 7.

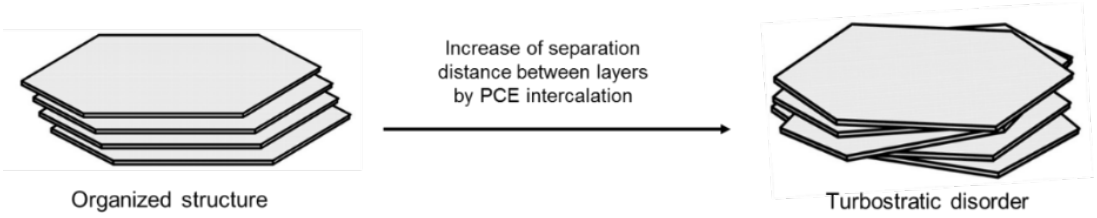

Figure 7. Illustration of turbostratic disorder by layer stacking (adapted from [33])

Since the distance between clay plates enlarges when the PCE dosage is increased, it makes sense to suggest that turbostratic disorder increases when the interlaminar space is being expanded by the intercalation of PCE side chains. Under these conditions, clay exfoliation can

be produced more easily [31]. Thus, it is hypothesized that the intercalation of PCE side chains has the capacity to promote exfoliation of montmorillonite clay and, as it is observed, this capacity increases in PCE polymers composed by large side chains and having high side chain density. An analogue behaviour is described in [34-38] by studying the effects of the length of linear PEO (poly-ethylene oxide) polymers for the synthesis of organo-clay nanocomposites from exfoliated clays, concluding that the longer the polymer chain, the higher the intercalation and the greater the exfoliation.

Observing the diffraction patterns presented in Figure 6(b), the initial d_{060} peak, key to following the intralayer structure of MNT clays, does not change at any PCE dosage. This firmly indicates that the polymer intercalation in the interlaminar space is produced along the *c*-axis (layer stacking), while the intralayer structure, the *ab* plane, does not change [10]. It means that the structural alterations produced by PCE intercalation only affects the layer arrangement forming the clay colloid; meanwhile, the structure of the single clay plates remains unaltered [39].

5.6 Saturation dosage of Na-MNT clay by intercalation of PCE side chains

Observing the evolution of the interlayer d-spacing from Figure 4(a) at the low dosage range of PCE admixture (at low PCE/clay ratio, where PCE is the limiting reactant), it can be noticed that the PCE polymers with the highest anionic charge (AA-3000 and AA-1100) produce a faster d-spacing increase.

Thus, at low PCE/clay ratio, PCE polymers with a high anionic charge can intercalate larger number of side chain layers and reach the stationary state at lower PCE dosage, likely promoted by their higher adsorption affinity.

The saturation of the interlaminar space of the clay by PCE intercalation is described as the dosage of PCE needed to reach the stationary state (the state in which the d-spacing remains nearly static in response to additional PCE dosage).

According to multiple intercalation mechanism proposed by [6], it is assumed to be the point at which the interlaminar space of MNT clay is saturated by intercalated PEO/PEG side chains, so almost no further units can be easily absorbed.

Figure 8(a) presents how the *saturation dosage* (D_{sat}, expressed as the percentage of PCE in the weight of clay) is calculated from the intersection point of the two lines, defined by the initial increase of d-spacing produced at a low dosage of PCE and the stationary state line.

Figure 8(b) displays the results of the saturation dosage - D_{sat} calculated for each studied PCE polymer.

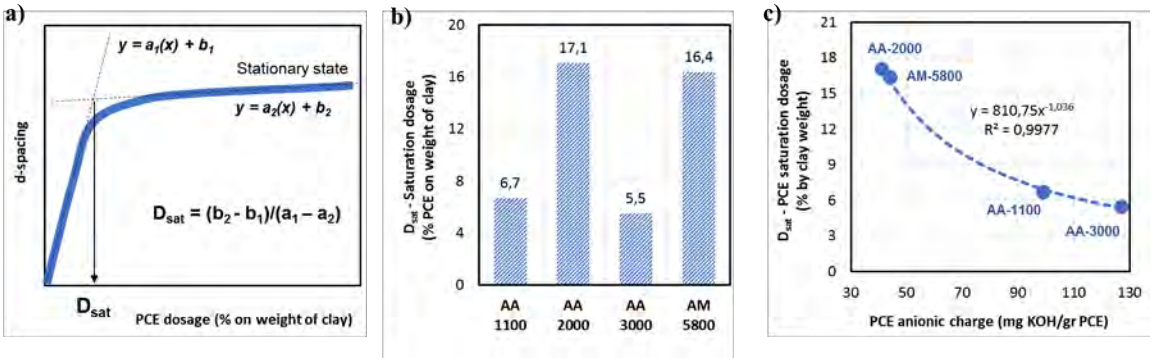

Figure 8. a) Methodology for D_{sat} – *saturation dosage* calculation; b) D_{sat} – *saturation dosage* of each PCE; c) Correlation between saturation dosage and PCE anionic charge

Since the anionic charge defines the affinity of PCE polymers to interact with the clay surface, a relationship between D_{sat} –saturation dosage and the PCE anionic charge is expected. As seen in Figure 8(c), the saturation dosage can be correlated with the PCE anionic charge. This relationship indicates that the saturation dosage decreases when the anionic charge of a PCE polymer increases but converges to a minimum residual value.

The reported type of relationship between the saturation dosage and PCE anionic charge seems more likely than just a linear correlation as this would mean that PCE polymers with very high anionic charge would reach a saturation dosage equal to 0. That would imply that for practical purposes, there would be no intercalation.

5.7 Sorption isotherms of PCE polymers on MNT clay

The results of the net sorbed amount of PCE measured in clay pastes containing increasing PCE dosages are presented in Table 6.

To identify the relative variations in the sorption rate at each PCE dosage, Figure 9(a,b) displays the relative incremental of sorbed PCE (S_{rel}). It is calculated using the expression $\Delta S(x)_{rel} = (S_x - S_y)/(D_x - D_y)$, where $\Delta S(x)_{rel}$ means the relative incremental of sorption at a PCE dosage of D_x (expressed as mg PCE/g clay), S_x is the sorbed amount at the D_x dosage and S_y is the sorbed amount at the previous PCE dosage (D_y).

PCE dosage (% by weight of clay)	Net sorbed amount of PCE on clay (mg/g)			
	AA-1100	**AA-2000**	**AA-3000**	**AM-5800**
0%	0	0	0	0
2%	19 ± 3	17 ± 2	20 ± 1	18 ± 3
5%	48 ± 6	36 ± 4	50 ± 2	43 ± 5
13%	90 ± 8	68 ± 6	107 ± 9	75 ± 3
50%	163 ± 13	143 ± 10	181 ± 6	188 ± 14
100%	204 ± 9	226 ± 15	228 ± 12	243 ± 11
150%	216 ± 12	259 ± 13	243 ± 16	290 ± 19
220%	218 ± 11	277 ± 13	263 ± 17	308 ± 21

Table 6. Net sorbed amount of PCE in clay pastes with increasing PCE dosages, including the standard deviation of the experimental results

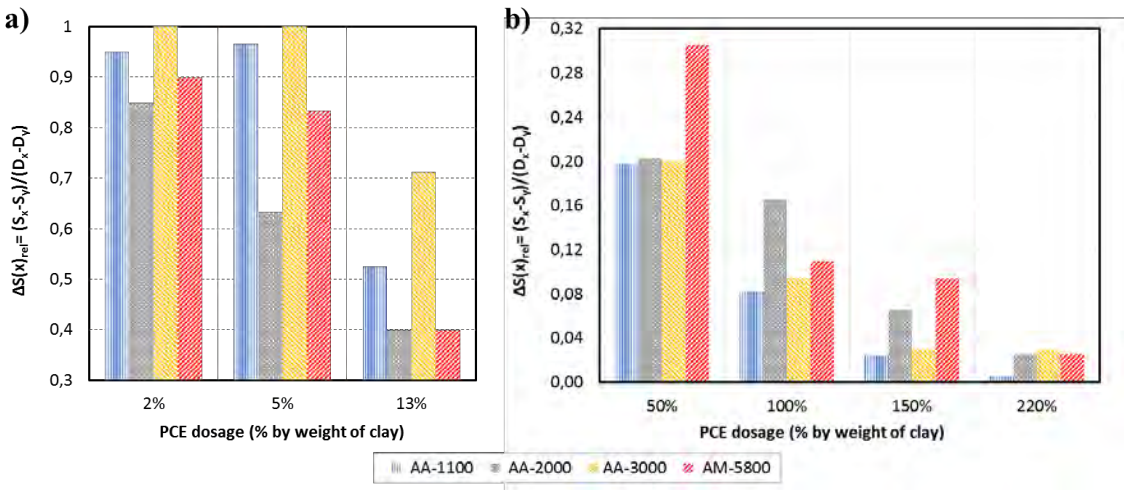

Figure 9. Relative incremental of sorption (ΔS_{rel}) at each PCE dosage; a) From 2% to 13% PCE dosage; b) From 50% to 220% PCE dosage

Interestingly, the relative incremental of sorbed PCE presented in Figure 9 is consistent with both the expansion profile of the clay and the exfoliation behaviour deducted from the XRPD patterns. At a low PCE/clay dosage ratio (Figure 9(a)), the PCE polymers with a higher anionic charge (AA-1100 and AA-3000) experience the greatest incremental of sorption, showing ΔS_{rel} values close to 1. It means that nearly 100% of the added polymer is being sorbed by the clay. It is the expected trend because the affinity for adsorption is driven by the PCE anionic charge. Conversely, when PCE/clay dosage ratio increases, Figure 9(b) demonstrates

that the greatest relative incremental of sorption is experienced by the AA-2000 and AA-5800 polymers. These are the PCE polymers with the highest side chain density, thus the polymers that are expected to promote the greatest clay exfoliation. Therefore, the trend observed in the sorption rates supports the proposed interpretation in regards of the consequences of the new, additional basal clay surface released by exfoliation.

5.8 Intercalation degree of PCE side chains

The number of PEO/PEG side chain units intercalated into Na-MNT clay can be calculated from the d-spacing results following the methodology proposed in [6]. Figure 10 presents the intercalation degrees (n_{PEG}) obtained for PCE polymers at each tested dosage, including the main clay specimen and the clay specimens likely originated by exfoliation.

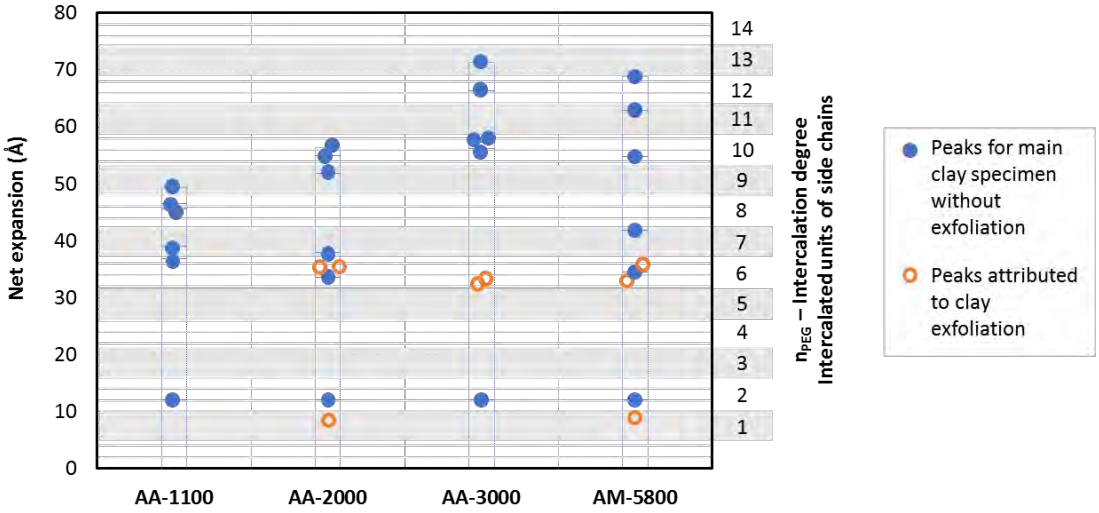

Figure 10. Intercalation degrees (n_{PEG}) of PCE side chains into Na-MNT clay

It is interesting to see that there are some *preferred degrees of intercalation* present in almost all PCE polymers. For the clay sample used, these preferred degrees are n_{PEG}= 6-7 and n_{PEG}= 9-10. Conversely, intercalation degrees corresponding to 3, 4 and 5 units of PEO/PEG side chains are not observed in any case. This behaviour suggests that some intercalation degrees are more stable than others and they are presumably defined by the properties of the clay and not by the PCE polymer.

For all the new clay specimens produced by exfoliation, two intercalation degrees are only identified. The first observed specimen from exfoliation always presents six units of intercalated side chains (n_{PEG}= 6). This intercalation degree is visible for all the PCE polymers

that are able to produce clay exfoliation (AA-2000, AA-3000 and AM-5800) but it is also commonly observed in the main, unexfoliated clay specimens, which suggests that it is a very stable configuration. Further exfoliation generates clay specimens with only one single intercalated side-chain layer (n_{PEG}= 1, at18.3 Å d-spacing), which corresponds to the minimum possible configuration of intercalation. The intercalation degree n_{PEG}= 1 is exclusively observed in PCE polymers with high side chain density like AA-2000 and AM-5800 and it is not present in AA-3000, which only produces exfoliated specimens with n_{PEG}= 6 (six intercalated side-chain layers).

Using Figure 10, it is also observed that a 2% dosage of any of the PCE polymers always produce the same intercalation degree of n_{PEG}= 2, with two units of side chains intercalated. Therefore, considering that the Na-MNT clay dispersed in calcium alkaline media presents an interlayer d-spacing equivalent to three water molecule layers absorbed into the interlaminar space [10] and, in parallel, the intercalation degree produced at the lowest PCE dosage always corresponds to two units of side chains (n_{PEG}= 2), it suggests that the mechanism of side chain intercalation is not based on the replacement of the absorbed water layers, but by the insertion of the PEO/PEG side chains in between the water layers that are already absorbed.

6. INTERPRETATION OF THE INTERCALATION MECHANISM OF SIDE CHAINS

It has been observed that the anionic charge of PCE is the main driver force defining the PCE dosage to saturate the interlaminar space of the clay. PCE polymers with higher anionic charge promote the adsorption of polymer on the clay surface, allowing it to reach the saturation dosage sooner.

In parallel, PCE polymers with longer side chain length and especially those with higher side chain density have an increased tendency to produce clay exfoliation. Therefore, for these polymeric structures, a greater fluidity loss and a higher level of sorption is expected due to the generation of new basal surface area produced when clay exfoliates. In this way, the results of relative reduction of paste flow presented in Figure 2(b) and the relative incremental of sorption presented in Figure 9(b) for AA-2000 and AA-5800 polymers match with this hypothesis, since these are the polymers with the highest side chain density.

Conversely, the AA-1100 polymer, having reduced side chain density and the shortest side chains, shows the lowest degree of intercalation. This behaviour aligns with the lowest reduction of paste flow observed in Figure 2(b) and with the lowest sorption rate at high dosage

of AA-1100, in Figure 9(b). Nevertheless, the AA-3000 polymer, having lower side chain density than AA-1100, demonstrates a fluidity loss profile more similar to AM-5800 than that of the AA-1100. This behaviour of the AA-3000 polymer can be attributed to its side chain length (which falls in between those of polymers AA-2000 and AM-5800).

Consequently, it can be proposed that the clay exfoliation induced by the intercalation of PCE polymers depends on the concentration of side chains in the edge opening between clay plates (being higher in the case of high side chain density) and on the capacity of the side chains to penetrate into the interlaminar space (being deeper in the case of large side chains [40]). This interpretation is consistent with the relative incremental of sorption presented in Figure 9(b) for the AA-300 polymer.

Based on this reasoned hypothesis, a model for the intercalation behaviour of PCE side chains into Na-MNT clay is presented in Figure 11 considering the adsorption location of the polymer. Since MNT clays that are dispersed in alkaline cement pore solution cumulates anionic charges in both the edge surface (by the ionization of the silanol, aluminate pH dependant terminals) and the basal surface (by the ionization of soluble cations balancing the permanent charges induced by octahedral substitution) [41-44], it is assumed that PCE polymers can be adsorbed on both clay locations.

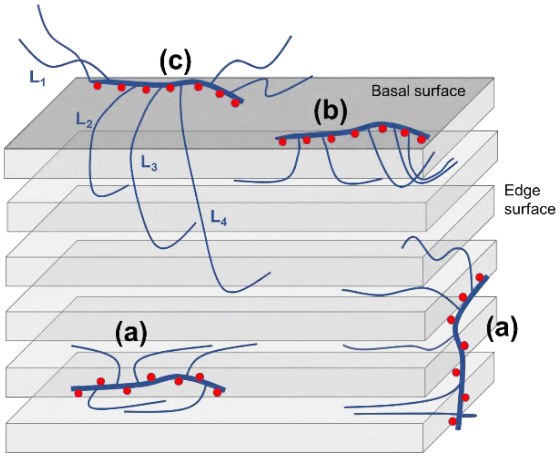

Figure 11. Intercalation models of side chains of PCE polymers depending on the adsorption location of the PCE on the Na-MNT clay surfaces (not at scale)

PCE units adsorbed on the edge surface -case (a) in Figure 11- will be easily intercalated, since the distance to the interlayer openings is reduced and accessible, even for PCE having short side chains.

The side chains of PCE units adsorbed in the basal surface of Na-MNT clay also can be intercalated if the location of adsorption is near the edge area -case (b) in Figure 10-, since the rotation of -C-O-C- bonds allows the side chains to be displayed optimally for intercalation. When the PCE units are adsorbed in the central locations of the basal surface -case (c)-, intercalation will only be possible if PCE side chains are long enough to rotate and reach the interlayer openings. Since the typical thickness/width ratio for montmorillonite clay is up to 1/200 [45], most PCE units adsorbed on the basal planes will be located too far to intercalate their side chains, except for PCE polymers with very long side chains.

This hypothesis justifies the behaviour of the AA-3000 polymer, which shows the largest d-spacing at the stationary state with similar value to AM-5800. The same argument is valid for AA-1100, which presents the lowest d-spacing, since the accessibility to the interlaminar spaces is restricted by its short side chains. The stationary d-spacing for AA-2000 is larger than AA-1100, but lower than both AA-3000 and AM-5800, despite having the highest side chain density. Once again, the same interpretation fits because AA-2000 contains shorter side chains than AA-3000 and AM-5800 but longer than AA-1100, thus limiting the intercalation of PCE units adsorbed on the basal surface of the clay but in a lesser extent than for AA-1100.

7. CONCLUSIONS

Using *In-situ* XRPD analysis on fresh, unaltered MNT pastes containing PCE-based superplasticizers, a new scenario for the intercalation behaviour of PCE side chains is revealed. The influence of the polymeric structure of the PCE on the intercalation behaviour can be distinguished from the d-spacing results and the experimental data of clay expansion allows for the establishment of a logic relationship with the results of paste flow loss and sorption behaviour.

Contrary to conclusions drawn from XRPD analysis performed on dried clay pastes, *in-situ* XRPD analysis on fresh, unaltered clay pastes confirms that the polymeric structure of PCE-based superplasticizers has a key role in the progression of the side chain intercalation and the evolution of the interlayer d-spacing, while meeting alignment with the experimental results of paste flow and sorption rate. The major parameters of the structure of PCE polymers influencing on the intercalation behaviour into Na-MNT clay are identified below:

- When the PCE/clay ratio is high, clay exfoliation is produced, generating additional exposed, accessible clay surface. It forces a reorganization of PCE arrangement around

the clay colloid. As consequence of clay exfoliation, there is an amplified impact on the fluidity loss. Experimental results of paste flow loss in cement pastes at low clay dosage support this scenario.

- PCE polymers with high side chain density produces earlier and more severe exfoliation, leading to an increase of fluidity loss even at a very high PCE/clay ratio (in which a very low amount of clay is present in the cement pastes).
- Maximum d-spacing (stationary d-spacing) is produced at the stationary state, when the PCE/clay ratio is highest. Stationary d-spacing is larger for PCE polymers having long side chains but is restricted by the stability of the clay structure (which exfoliates from a certain d-spacing value).
- When the PCE/clay ratio is low, d-spacing progression is controlled by the adsorption capacity, thus, by the anionic charge of the PCE polymer. Polymers with a higher anionic charge saturate the interlaminar space of the clay at a lower PCE/clay ratio.

Consequently, examining the d-spacing perspective, a consistent explanation has been found to justify that the PCE polymers with large side chains and high side chain density present higher sensitivity to MNT clays than PCE structures with shorter side chains and reduced side chain density. It matches with the behaviour observed with the AA-1100 polymer, which is the PCE with the lowest sensitivity to MNT clay within all polymers used.

Additionally, a new model is presented that explains the relationship between the structure of PCE polymers and the intercalation mechanism of side chains into MNT clays. This model is endorsed by the consistency between experimental results of paste flow and sorption rate and the d-spacing values obtained by *in-situ* XRPD measurements.

To complement this investigation and its corresponding conclusions, additional research is suggested to identify the influence of the PCE molecular weight in the intercalation behaviour. In addition, the potential influence of Na-MNT properties in the d-spacing evolution has not been investigated (either the octahedral substitution rate or shape and size of clay particles). Finally, the potential impact of mixing speed and shear energy and their influence on clay exfoliation and side chains intercalation degree is a topic for investigation.

Acknowledgments

Mr. Borralleras thanks all the support given by BASF Construction Chemicals to the development of this work. Dr. I. Segura is supported by the postdoctoral Torres Quevedo program of the Spanish Ministry of Economy and Competitiveness.

References

[1] L. Lei, J. Plank, Synthesis and properties of a vinyl ether-based polycarboxylate superplasticizer for concrete possessing clay tolerance, Industrial & Engineering Chemistry Research 53 (2014) 1048-1055. https://pubs.acs.org/doi/abs/10.1021/ie4035913

[2] H. Tan, Xin Li, M. Liu, B. Ma, B. Gu, X. Li, Tolerance of cement for clay minerals: effect of side-chain density in polyethylene oxide (PEO) superplasticizers additives, Clay and Clay Minerals 64-6 (2016) 732-742. https://doi.org/10.1346/CCMN.2016.064050

[3] H. Tan, B. Gu, B. Ma, X. Li, C. Lin, Mechanism of intercalation of polycarboxylate superplasticizer into montmorillonite, Applied Clay Science 129 (2016) 40-46. https://doi.org/10.1016/j.clay.2016.04.020

[4] S. Ng, J. Plank, Interaction mechanisms between Na-montmorillonite clay and MPEG-based polycarboxylate superplasticizers, Cement and Concrete Research 42 (2012) 847-854. https://doi.org/10.1016/j.cemconres.2012.03.005

[5] G. Xing, W. Wang, G. Fang, Cement dispersion performance of superplasticizers in the presence of clay and interaction between superplasticizers and clay, Advances in Cement Research 29 (2017) 194-205. https://doi.org/10.1016/j.arabjc.2017.12.027

[6] P. Borralleras, I. Segura, M. A. G. Aranda, A. Aguado, Influence of experimental procedure on d-spacing measurement by XRD of montmorillonite clay pastes containing PCE based superplasticizer, Cement and Concrete Research 116 (2019) 266-272. https://doi.org/10.1016/j.cemconres.2018.11.015

[7] S. Qian, H. Jiang, B. Ding, Y. Wang, C. Zheng, Z. Guo, Synthesis and performance of polycarboxylate superplasticizer with clay-inerting and high slump retention capability, Materials Science and Engineering 182 (2017). https://doi.org/10.1088/1757-899X/182/1/012033

[8] D. Atarashi, K. Yamada, A. Ito, M. Miyauchi, E. Sakai, Interaction between montmorillonite and chemical admixture, Journal of Advanced Concrete Technology 13 (2015) 325-331. https://doi.org/10.3151/jact.13.325

[9] R. Magarotto, I. Torresan, N. Zeminian, Effect of alkaline sulphates on the performance of superplasticizers. In: 11th International congress on the chemistry of cement (2003) 569–579.

[10] M. Matusewicz, K. Pirkkalainen, J.P. Suuronen, A. Root, A. Muurinen, R. Serimaa, M. Olin, Microstructural investigation of calcium montmorillonite, Clay Minerals 48 (2013) 267-276. https://doi.org/10.1180/claymin.2013.048.2.08

[11] D.L. Rowell, Soil science: methods and applications. Longman Scientific and Technical Publications, ISBN 0-470-22141-0 (1993) 133.

[12] A. Checchetti, J. Lanzo, Qualitative measurement of pH and mathematical methods for the determination of the equivalence point in volumetric analysis, World Journal of Chemical Education 3 (2015) 64-69. http:// doi.org/10.12691/wjce-3-3-2

[13] H. Tan, B. Gu, Y. Guo, B. Ma, J. Huang, J. Ren, F. Zou, Improvement in compatibility of polycarboxylate superplasticizers with poor-quality aggregate conatining montmorillonite by incorporating polymeric ferric sulfate, Construction and Building Materials 162 (2018) 566-575. https://doi.org/10.1016/j.conbuildmat.2017.11.166

[14] J. Plank, B. Sachsenhauser, Experimental determination of the effective anionic charge density of polycarboxylate superplasticizers in cement pore solution, Cement and Concrete Research 39 (2009) 1-5. https://doi.org/10.1016/j.cemconres.2008.09.001

[15] D. Wilinski, P. Lukowski, G. Rokicki, Polymeric superplasticizers based on polycarboxylates for ready-mixed concrete: current state of the art, Polimery 61 (2016) 474-481. https://doi.org/10.14314/polimery.2016.474

[16] R. J. Flatt, I. Schober, E. Raphael, C. Plassard, E. Lesniewska, Conformation of adsorbed comb copolymers dispersants, Langmuir 25 (2009) 845-855. https://doi.org/10.1021/la801410e

[17] X. Shu, Q. Ran, J. Liu, H. Zhao, Q. Zhang, X. Wang, Y. Yang, Tailoring the solution conformation of polycarboxylate superplasticizer toward the improvement of dispersing performance in cement paste, Construction and Building Materials 116 (2016) 289-298. https://doi.org/10.1016/j.conbuildmat.2016.04.127

[18] G. Xing, W. Wang, J. Xu, Grafting tertiary amine groups into the molecular structures of polycarboxylate superplasticizers lowers their clay sensitivity, RSC Advances 6 (2016) 106921-106927. https://doi.org/110.1039/C6RA22027D

[19] C. Zhi Li, N. Feng, Y. De Li, R. Chen, Effects of polyethylene oxide chains on the performance of polycarboxylate-type water-reducers, Cement and Concrete Research 25 (2005) 867-873. https://doi.org/10.1016/j.cemconres.2004.04.031

[20] J. Liu, Q. Ran, C. Miao, M. Qiao, Effects of grafting densities of comb-like copolymer on the dispersion properties of concentrated cement suspensions, Materials Transactions 53 (2012) 553-558. https://doi.org/10.2320/matertrans.M2011344

[21] L. Lei, J. Plank, A study on the impact of different clay minerals on the dispersing force of conventional and modified vinyl ether based polycarboxylate superplasticizers, Cement and Concrete Research 60 (2014) 1-10. https://doi.org/10.1016/j.cemconres.2014.02.009

[22] C. Giraudeau, J. d´Espinose de Lacaillerie, Z. Souguir, Surface and intercalation chemistry of polycarboxylate copolymers in cementitious systems, Journal of the American Ceramic Society 92 (2009) 2471-2488. https://doi.org/10.1111/j.1551-2916.2009.03413.x

[23] M. Szczerba, Z. Klapyta, A. Kalinichev, Ethylene glycol intercalation in smectites. Molecular dynamics simulation studies, Applied Clay Science 91 (2014) 87-97. https://doi.org/10.1016/j.clay.2014.02.014

[24] H. Li, Y. Zhao, S. Song, Y. Hu, Y. Nahmad, Delamination of Na-montmorillonite particles in aqueous solutions and isopropanol under shear forces, Journal of Dispersion Science and Technology 38 (2017) 1117-1123, https://doi.org/10.1080/01932691.2016.1224720

[25] X. Zhang, H. Yi, H. Bai, Y. Zhao, F. Min, S. Song, Correlation of montmorillonite exfoliation with interlayer cations in the preparation of two-dimensional nanosheets, RSC Advances 7 (2017) 41471-41478. https://doi.org/10.1039/C7RA07816A

[26] J. Torres-Lunam J. G. Carriazo, N. R. Sanabria, Arcillas delaminadas por especies de titanio – degradación de un colorante textil (amarillo reactivo 145), Proceedings XXIV Congreso Iberoamericano de Catálisis (2014) 112-119.

[27] E. C. Jonas, R. M. Oliver, Size and shape of montmorillonite crystallites, Clay and Clay Minerals 15 (1967) 27-33. https://doi.org/10.1346/CCMN.1967.0150103

[28] N. Güven, Smectites – Hydrous phyllosilicates, Reviews in Mineralogy 19 (1988) 497-560.

[29] S.W. Kim, W.H. Jo, M.S Lee, M.B. Ko, J.Y. Jho, Effects of shear on melt exfoliation of clay in preparation of Nylon 6/organoclay nanocomposites, Polymer Journal 34 (2002) 103-111. https://doi.org/10.1295/polymj.34.103

[30] T. Chen, Y. Yuan, Y. Zhao, F. Rao, S. Song, Effect of layer charges on exfoliation of montmorillonite in aqueous solutions, Colloids and Surfaces: Physicochemical and Engineering aspects 548 (2018) 92-95. https://doi.org/10.1016/j.colsurfa.2018.03.066

[31] R.F. Geise, The electrostatic interlayer forces of layer structure minerals, Clay and Clay Minerals 26 (1978) 51-57. https://doi.org/10.1346/CCMN.1978.0260106

[32] R. Ait-Akbour, P. Boustingorry, F. Leroux, F. Leising, C. Taviot-Guého, Adsorption of polycarboxylate poly(ehtylene glycol) (PCP) esters on montmorillonite (MNT): Effect of exchangeable cations (Na^+, Mg^{2+} and Ca^{2+}) and PCP molecular structure, Journal of Colloid and Interface Science 437 (2015) 227-234. https://doi.org/10.1016/j.jcis.2014.09.027

[33] A. Meunier, Why are clay minerals small?, Clay Minerals 41 (2006) 551-566. http://dx.doi.org/10.1180/0009855064120205

[34] S. Zhu, H. Peng, J. Chen, H. Li, Y. Cao, Y. Yang, Z. Feng, Intercalation behaviour of poly(ethylene glycol) in organically modified montmorillonite, Applied Surface Science 276 (2013) 502-511. https://doi.org/10.1016/j.apsusc.2013.03.123

[35] A. Kobayashi, M. Kawaguchi, T. Kato, A. Takahashi, Intercalation adsorption of poly(ethylene oxide) into montmorillonite, Kyoto University – Bulletin of the Institute for Chemical Research 66 (1989) 176-183.

[36] M. Reinholdt, R. Kirkpatrick, T. Pinnavala, Montmorillonite-poly(ethylene glycol) nanocomposites: interlayer alkali metal behaviour, The Journal of Physical Chemistry 109 (2005) 16296-16303. https://doi.org/10.1021/jp052601o

[37] T. Okada, Y. Seki, M. Ogawa, Designed nanostructures of clay for controlled adsorption of organic compounds, Journal of Nanoscience and Nanotechnology 14 (2014) 2121-2134. https://doi.org/10.1166/jnn.2014.8597

[38] R.W. Franco, C. Brasil, G. Mantovani, E. de Azevedo, T. Bonagamba, Molecular dynamics of poly(ethylene glycol) intercalated in clay, studied using ^{13}C solid-state NMR, Materials 6 (2013) 47-64. https://doi.org/10.3390/ma6010047

[39] R. Tettenhorst, H. E. Roberson, X-Ray diffraction aspects of montmorillonite, American Mineralogist 58 (1973) 73-80.

[40] H. Li, Y. Zhao, T. Chen, Y. Nahmad, S. Song, Restraining Na-montmorillonite delamination in water by adsorption of sodium dodecyl sulfate or octadecyl trimethyl ammonium chloride on the edges, Minerals 6 (2016) 87-97. https://doi.org/10.3390/min6030087

[41] T. Preocanin, A. Abdelmonem, G. Montavon, J. Luetzenkirchen, Charging behaviour of clays and clay minerals in aqueous electrolyte solutions. Experimental methods for measuring the charge and interpreting the results – Clays, clay minerals and ceramic materials based on clay minerals, ISBN 978-953-51-2259-3 (2016). https://doi.org/10.5772/62082

[42] X. Liu, X. Lu, M. Sprik, J. Cheng, E.J. Meijer, R. Wang, Acidity of edge surface sites of montmorillonite and kaolinite, Geochimica et Cosmochinica Acta 117 (2013) 180-190. https://doi.org/10.1016/j.gca.2013.04.008

[43] M. Alvarez-Silva, M. Mirnezami, A. Uribe-Salas, J. A. Finch, Point of zero charge, isolelectric poit and aggregation of phyllosilicate minerals, Canadia Metallurgical Quarterly 49 (2010) 405-410. https://doi.org/10.1179/cmq.2010.49.4.405

[44] E. Tombácz, M. Szekeres, Colloidal behaviour of aqueous montmorillonite suspensions: the specific role of pH in the presence of indifferent electrolytes, Applied Clay Science 27 (2004) 75-94. https://doi.org/10.1016/j.clay.2004.01.001

[45] R. Holtz, W. Kovacs, An introduction to geotechnical engineering, ISBN 013-484394-0 (1981), Prentice-Hall Inc.

3.3. JOURNAL PAPER III

ABSORPTION CONFORMATIONS IN THE INTERCALATION PROCESS OF POLYCARBOXYLATE ETHER-BASED SUPERPLASTICIZERS INTO MONTMORILLONITE CLAY

Published in Construction and Building Materials (August 2019) 116657.

Pere Borralleras[a], Ignacio Segura[b, c,*], Miguel A. G. Aranda[d] and Antonio Aguado[b]

[a] BASF Construction Chemicals Iberia, Ctra del Mig 219, E-08907 Hospitalet de Llobregat, Barcelona, Spain

[b] Department of Environmental and Civil Engineering, Universitat Politècnica de Catalunya-Barcelona Tech, Jordi Girona 1-3, C1, E-08034 Barcelona, Spain

[c] Smart Engineering Ltd, Jordi Girona 1-3, ParcUPC–K2M, E-08034 Barcelona, Spain

[d] ALBA Synchrotron, Carrer de la Llum 2-26, E-08290, Cerdanyola del Vallès, Barcelona, Spain

* Corresponding author: Ignacio Segura, Department of Environmental and Civil Engineering, Universitat Politècnica de Catalunya-Barcelona Tech, Jordi Girona 1-3, C1, E-08034 Barcelona, Spain. Email address: ignacio.segura@upc.edu Tel: +34 93 4054684

Abstract

The intercalation of polycarboxylate based superplasticizers (PCE) into montmorillonite clay (MNT) is arranged preferably by two types of absorption conformations: *one-to-one* conformation and *bridging* conformation. A third model named *plugged* conformation is described but it seems not appropriate to polymers having anionic charge and it would be possible only for very particular cases. The preferred conformation of absorption of the PCE polymer is determined by key properties of the polymer and the clay. For the polymer, the two main characteristics are the length of side chains and the side chain density.; For the MNT clay, the mains properties are the layer charge and to a lesser extent the morphology of the clay particle. PCE anionic charge is not a determining factor for the absorption conformation but is a key factor for the earlier saturation of the interlaminar space by intercalation. Since many variables are interplaying simultaneously and complementarily, the interaction process between PCE polymers and MNT clays is very complex that deserves further studies.

Keywords: Polycarboxylate, montmorillonite, conformation, intercalation, absorption, adsorption

1. INTRODUCTION

Concrete technology made a breakthrough with the introduction of polycarboxylate based superplasticizers (PCE) at the end of the 90´s [1]. Using PCE technology, it is possible to produce advanced concretes with improved fresh and mechanical properties [2], which are impossible to be achieved with the predecessor water-reducers admixtures. The advances made by PCE technology have been such to the point that new concrete types like self-compacting concrete and more recently ultra-high performance concrete [3,4] are possible nowadays.

Despite all the positive contributions made by this new chemistry, there is a point pending of improvement for PCE based admixtures related to their compatibility with sands of limited quality. It is well known that sands containing small quantities (<0,5%) of some specific clay types produce several affectations in the performance of PCE-based superplasticizers [5]. These clays are those that have swelling properties, such as smectite-montmorillonite clays [5-7], and they are able to totally inhibit the dispersing capacity of PCE polymers.

The interaction between clays and PCE polymers has been widely studied [8-16]. One of the most relevant conclusions from these investigations is the fact that montmorillonite clays

(MNT) can absorb PCE polymers from the intercalation of their PEG/PEO based side chains. The understanding of the intercalation mechanism has been complemented thanks to the measurements of interlayer d-spacing using *in situ* XRPD analysis on fresh, unaltered clay pastes [17].

Using this methodology, it is demonstrated that the expansion of MNT clays produced by the intercalation of PCE side chains is larger than that deduced from the aforementioned studies and revels the true influence of the structure of PCE polymers in the affinity for intercalating inside montmorillonite clays, as presented by the authors in [18]. None of these observations can be clearly identified by the typical analytical method used to measure the interlayer d-spacing, which is based on XRPD analysis performed on centrifuged and dried clay pastes [17].

This work is part of our ongoing research effort to better understand the interaction of PCE with clays [17,18] with the final aim to develop clay-resistant PCEs. In order to do so, the interaction between MNT and PCE polymers must be unravelled.

The objective of this investigation is to complement the models for the intercalation mechanism on the basis of the information offered by the interlayer d-spacing measurements of MNT clay with *in situ* XRPD analysis, as well as to identify the main aspects and the determining factors that control and direct this process.

2. MATERIALS

2.1 Cement

Cement used is a CEM I 52.5R. Table 1 presents oxide and mineral phase composition of the anhydrous cement (expressed in wt. %), determined by XRF (X-ray fluorescence) and Rietveld. The Blaine value reported in cement specifications is 4750 cm^2/g. The measured BET-specific surface is 1.6 m^2/g and the particle size (D_{50}), determined by laser diffraction, is 10 μm.

For the reproducibility of the experimental results obtained in this study, it should be stated that the amount of orthorhombic C_3A of cement is very low, while its sulphate content is high. This feature is important when conditioning the levels of adsorption of the admixtures [19].

Oxide composition (wt. %)		Mineral phases (wt. %)	
SiO_2	19.60	C_3S	58.9
Al_2O_3	5.38	C_2S	14.0
Fe_2O_3	2.41	C_3A total	9.4
CaO	65.29	C_3A ort/cub	99% cubic
Na_2O	0.05	$C_4(A,F)$	5.7
K_2O	0.84	$M_X(SO_4)$	5.5
MgO	0.82	Total	93.5
SO_3	3.34		
LOI	2.18		

Table 1. Oxide composition and mineral phases of anhydrous cement used

2.2 Sodium montmorillonite clay (Na-MNT)

The clay used in this investigation is a powder sodium montmorillonite (Na-MNT) sample. Oxide composition by XRF is shown in Table 2 (expressed in wt. %). The BET-specific surface is measured at 49.5 m^2/g (average of two measurements: 46.1 m^2/g and 52.8 m^2/g) and the average particle size (D_{50}), determined by laser diffraction, is 7.4 μm.

A d_{001} value of 12.3 Å is deduced from its 2θ position at 7.2º in XRPD analysis on raw (dry) clay powder. This value is typical for Na-MNT clays with one H_2O molecule layer inside the interlaminar space [11,17]. Some impurities are identified: 4.8 wt.% of quartz and 3.3 wt.% of calcite, which explains the loss-on-ignition (LOI) value and the amount of CaO identified. Before its use, the powder clay is dried at 70 ºC for 48 hours to remove its residual moisture.

Oxide composition of Na-MNT (wt. %)										
SiO_2	TiO_2	Al_2O_3	Fe_2O_3	MgO	MnO	NiO	CaO	K_2O	Na_2O	LOI
63.12	0.01	19.88	1.37	2.33	0.04	0.06	2.24	0.44	3.43	5.97

Table 2. Oxide composition of MNT clay used

2.3 Water-reducer/superplasticizer polymers

Two different pure polycarboxylate ether (PCE) polymers presented in aqueous solution are used (PCE-1100 and PCE-5800). Complementary to the PCE polymers, two PCE polymers blocked for adsorption (XPE-1100 and XPE-5800) are used in this investigation. The blockage of the free carboxylic groups (which are the promoters for the surface adsorption) is obtained by esterification of the carboxylic monomers of the PCE backbone and by the direct

polymerization of hydrolysable monomers, which allows to disable the effective anionic charge of the polymer [20].

By blocking the free carboxylic groups, XPE polymers cannot be adsorbed until the esterified terminals are released by hydrolysis (normally, from 30 to 60 minutes after mixing). Therefore, since the adsorption at an initial time is not possible, the blocked PCE polymers (XPE) are not able to generate any fluidification effect until the esterified carboxylic groups are not unblocked by hydrolysis.

Table 3 presents the characteristics of the PCE and XPE polymers used. The side chain frequency and the side chain density are calculated from the PCE anionic charge, determined by titration with KOH [18].

Parameter		PCE-1100	PCE-5800	XPE-1100	XPE-5800
Solid concentration (wt. %)		50.3%	46.4%	45.7%	42.2%
Main backbone monomer		Acrylic	Maleic	Acrylate-ester	
Anionic charge (mg KOH/g PCE)		99	44	--	--
Side chains	Type	IPEG	VPEG	IPEG	VPEG
	mol EO/side chain	25	132	25	132
	Mw (g/mol)	1100	5800	1100	5800
Side chain frequency (molar ratio side chain/backbone)		0.31	0.29	Not determined	
Side chain density (mol EO · side chain frequency)		7.8	38.3		

Table 3. Chemical structure and composition of PCE polymers

Complementary to the PCE and XPE polymers, a 60 wt.% solution of a linear sodium polymethacrylate polymer (PMA) with a molecular weight of 8000 g/mol and a calcium salt of β-naftalensulfonate-formaldehyde polymer (Ca-BNS) at 40 wt.% concentration are used for comparison purposes. All admixtures are tested at an equal solid concentration of 40 wt.%, prepared by dilution with distilled water.

2.4 Non-ionic polymers

Table 4 presents the four selected non-ionic, non-water-reducer polymers without any dispersing property (MPEG-500, PEO-4000 and APEO-440), used to support in the interpretation of the interaction conformations of the PCE polymers.

Non-ionic polymer	Composition	Mw (g/mol)	Structure	Calculated length (Å)
MPEG-500	Methoxy-polyethylene glycol	500	Linear	37
PEO-4000	Polyethylene oxide (91 EO)	4000	Linear	296
APEO-440	10-EO Ethoxylated nonylphenol	660	Linear	41

Table 4. Structure and composition of non-ionic polymers

The selection of non-ionic polymers is made to compare linear polymers of equal length but different polarity and of equal polarity but different length, that help the interpretation of the results. A comparison of the polymer length fof MPEG-500, APEO-440 and PEO-4000 is given in Figure 1.

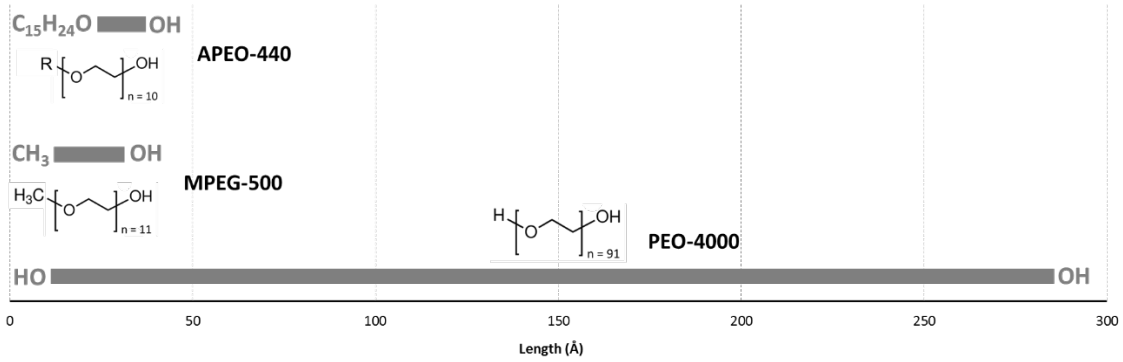

Figure 1. Scaled representation of the non-ionic polymers' length

One can observe that both MPEG-500 and APEO-440 are linear polymers based on a polyethoxylated (PEO/PEG) polar chain of equivalent length, whose composition is identical to that of the PCE side chains. However, MPEG-500 and APEO-440 present important differences in the polarity of the base terminal that lead to totally different behaviours. The methyl terminal of MPEG-500 is non-polar, but it is small enough to allow the 11 EO (ethylene oxide) mol composing the linear chain to make the polymer totally water-soluble and stable in a polar media.

Conversely, the nonylphenol base terminal of APEO-440 is very hydrophobic to the point that its solubility in water is only partial, despite of the 10 EO mol of the linear chain. It means that the APEO-440 polymer acquires micellar arrangements in polar medias such as water. The PEO-4000 is a linear polymer exclusively based on condensed units of ethylene oxide. Its composition is identical to MPEG-500 but its total length is up to 8 times longer.

2.5 Synthetic cement pore solution

All clay pastes are produced using synthetic cement pore solution as the liquid phase. The solution is prepared by dissolving 14.3 g of Na_2SO_4, 3.05 g of NaOH and 3.00 g of $Ca(OH)_2$ in 1 litre of distilled freshly-boiled water (equivalent to 0.157 mol/l of OH^-, 0.278 mol/l of Na^+, 0.100 mol/l of SO_4^{2-} and 0.040 mol/l of Ca^{2+} concentration). The synthetic cement pore solution is always freshly prepared to avoid carbonation.

3. EXPERIMENTAL METHODS

3.1 Preparation of cement and clay pastes

Clay pastes are prepared at 22 ºC by dispersing powdered Na-MNT clay in the synthetic cement pore solution at 17 wt.% concentration. The mixing process is done using a vertical shaft mixer equipped with a helical head, moving at 600 rpm. The total mixing time is four minutes, during which the admixture is added at the required dosage after the one-minute mark. Cement pastes are prepared following the same procedure as clay pastes but dispersing the cement with tap water at 22 ºC.

3.2 Measurement of paste fluidity

Fluidity of cement and clay pastes is determined by the measurement of paste flow in the mini-slump test. The test uses a metallic truncated mini-cone that is 55 mm high, with an upper diameter of 19 mm and a lower diameter of 38 mm. The mini-cone is arranged on a flat, clean glass surface. It is filled with fresh paste and then compacted with a crystal rebar to evacuate trapped air. The mini-cone is then lifted to let the paste to flow onto the glass surface until the paste reaches maximum spread. The paste spread (paste flow, expressed in mm) is measured in two perpendicular directions and the average value is taken. This test is widely used to evaluate the fluidity of fresh cementitious pastes.

3.3 Sorption of polymers on cement and clay

The total sorbed fraction of organic polymers (including the adsorbed and absorbed fraction) on both cement and clay is measured by determination of the total organic carbon (TOC) with a Shimadzu testing equipment. Freshly prepared pastes containing organic polymer are diluted with Millipore water and mixed for 30 seconds to facilitate the phase separation. Clay or cement suspensions are separated by centrifugation at 15000 rpm for 10 minutes and

the obtained liquid phase is filtrated with a 0.45 μm syringe Nylon filter. The final filtrate is acidified with concentrated HCl to remove inorganic carbon and is then submitted for TOC analysis by combustion at 900 ºC. Previously, calibration lines of each polymer were prepared by recording the TOC value of three different concentrations of polymers. The sorbed fraction of PCE is calculated by interpolation between the calibration lines from the difference of the total PCE dosage added and the non-sorbed fraction of PCE identified in the filtrate. Results are expressed as a percentage of sorption of the total PCE dosage and/or in sorbed mg of PCE per gram of cement or clay.

3.4 *In situ* XRPD patterns of fresh clay pastes

XRPD patterns for fresh, unaltered clay pastes are obtained following the experimental procedures previously described in [17]. In brief, *in-situ* XRPD analysis of fresh, unaltered clay pastes are performed using an MSPD diffractometer using synchrotron radiation at ALBA Synchrotron (Barcelona) and with a PANalytical X'Pert PRO MPD Cu Kα lab diffractometer (λ = 1.5418 Å). As some diffraction peaks display asymmetry, the peak positions were not determined by fitting the suitable range of the profiles to symmetric functions. The diffraction peak positions are determined from the maxima of the intensities.

4. RESULTS AND DISCUSSION

4.1 Dispersing capacity of water-reducer polymers in cement and clay pastes

The generation of initial fluidity produced by different dosages of the water-reducer polymers is presented in Figure 2. The results of paste flow measured in cement pastes at w/c ratio 0.26 and in clay pastes at 17% wt. concentration are presented in Figure 2(a,b), respectively.

The results shown in Figure 2(a) confirms that the dispersing capacity of the PCE polymers in cement paste is much superior than those of Ca-BNS and PMA water-reducers, as expected [8,21,22].

Nevertheless, this trend is reversed in the clay pastes (see Figure 2(b)), observing that the dispersing capacity of the PCE polymers results severally altered as consequence of the capacity of MNT clays to inhibit the dispersing performance of PCE polymers [11].

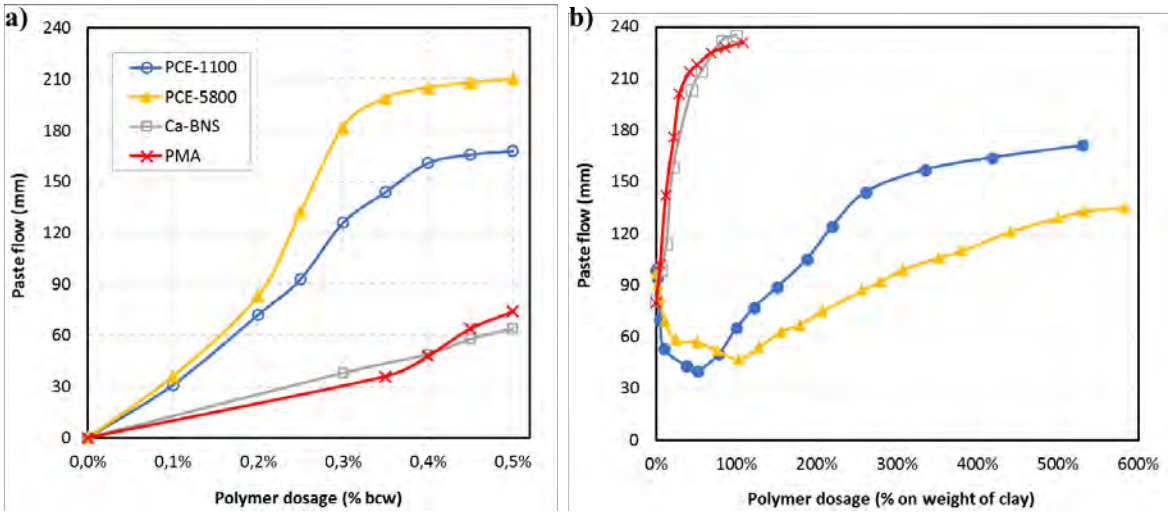

Figure 2. Paste flow at different dosage of water-reducer polymers; a) in cement pastes at w/c 0.26; b) in Na-MNT clay pastes at 170 mg/ml in synthetic cement pore solution

From the fluidity curves of the PCE polymers in clay pastes presented in Figure 2(b), it is detected that the first additions of PCE (from 0% to 100% dosage) produce a flocculation effect, despite the addition of a dispersing agent, and that a high dosage of PCE is required to start generating positive fluidification.

Conversely, the behaviour of Ca-BNS and PMA water-reducers in the paste flow evolution of clay pastes is not affected in the same magnitude than PCE polymers. On the one hand, the initial flocculation phase is not observed with Ca-BNS and PMA, and on the other, the generation of fluidity at equivalent dosage is higher than that of PCE polymers.

Therefore, despite demanding higher dosages than the PCE polymers in the cement pastes to achieve the same paste flow level, the affectation on the dispersing performance of Ca-BNS and PMA in clay pastes is by far not comparable to that of PCE polymers. It evidences that both Ca-BNS and PMA water-reducer polymers are almost clay insensitive [8,13,23,24].

4.2 Expansion of Na-MNT clay by *in situ* XRPD on fresh, unaltered clay pastes

In-situ XRPD analysis on fresh, unaltered clay pastes evaluates the evolution of the interlaminar space dimension (d_{001}) for Na-MNT clay produced by different dosages of PCE polymers. Synchrotron XRPD patterns in Kratky format are presented in Figure 3(a,b) for PCE-1100 and PCE-5800, respectively.

XRPD patterns for Na-MNT pastes with Ca-BNS and PMA are not performed because both polymers do not produce any variation in the interlayer d-spacing of the clay, since they are not absorbed into MNT clays at any dosage [8,13].

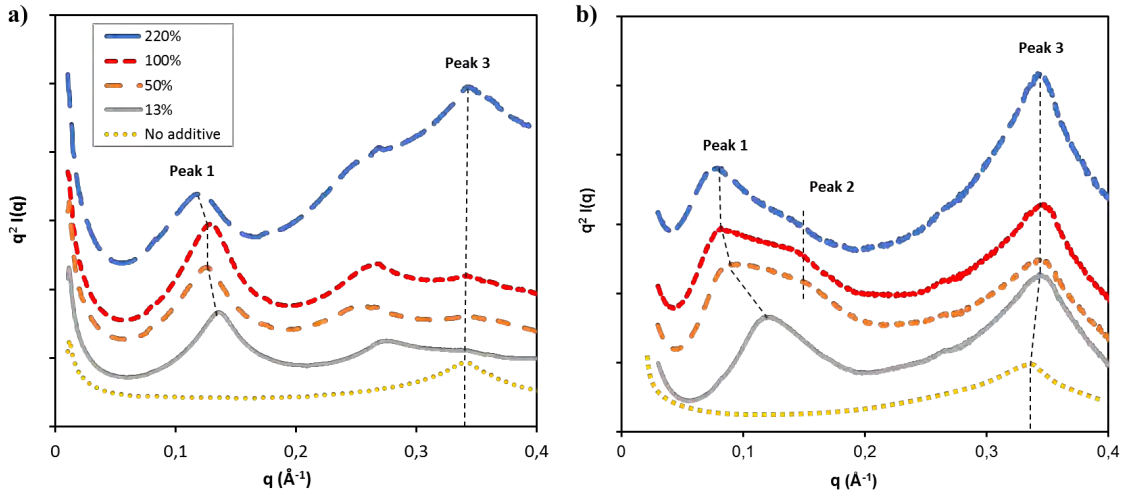

Figure 3. *In situ* synchrotron XRPD patterns of fresh, unaltered clay pastes as increasing dosage of PCE polymers; a) PCE-1100; b) PCE-5800

The initial peak at 18.5 Å (marked as Peak 3 in Figure 3) for the clay paste without any polymer is compatible to 3 water molecules absorbed in the interlayer region [25]. From this initial d-spacing, further clay expansion is produced at each addition of PCE polymer, referred as Peak 1 in Figure 3.

Peak 1 is not present in clay pastes without PCE polymer and it is being progressively displaced to lower angles when PCE dosage increases. According to the previous work of the authors [18], the larger increase of d-spacing observed with PCE-5800 is consequence of its longer side chains, larger than that of PCE-1100 polymer.

Additionally, Peak 2 is attributed to clay specimens originated by exfoliation of the dispersed clay particles, having diverse levels of intercalation which are coexisting with the main clay specimen with the largest expansion. From the different position and intensity of the peaks, it is confirmed that clay exfoliation induced by PCE-5800 is significantly more accused than of PCE-1100 due to the higher side chain density and the longer side chains.

From the multiple intercalation model of side chains proposed in [17], it is possible to estimate the number of water molecules layers and the number of side chains layers and intercalated for each result of d-spacing (intercalation degree, n_{PEG}). Figure 4 displays the

evolution of the maximum d-spacing (Peak 1) at each dosage of PCE polymers and its correspondence with the number of PCE side chains intercalated.

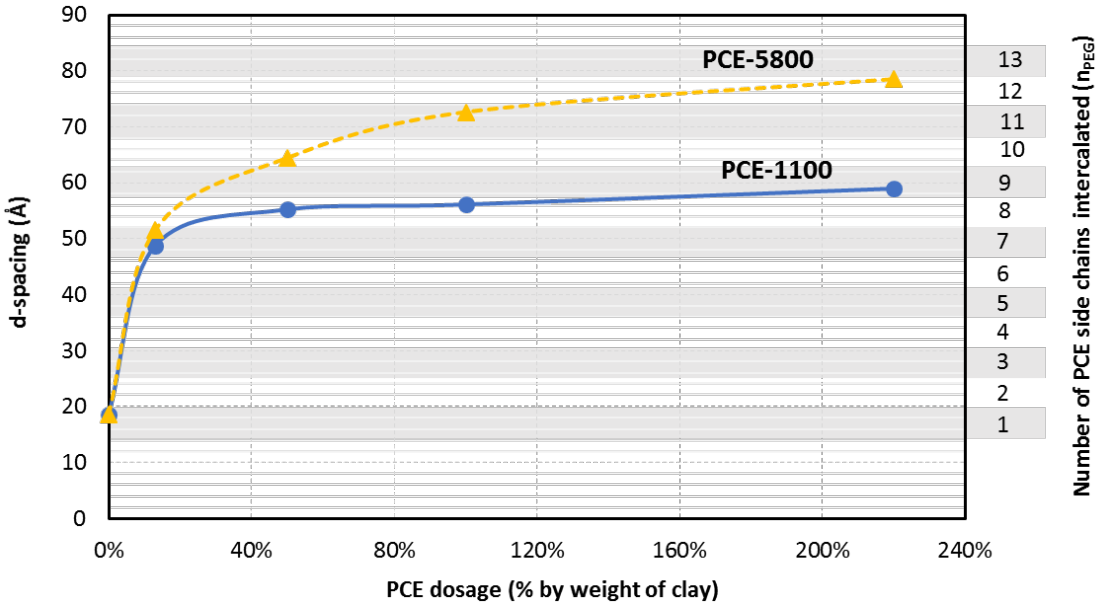

Figure 4. Maximum d-spacing and intercalation degree at each dosage of PCE polymers

Figure 4 shows that major d-spacing changes are produced at the initial additions of PCE while at higher dosage the d-spacing variations become more moderated and tend to stabilization.

By comparing d-spacing evolution against fluidity curves of clay pastes presented in Figure 2(b) for both PCE polymers, it can be stated that the dosage range when flocculation phase is observed matches with the PCE dosages where the biggest d-spacing variations are observed. Additionally, the threshold dosage of PCE polymer in clay pastes from which the positive generation of fluidity starts (see Figure 2(b)) is related with similar dosages at which the d-spacing variations stabilize.

According to the mechanism proposed by [17] based on the multiple intercalation of PCE side chains into the interlaminar space of MNT, the successive increase of number of side chains intercalated (n_{PEG}) forces the intercalation of one additional layer of water molecules to coordinate the PEO/PEG chains in the way that $n_{H20} = n_{PEG}+1$. Therefore, the experimented reduction of fluidity observed in clay pastes at the initial dosages of PCE could be justified by the additional water uptake of the clay promoted by the successive intercalation of side chains.

Figure 5(a,b) illustrates the changes produced in the number of absorbed water layers into the interlaminar space of MNT when PCE side chains are intercalated.

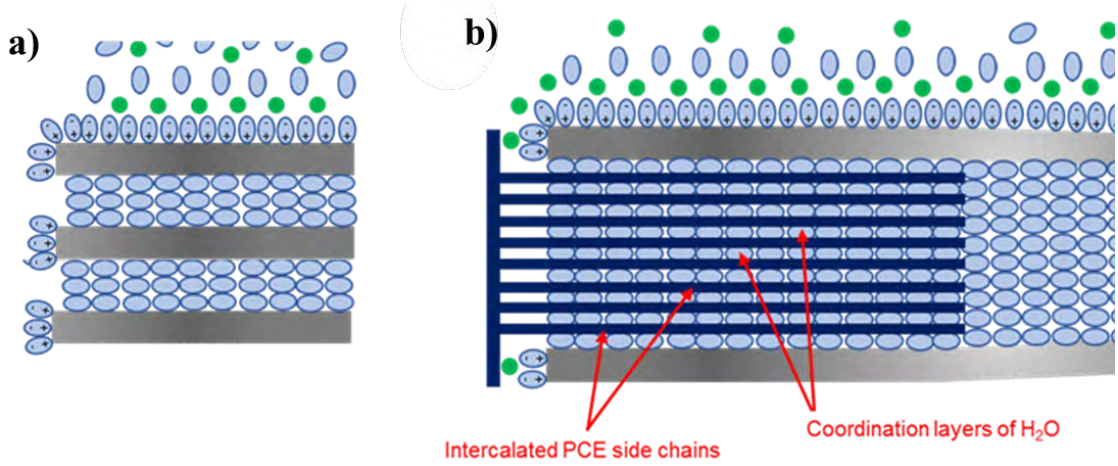

Figure 5. Arrangement of water layers absorbed into MNT in alkaline media; a) in absence of PCE polymer; b) when 8 side chains of PCE polymer are intercalated.

This representation highlights the enhanced water demand of PCE-intercalated MNT. From the initial conformation presented in Figure 5(a) where 3 water layers are absorbed in the interlaminar space of MNT clay, the intercalation of 8 units of PCE side chains forces to increase the number of absorbed water layers up to 9 to coordinate each side chain intercalated [17]. Since the additional water molecules absorbed are captured from the solution, it is plausible to state that this large water uptake promoted by the PCE intercalation is responsible for the initial flocculation observed in clay pastes at the early additions of PCE polymers, and this loss of fluidity is not stabilized until the interlaminar space of MNT clay is not saturated [18] and likely exfoliated.

From this hypothesis, the flocculation phase should be more pronounced for PCE polymers capable to produce higher intercalation levels. It is in agreement with the fluidity curves shown in Figure 2(b), since the dosage range where flocculation is being produced is larger for PCE-5800 polymer having longer side chains and higher side chain density than for PCE-1100 with shorter side chains and lower side chain density.

The consequences from the intercalation of side chains on the distribution of the interlayer cations is not fully understood yet. It is likely that some of these interlayer cations are exchanged by the intercalated PCE side chain, so being removed from clay interlaminar space. Nevertheless, various studies [26-28] propose models for the cation redistribution forced by the intercalation of organic polymers since it is confirmed that an important part of the interlayer cations remains inside the interlaminar space after the intercalation of lineal

polyethylene glycols (PEG), and that these cations are not directly coordinated by the oxygen atoms of PEG chains. Therefore, it is feasible to speculate that some of the interlayer cations are displaced by the intercalation towards the innermost part of the interlayer region thus creating a mismatch in the net charge balance. At this point, a local accumulation of positive charges could be created in the most inner region of the interlaminar space while in the locations closer to the periphery edge-area (from where side chains are intercalated) the repulsion between clay plates is increased due to the lack of cations balancing (at least partially) the permanent charges of the clay plates (layer charge).

The proposed model of *innermost cation displacemen*t is aligned with the poor layer stacking order and turbostratic disorder of stacked layers produced along the *c*-axis [25,29] and observed in the XRPD patterns of MNT clay pastes when PEG/PEO side chains are intercalated [16,18]. Figure 6 illustrates the proposed model of innermost cation displacement.

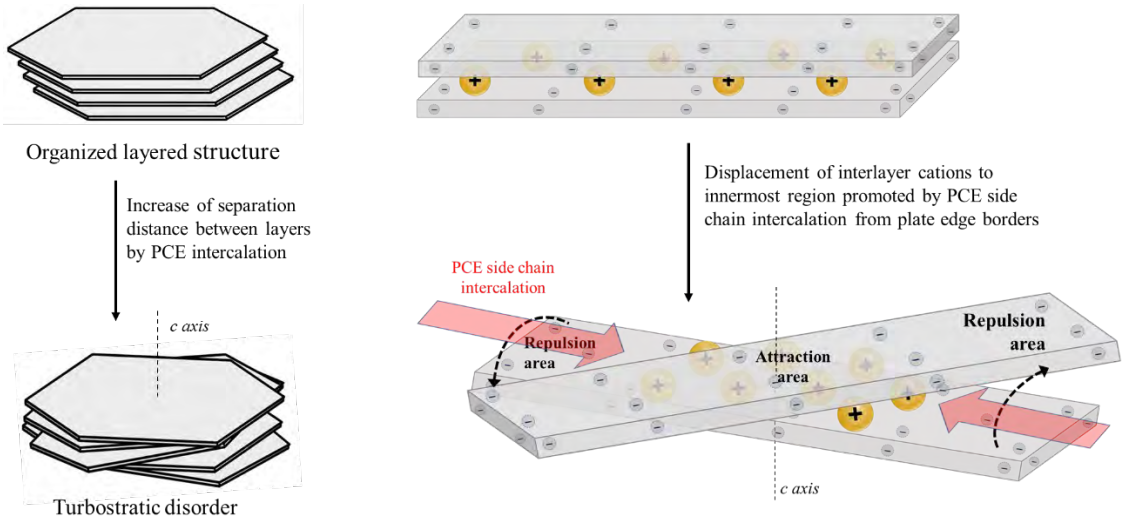

Figure 6. Illustration of the innermost cation displacement model induced by the intercalation of PCE side chains and its alignment with the loss of layer stacking order

The loss of stacking order (being the preliminary step to clay delamination) and the formation of new exfoliated clay specimens with lower number of stacked plates (along *c* axis) generate broader and asymmetric peaks in the XRPD patterns [29,30], as it can be clearly appreciated in Figure 3. Thus, according to the model presented in Figure 6, the longer the side chains the wider the region of repulsion generated between clay plates. It is also in agreement with the fact that PCE polymers with longer side chains are capable to induce higher levels of clay exfoliation [18].

Clay exfoliation generates new additional basal surface [24,31,32] being comparable to an effective reduction of PCE dosage in terms of fluidity generation and thus may be a plausible theory to explain why PCE polymers with such structure induce higher clay exfoliation.

This model, together with the hypothesis for the additional water uptake of MNT clay promoted by the intercalation of PCE side chains, is in agreement with the differences observed in the previous Figure 2(b) in regards of the fluidity evolution of clay pastes between PCE-1100 and PCE-5800, where the polymer having longer side chains contradictory denotes lower fluidification capacity at all dosages than PCE-1100 polymer, based on shorter side chains and reduced side chain density.

4.3 Effects on the fluidity of cement and clay pastes produced by XPE polymers (esterified PCE) and by the non-ionic polymers

The variations of fluidity of cement pastes at w/c 0.45 and of clay pastes at 170 mg/ml concentration produced by the addition of XPE-1100 and XPE-5800 blocked PCE polymers and by the addition of the non-ionic polymers (MPEG-500, PEO-4000 and APEO-440) are presented in Figure 7. Dosage used for all polymers is 0.3% on cement weight for cement pastes and 50% on clay weight for clay pastes. The results of paste flow obtained for these polymers are compared against the paste fluidity generated by the water-reducer polymers at the same dosage (from Figure 2(a)).

For both type of pastes, the changes in fluidity are represented in relative terms, referenced to the fluidity value of cement and clay paste without admixture, being 61 mm for cement paste and 99 mm for clay paste. In these terms, a relative value of 0 means no variation of paste flow, positive values mean increase of paste flow and the value -1 means the complete loss of fluidity.

As expected, while fluidity of cement pastes is increased by the addition of PCE-1100, PCE-5800, Ca-BNS and PMA (so all water-reducer polymers), the esterified PCE polymers XPE-1100 and XPE-5800 do not produce any significant variation in the paste flow.

The same behaviour is observed in cement paste for all the non-ionic polymers. In clay pastes, the addition of 50% of PCE-1100 and PCE-5800 generates a reduction of fluidity, so reproducing the same flocculation effect already presented in Figure 2(b), which is not observed for Ca-BNS and PMA water-reducers since an increase of fluidity is registered for both polymers in clay pastes.

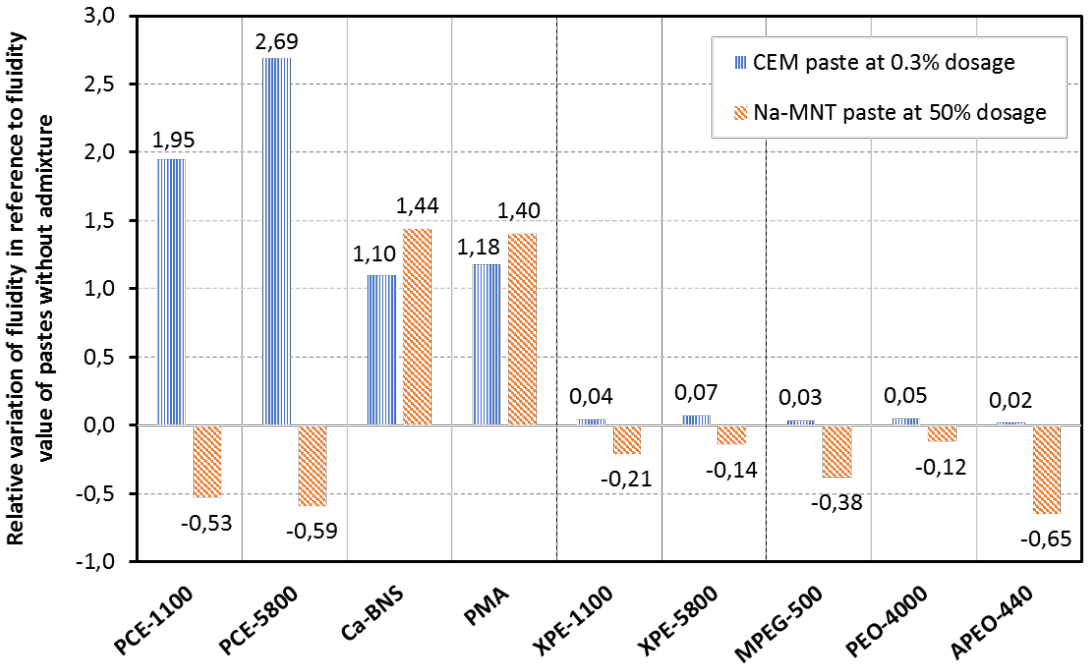

Figure 7. Relative variation of fluidity produced by 0.3% dosage in cement paste and by 50% dosage in clay paste of polymers tested.

The reduction of fluidity observed for the non-ionic polymers in clay pastes is of particular interest since they do not produce any variation of fluidity in cement pastes. The most pronounced reduction of fluidity observed in the clay pastes for all polymers tested corresponds to APEO-440. Both XPE-1100 and XPE-5800 esterified polycarboxylates also experience some fluidity loss but of lower level than those of PCE polymers. It is noticed that the fluidity reduction of XPE-1100 is higher than of XPE-5800, so keeping the same trend than observed in the case of PCE polymers in clay pastes, where reduction of fluidity of PCE-1100 is more pronounced than of PCE-5800 and aligned with the length of the side chains of each polymer. A similar trend is observed for MPEG-500 and PEO-4000 in relation to PCE-1100 and PCE-5800, but in this case the differences in paste flow between both polyglycols are more pronounced. The fluidity loss produced by MPEG-500 is of higher magnitude, being comparable to the fluidity reduction for PCE polymers. Conversely, the reduction of fluidity for PEO-4000 it is 3 times lower than for MPEG-500 and comparable to XPE-5800 blocked PCE.

This behaviour, together with the observations from Figure 2(b), suggests that the longer the side chains the lower the absolute fluidity reduction at the flocculation phase but prolonging the flocculation effect along the dosage range required to reactivate the positive

generation of fluidity. Therefore, it is an indicator that some differences in the intercalation mechanism must take place as a function of the length of PCE side chains.

4.4 Sorption of polymers on cement and clay

Experimental results of sorption for water-reducer polymers and for the non-ionic polymers on cement and on clay are presented in Figure 8(a,b) respectively. As previously described, polymer dosage used is 0.3% in cement pastes and 50% in clay pastes. The results of sorption on cement are in accordance with the typical sorption values reported in literature [33-38] and with the fluidity results presented in Figure 7, since the reduced sorption is correlated with the lower generation of fluidity and vice versa. Nevertheless, this correlation is not met in the case of clay pastes, except for Ca-BNS and PMA.

All other polymers present high sorption rates on Na-MNT clay but it is not translated into additional generation of fluidity. Therefore, as it already known in the case of MPEG-500 and PEO-4000, all these polymers are susceptible to being absorbed by the clay in a comparable way than PCE polymers since sorption results from TOC analysis do not distinguish between adsorbed polymer on the surface and absorbed polymer by intercalation.

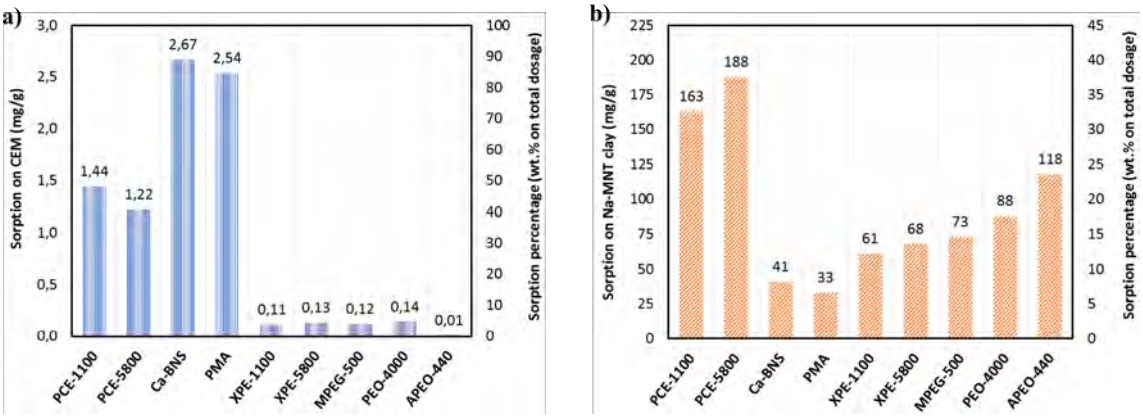

Figure 8. Sorbed amounts of polymer on; a) cement; b) Na-MNT clay

4.5 XRPD patterns for XPE (blocked PCE) and non-ionic polymers

In-situ XRPD on fresh, unaltered clay pastes measures the changes in the interlayer d-spacing of the clay produced by the addition of a 50% dosage of XPE-1100, XPE-5800 and the non-ionic polymers MPEG-500, PEO-4000, APEO-440. XRPD patterns obtained are displayed in Figure 9(a,b). For the sake of comparison, Figure 9(a) includes the XRPD pattern of the PCE-1100 polymer.

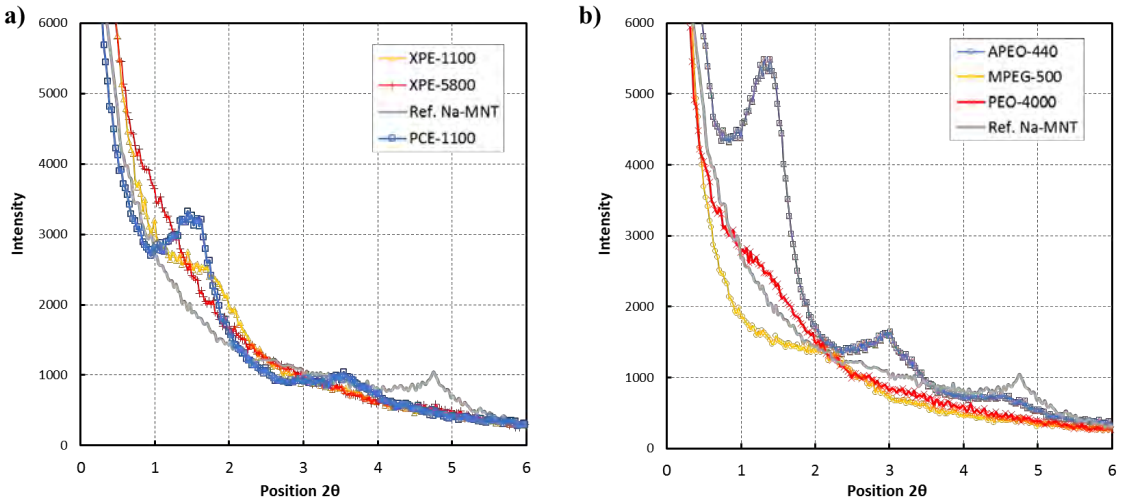

Figure 9. *in-situ* XRPD patterns for fresh, unaltered, clay pastes with 50% dosage of; a) XPE esterified polycarboxylates and PCE-1100; b) non-ionic polymers

The interlayer d-spacing associated to the main peaks identified in the XPRD patterns of Figure 9 and the degree of intercalation (n_{PEG}) calculated according to [17] are presented in Table 5, excluding the equivalent peaks by order of reflection. For the case of XPE-5800, the position of the main peak is hardly distinguishable.

This may be due to the required sample preparation when using a Cu Kα lab diffractometer for *in situ* XRPD, which is not needed when *in situ* XRPD analysis are performed with Synchrotron light. As observed in [17], Synchrotron light offers a much higher resolution than Cu Kα lab diffractometer. The d-spacing and n_{PEG} values displayed in Table 5 for PCE-1100 and PCE-5800 are extracted from the XRPD patterns presented in Figure 3.

	d-spacing (Å)			n_{PEG}		
XPE-1100	49.6	42.7	-	7	6	-
XPE-5800	49.6	-	18.5	7	-	0
MPEG-500	46.3	-	18.5	6	-	0
PEO-4000	63.6	44.9 42.3		10	6	-
APEO-440	64.5	-	18.6	10	-	0
POE-900	-	-	18.6	-	-	0
PCE-1100	55.2	-	18.3	8	-	1
PCE-5800	64.4	41.7	18.4	10	6	1

Table 5. Summary of d-spacing values and n_{PEG} for main diffraction peaks in Figure 10

The net clay expansion (obtained by subtracting 9.6Å from the results of d-spacing, being 9.6Å the typical thickness of the T-O-T layer of MNT clays [32,39]) and the associated intercalation degree (n_{PEG}) obtained at 50% dosage are represented in Figure 10.

For the sake of completeness, Figure 10 includes the intercalation levels from the previous work of the authors [18], for PCE-1100 and PCE-5800 at different dosages than 50% and with two polycarboxylate polymers different than PCE-1100 and PCE-5800, taking advantage of the fact that the test conditions in both works are identical.

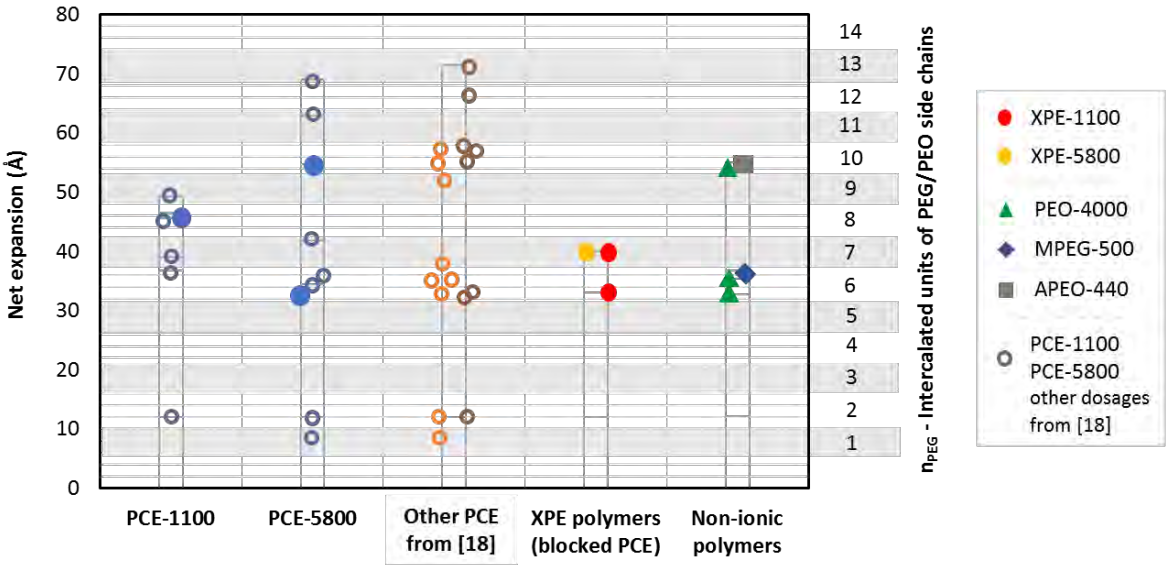

Figure 10. Intercalation degree (n_{PEG}) for PCE, XPE and non-ionic polymers, including the results of intercalation degree obtained in [18], using the same clay sample and PCE dosages of 2%, 5%, 13%, 50%, 100% and 220% by weight of clay

The variations in d-spacing deduced from *in situ* XRPD analysis confirms that the high sorption rates observed in Figure 8(b) for XPE and for the non-ionic polymers in clay pastes are consequence of their intercalation into Na-MNT clay, producing clay expansion. In the previous publication of the authors [18], it is deduced that there are some preferred levels of intercalation for the PCE polymers that seems to be maintained both in the case of XPE polymers and of the non-ionic polymers. It can be observed that the most common intercalation levels correspond to $n_{PEG} = 6$, $n_{PEG} = 7$ and $n_{PEG} = 10$, which coincide with the preferred levels identified in [18] for the same clay sample.

Therefore, taking into account the fact that preferred levels of intercalation are reproduced even with polymers of very different structure from PCE, it seems appropriate to

postulate that it is the nature of the clay itself that conditions these preferred levels and not so much the type of polymer. If this finding is validated, the composition and structure of the MNT clay would acquire a relevant importance as the structure of the PCE polymer in the interference process that has been largely ignored until now.

4.6 Absorption conformations for XPE and non-ionic polymers

It is known that the amount of intercalated polyethylene glycol (PEG) into MNT and its arrangement depend on both the length of the polymer and on the layer charge of the clay [40-44]. In terms of adsorbed amount, it increases as the layer charge of the clay is higher, but at very high layer charge values it begins to decrease [26].

The same trend is observed in regards of the length of PEG since the adsorbed amounts increase as the longer the chain length is, but it begins to decrease from molecular weights of 100.000 g/mol [44]. In terms of absorption conformations, the layer charge of the clay modifies the internal arrangement of the linear PEG polymers as Figure 11 shows.

From a PEG layered sequence arranged in parallel to clay plates when layer charge is low (Figure 11(a)), the orientation of the chains is evolving towards a perpendicular arrangement as the clay charge increases (Figure 11(b)) until describing the pillared arrangement shown in Figure 11(c) [41]. Nevertheless, the pillared arrangement is only affordable for short chain PEGs.

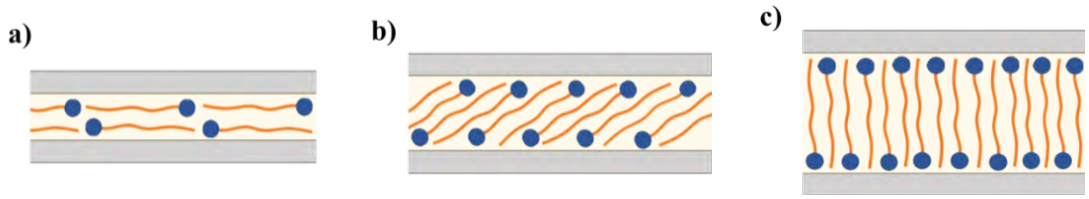

Figure 11. Arrangement for intercalated PEG in function of layer charge of MNT clay

Assuming the parallel conformation illustrated in Figure 11(a), the calculated number of intercalated chains deducted from the net expansion obtained for MPEG-500 is 6 unit-layers. This possible conformation for MPEG-500 intercalation is represented in Figure 12(a). Nevertheless, the measured net expansion of 36.7Å is suspiciously equivalent to the length of the MPEG-500 polymer, suggesting that the intercalated units of MPEG-500 could be arranged in the pillared conformation, as represented in Figure 12(b).

For PEO-4000, three different intercalation degrees are identified. Maximum d-spacing at 63.6 Å is associated to 10 units of PEO-4000 intercalated and arranged as it is illustrated in

Figure 12(a). The next two levels at 44.9 Å and 42.3 Å are so close that they are both associated to 6 units of PEO-4000 intercalated in the same conformation.

Because the estimated length of PEO-4000 is close to 300 Å, the pillared arrangement for this polymer is not possible. Nevertheless, the long size of PEO-4000 allows alternative arrangements such as the helical conformation represented in Figure 12(c) or as a kind of wave-like arrangement like the one represented in Figure 12(d) [43]. Since up to 3 different intercalation degrees are identified for PEO-4000 and two of them likely correspond to the same number of intercalated chains, it must be considered the possibility of coexistence of different absorption conformations.

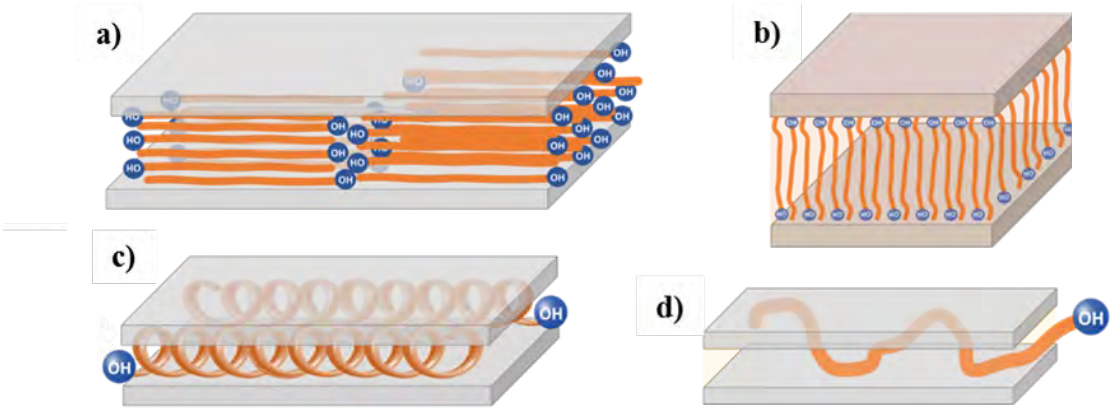

Figure 12. Intercalation confirmations for; a) MPEG-500, PEO-4000 in overlapped layers; b) MPEG-500 pillared; c) PEO-4000 helical; d) PEO-4000 wave-like

Since clay charge is a key factor defining which of those conformations is taking place, it is another indicator suggesting that the characteristics of the clay are determinant in the intercalation profile and therefore for the magnitude of the interference produced in the fluidity of cementitious systems containing clays. Supporting this hypothesis, it is known that the arrangement taken by zwitterionic surfactants change as function of the cation exchange capacity of MNT clays [27].

One unique intercalation degree at 64.5 Å interlayer d-spacing is observed for APEO-440. An arrangement based on overlapped chains parallel to clay plates is ruled out due to the highly hydrophobicity of nonylphenol terminal that cannot be exposed to the polar siloxane groups of the internal clay surface neither to the aqueous media.

Therefore, the conformation taken needs to protect the nonylphenol terminals from the polar environment so only the arrangements where nonylphenol terminals remain isolated are

feasible. This could be achieved by a pillared double-layer conformation where hydrophobic groups are located in the centre of the interlaminar space, as far as possible from the internal, polar clay surface although semi-pillared or L-like double-layer conformations are also possible for APEO-440 since these arrangements are already known for molecules of similar characteristics [27].

Whatever the absorption conformation is, the fact the APEO-440 is intercalated proves that the mere presence of polar linear chains is sufficient to trigger the absorption of the entire molecule. Thus, since only 10 EO mol chains are enough to force the intercalation of an ethoxylated polymer having highly hydrophobic terminals such as APEO-440, it can be considered that side chains can be even a more determining factor than adsorption on surface so that intercalation occurs or not.

This is corroborated by XPE blocked-PCE polymers. XPE-1100 and XPE-5800 intercalate 6 and 7 side chains units. Therefore, the intercalation rates for both XPE are lower than those of the respective PCE polymers with equivalent side chain length.

The fact that the sorption results on clay for XPE polymers are more than 60% lower than that for the PCE polymers and that XPE polymers show almost no sorption on cement, suggests that the intercalation into the interlaminar space is produced despite there is no adsorption of XPE polymer on clay surface.

Thus, sorption results for XPE polymers only reflects absorbed polymer into clay. In any case, since unique intercalation degrees of XPE polymers are 6 and 7, corresponding with the preferred degrees of intercalation observed also for all polymers intercalated into the clay used, this suggests that for this type of polymers the nature of the clay may have more influence that the polymer itself in the intercalation behaviour.

And in addition, the intercalation observed for XPE polymers confirms that the absorption of branched polymers having polar side chains is feasible without the need for surface adsorption. Nevertheless, the lack of polymer adsorption on clay surface leads to lower expansion so, to lower side chain intercalation degrees, in agreement with the experimental results.

5. INTERACTION MODELS BETWEEN PCE-POLYMER AND Na-MNT CLAYS

5.1 Absorption conformations

Based on the conformation models and arrangements proposed for the non-ionic polymers and for the XPE esterified polycarboxylates, and considering the results of fluidity, adsorption and intercalation of PCE polymers, three models of absorption conformations in MNT are proposed in Figure 13.

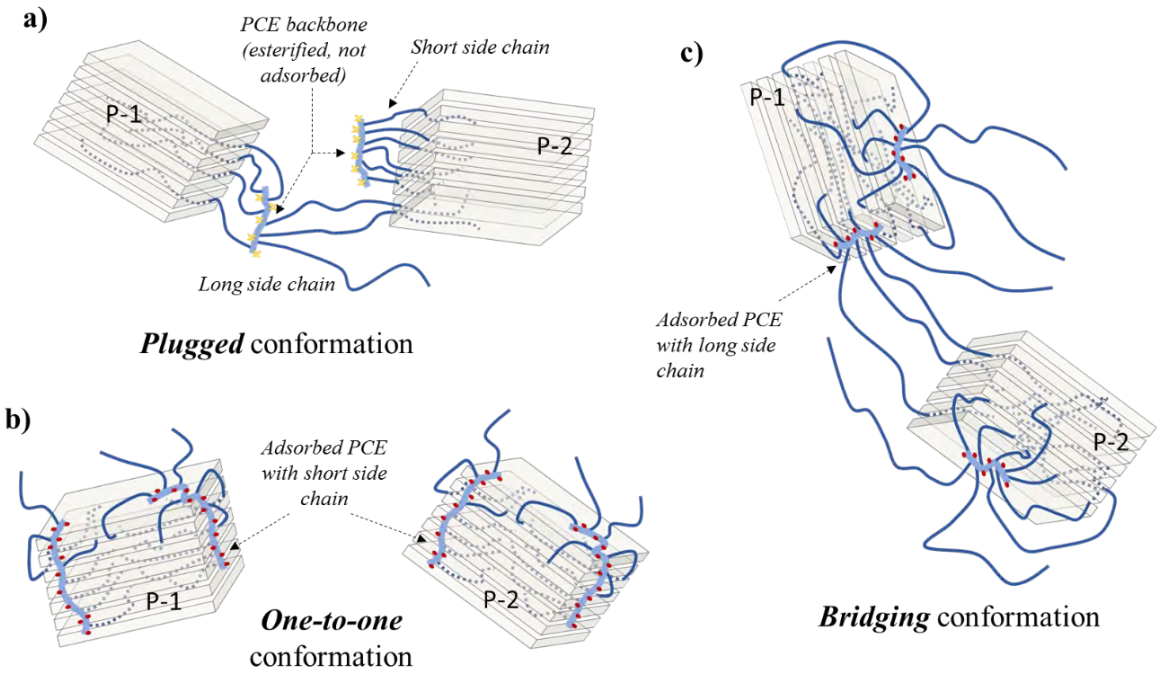

Figure 13. Absorption conformations for PCE polymers into Na-MNT

In the *plugged* conformation of absorption presented in Figure 13(a), the intercalation of side chains is produced without previous or neither simultaneous adsorption of polymer on clay surface, so side chains are directly intercalated into clay from polymer units not adsorbed (so, like plugged). Therefore, the absorption process is promoted exclusively by the direct intercalation of side chains so controlled by the affinity for being intercalated into the clay.

This is the conformation arranged by XPE polymers since adsorption on clay surface is not possible because the anionic charge of PCE is temporally blocked by esterification. In the *plugged* conformation, it is possible that side chains from one single unit of polymer are

intercalated by more than one clay particle (P-1 and P-2 in Figure 13) if the length of the chains is long enough to keep the clay particles away and avoid electrostatic repulsion between them.

The *plugged* conformation seems not feasible for PCE polymers owning effective anionic charge. It is deducted from the high sorption rates observed for PCE polymers, which confirms that when anionic charge is available, adsorption on clay surface is produced. Thus, the *plugged* conformation could only occur in the case of PCE polymers with very little anionic charge that interact with MNT clays with very little layer charge.

Figure 13(b) corresponds to the *one-to-one* absorption conformation. In this case, the adsorbed units of PCE intercalate their side chains only and exclusively in the clay particle they are adsorbed on and without the possibility of sharing (intercalating) side chains into another neighbouring clay particle. It happens when PCE adsorption is concentrated in the edge surface of clay, therefore making very accessible the interlaminar spaces. Since the edge surface of MNT clays is typically very small in relation to total clay surface [45,46], it is expected that edge area will become saturated very rapidly by the adsorbed PCE.

Thus, the possibility to share intercalated side chains from one single PCE unit with some nearby particles having also the edge-surface saturated by PCE seems difficult due to hindrance aspects.

The *one-to-one* conformation is the most appropriate for MNT clays with reduced basal surface charge (so low isomorphic substitution, small CEC). In clays like this, the total layer charge is mostly located in the particle edges while basal planes are more neutral [47-50], therefore the adsorption of PCE polymer is mainly concentrated on the edge surface rather than on the basal surface. According to this hypothesis, clays having these characteristics should lead to an earlier saturation of the interlaminar space by intercalation, thus demanding low PCE dosage to reach the D_{sat} – saturation dosage, as defined in [18].

To a lesser extent, MNT clays with large number of stacked plates per particle are more likely to acquire *one-to-one* conformation simply because the increased ratio of total edge surface, providing larger number of accesses for intercalation. The *one-to-one* conformation is also the most appropriate for PCE polymers with short side chains because the reduced length will not allow shared intercalation of side chain from one PCE unit with other nearby clay particles, which must be too close and so subjected to electrostatic repulsion.

In the *bridging* conformation depicted in Figure 13(c), adsorption on clay surface and shared intercalation with neighbouring clay particles (P-1 and P-2) are produced at the same time. The *bridging* conformation is the preferred one when MNT has high basal surface charge

and large aspect ratio. In these conditions, PCE units are adsorbed in both basal and edge surface of clay.

Due to the morphology of clay particles, basal surface is much larger than edge surface and far more accessible to adsorption. Thus, it can be considered that adsorption on basal surface will be preferred in clays such as these. PCE units adsorbed on basal surface can be intercalated only if side chains are long enough to reach the interlayer openings located at the particle edges [18].

Otherwise, the intercalation in the same particle (P-1) is not feasible. In this case, the free-oriented side chains of the PCE unit adsorbed on the basal surface of one clay particle can be intercalated by neighbouring particles (P-2) because the occupation is mainly concentrated in the basal surfaces and, consequently, the edge surfaces remain accessible for intercalation.

From the polymer perspective, PCE polymers having large side chains and high side chain density acquire *bridging* conformation due to the high steric repulsion that prevents all the side chains belonging to one single PCE from being intercalated within the same clay particle on which it is adsorbed.

5.2 Promoters of intercalation

From the previous section, it can be deduced that the absorption conformation to be acquired is controlled by: i) clay properties such as layer charge by isomorphic substitution and, to a lesser degree, by the particle morphology (number of stacked plates, aspect ratio); and ii) PCE polymer properties such as the length and density of side chains.

Surprisingly, PCE anionic charge seems to be of little relevance in the definition of the conformation models, but as it was reported in the previous work of the authors [18], the anionic charge of the polymer defines the saturation dosage (D_{sat}) at the time when the interlaminar space of MNT clay is almost fully intercalated by side chains (so, saturated).

Therefore, it can be stated that while the absorption conformation is determined by the factors previously mentioned, the anionic charge of PCE polymer determines the efficiency of the intercalation.

To determine the contribution of PCE anionic charge in the evolution of total sorption rate of polymer on MNT pastes, the sorption isotherms on Na-MNT clay for PCE and XPE polymers, PMA linear polymethacrylate and for the non-ionic polymers are presented in Figure 14.

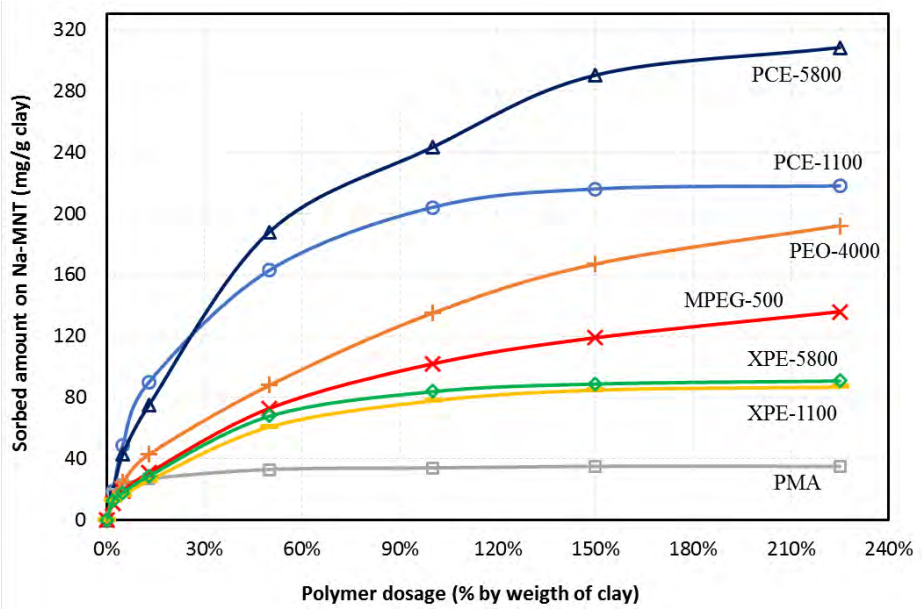

Figure 14. Sorption isotherms on Na-MNT of the studied polymers.

The profile of the isotherms shown in Figure 14 for PCE polymers confirms that, when the polymer has anionic charge, the sorption evolves more efficiently than any polymer without an effective charge. Apart from PMA that is not absorbed/intercalated, and hence its rapid saturation at the lowest levels of uptake, all other polymers base their measured sorption mainly on the intercalation into MNT, and only PCE polymers experience simultaneously adsorption on clay surface and absorption by intercalation. Nevertheless, from the sorption saturation levels of PMA in comparison with that for PCE, it can be inferred that most of the sorbed amount measured for PCE polymers is likely due to intercalation and not to surface adsorption.

XPE esterified polycarboxylates, in agreement with the proposed *plugged* conformation of absorption, present the most reduced affinity for intercalation since both XPE-1100 and XPE-5800 stabilize its sorption rate at the lowest dosage within all polymers, on total sorbed amounts being 60-70% lower that of PCE polymers. Sorption evolution of polyglycols MPEG-500 and PEO-4000 (so absorption by intercalation since, as seen in Figure 8(a) with cement, they are not surface sorbed) evolves more progressively than PCE polymers and its saturation is not observed within the range of dosages tested.

Finally, sorption of PCE polymers at low dosage evolves much efficiently than any other polymer and the stabilization is reached at the highest amounts of sorption. Therefore, it denotes that the anionic charge promotes a more efficient intercalation into MNT clay and it is

the determining factor that allows the intercalation of a large number of side chains in a reduced space, overcoming part of the steric hindrances that would not allow such grouping of chains under normal conditions, as shown by the sorption isotherms of the other polymers not having anionic charge.

For PCE-5800 it is expected the *bridging* conformation because its long side chains. For this conformation, it can be deduced that the total sorption progresses faster than the intercalation degree since the intercalation of side chains from the adsorbed units of PCE is shared with other clay particles. Therefore, there is no massive, punctual intercalation. Conversely, PCE-1100 having shorter side chains is expected to arrange in the *one-to-one* conformation. In this conformation, supported by the higher anionic charge of this PCE, the intercalation degree and the polymer sorption progress more smoothly because the intercalation is concentrated on the same clay particle where the polymers units are adsorbed on, thus creating large intercalation but only in local sites of the clay particle. This is evident for the two PCE polymers by comparing the evolution of the interlayer d-spacing presented in Figure 4 with the sorption isotherms displayed in Figure 14.

According to the previous reasoning, when *bridging* conformation is taken place, it is expected that clay particles with high intercalation degrees coexist with particles with lower intercalation degrees as consequence of a more random process. Conversely, for the *one-to-one* conformation, most of the clay particles would have similar, homogeneous degree of intercalation. This is confirmed by the intensity of Peak 3 in the XRPD patterns of PCE-1100 and PCE-5800 displayed in Figure 3. It can be observed that Peak 3 at 18.3 Å (corresponding to n_{PEG} =1) for PCE-5800 is always visible and of high intensity, coexisting with Peak 1. Therefore, different clay specimens with different intercalation degree are present at the same time. For PCE-1100, Peak 3 disappears at the first addition of PCE and it does not appear until the highest dosage of PCE-1100 is added, thus only a unique intercalation degree is observed at almost all dosages tested. The same affirmation works to understand why PCE-5800 having higher side chain density and longer side chains than PCE-1100 experiences lower absolute reduction of paste flow in the flocculation phase of clay pastes presented in Figure 2(b), but the dosage range where flocculation is produced is larger than that of PCE-1100.

6. CONCLUSIONS

PCE polymers intercalated into MNT can be arranged preferably in two possible absorption conformations: *one-to-one* conformation and *bridging* conformation. A third model

described, *plugged* conformation, seems to be not appropriate to polymers having anionic charge and it would be possible only for very particular cases.

The preferred conformation for PCE absorption is dictated by key properties of the polymer(s) and the clay(s). For the polymer, the two main characteristics are the length of side chains and the side chain density. For the MNT, the mains properties are the layer charge and to a lesser extent the morphology of the clay particle. PCE anionic charge is a key factor for the earlier saturation but not for the absorption arrangement.

The models of adsorption conformation proposed allow a reasonable and consistent explanation about the interaction processes between PCE polymers and MNT that fits the experimental results. But at the same time, also highlight the importance of the properties of clay for the understanding of the intercalation arrangements. Therefore, in any experimental work where PCE-MNT interaction is studied, it is needed to specify as much as possible the properties of the clay used otherwise the comparison of results from different studies is not feasible.

Acknowledgments

Mr. Borralleras thanks all the support given by BASF Construction Chemicals to the development of this work. Dr. I. Segura is supported by the postdoctoral Torres Quevedo program of the Spanish Ministry of Economy and Competitiveness.

References

[1] E. Sakai, A. Ishida, A. Ohta, New trends in the development of chemical admixtures in Japan, Proceedings Journal of Advanced Concrete Technology 4 (2006) 211-223.

[2] F. Puertas, H. Santos, M. Palacios, S. Martínez-Ramírez, Polycarboxylate superplasticizers admixtures: effect on hydration, microstructure and rheological behaviour in cement pastes, Advances in Cement Research 17 (2005) 77-89.

[3] P.C. Aïtcin, R.J. Flatt, Science and technology of concrete admixtures, ISBN 978-0-08-100693-1 (2016).

[4] J. Plank, C. Schroefl, M. Gruber, M. Lesti, R. Sieber, Effectiveness of polycarboxylate superplasticizers in ulta-high strength concrete: the importance of PCE compatibility with silica fume, Journal of Advanced Concrete Technology 7 (2009) 5-12.

[5] D. Atarashi, Interaction between superplasticizers and clay minerals, Japan Cement Association (2005) 287-292.

[6] D. Atarashi, K. Yamada, A. Ito, M. Miyauchi, E. Sakai, Interaction between montmorillonite and chemical admixture, Journal of Advanced Concrete Technology 13 (2015) 325-331.

[7] L. Xoing, G. Zheng, Y. Bi, C. Fu, Effect of typical clay upon the dispersion performance of polycarboxylate superplasticizer, Proceedings International Conference on Materials, Environmental and Biological Engineering (2015) 226-229.

[8] L. Lei, J. Plank, A study on the impact of different clay minerals on the dispersing force of conventional and modified vinyl ether based polycarboxylate superplasticizers, Cement and Concrete Research 60 (2014) 1-10.

[9] S. Qian, H. Jiang, B. Ding, Y. Wang, C. Zheng, Z. Guo, Synthesis and performance of polycarboxylate superplasticizer with clay-inerting and high slump retention capability, Materials Science and Engineering 182 (2017).

[10] X. Shu, Q. Ran, J. Liu, H. Zhao, Q. Zhang, X. Wang, Y. Yang, Tailoring the solution conformation of polycarboxylate superplasticizer toward the improvement of dispersing performance in cement paste, Construction and Building Materials 116 (2016) 289-298.

[11] L. Lei, J. Plank, Synthesis and properties of a vinyl ether-based polycarboxylate superplasticizer for concrete possessing clay tolerance, Industrial & Engineering Chemistry Research 53 (2014) 1048-1055.

[12] H. Tan, Xin Li, M. Liu, B. Ma, B. Gu, X. Li, Tolerance of cement for clay minerals: effect of side-chain density in polyethylene oxide (PEO) superplasticizers additives, Clay and Clay Minerals 64-6 (2016) 732-742.

[13] H. Tan, B. Gu, B. Ma, X. Li, C. Lin, Mechanism of intercalation of polycarboxylate superplasticizer into montmorillonite, Applied Clay Science 129 (2016) 40-46.

[14] S. Ng, J. Plank, Interaction mechanisms between Na-montmorillonite clay and MPEG-based polycarboxylate superplasticizers, Cement and Concrete Research 42 (2012) 847-854.

[15] G. Xing, W. Wang, G. Fang, Cement dispersion performance of superplasticizers in the presence of clay and interaction between superplasticizers and clay, Advances in Cement Research 29 (2017) 194-205.

[16] H. Tan, B. Gu, Y. Guo, B. Ma, J. Huang, J. Ren, F. Zou, Improvement in compatibility of polycarboxylate superplasticizers with poor-quality aggregate conatining montmorillonite by incorporating polymeric ferric sulfate, Construction and Building Materials 162 (2018) 566-575.

[17] P. Borralleras, I. Segura, M. A. G. Aranda, A. Aguado, Influence of experimental procedure on d-spacing measurement by XRD of montmorillonite clay pastes containing PCE based superplasticizer, Cement and Concrete Research 116 (2019) 266-272. https://doi.org/10.1016/j.cemconres.2018.11.015

[18] P. Borralleras, I. Segura, M. A. G. Aranda, A. Aguado, Influence of polymer structure of polycarboxylate based superplasticizers in the intercalation mechanism in montmorillonite clay, Cement and Concrete Composites (*under review*).

[19] Magarotto R, Torresan I, Zeminian N. Effect of alkaline sulphates on the performance of superplasticizers. In: 11th International congress on the chemistry of cement; 2003. p. 569–79.

[20] D. Wilinski, P. Lukowski, G. Rokicki, Polymeric superplasticizers based on polycarboxylates for ready-mixed concrete: current state of the art, Polimery 61 (2016) 474-481.

[21] R. Qianping, X. Wang, X. Shu, J. Liu, Effects of sequence structure of polycarboxylate superplasticizers on the dispersion behavior of cement paste, Journal of Dispersion Science and Technology 37 (2016) 431-441.

[22] Y. Zhang, X. Kong, Correlations of the dispersing capability of NSF and PCE types of superplasticizer and their impacts on the cement hydration with the adsorption in fresh cement pastes, Cement and Concrete Research 69 (2015) 1-9.

[23] G. Xing, W. Wang, J. Xu, Grafting tertiary amine groups into the molecular structures of polycarboxylate superplasticizers lowers their clay sensitivity, RSC Advances 6 (2016) 106921-106927.

[24] L. Lei, J. Plank, A concept for a polycarboxylate superplasticizer possessing enhanced clay tolerance, Cement and Concrete Research 42 (2012) 1299-1306.

[25] M. Matusewicz, K. Pirkkalainen, J.P. Suuronen, A. Root, A. Muurinen, R. Serimaa, M. Olin, Microstrcutural investigation of calcium montmorillonite, Clay Minerals 48 (2013) 267-276.

[26] J. Bujdak, E. Hackett, E.P. Giannelis, Effect of layer charge on the intercalation of polyethylene oxide in layered silicates: implications on nanocomposite polymer electrolytes, Chemistry of Materials 12 (2000) 2168-2174.

[27] J. Zhu, P. Zhang, Y. Qing, K. Wen, X. Su, L. Ma, J. Wei, H. Liu, H. He, Y. Xi, Novel intercalation mechanism of zwitterionic surfactant modified montmorillonites, Applied Clay Science 141 (2017) 265-271.

[28] R.L. Parfitt, D.J. Greenland, Adsorption of water by montmorillonite-poly(ethylene glycol) adsorption products, Clay Minerals 8 (1970) 317-324.

[29] A. Meunier, Why are clay minerals small?, Clay Minerals 41 (2006) 551-566.

[30] R. Tettenhorst, H. E. Roberson, X-Ray diffraction aspects of montmorillonite, American Mineralogist 58 (1973) 73-80.

[31] R. F. Geise, The electrostatic interlayer forces of layer structure minerals, Clay and Clay Minerals 26 (1978) 51-57.

[32] E. C. Jonas, R. M. Oliver, Size and shape of montmorillonite crystallites, Clay and Clay Minerals 15 (1967) 27-33.

[33] R. Qianping, X. Shu, Y. Yang, J. Zhang, Effect of molecular weight of polycarboxylate superplasticizer on its dispersion, adsorption and hydration of a cementitious system, Journal of Materials in Civil Engineering 28 (2016) 184-188.

[34] H. Feng, L. Pan, Q. Zheng, J. Li, N. Xu, S. Pang, Effects of molecular structure of polycarboxylate superplasticizers on their dispersion and adsorption behaviour in cement paste with two kinds of stone powder, Construction and Building Materials 170 (2018) 182-192.

[35] C.Z. Li, N.Q. Feng, Y.D. Li, R.J. Chen, Effects of polyethylene oxide chains on the performance of polycarboxylate-type water-reducers, Cement and Concrete Research 35 (2005) 867-873.

[36] J. Liu, Q. Ran, C. Miao, M. Qiao, Effects of grafting densities of comb-like copolymer on the dispersion properties of concentrated cement suspensions, Materials Transactions 53 (2012) 553-558.

[37] H. Lombois-Burger, P. Colombet, J. Halary, H. Van Damme, On the frictional contribution to the viscosity of cement and silica pastes in the presence of adsorbing and non-adsorbing polymers, Cement and Concrete Research 38 (2008) 1306-1314.

[38] H. Bessaies-Bey, R. Baumann, M. Schmitz, M. Radler, N. Roussel, Effect of polyacrylamide on rheology of fresh cement pastes, Cement and Concrete Research 76 (2015) 98-106.

[39] M.J. Wilson, Sheet silicates: clay minerals, ISBN 978-1-86239-359-2, The Geological Society Publishing House, Second edition (2013).

[40] S. Zhu, H. Peng, J. Chen, H. Li, Y. Cao, Y. Yang, Z. Feng, Intercalation behavior of poly(ethylene glycol) in organically modified montmorillonite, Applied Surface Science 276 (2013) 502-511.

[41] T. Okada, Y. Seki, M. Ogawa, Designed nanostructures of clay for controlled adsorption of organic compounds, Journal of Nanoscience and Nanotechnology 14 (2014) 2121-2134.

[42] R.W.A. Franco, C.A. Brasil, G.L. Mantovani, E.R. de Azevedo, T.J. Bonagamba, Molecular dynamics of poly(ethylene glycol) intercalated in clay, studied using ^{13}C solid-state NMR, Materials 6 (2013) 47-64.

[43] M.X. Reinholdt, R.J. Kirkpatrick, T.J. Pinnavala, Montmorillonite-poly(ethylene glycol) nanocomposites: interlayer alkali metal behavior, The Journal of Physical Chemistry 109 (2005) 16296-16303.

[44] A. Kobayashi, M. Kawaguchi, T. Kato, A. Takahashi, Intercalation adsorption of poly(ethylene oxide) into montmorillonite, Kyoto University – Bulletin of the Institute for Chemical Research 66 (1989) 176-183.

[45] P.H. Nadeau, The physical dimensions of fundamental clay particles, Clay Minerals 20 (1985) 499-514.

[46] A. Kahn, Studies on the size and shape of clay particles in aqueous suspension, Clays and Clay Minerals 6 (1959) 220-236.

[47] H. Zhao, S. Bhattarcharjee, R. Chow, D. Wallace, J.H. Masliyah, Z. Xu, Probing surface charge potentials of clay basal planes and edges by direct force measurements, Langmuir 24 (2008) 12899-12910.

[48] T. Preocanin, A. Abdelmonem, G. Montavon, J. Luetzenkirchen, Charging behavior of clays and clay minerals in aqueous electrolyte solutions. Experimental methods for measuring the charge and interpreting the results – Clays, clay minerals and ceramic materials based on clay minerals, ISBN 978-953-51-2259-3 (2016).

[49] X. Liu, X. Lu, M. Sprik, J. Cheng, E.J. Meijer, R. Wang, Acidity of edge surface sites of montmorillonite and kaolinite, Geochimica et Cosmochinica Acta 117 (2013) 180-190.

[50] E. Tombácz, M. Szekeres, Surface charge heterogeneity of kaolinite in aqueous suspension in comparison with montmorillonite, Applied Clay Science 34 (2006) 105-124.

3.4. CONFERENCE PAPER I

MODELIZACIÓN DEL MECANISMO DE PÉRDIDA DE CONSISTENCIA PROVOCADO POR ARCILLAS EN PASTAS DE CEMENTO CON SUPERPLASTIFICANTES BASE POLICARBOXILATO

Published in the Proceeding of the HAC2018 – Congreso Iberoamericano de Hormigón Autocompactacnte y Hormigones Especiales (March 2018), 279-289

Pere Borralleras[a], Ignacio Segura[b, c,*], and Antonio Aguado[b]

[a] BASF Construction Chemicals Iberia, Ctra del Mig 219, E-08907 Hospitalet de Llobregat, Barcelona, Spain

[b] Department of Environmental and Civil Engineering, Universitat Politècnica de Catalunya-Barcelona Tech, Jordi Girona 1-3, C1, E-08034 Barcelona, Spain

[c] Smart Engineering Ltd, Jordi Girona 1-3, ParcUPC–K2M, E-08034 Barcelona, Spain

* Corresponding author: Pere Borralleras Mas, Technical & Marketing Department, BASF Construction Chemicals España, Ctra. Del Mig 219, E-08907 Hospitalet de Llobregat, Spain. Email address: pere.borralleras@basf.com Tel: +34 93 2616158

Resumen

Este trabajo investiga acerca del mecanismo de interferencia provocado por arcillas sobre la fluidez de sistemas cementosos con condiciones asimilables al HAC en cuanto a baja relación agua/cemento y alta dosis de aditivo basado en polímeros de éter policarboxílico. Se propone una sistemática para determinar cómo repercuten de forma aislada la absorción de agua y la inhibición del efecto dispersante del aditivo, a partir de la cual se describe el mecanismo de sobre-absorción de la arcilla provocado por la intercalación múltiple de cadenas laterales.

Palabras clave: arcilla, montmorillonita, policarboxilato, fluidez, absorción

1. INTRODUCCIÓN

En el diseño del hormigón autocompactante (HAC) se emplean elevadas fracciones de arena y bajas relaciones agua/cemento (R W/C) y agua/finos (R W/F_{vol}), que requieren de altas dosis de aditivos basados en policarboxilatos (PCE) para aportar el nivel de fluidez requerido. Estos condicionantes de diseño actúan como amplificadores del efecto interferente, de tal modo que la presencia de muy pequeñas cantidades de arcilla en la arena es suficiente para generar severas pérdidas de fluidez y penalizar el mantenimiento de consistencia.

Las arcillas son minerales sedimentarios de estructura laminar y elevada finura, que pertenecen al grupo de los filosilicatos. Su estructura, representada en la Fig. 1(a), puede describirse como láminas superpuestas formadas por secuencias repetitivas de tetraedros SiO_4 (capa T) y octaedros $Al(OH)_6$ (capa O) que comparten vértices [1]. En función de la organización de las capas T y capas O que componen las láminas, se distinguen los diferentes tipos de arcilla (caolinitas, micas, esmectitas, cloritas), definiéndose las arcillas tipo T-O y las arcillas tipo T-O-T, cuyas conformaciones se muestran en la Fig. 1(b).

Los átomos de Si de los tetraedros y los de Al de los octaedros pueden experimentar substitución isomórfica por cationes de carga no equivalente como Al^{3+} o Fe^{3+} y Mg^{2+}, provocando la acumulación de cargas residuales en las láminas. Estas cargas aniónicas acumuladas originan la repulsión entre láminas contiguas, haciendo que se separen entre ellas y creen un espacio interlaminar, donde se acumulan los cationes que balancean las cargas.

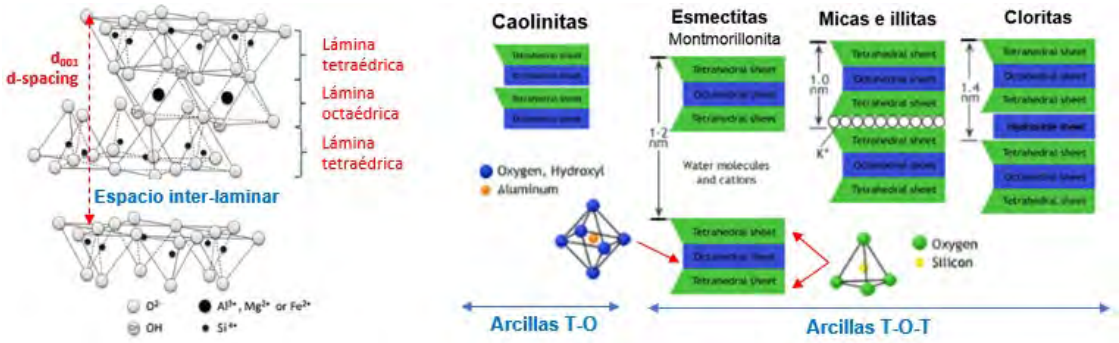

Figura 1. a) Estructura de las arcillas; b) Tipologías de arcillas en función de la estructura laminar

El espacio interlaminar es particular de cada tipo de arcilla y su apertura se caracteriza por difracción de rayos-X (d-spacing – d_{001}). La capacidad de intercambio y la accesibilidad de este espacio son determinantes para la capacidad interferente de las arcillas, porqué condicionan la absorción de agua y de moléculas polares de la arcilla.

Las arcillas del tipo esmectita-montmorillonita (MNT) son las que disponen de un espacio interlaminar más amplio y accesible, que hace que su superficie específica aumente exponencialmente. Debido a esta propiedad, estas arcillas son la que provocan una mayor interferencia sobre la fluidez de hormigones, siendo consideras las más problemáticas.

2. IMPACTO EN LA FLUIDEZ DEL HAC PROVOCADO POR ARCILLAS MNT

Para caracterizar el impacto que ejercen las arcillas en la fluidez del HAC, se registra la pérdida de consistencia que provoca la adición de diferentes cantidades de arcilla Na-MNT sobre una arena caliza con 0,4 gr/100gr de azul de metileno (MB).

La Fig. 2(a) muestra los resultados de MB de la arena resultante obtenida por cada adición de arcilla, y la Fig. 2(b) el impacto producido sobre la fluidez inicial en un HAC de extensión de flujo 670 mm.

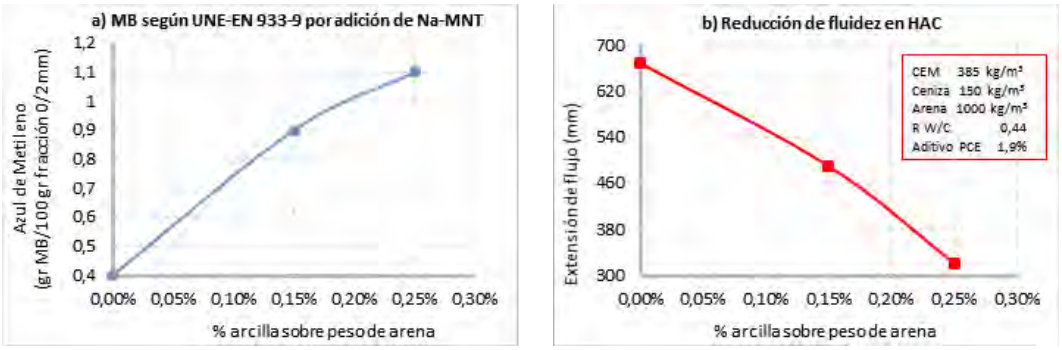

Figura 2. a) Valores de MB de la arena por adición de arcilla; b) Reducción de fluidez en HAC

Se observa que la arcilla Na-MNT provoca la total pérdida de la capacidad autocompactante incluso en cantidades tan bajas que el valor de MB resultante no excede los límites permitidos por la EHE-08. De confirmarse esta limitación, podría ponerse en cuestión la viabilidad de este método de caracterización de arenas cuando éstas se usan en hormigones de las características del HAC.

3. MECANISMO DE INTERFERENCIA DE LAS ARCILLAS

Las arcillas MNT fundamentan su efecto interferente a partir de dos procesos diferentes que se manifiestan de forma paralela [2]. Por un lado, absorben parte del agua de amasado y, simultáneamente, inhiben el efecto dispersante de los polímeros de PCE. La suma de ambos efectos origina la pérdida de fluidez del hormigón, que se experimenta tanto justo en el momento inicial como también durante los 30-60 minutos posteriores.

Para obtener una mejor comprensión del mecanismo de interferencia completo se pretende estudiar ambos efectos de forma aislada. Se evaluará por un lado el impacto provocado por arcillas en pastas de cemento sin aditivo, para posteriormente incluir la variable del aditivo.

3.1. Factor de interferencia por absorción de agua

Para caracterizar el impacto causado por la capacidad de absorción de agua de arcillas del tipo Na-MNT, se evalúa la pérdida de fluidez inicial de pastas de cemento inducida por diferentes cantidades de dos arcillas Na-MNT de diferente origen.

La finura y tamaño de partícula de las dos arcillas y del cemento se presenta en la Tabla 1.

	CEM I-52,5R	*Na-MNT (A)*	*Na-MNT (B)*
D_{50} (µm)- Malvern	9,98	7,35	36,90
Superficie específica BET (m^2/kg)	9260	49450	45220

Tabla 1. Descripción de los materiales utilizados

El primer paso es determinar la curva de fluidez del cemento por efecto de la R W/C, mostrada en la Fig. 3(a). Se observa que la curva obtenida se asimila a una función logística, de tal modo que puede ser linealizada según la Fig. 3(b). La regresión lineal resultante, expresada en función de los litros de agua por metro cuadrado de cemento (transformando el peso con la superficie específica), se presenta en la Fig. 3(c).

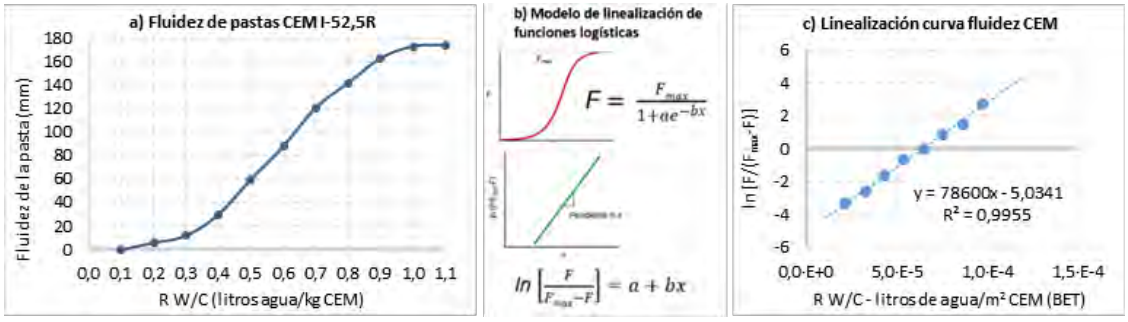

Figura 3. a) Fluidez de pastas de cemento a diferente R W/C; b) Modelo de regresión lineal de funciones logísticas. c) Resultado de la linealización de los resultados de fluidez de las pastas

La fluidez máxima (F_{max}) corresponde al valor de fluidez (en mm) de la pasta con R W/C 1,0. Esta asociación es una aproximación, ya que el valor, aunque sí tiende a estabilizarse, no es matemáticamente asintótico. Pero partir de esta R W/C, las pastas dejan de ser estables y presentar disgregación, pudiendo asumir que en el valor de fluidez a R W/C=1 corresponde con el límite de estabilidad de la pasta de cemento, que define el valor de F_{max}.

Con la regresión lineal es posible obtener los valores *a* y b de la función y proponer la ecuación matemática Ecs. (1) de la Fig. 4(a), que expresa la fluidez de la pasta en función de la R W/C y de la superficie específica del cemento (en m^2/kg). La correlación presentada en la Fig. 4(b) entre los valores teóricos y los experimentales muestra una correlación aceptable.

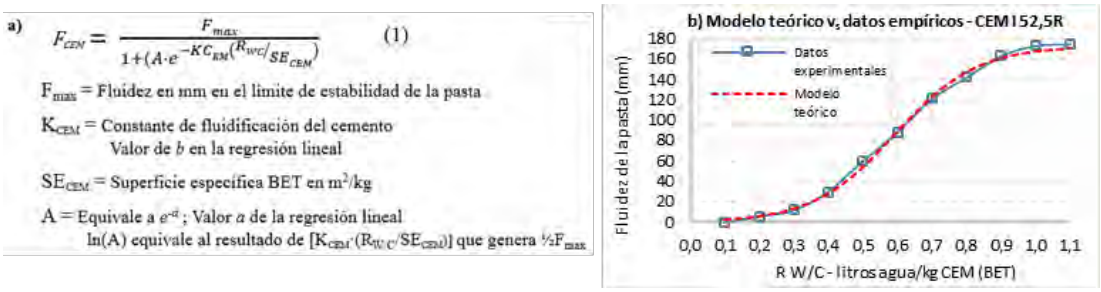

Figura 4. a) Ecuación de fluidez de pastas de cemento; b) Comparación del modelo con los resultados

El impacto en la fluidez de pastas de cemento provocado por diferentes cantidades de arcilla se presenta en la Fig. 5. Los resultados con la arcilla Na-MNT (A) se presentan en la Fig. 5(a) y con Na-MNT (B) en la Fig. 5(b). Las curvas de fluidez obtenidas muestran que la pérdida de fluidez no es lineal con el porcentaje de arcilla, sino que disminuye proporcionalmente cuando aumenta.

Complementariamente, las Fig. 5(c) y 5(d) representan la pérdida de fluidez relativa unitaria para cada una de las arcillas, calculada sobre el valor de fluidez de la pasta de cemento sin arcilla a la misma R W/C. CEM y expresado según los m^2 de arcilla por kg de cemento. Se observa que estas curvas describen una función potencial del tipo $y=A \cdot x^n$, que se ajusta automáticamente para obtener los valores de *A* y *n*.

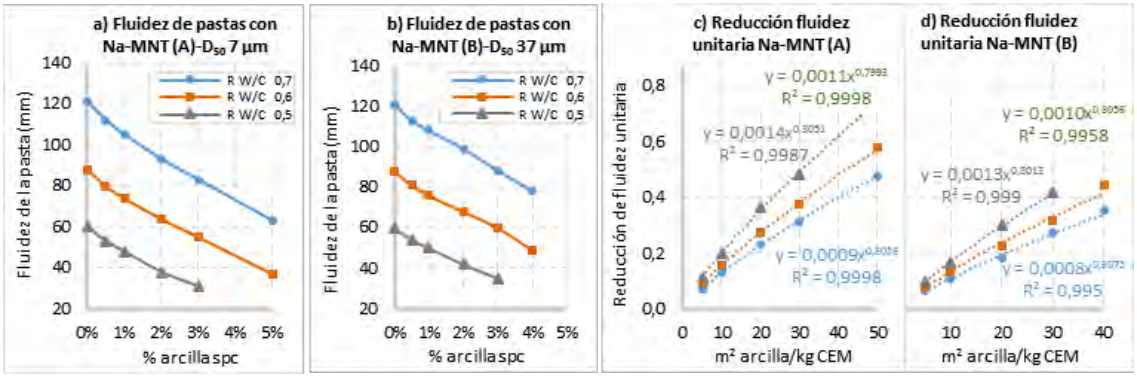

Figura 5. a) Fluidez de pastas con Na-MNT (A); b) Con Na-MNT (B); c) Reducción de fluidez unitaria con Na-MNT (A); d) Con Na-MT (B)

Se observa que el exponente *n* muestra valores casi idénticos en todos los casos, pudiendo intuir que se trata de un valor característico y constante de cada tipología de arcilla. *n* define la progresión de la pérdida de fluidez con la cantidad de arcilla, y podría relacionarse con un factor cinético por el cual, cuando la relación entre la cantidad de arcilla y el volumen de agua es baja, la absorción de agua progresa más rápidamente.

Asumiendo esta hipótesis, el valor *n* se denominará *factor de cinética de absorción*, y se expresará con el símbolo K_A. Cuando el factor K_A tiene un valor de 1, la cinética de adsorción es independiente de la cantidad de arcilla. Cuando $K_A<1$ (como en este caso), el efecto de pequeñas cantidades de arcilla tiene un mayor impacto relativo sobre la fluidez inicial, y si $K_A<1$ la absorción inicial relativa se aceleraría exponencialmente con la cantidad de arcilla.

log*A* equivale a la reducción de fluidez unitaria causada por 1 $gr_{arcilla}/kg_{cemento}$. Como se observa en la Fig. 6(a) y 6(b), puede relacionarse linealmente con la R W/C. Esta relación se observa en las dos arcillas Na-MNT, las cuales no tienen composición idéntica (impurezas diferentes que acompañan a la arcilla en cada una de ambas muestras) ni similar superficie específica y diámetro medio de partícula. De este modo, el valor *A* puede expresarse en función de la R W/C con los parámetros del ajuste lineal *a* y *b* (que se denominarán α_A y β_A respectivamente), obteniendo la Ecs. (2) presentada en la Fig. 6(c), que modeliza la interferencia unitaria provocada por la arcilla sobre la fluidez inicial de pastas de cemento y se representa como Ψ_A.

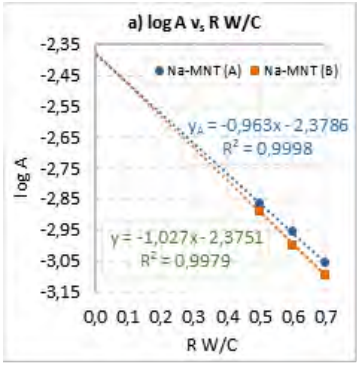

b)

$$\Psi_A = 10^{[\beta_A + \alpha_A(R_{W/C})]} \cdot [(SE_A[A])^{K_A}] \qquad (2)$$

Ψ_A = Factor de interferencia unitaria de la arcilla

[A] = Concentración de arcilla, en kg/kg CEM

K_A = *Factor de cinética de absorción* - Valor de *n* en el ajuste potencial
Define la capacidad de absorción inicial de la arcilla

β_A = *Factor de interferencia residual* - Valor de *b* en la regresión lineal de logA v. R W/C
Cuando [A]= SE_A=1 ($1m^2$ de arcilla) y $R_{W/C}$= 0 (situación teórica) → $\Psi_A = 10^{\beta_A}$

α_A = *Factor de sensibilidad* - Valor de *a* en la regresión lineal de logA v. R W/C
Expresa como la R W/C modula el factor Ψ_A
Para que Ψ_A = 0,5 ($F = \frac{1}{2}F_{cem}$) con $1m^2$ de arcilla → $R_{W/C} = -(0,3+\beta_A)/\alpha_A$

SE_A = Superficie específica BET en m^2/kg

Figura 6. Representación del valor A frente a R W/C; a) Para Na-MNT (A); b) Para Na-MNT (B); c) Ecuación que describe la interferencia unitaria provocada por la arcilla sobre la fluidez inicial

Del mismo que K_A, el valor β_A es muy similar entre ambas arcillas, permitiendo también pensar que puede tratarse de un valor constante y característicos de las arcillas Na-MNT. Integrando la Ecs. (2) en la Ecs. (1) del cemento se puede modelizar la fluidez inicial de las pastas de cemento con arcilla, dando como resultado la Ecs (3) presentada en la Fig. 7(a), mediante la cual es factible evaluar de manera aislada el efecto interferente sobre la fluidez inicial en pastas de cemento que provoca la arcilla Na-MNT debido a su absorción de agua.

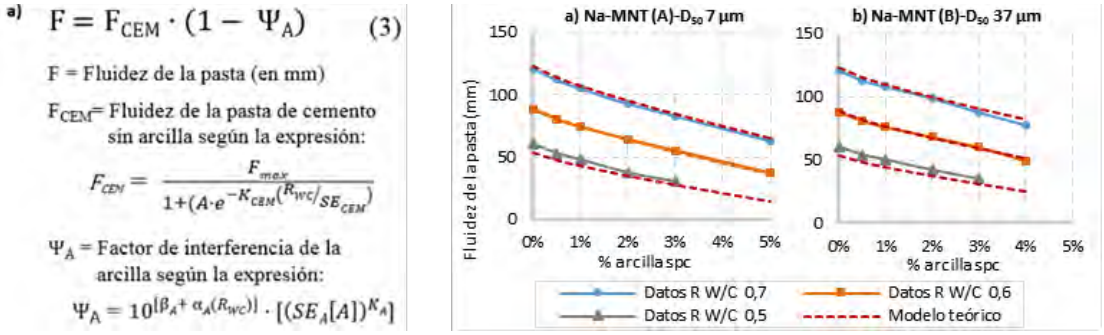

Figura 7. a) Modelo matemático propuesto para determinar la fluidez inicial de pastas de cemento con arcilla; b) Correlación entre los valores teóricos y los resultados experimentales de las dos arcillas

El modelo en general presenta una correlación. La correlación entre el modelo teórico y los datos experimentales se presenta en la Fig. 7(b-c). Se observa una correlación aceptable, que muestra mayores desviaciones a R W/C bajas que son inducidas, en este caso, por la desviación entre el valor inicial de F_{CEM} deducido por la Ecs. (1) y el valor de fluidez inicial experimental obtenido en la pasta de cemento.

3.2. Factor de interferencia por inhibición del efecto dispersante de los aditivos

El segundo factor de interferencia de las arcillas se basa en la inhibición de la capacidad dispersante de los aditivos superplastificantes basados en PCE. Esta inhibición generada por arcillas tipo MNT es conocido y existen publicaciones científicas al respeto que permiten concluir que el mecanismo de inhibición se explica por la intercalación de las cadenas laterales de PEO del polímero de PCE dentro del espacio interlaminar de la arcilla [3]. El fenómeno de intercalación de cadenas puede demostrarse con la observación de la variación de la apertura del espacio interlaminar de la arcilla mediante difracción de rayos-X (XRD). Las arcillas Na-MNT en estado sólido y semi-deshidratadas presentan un valor d_{001} entre 1,23 y 1,26 nm, que define una apertura del espacio interlaminar de 2,7-3,0 Å.

Analizando este parámetro en pastas de arcilla y agua con aditivo (separando la fase sólida por centrifugación y secando el sólido filtrado), se observa que d_{001} aumenta hasta 1,73-1,77 nm, significando que el espacio interlaminar ha expandido hasta 4,7-5,4 Å. El incremento registrado (aprox. 2,7-3,0 Å) se corresponde en distancias a una cadena de PEO coordinada por dos moléculas de agua [3], confirmando la intercalación de cadenas laterales de tal modo que el aditivo pierde su capacidad dispersante.

Para caracterizar el efecto interferente de las arcillas sobre los aditivos se emplean tres polímeros de PCE diferentes, identificados como PCE-1 y PCE-5. La estructura de los

polímeros se representa en la Fig. 8, que incluye la escala en Å y los valores de carga aniónica (λ) obtenida mediante la valoración de los grupos –COOH totales de cada PCE.

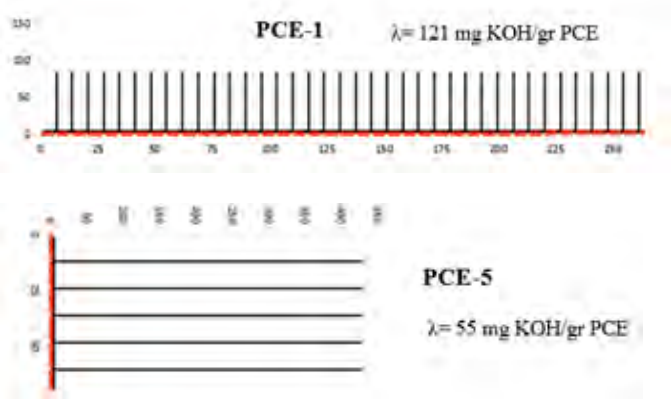

Figura 8. Representación de la estructura de los PCE empleados y carga aniónica

El polímero PCE-1 puede definirse como un PCE con cadena principal larga, cadenas laterales cortas y alta carga aniónica, mientras que PCE-5 está formado por largas cadenas laterales sobre una cadena principal de corta longitud y reducida carga aniónica.

Sobre pastas de cemento con aditivo, se evalúa el impacto sobre la fluidez inicial provocado por diferentes concentraciones de arcilla Na-MNT (A) empleando diferentes dosificaciones de cada PCE (expresada en porcentaje de materia activa sobre peso de cemento) y diferentes R W/C. Los resultados se muestran en la Fig. 9.

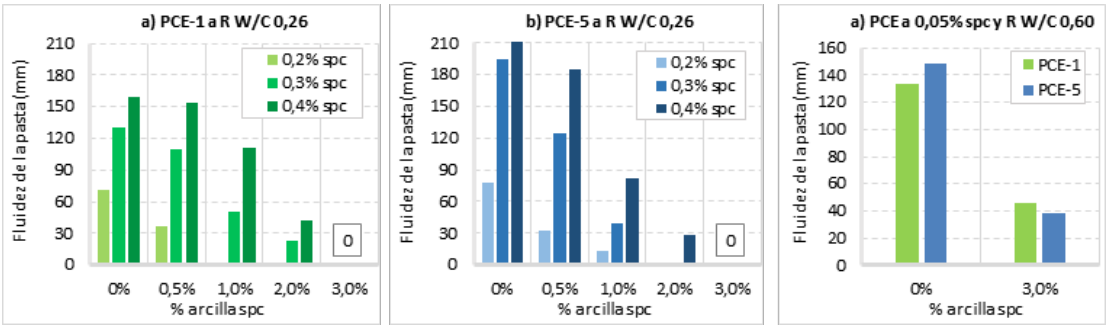

Figura 9. Fluidez de pastas de cemento con arcilla, a) PCE-1; b) PCE-5; c) a R W/C 0,6

El análisis de los resultados presentados en la Fig. 9 permite concluir que la magnitud de la inhibición de la capacidad dispersante del aditivo está relacionada con la estructura del PCE, observándose un mayor impacto cuando mayor es la longitud de las cadenas laterales. Al 3% de Na-MNT todas las pastas con aditivo pierden por completo su fluidez, incluso a dosis

altas de aditivo, salvo a R W/C más elevada. Sin embargo, la reducción de fluidez a R W/C 0,6 presenta una contradicción aparente con los resultados que podrían esperarse, tal y como presenta de forma esquemática la Fig 10 considerado los efectos de absorción y de inhibición.

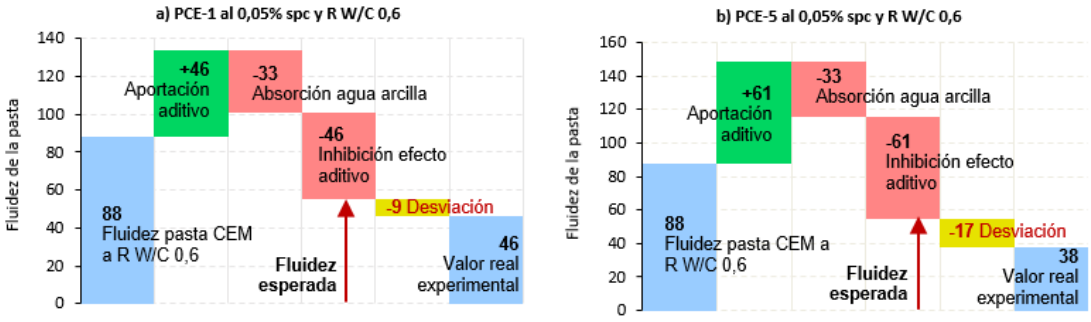

Figura 10. Segmentación de la fluidez a R W/C 0,6 mediante factores aislados. a) Para PCE-1; b) Para PCE-5

Cuando R W/C= 0,26, la fluidez inicial de la pasta de cemento sin arcilla y sin aditivo es 0 a efectos prácticos, de tal modo que se asume que la fluidez generada es contribución exclusiva del aditivo. A R W/C= 0,6 la fluidez inicial de la pasta sin aditivo registrada experimentalmente es de 88 mm, y con la hipótesis de que la arcilla al 3% inhibe por completo el efecto del aditivo, la fluidez residual de la pasta debería mostrar un valor aproximado de 55 mm aplicando la Ecs. (3).

Sin embargo, todas las pastas a R W/C 0,60 con el 3% de Na-MNT y 0,05% spc de aditivo pierden más fluidez de la esperada, indicando que se experimenta un nivel de interferencia mayor al de la suma de los dos efectos interferentes individuales planteados (absorción de agua e inhibición del efecto dispersante).

4. INTERACCIÓN PCE-ARCILLA

Con el objetivo de comprender la desviación de reducción de fluidez observada entre el dato experimental y el valor teórico definido por el modelo en las pastas de cemento a R W/C 0,60 con 3% de arcilla y 0,05% de aditivo, se realizan las curvas de fluidez de pastas de arcilla con aditivo (sin cemento) que se presentan en la Fig. 10(a). Estas pastas se preparan con solución de poro de cemento, con una concentración de arcilla Na-MNT (A) del 20%.

Sobre estas pastas, se obtienen los espectros XRD con Na-MNT (A) y PCE-1 en algunos puntos seleccionados (indicados en la Fig. 11(a)) para determinar la apertura del espacio interlaminar. Pero a diferencia de lo publicado en la literatura disponible, en este caso

las difracciones se realizan sobre las muestras en estado fresco (sin centrifugar para separar y posteriormente secar la fase sólida). La Figura 11(b) muestra los espectros XRD obtenidos.

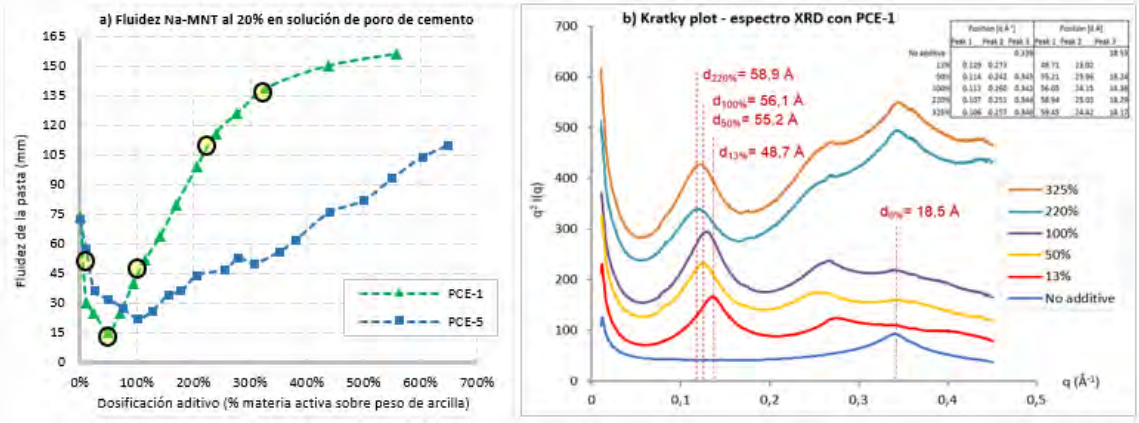

Figura 11. a) Curvas de fluidez de las pastas de arcilla; b) Espectros XRD en fresco

Las curvas de fluidez arcilla-aditivo presentan una zona inicial donde la adición de PCE provoca incluso que la fluidez disminuya, hasta alcanzar una dosis específica a partir de la cual la fluidez ya empieza a incrementar. Esta dosificación umbral es claramente menor en el caso de PCE-1, mostrando un comportamiento coherente con los resultados de fluidez en pastas de cemento de la Fig.9 donde se ha observado una mayor sensibilidad en el PCE de cadenas laterales de mayor longitud.

Los resultados de apertura del espacio interlaminar obtenidos por XRD muestran una dimensión muy superior a la que se registra cuando la difracción se realiza sobre muestras secadas [3].

Resulta evidente que el procedimiento seguido en este caso, realizando las difracciones sobre pastas frescas, es más representativo de la situación real, por lo que podría poner en cuestión la representatividad de los resultados que se obtienen cuando las muestras de pastas de arcilla con aditivo se someten a centrifugación y secado.

Con los valores de q($Å^{-1}$) del espectro, se determina el valor d_{001} y la apertura del espacio interlaminar $d_{T\text{-}T}$, considerando que el espesor de la lámina T-O-T es de 9,6 Å [1]. A partir de este valor, puede estimarse el número de moléculas de agua y de cadenas de PEO contenidas en su interior. Los valores obtenidos se presentan en la Tabla 2, estimados a partir de las distancias de enlace C-O y O-H y la compresión que ejerce el puente de hidrógeno.

PCE-1	*Datos del espectro XRD*		*Interpretación de los valores*	
(% spa)	*d-spacing, d_{001} (Å)*	*$d_{T\text{-}T}$ (Å)*	*Unidades H_2O*	*Cadenas PEO*
0%	19	9	3	-
13%	49	39	8	7
50%	55	46	9	8
100%	56	46	9	8
220%, 325%	59	49	9-11	8

Tabla 2. Interpretación del espectro XRD de las pastas de arcilla con PCE-1

A partir de las interpretaciones de la Tabla 2 se puede idealizar la disposición molecular en el interior del espacio interlaminar, donde las cadenas de PEO intercaladas están flanqueadas por moléculas de agua. De este modo, se presenta el modelo de la Fig. 12(a), donde la unidad L_d constituida por una cadena de PEO y una molécula de agua coordinadas por puentes de hidrógeno se repite *n* veces hasta un valor de intercalación máximo (*n*=8 en este caso). A partir del valor máximo de *n* (a d_{001}>55Å) la expansión del espacio interlaminar se estabiliza, y la reducción de intensidad del primer pico a 220% y 325% (Fig. 10(a)) y la clara reaparición del pico original a d_{001}=19Å sugiere que la arcilla empieza a experimentar delaminación.

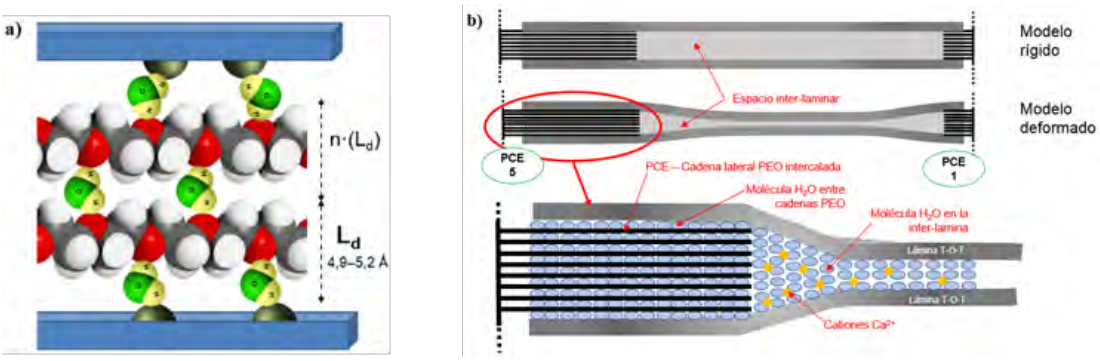

Figura 12. a) Conformación de la intercalación múltiple de cadenas laterales; b) Modelo de intercalación múltiple de cadenas laterales en arcillas MNT

La intercalación múltiple con hasta 8 cadenas laterales en un espacio tan reducido permite plantear que todas las cadenas intercaladas corresponden a la misma molécula de PCE. Esta configuración de intercalación sería inviable con la intervención de varias unidades de PCE debido a los impedimentos estéricos entre los polímeros.

Con la modelización del mecanismo propuesto en la Fig. 12(b) se deduce que en la zona de intercalación el número de moléculas de agua absorbidas incrementa hasta 3 veces, lo que permite explicar la desviación de pérdida de fluidez observada en la Fig. 10 a partir de un

proceso de sobre-absorción provocado por la intercalación múltiple de cadenas laterales, que es mayor cuanto mayor es la longitud de las cadenas laterales.

La expansión interlaminar provocada por las cadenas intercaladas se experimenta en la parte más superficial de la arcilla. De este modo, como se ilustra en la Fig. 12(b), la arcilla podría presentar un modelo rígido, en el cual la separación entre láminas es equivalente en todo el plano, o un modelo deformado, en el que la apertura provocada por el PCE va contrayéndose hasta los 19Å (con solamente 3 moléculas de agua). Inicialmente el modelo rígido parecería el más lógico, pero la reaparición del pico correspondiente a 19Å a partir del 50% de aditivo (cuya intensidad aumenta a dosis superiores) y la pérdida de agudeza del pico principal con el aumento de aditivo (relacionado con deformaciones de la estructura laminar) [3] son más coherentes con el modelo deformado.

5. CONCLUSIONES

La interpretación de los resultados de los ensayos permite extraer las siguientes conclusiones:

- El efecto interferente sobre la fluidez asociado a la absorción de agua de Na-MNT se ha descrito matemáticamente, permitiendo aislar este efecto del provocado por el aditivo.
- Con el modelo teórico de absorción de agua de Na-MNT se identifica la sobre-absorción de moléculas de agua que promueve la intercalación múltiple de cadenas de PEO en el espacio interlaminar.
- El espectro XRD sugiere que se intercalan de forma simultánea hasta 8 cadenas de PEO, coordinadas por moléculas de agua dispuestas entre cada cadena y entre la superficie interna del espacio, describiendo una secuencia repetitiva H_2O-PEO.
- Se han observado diferencias relevantes entre los valores de d_{001} obtenidos con XRD de pastas frescas y con la fase sólida seca (por centrifugación y secado de las pastas). De confirmarse, significaría que en el procedimiento de centrífuga y/o secado se liberan cadenas de PEO absorbidas que arrastran también moléculas de agua fuera del espacio, restando representatividad a los resultados que se obtendrían.
- La hipótesis de la sobre-absorción de agua por la intercalación múltiple de cadenas de PEO permite explicar también por qué los PCE con cadenas laterales de mayor longitud experimentan un nivel de interferencia con arcillas mayor que los tipos con cadena corta.

Los modelos e hipótesis planteadas se ajustan al comportamiento observado con los materiales particulares empleados, y deberían ser validados con estudios complementarios.

Referencias

[1] Domínguez, Schifter (1995). “Las arcillas: el barro noble”. Instituto Latinoamericano de la Comunicación Educativa. México DF (México).

[2] Xing, Fang, Wang (2017). “Cement dispersion performance of superplasticizers in the presence of clay and interaction between superplasticizers and clay”. Advances in Cement Research, vol. 29, issue 5, pág. 194-205. Hefei (China).

[3] Plank (2012). “Interaction mechanism between Na-montmorillonite clay and MPEG-based polycarboxylate superplasticizers”. Cement and Concrete Research vol. 42, pág. 847-854. Technische Universitat Munich, Garching (Alemania).

3.1. OTHER PUBLICATIONS I

LUZ SINCROTRÓN PARA ILUMINAR EL DESARROLLO DE ADITIVOS SUPERPLASTIFICANTES DE ALTAS PRESTACIONES INSENSIBLES A LAS ARCILLAS

Published in Cemento Hormigón 993 (Julio 2019) 52-55.

Pere Borralleras[a], Ignacio Segura[b, c,*], Miguel A. G. Aranda[d] and Antonio Aguado[b]

[a] BASF Construction Chemicals Iberia, Ctra del Mig 219, E-08907 Hospitalet de Llobregat, Barcelona, Spain

[b] Department of Environmental and Civil Engineering, Universitat Politècnica de Catalunya-Barcelona Tech, Jordi Girona 1-3, C1, E-08034 Barcelona, Spain

[c] Smart Engineering Ltd, Jordi Girona 1-3, ParcUPC–K2M, E-08034 Barcelona, Spain

[d] ALBA Synchrotron, Carrer de la Llum 2-26, E-08290, Cerdanyola del Vallès, Barcelona, Spain

* Corresponding author: Pere Borralleras Mas, Technical & Marketing Department, BASF Construction Chemicals España, Ctra. Del Mig 219, E-08907 Hospitalet de Llobregat, Spain. Email address: pere.borralleras@basf.com Tel: +34 93 2616158

Resumen

Investigadores de BASF Construction Chemicals España, la Universitat Politècnica de Catalunya y del sincrotrón ALBA de Cerdanyola del Vallès, desarrollan un nuevo método analítico empleando rayos-X generados por luz sincrotrón para determinar la expansión de arcillas montmorillonitas inducida por la intercalación de aditivos superplastificantes basados en policarboxilatos. Los resultados experimentales obtenidos con el nuevo método aportan una mayor y mejor comprensión del proceso de interacción entre este tipo de superplastificantes y las arcillas expansivas, abriendo nuevos escenarios para el desarrollo de aditivos que promuevan un uso más eficiente de las arenas en la fabricación de hormigones y contribuyan al desarrollo sostenible del sector

Abstract

Researchers from BASF Construction Chemicals Spain, Universitat Politècnica de Catalunya and ALBA synchrotron from Cerdanyola del Vallès, develop a new analytical method by using X-rays generated by synchrotron light to determine the expansion of montmorillonite clays induced by the intercalation of polycarboxylate-based superplasticizers. The experimental results obtained with the new method provide greater and better understanding of the interaction process between this type of superplasticizers and expansive clays, opening new scenarios for the development of admixtures that promote a more efficient use of sands in the manufacture of concretes and contribute to the sustainable development of the sector.

1. INTRODUCCIÓN

Los aditivos superplastificantes de nueva generación basados en polímeros de éter de policarboxilato (PCE) son, en todos los aspectos, el tipo de reductores de agua para hormigón de mayores prestaciones [1-3]. Su introducción en el mercado del hormigón empezó en el año 2000, como alternativa a los aditivos superplastificantes convencionales basados en polímeros de naftalensulfonato (BNS) y melamina sulfonada (MNS), y ofreciendo un gran número de nuevas oportunidades a explorar, hasta el punto de que en la actualidad ya son el tipo de aditivos más empleado.

De forma directa o indirecta, los últimos avances tecnológicos con mayor trascendencia para el sector del hormigón están estrechamente vinculados con los superplastificantes de nueva generación. Por ejemplo, el diseño de nuevos hormigones como el hormigón de altas prestaciones (HPC), el hormigón autocompactante (SCC) o el UHPC (Ultra-High Performance

Concrete) era técnicamente inviable con las tecnologías predecesoras porque precisa de unos niveles de reducción de agua solamente al alcance de los aditivos basados en polímeros de PCE [4,5].

A partir de 2004, se consolidó el uso regular de este tipo de aditivos para fabricar los hormigones convencionales de consumo diario (tipo HA-25/B), ya que permiten obtener interesantes optimizaciones de los costes de producción, al mismo tiempo que reducen el impacto ambiental asociado y contribuyen de manera activa en el desarrollo sostenible del sector.

Sin embargo, es conocido que los aditivos superplastificantes de nueva generación basados en polímeros de PCE presentan una alta sensibilidad a las arcillas [6-10]. De este modo, cuando las arenas contienen ciertas arcillas en su composición (aunque sea en muy baja cantidad), la capacidad dispersante de estos aditivos queda significativamente mermada y no es posible acceder a todas sus ventajas. En consecuencia, la interferencia en el rendimiento de los polímeros de PCE causada por la presencia de arcillas en la arena restringe y limita los beneficios que esta tecnología es capaz de aportar, tanto técnicos, como económicos y ambientales.

Las arenas para hormigón, incluso siendo aptas para su uso según el criterio del ensayo del azul de metileno UN-EN 933-9, pueden contener pequeñas cantidades de ciertas arcillas que son suficientes para perturbar de forma crítica la capacidad dispersante de los aditivos superplastificantes [6]. Los efectos no deseados provocados son la falta de fluidez inicial del hormigón, que obliga a aumentar el contenido de agua en el momento de su fabricación, y la pérdida prematura de consistencia durante el transporte, que incrementa el riesgo de adición de agua en obra y las consecuentes pérdidas incontroladas de resistencia y durabilidad. La envergadura y magnitud de esta interferencia depende de la cantidad y del tipo de arcillas presentes en la arena, pero, en cualquier caso, obliga a considerar medidas correctoras o preventivas para contrarrestar los efectos no deseados provocados por las arcillas.

Las arcillas contenidas en las arenas interfieren en el rendimiento de cualquier tipo de aditivo en mayor o menor medida. Sin embargo, cuando estas arcillas son del tipo expansivo, como por ejemplo las montmorillonitas (MNT), la pérdida de capacidad dispersante experimentada por los aditivos basados en PCE es muy superior a la que experimentan los superplastificantes convencionales basados en BNS y MNS [7-10].

Este comportamiento se puede constatar en la Figura 1, donde se presenta la fluidez de pastas de cemento que contienen diferentes tipos de arcilla y de aditivos superplastificantes. Se observa que la pérdida de fluidez de la pasta de cemento que contiene 2% de arcilla del tipo

MNT y aditivo basado en PCE es superior al 80% (respeto a la pasta de cemento sin arcilla), mientras que para los aditivos basados en BNS y MNS la pérdida de fluidez es del orden del 45%.

Contrariamente, con las arcillas de naturaleza no expansiva (caolín, moscovita), las pérdidas de fluidez son muy inferiores a las provocadas por la arcilla MNT y, en cualquier caso, sin apenas diferencias entre los polímeros de PCE y los de BNS y MNS. En el mismo sentido, la Figura 2, que indica como aumenta la demanda de agua relativa del hormigón cuando aumenta el valor del azul de metileno (MBV) de la arena, demuestra el mismo comportamiento, evidenciando que los polímeros de PCE son mucho más sensibles a la presencia de arcillas que los polímeros de BNS.

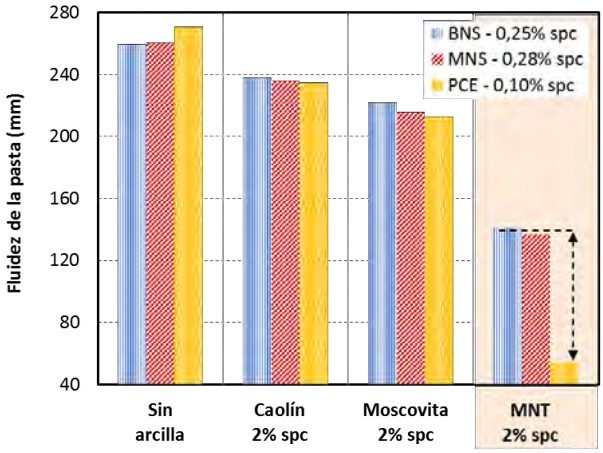

Figura 1.- Fluidez de pastas de cemento que contienen diferentes tipos de arcilla y de aditivo superplastificante a diferentes dosificaciones para equilibrar la fluidez de la pasta de cemento sin arcilla

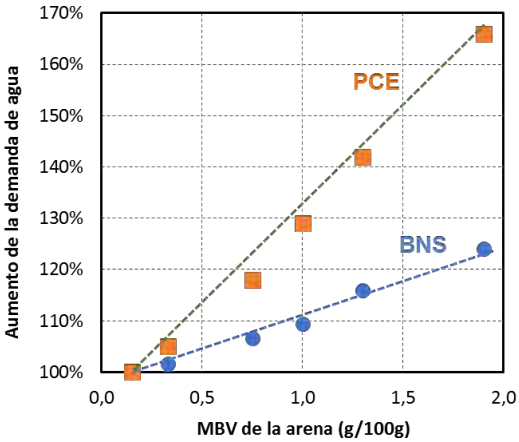

Figura 2.- Aumento de la demanda de agua del hormigón por el incremento del valor del azul de metileno (MBV) de la arena para un superplastificante convencional basado en BNS y un superplastificante de nueva generación basado en PCE

2. DESARROLLO DE ADITIVOS SUPERPLASTIFICANTES DE ALTO RANGO INSENSIBLES A TODO TIPO DE ARCILLAS

2.1. Objetivos planteados

La investigación dirigida a desarrollar aditivos superplastificantes de alto rango con alta tolerancia a las arcillas se plantea a partir de dos objetivos diferentes a alcanzar. El primero tiene como finalidad diseñar estructuras poliméricas con baja sensibilidad a las arcillas no-expansivas. En esta línea, BASF Construction Chemicals presentó en 2017 *MasterSuna*, el último avance en

aditivos superplastificantes de altas prestaciones caracterizado por una mayor tolerancia a las arcillas. Los aditivos superplastificantes *MasterSuna* permiten fabricar hormigones estructurales con arenas de baja calidad pero aún aptas para su uso, debido a que contienen arcillas del tipo no-expansivo.

La Figura 3 muestra las mejoras de compatibilidad de *MasterSuna* comparando la demanda de aditivo y el mantenimiento de consistencia de un hormigón tipo HA-25/F fabricado con aditivo superplastificante *MasterSuna* y con un aditivo basado en polímeros convencionales de PCE, donde se puede observar el mejor comportamiento en el mantenimiento de consistencia del hormigón con *MasterSuna* con un 33% menos de dosificación de aditivo.

En estas condiciones, la menor sensibilidad de *MasterSuna* a las arcillas no-expansivas permite evitar el uso de arenas correctoras o ahorrar el incremento habitual de cemento que se precisa al trabajar con arenas de baja calidad. Esto resulta en ahorros directos del coste de producción del hormigón y en la optimización de las variables ambientales, la magnitud media de los cuales se muestra en la Figura 4 para un diseño típico de un hormigón HA-25/F fabricado con una arena granítica que contiene arcillas clorita y moscovita, comparativamente al mismo diseño de hormigón. pero empleando una arena sin arcilla.

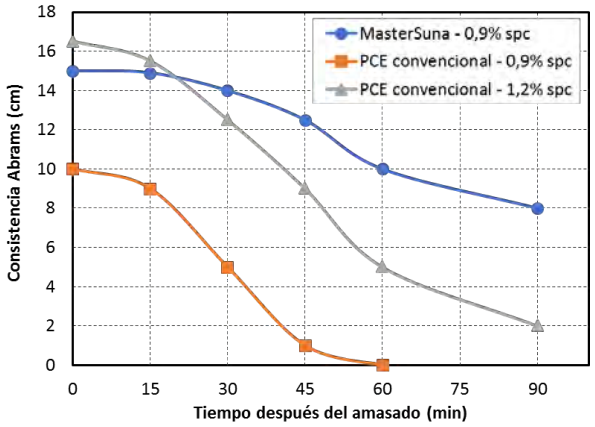

Figurra 3.- Evolución de consistencia Abrams de hormigones HA-25/F fabricados con superplastificante *MasterSuna* al 0,9% spc y con superplastificante basado en PCE al 0,9% spc y 1,2% spc

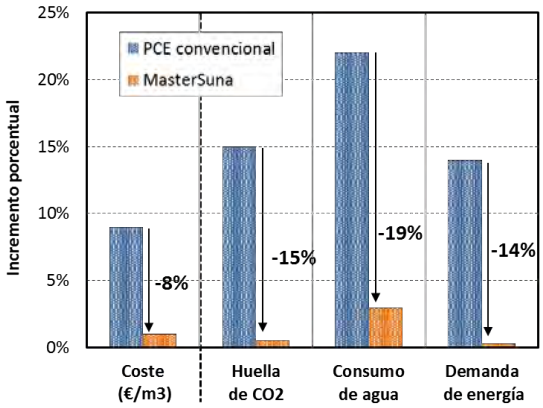

Figura 4.- Impacto relativo en el coste del hormigón y en la huella de CO_2, consumo de agua y demanda de energía asociada motivo por el incremento de cemento en la dosificación de un hormigón HA-25/F

La mejor tolerancia de *MasterSuna* a las arcillas no-expansivas se consigue a partir del control de las afinidades de adsorción de los polímeros que componen estos aditivos, haciendo que la captura de aditivo por parte de las partículas de arcillas sea mínima y quede más aditivo disponible para interaccionar con el cemento [11].

Gracias a estas ventajas, con *MasterSuna* se están optimizando con éxito hormigones fabricados con arenas problemáticas que contienen arcillas del tipo mica y clorita, las más frecuentes en arenas calizas y graníticas, aportando ahorros de coste para el productor de hormigón y mejoras en el impacto ambiental asociado. De este modo, se puede considerar que el primer objetivo del desarrollo de superplastificantes de alto rango insensibles a las arcillas del tipo no-expansivo en buena parte ya se ha alcanzado. A pesar de este logro, la tecnología *MasterSuna* sigue en continuo desarrollo para llegar a alcanzar el segundo y más ambicioso objetivo planteado: hacer técnicamente viable el empleo de arenas que contienen cantidades relevantes de arcillas expansivas (tipo MNT) para fabricar hormigón.

Todos los antecedentes sugieren que este es un reto ambicioso debido a la complejidad del proceso de interacción entre los polímeros de PCE y las arcillas MNT, que combina simultáneamente los procesos de adsorción superficial competitiva típica de todas las arcillas con todos los tipos de aditivos con los procesos de absorción por intercalación de las cadenas laterales del polímero de PCE exclusivos de la combinación entre arcillas MNT y polímeros de PCE [12,13]. Este proceso de intercalación es el responsable de la casi total inhibición de la capacidad dispersante de los superplastificantes de nueva generación.

La consecución de este segundo objetivo permitirá sin duda un uso más eficiente de las arenas, por ejemplo, minimizando o incluso evitando el proceso de lavado. La Figura 5 (izquierda) muestra los impactos negativos en pérdida de productividad, consumo de agua y generación de residuos sólidos producidos por tonelada de arena comercial en una instalación de lavado con una capacidad de entrada de 100 Tn/h. La optimización de la necesidad de lavado hará factible optimizar el aprovechamiento de los recursos naturales, maximizar el rendimiento de los centros de extracción de áridos y minimizar su impacto paisajístico, así como reducir la generación de residuos sólidos y el impacto ambiental (Figura 6-derecha).

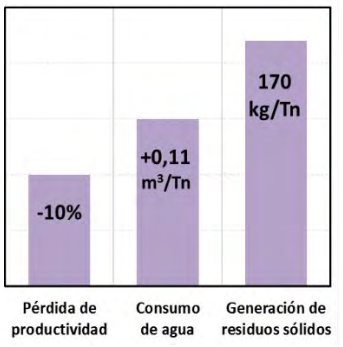

Figura 5.- Consecuencias del lavado de arena - Fig 6.- Ejemplos de impacto paisajístico de los centros de extracción de áridos

A pesar de que en varias publicaciones científicas se han estudiado nuevos diseños de polímeros para reducir su sensibilidad a estas arcillas [14-18], ninguna de estas soluciones es, hasta la fecha, lo suficientemente robusta, eficiente e industrialmente viable para permitir resolver este problema de forma definitiva. En consecuencia, se puede concluir que, sin la plena compresión del mecanismo de interacción, el desarrollo de aditivos superplastificantes de altas prestaciones insensibles a todo tipo de arcillas resulta extremamente complicado.

2.2. Limitaciones para la comprensión del mecanismo de interacción entre polímeros de PCE y arcillas MNT (montmorillonitas). Método convencional para determinar la expansión de la arcilla

A diferencia de las arcillas no-expansivas, las montmorillonitas (MNT) se caracterizan por disponer de un espacio interlaminar muy accesible que les confiere la capacidad para absorber agua y otras moléculas polares. Son muy frecuentes en arenas extraídas de lechos de río o en yacimientos sedimentarios, de tal modo que, en definitiva, la finalidad de los procesos de lavado de las arenas silíceas naturales no es otra que eliminar esta fracción arcillosa y prevenir así los efectos dañinos que provoca en la calidad final del hormigón.

Del mismo modo que cuando las arcillas MNT absorben agua, la intercalación de polímeros de PCE dentro del espacio interlaminar provoca la expansión de la arcilla. La manera en cómo progresa y evoluciona esta expansión resulta de gran interés para comprender la naturaleza de la interacción PCE-MNT, de tal modo que registrar los cambios en la apertura del espacio interlaminar de estas arcillas (d_{001} - d-spacing) es fundamental.

Destacar que este valor, d_{001}, es una medida directa de la distancia entre dos láminas consecutivas de arcilla y por tanto su aumento en el proceso de intercalación da información sobre la especie que se inserta entre las láminas de la arcilla.

La técnica analítica para medir el grado de expansión de las arcillas es la difracción de rayos X de polvo (XRPD, de sus siglas en inglés). El procedimiento experimental aplicado en todas las referencias bibliográficas encontradas consiste en preparar pastas de arcillas dispersando la arcilla en polvo en una solución de poro de cemento sintética y con superplastificante basado en PCE. Estas pastas se centrifugan o filtran para separar y recuperar la fracción sólida, la cual se seca hasta obtener una muestra en polvo que se somete a la prueba analítica, difracción de rayos X.

Sin ir más lejos, gracias a la difracción de rayos X ha sido posible deducir las diferencias entre el tipo de interacción de los polímeros de PCE con las arcillas expansivas y las no-

expansivas, como demuestran los espectros mostrados en la Figura 7 obtenidos a partir de pastas de arcilla desecadas de caolín, moscovita y montmorillonita.

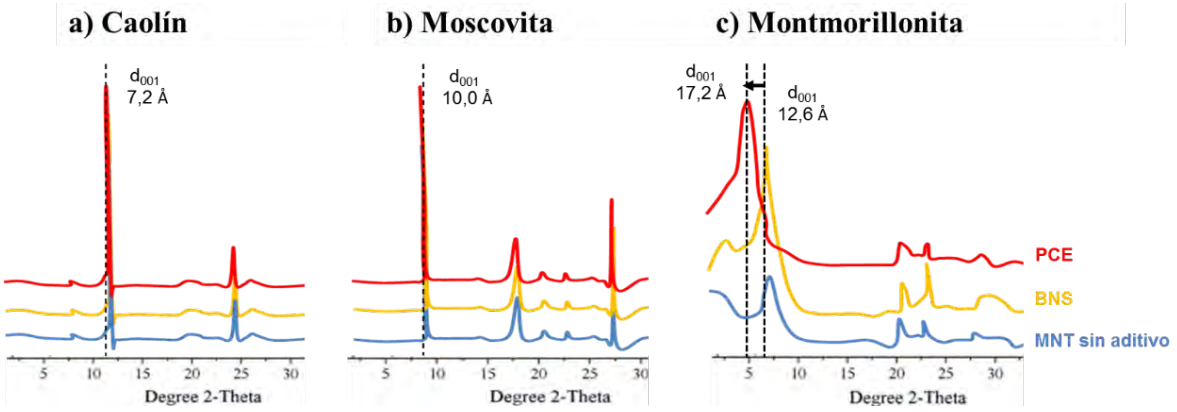

Figura 7.- Difractogramas XRPD y valores de d-spacing (d_{001}) obtenidos a partir de pastas de arcillas desecadas; a) Caolín, arcilla no-expansiva; b) Moscovita, arcilla no expansiva de la familia de las micas; c) Arcilla expansiva del tipo montmorillonita (adaptado de [10])

Las Figuras 7(a) y 7(b) muestran, que en todos los casos con arcillas no-expansivas (p.ej. caolín y moscovita), tanto para el PCE como para BNS no cambia la distancia interlaminar con respecto al blanco (arcilla sin aditivo). Esta afirmación se basa en la evidencia experimental de que d_{001} tiene el mismo valor en las diferentes condiciones.

Los difractogramas de la Figura 7(c) de pastas de arcilla montmorillonita tampoco registran cambios cuando la pasta contiene aditivo basado en BNS, pero en el caso del polímero de PCE, se constata que hay un desplazamiento de la posición 2θ hacia ángulos menores. Esto significa que la separación entre las láminas de la arcilla ha aumentado y, por lo tanto, que ha habido una expansión del espacio interlaminar de la montmorillonita provocada por el polímero de PCE. Y a partir del incremento del valor de espaciado d_{001}, es posible deducir el número de capas de cadenas laterales del PCE intercaladas dentro de la arcilla.

Desafortunadamente, hay claros indicios que evidencian que los resultados de expansión de la arcilla (d_{001} - d-spacing) obtenidos con esta técnica analítica no se ajustan con el comportamiento real. La principal razón son las discrepancias identificadas entre los valores de d-spacing y los resultados de pérdida de fluidez y de sorción de aditivo.

Este desajuste entre los perfiles de expansión de la arcilla y los resultados experimentales de fluidez y sorción se refleja en la Figura 8(a,b), donde se muestran respectivamente los resultados de fluidez de pastas de cemento y de sorción de aditivo en pastas de arcilla para tres

montmorillonitas diferentes (MNT-1, MNT-2 y MNT-3) combinadas con tres polímeros de PCE con claras diferencias en su estructura polimérica.

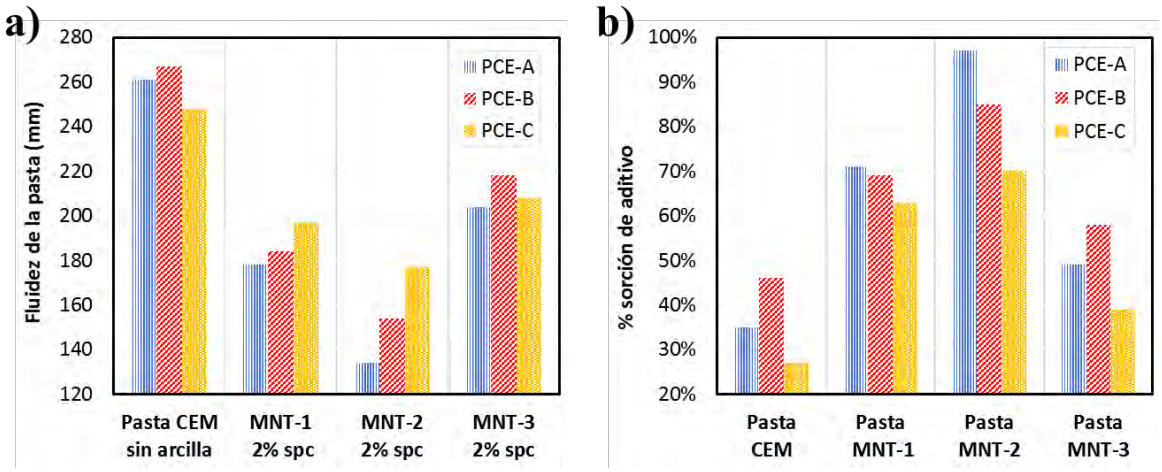

Figura 8.- Comparación de resultados experimentales entre combinaciones de tres arcillas MNT y tres polímeros de PCE (adaptado de [13,19,20]); a) Fluidez de pastas de cemento; b) Sorción de aditivo en pastas de arcilla

Estos resultados de la Figura 8 se contrastan con los valores experimentales de d-spacing obtenidos por XRPD de pastas de arcilla desecadas que presenta la Figura 9. Se puede detectar que, mientras los datos de fluidez y de sorción evidencian claras diferencias de comportamiento entre las tres arcillas y los tres PCE, los resultados de d-spacing de la Figura 9 para las mismas pastas indican un perfil de expansión idéntico para todas las combinaciones MNT-PCE. Esta afirmación se basa en que, en todos los casos, las diferencias de d-spacing son inferiores a 3 Å, que es la dimensión equivalente a una capa de moléculas de agua absorbidas en la inter-lámina.

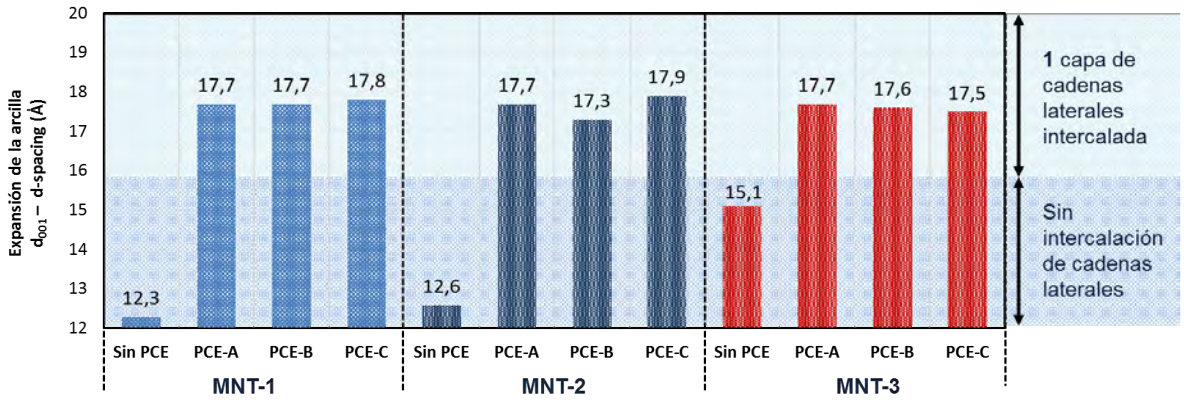

Figura 9.- Resultados de d-spacing obtenidos por XRPD de pastas de arcilla desecadas (adaptado de [13,19,20])

En consecuencia, atendiendo a los valores obtenidos de expansión neta de la arcilla, debe deducirse que todas las montmorillonitas y todos los polímeros de PCE tienen el mismo comportamiento en cuanto a la intercalación, en el cual una sola capa de cadenas laterales es intercalada dentro del espacio interlaminar siguiendo un *modelo de intercalación monocapa* que se ilustra en la Figura 10.

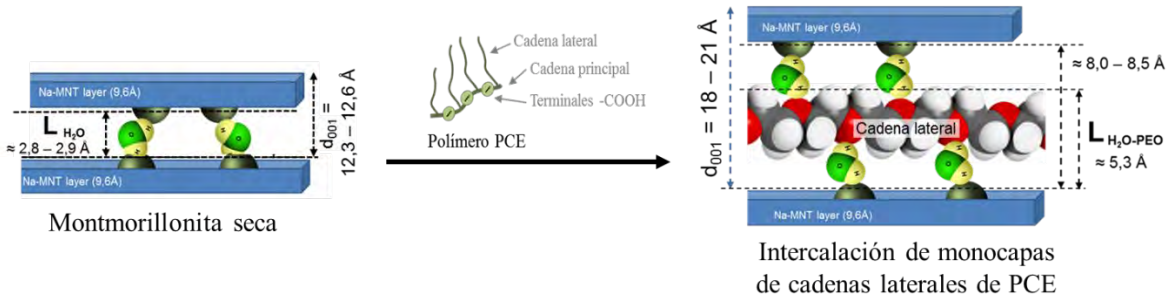

Figura 10.- Modelo de intercalación monocapa de cadenas laterales de PCE deducido a partir de los resultados de expansión obtenidos por XRPD de pastas de arcilla desecadas (adaptado de [21])

Según este modelo de intercalación monocapa, una sola capa de cadenas laterales del PCE en disposición planar tipo zig-zag queda intercalada dentro del espacio interlaminar, coordinada por dos capas de moléculas de agua [20], con independencia de las propiedades de la montmorillonita y de la estructura del polímero de PCE.

Las mismas discrepancias con los valores de d-spacing se identifican cuando se compara la influencia de la dosificación de aditivo, tal y como se muestra en la Figura 11. Se observa que en la Figura 11(a) la dosificación de aditivo genera cambios apreciables tanto en la fluidez de la pasta y en el perfil de sorción. Sin embargo, en la Figura 11(b) no se detecta ningún cambio significativo en la expansión de la arcilla porque las diferencias de d-spacing entre todas las dosificaciones de PCE ensayadas son inferiores a 3 Å. Esto debe asimilarse a que la dosificación de aditivo no altera el modelo de intercalación monocapa deducido por los resultados de expansión obtenidos por XRPD de pastas de arcilla desecadas.

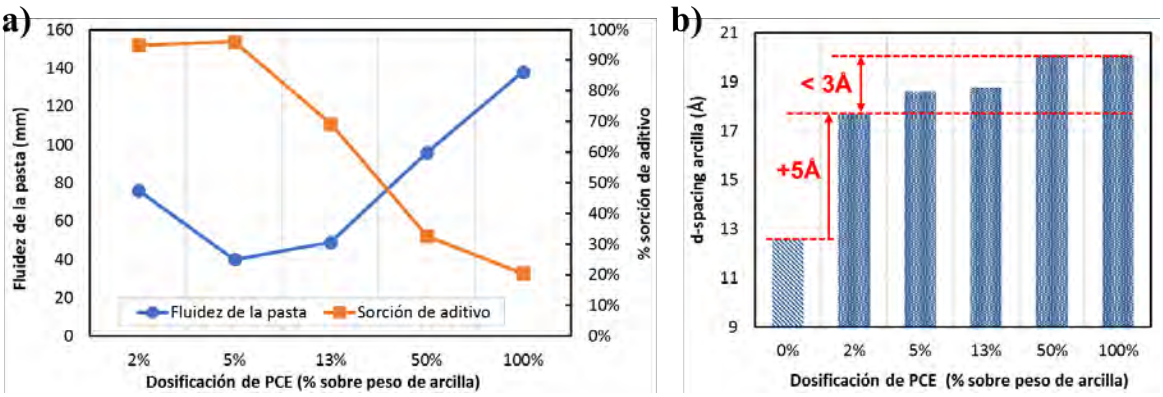

Figura 11.- a) Fluidez y porcentaje de sorción de aditivo de pastas de arcilla con diversas dosificaciones de PCE; b) d-spacing por XRPD de pastas de arcilla desecadas con diferentes dosis de PCE (adaptado de [21,22])

De forma general, los valores de expansión de la arcilla obtenidos por la difracción de rayos X del polvo desecado de pastas de arcilla siempre están comprendidos entre 17-21Å que, a efectos prácticos, se pueden considerar como invariables con independencia de la dosificación y del tipo de polímero de PCE y de las propiedades de la arcilla montmorillonita. Sin embargo, sí se revelan comportamientos muy diferenciados de fluidez y sorción.

En consecuencia, puede afirmarse que los resultados de expansión obtenidos con el método de ensayo convencional no son consistentes con el comportamiento observado en la fluidez y la sorción de aditivo y no reproducen la influencia de la dosificación y de la estructura del polímero de PCE ni de las diferencias entre propiedades de la arcilla.

Estas desavenencias entre datos experimentales no permiten plantear de forma coherente ninguna interpretación del mecanismo de interacción/intercalación. Con el método de ensayo empleado hasta esta investigación, para determinar la expansión de la arcilla provocada por la absorción de polímeros de PCE, no se pueden establecer correlaciones por lo que la generación de los nuevos conocimientos necesarios para interpretar el mecanismo de interacción queda estancada.

3. NUEVO PROCEDIMIENTO DE ENSAYO PARA DETERMINAR LA EXPANSIÓN DE LA ARCILLA PROVOCADA POR LA INTERCALACIÓN DE POLÍMEROS DE PCE

Fruto de la suma de esfuerzos entre la empresa privada, centros tecnológicos y la universidad, investigadores de BASF Construction Chemicals, la Universistat Politécnica de

Catalunya y el Sincrotrón ALBA han desarrollado un nuevo método de ensayo para determinar la expansión de la arcilla (d-spacing, d_{001}) producida por la intercalación de cadenas laterales de los polímeros de PCE [21].

El nuevo método, al igual que el método convencional, se basa en la técnica de difracción de rayos-X de polvo (XRPD). Sin embargo, la difracción se realiza directamente sobre las pastas de arcilla en fresco, evitando todos los tratamientos previos de las muestras, tanto la separación de fases (centrifugado o filtración) como el secado de la pasta.

Para disponer de la resolución necesaria para detectar los cambios de expansión de la arcilla en estas condiciones, las difracciones se realizan con rayos-X generados por luz sincrotrón en el Sincrotrón ALBA de Cerdanyola del Vallès (Figura 12).

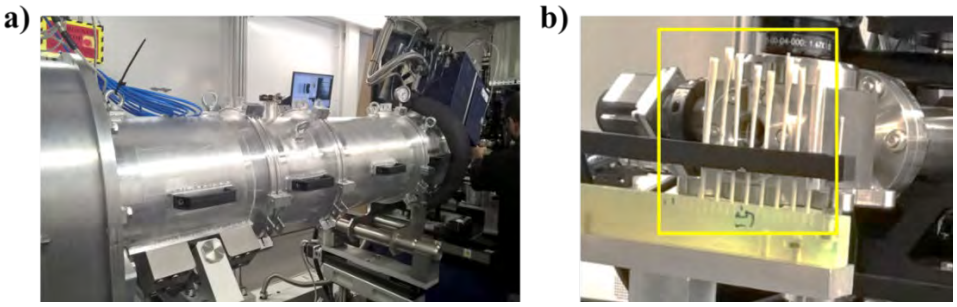

Figura 12.- a) Línea de luz NCD-SWEET del Sincrotrón ALBA; b) Capilares con las pastas frescas montados en el rack del equipo de difracción

Los resultados de d-spacing obtenidos con este nuevo método revelan aspectos imposibles de vislumbrar con el método convencional. Por un lado, se observa que la intercalación de polímeros de PCE provoca expansiones de la arcilla hasta tres veces superior, y permite distinguir la influencia en los perfiles de expansión tanto de la dosificación de aditivo como de las propiedades del polímero de PCE y de la arcilla.

La Figura 13 compara los difractogramas de pastas de arcilla con dos dosificaciones de polímero de PCE. La Figura 13(a) corresponde a los espectros obtenidos con el nuevo método de ensayo por XRPD directamente sobre pastas frescas inalteradas con luz sincrotrón, y la Figura 13(b) a los espectros obtenidos por XRPD del polvo desecado de pastas de arcilla, empleando un difractómetro Kα Cu. Comparando las posiciones de los picos de cada espectro y la dimensión del espacio interlaminar asociado (d_{001} – d-spacing), queda evidenciado que la difracción sobre pastas frescas revela un perfil de expansión totalmente diferente al que ofrece el método convencional.

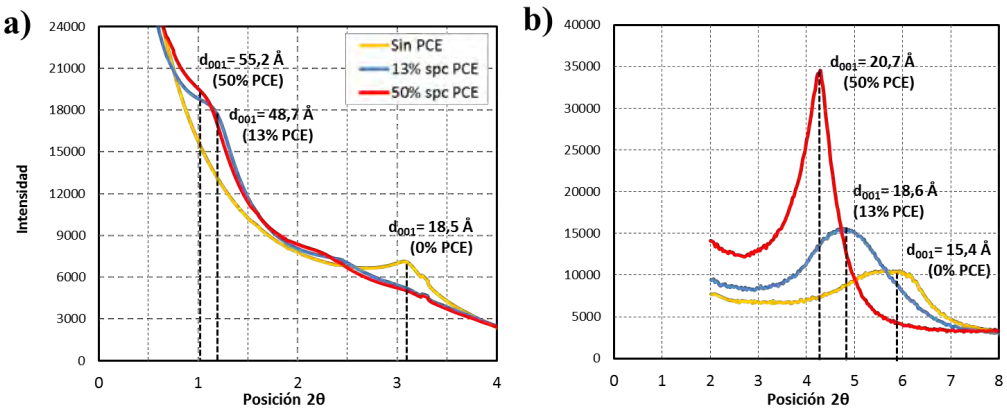

Figura 13.- Espectros de difracción de pastas de arcilla con polímero de PCE al 0%, 13% y 50% sobre peso de arcilla (de [21]); a) Sobre pastas frescas inalteradas empleando rayos X generados con luz sincrotrón; b) Sobre pastas desecadas empleando rayos X generados por un difractómetro Kα Cu

Para el caso de la Figura 13(a), el nuevo método de ensayo confirma que la dosificación de aditivo influye en el grado de expansión de la arcilla, en la línea que sugieren los datos experimentales de fluidez y de sorción pero que no se reproduce en los valores de expansión obtenidos por el método convencional. Esta aportación del nuevo método se presenta en la Figura 14(a), que compara los resultados de d-spacing obtenidos con ambos métodos en pastas de arcilla con diferente dosificación de aditivo.

Adicionalmente a la influencia de la dosificación de PCE, los espectros de difracción con luz sincrotrón sobre pastas frescas también revelan que polímeros de PCE con diferentes estructuras poliméricas y arcillas con propiedades diferentes generan diferentes valores de espaciado. En consecuencia, la influencia deducida a partir otras evidencias experimentales puede ser reproducida en el perfil de expansión de la arcilla obtenido por XRPD sobre pastas de arcillas frescas.

Esta notable aportación se muestra en las Figuras 14(b) y 14(c), donde se compara respectivamente el d-spacing generado por tres tipos de polímeros de PCE y tres tipos de arcillas MNT, empleando XRPD sobre pastas frescas y sobre pastas desecadas.

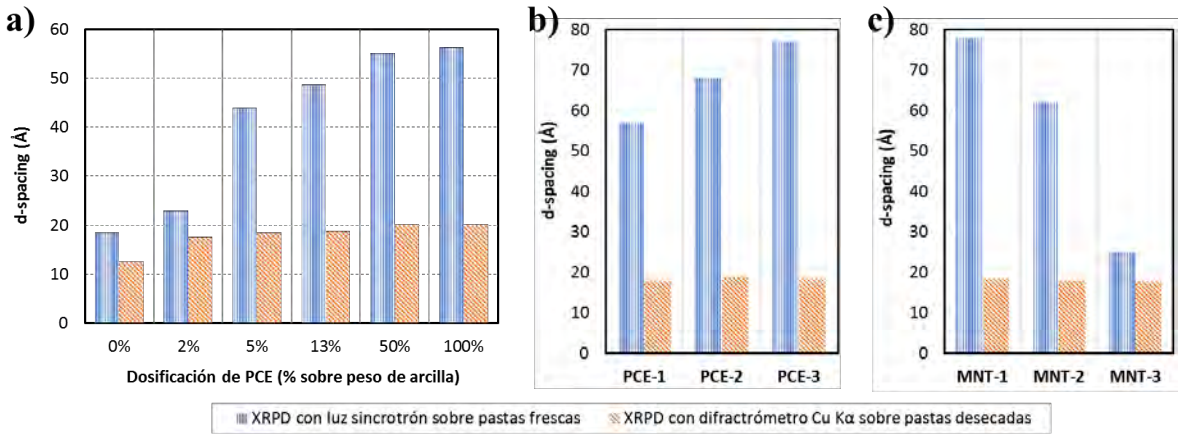

Figura 14.- Comparativa de resultados de d-spacing obtenidos por XRPD con luz sincrotrón sobre pastas de arcilla frescas y por XRPD sobre pastas desecadas con un difractómetro Kα Cu

Además de todas estas nuevas revelaciones, es importante destacar que los resultados de d-spacing obtenidos con pastas frescas son coherentes con los resultados de fluidez y de sorción, sugiriendo que el nuevo método es más representativo del comportamiento real. En cualquier caso, los resultados del nuevo método indican que el tratamiento de las muestras previo a la adquisición de los datos de XRPD altera el resultado del análisis y, en consecuencia, los perfiles de expansión obtenidos a partir de pastas de arcilla desecadas no reproducen el fenómeno de intercalación experimentado en estado fresco.

Por otro lado, es fundamental conocer las diferentes expansiones de la arcilla MNT con diversos polímeros de PCE diversos para poder optimizar el diseño de polímeros que minimicen la intercalación, ya que la fracción intercalada no está disponible para la dispersión de las partículas de cemento.

4. CONCLUSIONES

Con las investigaciones realizadas en el sincrotrón ALBA se ha desarrollado un nuevo método de ensayo para determinar la expansión de arcillas MNT provocada por la intercalación de polímeros de PCE. El nuevo procedimiento resuelve las limitaciones del método convencional y revela la influencia real de la estructura del polímero de PCE y de las propiedades de la arcilla en el fenómeno de intercalación, reportando resultados de d-spacing que son coherentes con los resultados de fluidez de pastas y de sorción de aditivo.

Este avance en la tecnología analítica abre la oportunidad para profundizar en el conocimiento del mecanismo de interacción entre polímeros de PCE y arcillas expansivas, conocer la influencia de cada una de las variables y, en definitiva, explorar nuevos horizontes en

el desarrollo tecnológico de los aditivos superplastificantes para hormigón de altas prestaciones e insensibles a todo tipo de arcillas.

La trascendencia de este hallazgo ha originado una publicación en la revista científica más prestigiosa de este ámbito, Cement and Concrete Research, pero también pone de manifiesto el potencial de la investigación multidisciplinar entre empresas privadas, centros de investigación y universidades.

Publicación científica: "*Influence of experimental procedure on d-spacing measurement by XRD of montmorillonite clay pastes containing PCE-based superplasticizer*". Pere Borralleras, Ignacio Segura, Miguel A.G. Aranda, Antonio Aguado. Cement and Concrete Research, 116 (2019) 266–272.

Referencias

[1] E. Sakai, A. Ishida, A. Ohta, New trends in the development of chemical admixtures in Japan, Proceedings Journal of Advanced Concrete Technology 4 (2006) 211-223.

[2] J.E. Ujhelvy, Water demand of concrete mixtures, Periodica Polytechnica 41 (1997) 199-225.

[3] F. Puertas, H. Santos, M. Palacios, S. Martínez-Ramírez, Polycarboxylate superplasticizers admixtures: effect on hydration, microstructure and rheological behaviour in cement pastes, Advances in Cement Research 17 (2005) 77-89.

[4] G. Gelardi, S. Mantellato, D. Marchon, M. Palacios, A.B. Eberhardt, R.J. Flatt, Chemistry of chemical admixtures - Science and technology of concrete admixtures, ISBN 978-0-08-100693-1 (2016).

[5] J. Plank, C. Schroefl, M. Gruber, M. Lesti, R. Sieber, Effectiveness of polycarboxylate superplasticizers in ulta-high strength concrete: the importance of PCE compatibility with silica fume, Journal of Advanced Concrete Technology 7 (2009) 5-12.

[6] V.A. Fernandes, P. Purnell, G.T. Still, T.H. Thomas, The effect of clay content in sands used for cementitious materials in developing countries, Cement and Cocnrete Research 37 (2007) 751-758.

[7] D. Atarashi, Interaction between superplasticizers and clay minerals, Japan Cement Association (2005) 287-292.

[8] L. Xoing, G. Zheng, Y. Bi, C. Fu, Effect of typical clay upon the dispersion performance of polycarboxylate superplasticizer, Proceedings International Conference on Materials, Environmental and Biological Engineering (2015) 226-229.

[9] D. Atarashi, K. Yamada, A. Ito, M. Miyauchi, E. Sakai, Interaction between montmorillonite and chemical admixture, Journal of Advanced Concrete Technology 13 (2015) 325-331.

[10] L. Lei, J. Plank, A study on the impact of different clay minerals on the dispersing force of conventional and modified vinyl ether based polycarboxylate superplasticizers, Cement and Concrete Research 60 (2014) 1-10.

[11] P. Borralleras, Arenas con arcillas y sus problemáticas en la producción de hormigón. Interferencia con los aditivos superplastificanes basados en PCE, Proceedings of the V Congreso Nacional de Áridos - Spain (2018), Area A, 27-53.

[12] H. Tan, B. Gu, B. Ma, X. Li, C. Lin, Mechanism of intercalation of polycarboxylate superplasticizer into montmorillonite, Applied Clay Science 129 (2016) 40-46.

[13] S. Ng, J. Plank, Interaction mechanisms between Na-montmorillonite clay and MPEG-based polycarboxylate superplasticizers, Cement and Concrete Research 42 (2012) 847-854.

[14] L. Lei, J. Plank, Synthesis and properties of a vinyl ether-based polycarboxylate superplasticizer for concrete possessing clay tolerance, Industrial & Engineering Chemistry Research 53 (2014) 1048-1055.

[15] L. Lei, J. Plank, A concept for a polycarboxylate superplasticizer possessing enhanced clay tolerance, Cement and Concrete Research 42 (2012) 1299-1306.

[16] R. Qianping, X. Wang, X. Shu, J. Liu, Effects of sequence structure of polycarboxylate superplasticizers on the dispersion behavior of cement paste, Journal of Dispersion Science and Technology 37 (2016) 431-441.

[17] G. Chen, J. Lei, Y. Du, X. Du, X. Chen, A poycarboxylate as a superplasticizer for montmorillonite clay in cement: adsoprtion and tolerance studies, Arabian Jorunal of Chemistry – article in press (2017) 1-8.

[18] G. Xing, W. Wang, J. Xu, Grafting tertiary amine groups into the molecular structures of polycarboxylate superplasticizers lowers their clay sensitivity, RSC Advances 6 (2016) 106921-106927.

[19] H. Tan, Xin Li, M. Liu, B. Ma, B. Gu, X. Li, Tolerance of cement for clay minerals: effect of side-chain density in polyethylene oxide (PEO) superplasticizers additives, Clay and Clay Minerals 64-6 (2016) 732-742.

[20] R. Ait-Akbour, P. Boustingorry, F. Leroux, F. Leising, C. Taviot-Guého, Adsorption of polycarboxylate poly(ehtylene glycol) (PCP) esters on montmorillonite (MNT): Effect of exchangeable cations (Na+, Mg2+ and Ca2+) and PCP molecular structure, Journal of Colloid and Interface Science 437 (2015) 227-234.

[21] P. Borralleras, I. Segura, M.A. G. Aranda, A. Aguado, Influence of experimental procedure on d-spacing measurement by XRD of montmorillonite clay pastes containing PCE-based superplasticizer, Cement and Concrete Research, 116 (2019) 266–272.

[22] P. Borralleras, I. Segura, A. Aguado, Modelización del mecanismo de pérdida de consistencia provocado por arcillas en pastas de cemento con superplastificantes base policarboxilato, Proceeding del HAC2018 – Congreso Iberiamericano de Hormigón Autocompactante y Hormigones Especiales, Valencia (2018) 279-289.

Chapter 4
SUBMITTED PAPERS

This chapter reproduces the journal papers derived from this thesis that are currently under revision in different journals. Since these are still not published, the papers presented in this chapter cannot be considered as part of the official compendium of publications. However, the outcomes of these works answer important aspects discussed in the previous chapters. Consequently, these are reproduced before the general discussion of the results. Each paper follows its own numbering of sections, figures, equations and references.

Contents

4.1. JOURNAL PAPER IV

INFLUENCE OF THE PROPERTIES OF MONTMORILLONITE CLAYS IN THE PERFORMANCE OF PCE-BASED SUPERPLASTICIZERS

Published in Construction and Building Materials XXX (XXX 2019) XXX-XXX.

Pere Borralleras[a], Ignacio Segura[b, c,*], Miguel A. G. Aranda[d] and Antonio Aguado[b]

[a] BASF Construction Chemicals Iberia, Ctra del Mig 219, E-08907 Hospitalet de Llobregat, Barcelona, Spain

[b] Department of Environmental and Civil Engineering, Universitat Politècnica de Catalunya-Barcelona Tech, Jordi Girona 1-3, C1, E-08034 Barcelona, Spain

[c] Smart Engineering Ltd, Jordi Girona 1-3, ParcUPC–K2M, E-08034 Barcelona, Spain

[d] ALBA Synchrotron, Carrer de la Llum 2-26, E-08290, Cerdanyola del Vallès, Barcelona, Spain

* Corresponding author: Ignacio Segura, Department of Environmental and Civil Engineering, Universitat Politècnica de Catalunya-Barcelona Tech, Jordi Girona 1-3, C1, E-08034 Barcelona, Spain. Email address: ignacio.segura@upc.edu Tel: +34 93 4054684

Abstract

This work focusses on the influence of the properties of montmorillonite clays (MNT) in the interaction process with polycarboxylate (PCE) based superplasticizers by using in-situ XRPD analysis on fresh, unaltered clay pastes. With this methodology, the agreement between clay expansion results with paste flow loss behaviour and sorption rate is met. The octahedral layer charge of the MNT clays is identified as the most relevant feature controlling the intercalation process. However, the relevance of the key-parameters controlling the process is dependent on the PCE/clay ratio (as per mg/m^2). At low PCE/clay ratio, the interaction is defined by the octahedral layer charge and by the morphology of the clay particle. However, at high PCE/clay ratio, there is almost no influence of the particle morphology, being the octahedral layer charge the property which mainly controls the interaction process.

Keywords: Clay (-), Montmorillonite (-), Polycarboxylate (-), Layer charge (-), Particle morphology (-)

1. INTRODUCTION

The presence of clays in the sands used for concrete production causes several affectations on the fluidity of fresh concrete [1]. Since sands are the major ingredient of concrete the quality of sands is one of the most critical factors for the industrial production of concrete. Inadequate quality of sands negatively affects the performance of concrete in fresh and hardened state. Therefore, to allow the optimal fabrication of concrete and ensure that the concrete structures meet their mechanical requirements and the expected service life, most of the regulations addressed to the concrete industry include some minimum quality requirements for the sand. Much of these requirements are intended to limit the amount of clays present in sands, since clays are the most problematic (unwanted) component contaminating sands.

Clays in sands increase the water demand of concrete and restrict the slump retention, thus forcing to increase the total amount of mixing water. When extra water is added, the final performance of the concrete is compromised. Clay content in sands is defined by specifying minimum compliance values in, for example, the methylene blue or the sand equivalent test. Within the different clay families, smectite-montmorillonite (MNT) is the type of clay generating the highest impacts on water demand increase and on slump loss, being especially critical when polycarboxylate based superplasticizers (PCE) are used [2,3].

Montmorillonite clays, differently from kaolinite, mica or chlorite clays, are characterized for their swelling properties, so they can expand by absorption of water and other organic molecules into their interlaminar space [4].

The interaction process between PCE based admixtures and MNT clays has been widely studied [5-11]. These works confirm that the interference on concrete slump is mainly generated by the absorption of polymer through a mechanism based on the intercalation of PCE side chains into the interlaminar space of MNT clay.

When the PCE polymer is absorbed by the clay, its dispersing capacity becomes almost totally inhibited. By performing *in-situ* X-ray Powder Diffraction (XRPD) analysis on fresh, unaltered clay pastes, our previous works [12,13] have revealed a more complex pattern of intercalation, reporting d-spacing results in agreement with the paste flow loss and sorption rates.

While there are many works focussed on the properties of water-reducer admixtures and their interaction with a given specific clay, there are just a few studies explicitly focused on the influence of the properties of MNT clays [14] . Therefore, most of the aspects related to how the particular characteristics of clays influence in the slump loss of concrete are not sufficiently understood. With the objective of generating complementary knowledge about the influence of MNT clays properties interfering in the dispersing capacity of PCE polymers, this study aims to identify the key-parameters of MNT clays controlling the interaction process with PCE based superplasticizers.

1.1 Structure of clays

Clay minerals are layered silicates belonging to phyllosilicate group, occurring as very fine laminar aggregates with very large width/thickness ratio (aspect ratio) and very high specific surface [4]. Clay particles are formed by individual layers of hexagonal platy sheets stacked one on top of another, so forming a book-like structure generating an interlaminar space in between the stacked plates.

Individual clay plates are formed by tetrahedral silicate layers and octahedral aluminate layers covalently bonded through the oxygen atoms of the vertices. Depending on the sequence arrangement of the silicate and aluminate layers, two different type of clay structures are defined [16]. T-O clays are based on clay plates formed by one silicate tetrahedral layer and one aluminate octahedral layer. This is the typical structure of *kaolinites*. On the other hand, T-O-T clays are based on plates formed by one aluminate octahedral layer sandwiched by two silicate tetrahedral layers. *Micas*, *chlorites* and *smectites* are based on T-O-T structures [17]. Both structures are depicted in Figure 1.

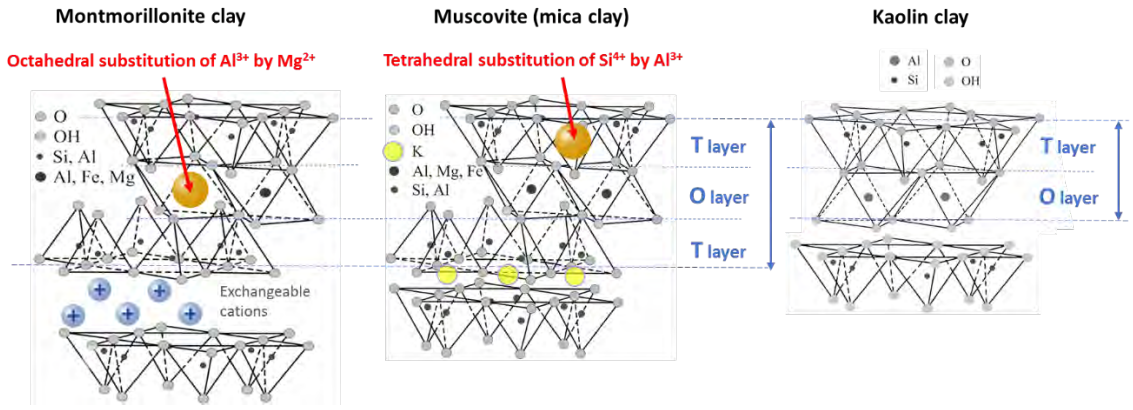

Figure 1. Clay types by the structure of individual plates and by isomorphic substitution

Another key factor differentiating clay families is the isomorphic substitution. It is based on the partial replacement of Si atoms in the T-layer and/or of Al atoms in the O-layer by cations of similar size but with lower charge. Since isomorphic substitution generates a charge deficiency in the structure, it creates an accumulation of residual charges in the clay plates (named as layer charge, ξ) that need to be balanced. Generally, T-O clays do not experience significant isomorphic substitution and this pattern is more typical in T-O-T clays. *Pyrophyllite* and *talc* are the T-O-T clays without isomorphic substitution representing the ideal dioctahedral and trioctahedral smectites, so they are electrically neutral [4] and do not have any swelling properties.

When Si atoms (formally Si^{4+}) in the tetrahedral layer are replaced by Al^{3+} or Fe^{3+} cations (aliovalent substitution), a residual charge of -1.0 per half-cell unit is generated in the T layer (tetrahedral layer charge, ξ_{tet}). This is the typical structure of *mica* clays and *illites*. Since the tetrahedral layers mean the external surface of clay plates, the residual charge of -1.0 can be balanced by monovalent cations, typically potassium K^+, creating a very stable structure that restricts the accessibility of the interlaminar space to the point that micas are not usually expandable clays [17].

When Al^{3+} cations in the octahedral layer are aliovalently replaced by divalent cations such as Mg^{2+}, Fe^{2+}, Ti^{2+} or other metallic divalent cations of comparable size, a non-stochiometric charge of -0.33 per cell unit is generated in the O layer (octahedral layer charge, ξ_{oct}) [4]. Contrary to tetrahedral substitution, the charge deficiency created by the octahedral substitution cannot be balanced with the same efficiency because it is not stoichiometric and because it is located in the inner-region of the clay plate. Therefore, these residual charges can be compensated by hydrated cations arranged in the interlaminar space, typically Na^+ and Ca^{2+}. As consequence, the resulting structures are not as stable as micas [4] because there is a natural

electrostatic repulsion between the individual clay plates. For this reason, the interlaminar space of these clays is easily accessible, allowing the interlayer cations to be exchanged by other cations or by polar molecules and giving the clay expansive properties [18]. In addition to octahedral substitution, typically smectite clays may also have some substitution in the tetrahedral layer. From the corresponding formula unit $M^{(+)}_{(x+y)}(Al_{(2-y)},Mg_y)(Si_{(4-x)}Al_x)O_{10}(OH)_2$, *x* represents the tetrahedral substitution and *y* the octahedral substitution, while $M^{(+)}$ means the interlayer hydrated monovalent cations balancing both residual layer charges *(x+y)*. In this respect, for montmorillonite clays $y > x$ [4].

Chlorites are the clay types having both tetrahedral and octahedral isomorphic substitution at the same time. These structures are possible because the interlaminar space is occupied by a hydroxide layer named *brucite-like layer*, which has electropositive behaviour to compensate the negative residual charges cumulated in the clay plates [19]. Brucite-like layer of chlorites is composed by mixed aluminum, ferric hydroxides and $M(OH)_2$ hydroxides, typically magnesium and ferrous but also others such as nickel or manganese, and in practical terms, it makes the interlaminar space non-accessible.

1.2 Morphology and active sites of clay particles

Clay particles are characterized by large aspect ratio. The thickness of clay particles is determined by the number of stacked layers, so the larger the number of plates forming the particle, the larger the thickness [4]. According to this morphology, two types of clay surfaces are differentiated in the clay particle, as displayed in Figure 2: *edge surface* and *basal surface.*

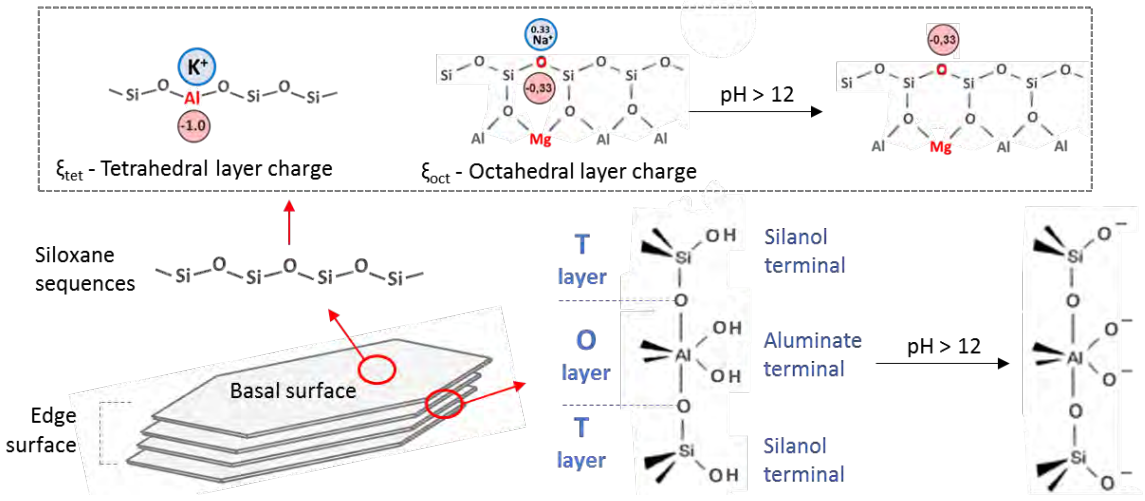

Figure 2. Morphology of clay particles (not at scale) and ionization of active sites on clay surfaces

The edge surface corresponds to the lateral surface defined by the exposed borders of the stacked clay plates forming the pristine particle. It is based on exposed silanol and aluminate terminals. From the typical morphology of clay particles, edge surface is much smaller than basal surface [20,21]. The edge groups are pH sensitive and can be ionized as function of the pH. For this reason, the *edge surface charges* of clays are commonly named as *pH-dependant charges*, which are directly defined by the shape of the particle so by the aspect ratio and the number of stacked layers.

The major fraction of the external clay surface is basal surface. It is the exposed surface of the T layers defined by the end-layers forming the clay particle and it is based on siloxane -Si-O-Si-O- sequences. If there is no isomorphic substitution, the basal surface is electrically neutral. Nevertheless, the basal planes of MNT clays experience ionization promoted by the unbalanced charges induced by aliovalent isomorphic substitution. It creates the *basal surface charges*, also named as *permanent charges* [22]. The permanent charges of the basal surface are independent of pH [23] and only occur in clays with aliovalent isomorphic substitution. Therefore, the total charge supported by the clay plates (named as layer charge, ξ) means $\xi = (\xi_{tet} + \xi_{oct})$ [24], but for practical purposes only the charges not efficiently stabilized have direct consequences on the behaviour of clays. In this way, the tetrahedral layer charges balanced with potassium cations will hardly generate basal surface charge, while the octahedral layer charges will always generate basal surface charge [25].

When clays are dispersed in polar solvents such as water, the terminals from edge surface as well as from the exposed basal surface for MNT clays ionize, so the clay colloids become charged. At high pH, both aluminate and silanol edge terminals and the electronegative siloxane sequences of the basal planes are ionized in their anionic state, thus creating an accumulation of negative charges in the dispersed clay colloids [26,27].

1.3 Sorption behaviour of clays

The sorption behaviour (adsorption and absorption) of clays is related to the ionization degree of the clay colloids. As all clays have pH-dependant charges, all types of clays show a minimal sorption capacity on the edge surface that allow to adsorb polar molecules on their lateral surface [25,28]. For MNT clays, in addition to the edge surface, the basal planes also have some sorption capacity due to the ionization of the soluble cations balancing the residual octahedral layer charge. The sorption capacity of the basal surface is defined by the amount of layer charge, being higher as the basal surface charge increases [18,29]. Therefore, the octahedral layer charge defines the accessibility of the interlaminar space so the expansion and the swelling behaviour of MNT clays, as well as the cation exchange capacity and the ability to interact with water and other polar molecules [30-33]. Other properties of MNT clays such as the tendency to

exfoliate and their dispersibility also increase as the layer charge increases [25,34,35]. In any case, since the high ratio between basal surface and edge surface, clays presenting active basal surface develop the highest sorption capacity.

2. RESEARCH SIGNIFICANCE

As far as known, this is the first study explicitly focused on the influence of montmorillonite clay properties on the intercalation mechanism of PCE based superplasticizers by using *in situ* XRPD measurements on fresh, unaltered clay pastes.

Previous investigations are supported by experimental data of clay expansion obtained with the traditional XRD analysis performed on centrifuged and dried clay pastes [5-11], and the conclusions extracted from these experimental results do not offer a clear view on the influence of the properties of clay in the intercalation mechanism and, at the same time, the d-spacing values obtained are not in agreement with other experimental results such as paste flow loss and sorption behavior [12-14]. Therefore, new insights of the intercalation behavior being in agreement with the experimental paste flow and sorption results are expected to be found by using *in situ* XRPD analysis.

3. MATERIALS

3.1 Cement

The cement used for the preparation of the pastes is a CEM I 52.5R. Blaine surface reported in the product specifications is 4750 cm^2/g. Oxide composition of anhydrous cement by X-ray Fluorescence (XRF) is presented in Table 1.

Oxide	SiO_2	Al_2O_3	Fe_2O_3	CaO	Na_2O	K_2O	MgO	SO_3	LOI	Total
(wt.%)	19.60	5.38	2.41	65.29	0.05	0.84	0.82	3.34	2.18	99.91

Table 1. Oxide composition of CEM I-52.5R by XRF

3.2 Montmorillonite clay samples

Three samples commercially available of smectite-montmorillonite (MNT) clay are used: two sodium MNT (M-Na7, M-Na18) and one calcium MNT (M-Ca6). Table 2 reports the density of each clay sample reported in the product specifications and the oxide and mineral composition, obtained by XRF and XRPD. Despite some impurities are present in the clay

samples, they are used as per obtained, being previously dried at 60 ºC for 48 hours to remove residual moisture. It is assumed that the impurities identified in the clay samples are not relevant for the interpretation of the results because any of them have the absorption properties of montmorillonites.

Calcite, quartz and dolomite are not layered minerals and the identified clays kaolin and muscovite do not have an accessible interlaminar space with the capacity to absorb and intercalate polar molecules, despite being layered materials [2].

Property		M-Na7	M-Na18	M-Ca6
Density (g/cm^3)		2.36	2.39	2.41
Mineral composition (wt. %)	Montmorillonite	84.7	80.1	85.4
	Muscovite	-	-	2.2
	Kaolin	-	4.4	-
	Calcite	3.3	-	2.7
	Quartz	4.8	6.9	3.1
	Dolomite	-	1.8	-
Oxide composition (wt. %)	SiO_2	63.12	63.81	63.03
	TiO_2	0.01	-	0.29
	Al_2O_3	19.88	22.37	23.93
	Fe_2O_3	1.37	1.83	0.63
	MgO	2.33	2.11	2.28
	MnO	0.04	-	-
	NiO	0.06	-	-
	Na_2O	3.43	2.36	0.11
	K_2O	0.40	0.89	0.96
	CaO	2.24	0.53	2.27
	LOI	5.97	4.11	4.98
	Total	98.85	98.01	98.48

Table 2. Density and mineral and oxide compositions for the clay samples used

From the oxide composition presented in Table 2, it is possible to calculate the layer charge for each MNT clay sample [4,19,36,37]. The values for the ξ – *total layer charge* per half-cell unit $O_{10}(OH)_2$ of smectites are obtained from the sum of the calculated values for the ξ_{tet} – *tetrahedral layer charge* and for the ξ_{oct} – *octahedral layer charge*.

The oxide composition used for the calculation of the layer charge is that obtained after subtracting the amount of oxides associated to the impurities identified in each clay sample. The calculated layer charge for the three MNT clay samples is shown in Table 3.

Layer charge per half-cell unit - $O_{10}(OH)_2$	M-Na7	M-Na18	M-Ca6
ξ – total layer charge	0.54	0.49	0.21
ξ_{oct} – octahedral layer charge	0.53	0.43	0.16
ξ_{tet} – tetrahedral layer charge	0.01	0.06	0.05
% of tetrahedral charge	2.4	12.8	24.6
Ratio (K^+/ ξ_{tet})	2.7	1.3	1.1

Table 3. Calculated results for layer charge from oxide composition of clay samples

The results for the layer charge per half-cell unit obtained for the three MNT clay samples used are comprised within the defined range for MNT clays ($0.2< \xi <0.6$) [15]. Despite the results in Table 3 are presented as positive values, the layer charges are anionic. It is denoted that the total layer charge of M-Ca6 sample is the lowest among all the clays because its very low octahedral layer charge. The total layer charge of M-Na7 and M-Na18 clays presents small differences. Nevertheless, it can be seen that the difference in the octahedral layer charge ξ_{oct} between these two clay samples is significantly larger. The M-Na7 has the highest octahedral layer charge, while the tetrahedral layer charge of M-Na18 and M-Ca6 is higher than that of M-Na7. However, since the ratio K^+/ξ_{tet} is higher than 1.0 for all the clay samples, it can be assumed that the tetrahedral layer charge is efficiently balanced by the K^+ cations, thus, its role in the intercalation behaviour of each clay has likely a much lower relevance than the octahedral layer charge [25].

3.3 Synthetic cement pore solution

All clay pastes are produced using synthetic cement pore solution as the liquid phase. The solution is prepared by dissolving 14.3 g of Na_2SO_4, 3.05 g of NaOH and 3.00 g of $Ca(OH)_2$ in 1 litre of distilled freshly-boiled water (equivalent to 0.157 mol/l of OH^-, 0.278 mol/l of Na^+, 0.100 mol/l of SO_4^{2-} and 0.040 mol/l of Ca^{2+} concentration). The synthetic cement pore solution is always freshly prepared to avoid carbonation.

3.4 Water-reducer / superplasticizer admixtures

A non-formulated polycarboxylate polymer based on polyethylene oxide polyacrylate ether (PCE) sodium salt is used as water-reducer/superplasticizer admixture. It is presented in

46 wt. % aqueous solution. The average molecular weight (Mw) for the PCE polymer is 50000 g/mol and it is composed by VPEG side chains having a molecular weight of 3000 g/mol (68 ethylene oxide units per side chain). The polymerization ratio of side chains in the acrylate backbone is 2.8:1 (acrylic monomer : side chain monomer) and the anionic charge of the polymer is 49 mg KOH/g PCE (obtained by titration with KOH). It means a grafting ratio of 0.36 (side chain : total backbone monomers) and a side chain frequency of 0.26 (side chain : acrylic monomer).

The structure of the PCE polymer used is illustrated in Figure 3(a). It is an idealized representation, since the polymer in water solution is always coiled. From the structural parameters *n*, *N* and *P* defined in Figure 3(b), the conformation in solution taken by the PCE polymer is deduced [38] and represented in Figure 3(c). The diagram shows that the conformation taken by the PCE polymer in water solution is the SBW (stretched backbone worm). Therefore, from the SBW conformation and from the high value of 17.9 for the side chain density (calculated according to [13]), it is expected that the PCE polymer has a high dispersing capacity, but it will be limited by its adsorption behaviour, which is restricted by steric hindrance factors.

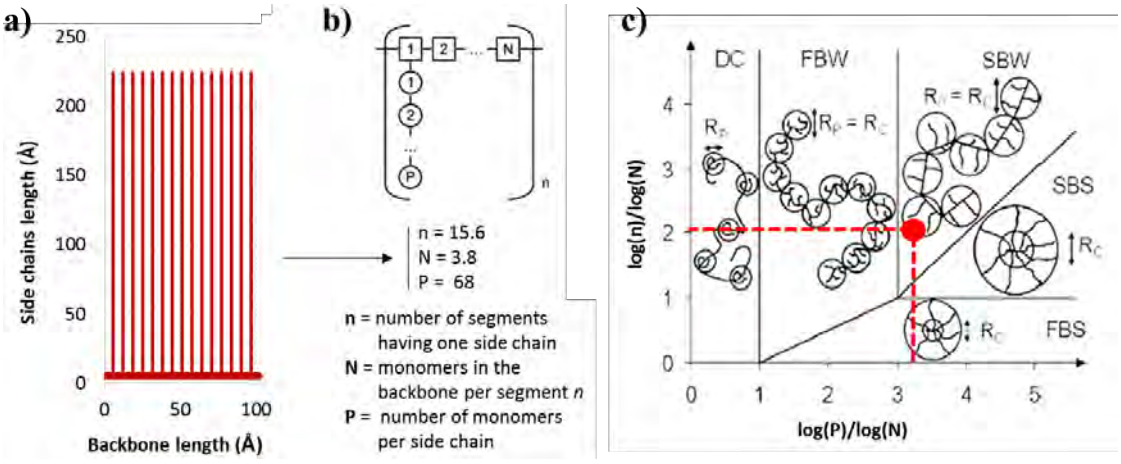

Figure 3. a) Idealized structure and dimensions for the PCE polymer; b) meaning and values for the structural parameters *n*, *N* and *P*; c) phase diagram for comb-shaped homopolymers (adapted from [38]) and conformation taken by the PCE polymer used

One additional water-reducer polymer complementary to the PCE-based superplasticizer is used only for comparison purposes. It is based on a formaldehyde β-naphthalene sulfonate condensate calcium salt (BNS), presented in 42 wt. % solution. Contrary to the PCE, BNS polymers cannot be intercalated into the interlaminar space of MNT clays as consequence of their linear polymeric structure, based on sulfonated naphthalene rings without PEG/PEO side

chains [2]. The solid content of both water-reducer admixtures is equalized at 40 wt. % concentration by dilution distilled water.

4. EXPERIMENTAL METHODS

4.1. Specific surface and particle size

The BET specific surface of cement and clay powders is measured with a TriStar 3000 V6 equipment from Micrometrics Instrument. The particle size distribution, expressed as D_{10}, D_{50} and D_{90}, is obtained by laser granulometry.

4.2. Preparation of cement and clay pastes

Clay pastes are prepared at 22 ºC by dispersing 10 g of clay powder in 50 g of synthetic cement pore solution. The mixing process is done using a vertical shaft mixer equipped with a helical head, moving at 600 rpm. The total mixing time is four minutes, during which the admixture is added at the required dosage after the one-minute mark. Cement pastes are prepared following the same procedure as clay pastes, using a water-to-cement (w/c) mass ratio of 0.26 and dispersing cement (and clay when used) with tap water at 22 ºC. For cement pastes containing clay, both powders are dry-mixed prior to the addition of water.

4.3 *In situ* XRPD analysis on fresh, unaltered clay pastes

In situ XRPD patterns of fresh, unaltered clay pastes are performed using a PANalytical X'Pert PRO MPD Cu Kα lab diffractometer (λ = 1.5418 Å), by following the experimental procedure described in [12]. In short, XRPD measurements are performed directly on the fresh clay pastes, avoiding centrifugation and drying.

4.4 Sorption of water reducer polymers on clay and on cement

The sorbed fraction of polymers (including both the adsorption on external surface and the absorption in the interlayer) is obtained by measuring the total organic carbon (TOC), using a Shimadzu testing equipment. Freshly clay pastes prepared with synthetic cement pore solution and containing water-reducer admixture are diluted with 50 ml of Millipore water. The suspension is separated by centrifugation at 15000 rpm for 10 minutes and the obtained liquid phase is filtrated with a 0.45 µm syringe Nylon filter. The final filtrate is acidified with concentrated HCl to remove inorganic carbon and is then submitted for TOC analysis by

combustion at 900 ºC. Same procedure is applied to measure PCE sorption in clay pastes prepared with synthetic cement pore solution.

Previously, calibration lines of each pure PCE polymer were prepared by recording the TOC value of three different concentrations of PCE. The sorbed fraction of PCE is calculated by interpolation between the calibration lines from the difference of the total PCE dosage added and the non-sorbed fraction of PCE identified in the filtrate. Results are expressed as a percentage of sorption of the total PCE dosage and/or in sorbed mg of PCE per gram of cement or clay.

4.5. Measurements of paste fluidity

Fluidity of cement and clay pastes is determined by the measurement of paste flow in the mini-slump test. The test uses a metallic truncated mini-cone that is 55 mm high, with an upper diameter of 19 mm and a lower diameter of 38 mm. The mini-cone is arranged on a flat, clean glass surface. It is filled with fresh paste and then compacted with a crystal rebar to evacuate trapped air. The mini-cone is then lifted to let the paste to flow onto the glass surface until the paste reaches maximum spread. The paste spread (paste flow, expressed in mm) is measured in two perpendicular directions and the average value is taken. This test is widely used to evaluate the fluidity of fresh cementitious pastes.

5. RESULTS AND DISCUSSION

5.1 Specific surface and granulometry of clay samples

Results for BET specific surface and for particle size distribution referred as D_{10}, D_{50}, and D_{90} for each powder clay sample and for the used cement are presented in Table 4. BET surface only reproduce the total external surface of clays but not the internal surface defined by the interlaminar space [39].

Since the thickness of clay particles is defined by the number of stacked plates (n_L), the typical high BET values for MNT clays is consequence of the short number of plates forming the elemental particles [21]. Thus, large basal surface is exposed as consequence of the almost 2-dimensional morphology of MNT clay particles [4,20]. This morphology explains the huge differences in BET surface between the MNT samples and the cement, since the shape of cement particles is rather isotropic (close to cubic or spherical) and the MNT particles are very anisotropic (plate-like).

Properties	CEM I	M-Na7	M-Na37	M-Ca6
BET (m^2/g)	1.6	49.5	36.5	54.5
D_{10} (µm)	1.5	2.0	1.9	1.7
D_{50} (µm)	10.0	7.4	18.3	6.0
D_{90} (µm)	31.3	17.0	23.7	16.4

Table 4. Experimental results of BET specific surface and particle size distribution

From the parameters presented in Table 4, it is possible to theoretically estimate the particle morphology of each MNT sample. Despite there are various experimental technics for measuring the thickness of clay particles [40-43], the empirical results obtained for the aspect ratios of MNT clays (and therefore for the number of plates forming the pristine clay particle) sometimes are not consistent within the different methodologies, thus leading to debatable results [44,45].

The potential delamination produced during the sample preparation is presumably the most relevant factor generating discrepancies of results [46] although the validity of some assumptions for data treatment is another source of errors. In this work it is used a simplified mode to theoretically calculate the *average number of stacked plates per clay particle* (n_L) from the D_{50} value, the BET surface and the real density, by applying the same mathematical model than in [19]. In this approach, the clay particle is assumed to be modelled like a square-base prism defined by (*a*,*a*,*h*) sides, where D_{50} is equivalent to the longest diagonal and the height of the prims *h* is the particle thickness. Therefore, from the assumed particle geometry, the specific surface and the corresponding volume for one single clay particle is assumed to be equal to the total prism area defined as ($S= 2a^2 + 4ah$) and to the prism volume defined as ($V= a^2 \cdot h$), respectively, while the ratio *a*/*h* between *a* and *h* sides means the *aspect ratio* (R_p) of the clay particle.

The calculated particle thickness and width (*h*,*a* sides of the idealized geometry), the number of stacked plates per clay particle (n_L) and the aspect ratio R_p (width/thickness ratio) for each clay sample are presented in Table 5. Despite the assumptions considered, the calculated results for n_L obtained are comprised within the typical ranges of MNT clays [4,20,21].

Particle morphology	M-Na7	M-Na18	M-Ca6
Particle thickness (Å)	172	230	153
Particle width (µm)	5.2	13.0	4.3
n_L (number of stacked plates per particle)	13.7	18.3	12.2
R_p – aspect ratio (width/thickness)	301	562	277

Table 5. Calculated results for particle thickness, n_L and R_p for each MNT sample

The high aspect ratio (R_p) calculated for the MNT clay samples and the resulting value of n_L confirm that the particles of MNT clays are formed by a reduced number of stacked plates, resulting in much thinner particles in comparison to other clay typologies such as micas, chlorites or kaolinites, with n_L values up to 10 times larger than those of MNT clays [4,19,21,42,44]. The limited number of stacked plates typical for MNT clays is consequence of the natural repulsion between the individual clay plates [18-20] originated by the permanent charges.

From the morphology parameters reported in Table 5 and assuming the idealized geometry, the particle size for each clay samples is illustrated in Figure 4(a). It can be deduced that the particles of M-Na7 and M-Ca6 montmorillonite samples are of similar shape and dimensions, while the particles of M-Na18 sample occurs with the highest aspect ratio and the widest basal plates despite having a larger particle thickness. Complementary, the thickness of each particle is represented in Figure 4(b), together with the calculated length of the backbone and of the side chains of the PCE polymer (in their fully stretched, idealized arrangement).

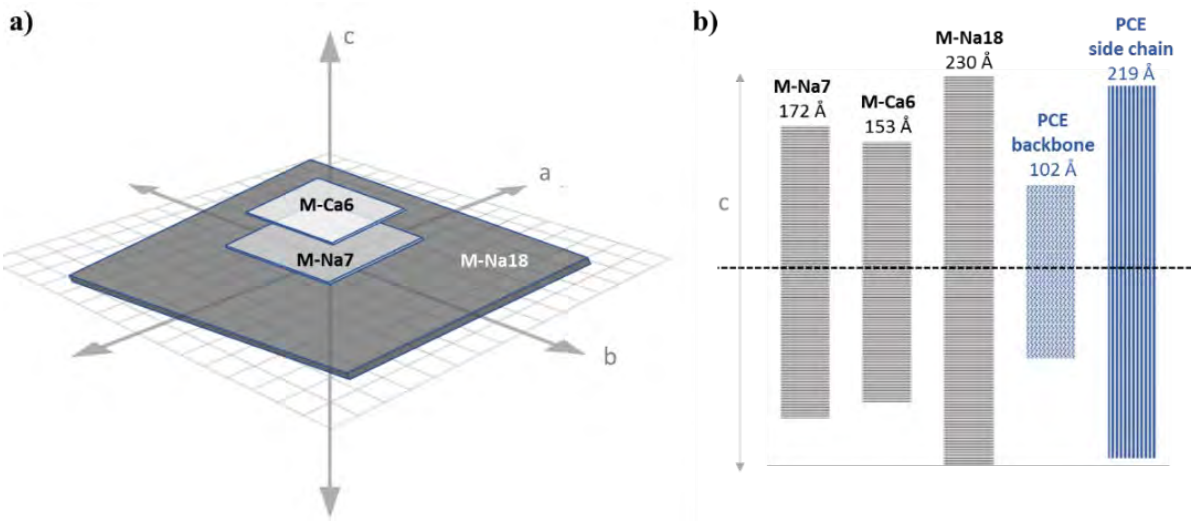

Figure 4. a) Illustration of the particle size for the clay samples; b) comparison between clay particle thickness and the idealized length of the backbone and side chains of PCE

One can note that both the length of the PCE backbone and of the side chains are of comparable size than the particle thicknesses. With this observation and considering that the polymeric structure of the PCE used is propitious to offer steric hindrance, it can be deduced an early and rapid saturation of the edge surface by polymer adsorption.

5.2 *In situ* XRPD patterns of fresh, unaltered clay pastes with water reducers

The evolution of the interlayer d-spacing for each MNT clay sample produced by different dosages of PCE and BNS water reducers are presented in Table 6, excluding the equivalent peaks being second order reflections.

The polymer dosages used are representative of the weight ratios between the total amount of admixture and the clay content provided by the sands in typical concrete mix designs. To show the criteria used for the assignation of the main peaks, Figure 5 displays the XRPD patterns of the three MNT clay samples only for some of the PCE dosages used.

Polymer dosage (wt.% clay)	Main peaks	PCE			BNS		
		M-Na7	M-Na18	M-Ca6	M-Na7	M-Na18	M-Ca6
0	Peak 3	18.5	18.5	18.5	18.5	18.5	18.5
2	Peak 1	21.7	21.6	21.7	*Not measured*		
5	Peak 1	43.3	33.4	22.1			
13	Peak 1	59.7	60.8	24.1	-	-	-
	Peak 3	18.3	-	-	18.6	18.5	18.7
50	Peak 1	73.2	61.7	25.2	*Not measured*		
	Peak 2	44.4	-	-			
	Peak 3	18.3	-	-			
100	Peak 1	73.3	64.0	28.4	-	-	-
	Peak 2	45.6	33.7	-	-	-	-
	Peak 3	18.3	18.3	-	18.5	18.8	18.6
200	Peak 1	76.1	66.6	28.7	-	-	-
	Peak 2	--	32.4	-	-	-	-
	Peak 3	18.3	18.3	-	18.6	18.7	18.8

Table 6. Interlayer d-spacing (Å) from main peaks obtained by *in situ* XRPD analysis

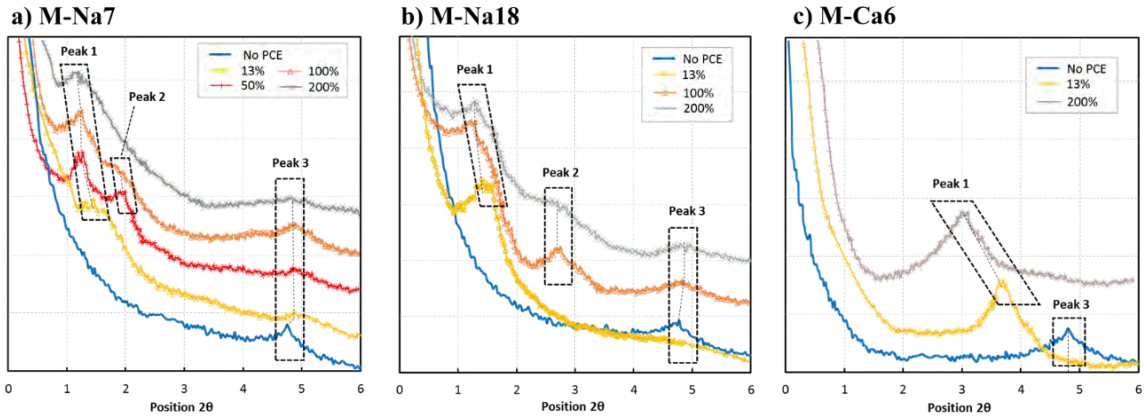

Figure 5. XRPD patterns obtained by *in situ* XRPD analysis on fresh, unaltered clay pastes containing diverse dosages of PCE polymer

As it can be seen in Table 6, Peak 3 is referred to that located between 18-19 Å. It corresponds to the peak identified in the clay pastes without any polymer addition and it is associated to 3 water layers intercalated into the interlaminar space [20]. Peak 1 corresponds to the peak of maximum interlayer d-spacing (see Figure 5) and its evolution as the dosage of PCE polymer increases is presented in Figure 6(a) for each MNT clay sample. As expected, this peak is not observed at any dosage of BNS, thus confirming that BNS is not absorbed by any of the MNT clay samples tested. For the PCE water reducer, the position of Peak 1 is shifted towards smaller angles (larger d-spacings) as the dosage of PCE increases. Peak 2 is observed for M-Na7 and M-Na18, but it only appears from certain PCE dosages. Interestingly, Peak 2 is not shown for M-Ca6 sample. In the cases where Peak 2 is shown, it can be observed that it is always coexisting with Peak 1 (located at lower 2θ position so associated to a larger expansion of the clay) and, at the same time, with Peak 3 at 18,3Å interlayer d-spacing. For this reason, Peak 2 is attributed to clay specimens derived from the exfoliation of the pristine clay particles having intercalated side chains, in the same way than deducted in [13]. Same attribution is given to Peak 3 at 18,3Å interlayer d-spacing when it is coexisting with other peaks of lower 2θ position (situation exclusively observed when PCE polymer is used).

The calculated intercalation degree (n_{PEG}) expressing the number of intercalated layers of side chains into the interlaminar space of the clay is displayed in Figure 6(b). It is calculated for all the peaks presented in Table 6 by applying the methodology described in [12], based on the bonding distances and the spatial arrangements of the -CH_2-O-CH_2- sequences of the PCE side chains and of the H-O-H of the water molecules.

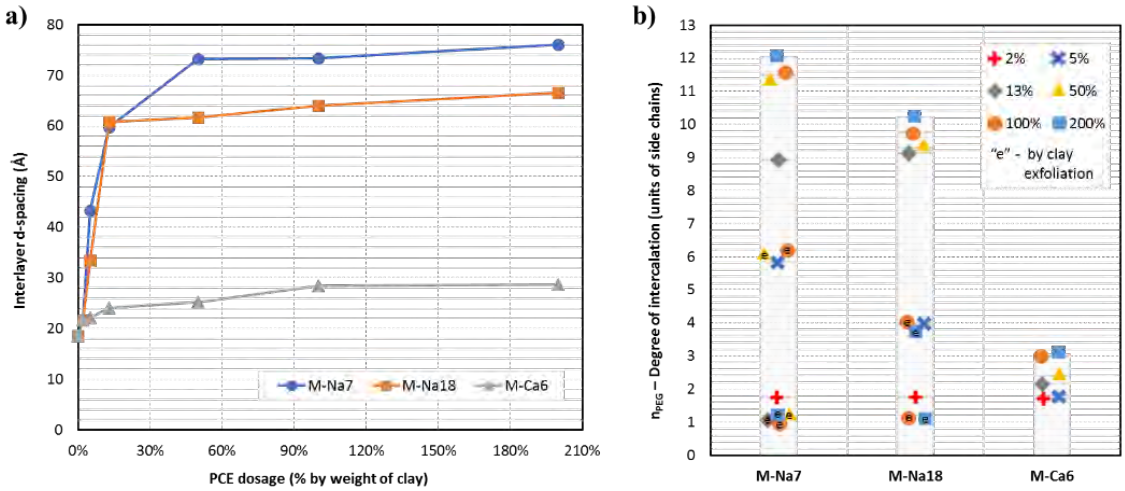

Figure 6. a) Evolution of the interlayer d-spacing for MNT clay pastes containing PCE admixture; b) intercalation degree of side chains calculated according to [12]

Figure 6(a) shows clear differences between the three MNT samples in both the progression of the interlayer d-spacing as PCE dosage increases and in the maximum value of d-spacing observed for the stationary phase (*stationary d-spacing*). Therefore, it can be confirmed that *in-situ* XRPD analysis performed on fresh, unaltered clay pastes reflects the influence of the properties of MNT clays on the intercalation behavior of PCE side-chains. This is significant since by using XRPD analysis performed on dried clay pastes containing PCE, no relevant differences in the d-spacing values are observed between clays of different properties, despite evidencing different behavior in paste flow loss and in sorption rates [14]. The maximum expansion (stationary d-spacing) observed for M-Ca6 is significantly lower than those of M-Na7 and M-Na18. For the stationary phase, the maximum intercalation degree for M-Ca6 corresponds to 3 layers of side chains (n_{PEG}=3), which is clearly much lower than for M-Na7 and M-Na18, having 12 and 10 layers of intercalated side chains, respectively. This finding is in agreement with previous results [25,30], where it was proposed that calcium montmorillonites, typically associated with low layer charges, swell to a much lower extension than sodium montmorillonites

In the same way, from Figure 6(b) it is deduced that for the same PCE polymer structure, the three MNT clay samples present very different intercalation behaviors. In addition, Figure 6(b) suggests the existence of some *preferred intercalation degrees*, identified as the most repeated number of intercalated side chains observed even at different dosages of PCE. The presence of the preferred intercalation degrees is also observed in [13] when using PCE polymers of diverse structures and at different dosages. Figure 6(b) shows that each MNT clay used presents some specific preferred intercalation degrees when the same PCE polymer structure is

used. Conversely, from the findings presented in the previous work [13], it is shown that when the same clay is used, the preferred intercalation degrees are replicated despite using PCE polymers of different structure. Therefore, it can be stated that the preferred intercalation degrees are mainly defined by the properties of the MNT clay and not by the structure of the PCE polymer.

The preferred intercalation degrees identified for M-Na7 clay sample are n_{PEG}= 6 and n_{PEG}= 11-12, meanwhile for M-Na18 clay they are n_{PEG}= 4 and n_{PEG}= 9-10. Since M-Ca6 clay only shows two intercalation degrees n_{PEG}= 2 and n_{PEG}= 3 throughout the entire dosage range of PCE used, these are assumed to be the preferred ones for this clay. Taken all together, these observations suggest that the preferred degrees of intercalation are an own characteristic of each particular clay, not being influenced by the structure of PCE polymers. At the same time, it is consistent with the hypothesis presented in [47] by which the spatial arrangement adopted by the PCE polymer is mainly controlled by the properties of the clay and, in a lesser extent, by the polymeric structure of the PCE.

In Table 6 and in Figure 6(b), it can be seen that some new peaks appear from certain dosages of PCE (referred as Peak 2). These peaks are attributed to new clay specimens produced by the partial exfoliation of the clay particles, whereby the pristine particle delaminates generating new particles with reduced number of stacked plates [48,49]. It can be noted that the profile of exfoliation is different for each MNT clay, since this pattern is determined by the charges supported by the stacked plates and by the type of bond that holds the individual plates stacked, in addition to other factors related to the media conditions [50].

At the testing experimental conditions, it is seen that M-Na7 clay experiences exfoliation from 13 wt. % PCE dosage upwards. For M-Na18, exfoliation starts at 100 wt. % dosage. Moreover, exfoliated specimens able to intercalate PCE polymer are not identified for M-Ca6. Nevertheless, a minor delamination degree for M-Ca6 clay releasing single clay plates cannot be excluded (also for M-Na7 and M-Na18), since isolated plates dispersed in the solution are not measured by XRPD [43,51]. Of course, isolated clay plates cannot intercalate PCE side chains since there is no interlaminar space, but they can adsorb large amounts of polymer (and water) on their new released basal surface.

The results of d-spacing presented in Table 6 also identify clay specimens from exfoliation of the pristine particles at 18.3 Å for M-Na7 and M-Na18 (referred as Peak 3). The peak at 18.3 Å appears from 13 wt. % dosage upwards for M-Na7 and from 100 wt. % for M-Na18, while Peak 3 is not observed for M-Ca6. This is the expected minimum configuration for a clay particle allowing the intercalation of side chains and, as represented in Figure 6(b), it is

associated to one single PEG/PEO side chain intercalated (n_{PEG}= 1) coordinated by two water molecules [14].

In addition to the exfoliated clay specimen at 18.3 Å, Figure 6(b) shows that the exfoliation of M-Na7 and M-Na18 particles produces other clay specimens of larger number of stacked plates (referred as Peak 2 in Table 6). In Figure 6(b) it is observed that all the clay specimens from exfoliation corresponding to Peak 2 show the same intercalation degree from which the preferable intercalation degrees are established, thus n_{PEG}= 6 for M-Na7 and n_{PEG}= 4 for M-Na18. Since at each delamination the basal surface is doubled [29], the exfoliation of MNT clays is critical for the increase of water demand, thus having a direct impact on the fluidity behavior of cementitious systems [52] and forcing to re-arrangements of the PCE units already adsorbed on the clay surface [13].

Saturation dosage (D_{sat}) is defined in our previous work [13] as the amount of PCE polymer needed to saturate the interlaminar space by intercalation of PCE side chains. In [13] it is proposed a methodology to calculate D_{sat} from the plot of the evolution of the d_{001} interlayer d-spacing obtained by *in situ* XRPD analysis on fresh, unaltered clay pastes as the PCE dosages increases.

Figure 7 illustrates how D_{sat} is calculated from the intersection of the two lines adjusted. From the results displayed in Figure 6(a), and by applying the methodology described in [13], D_{sat} – saturation dosage for each MNT clay is calculated and the obtained results are presented in Table 7.

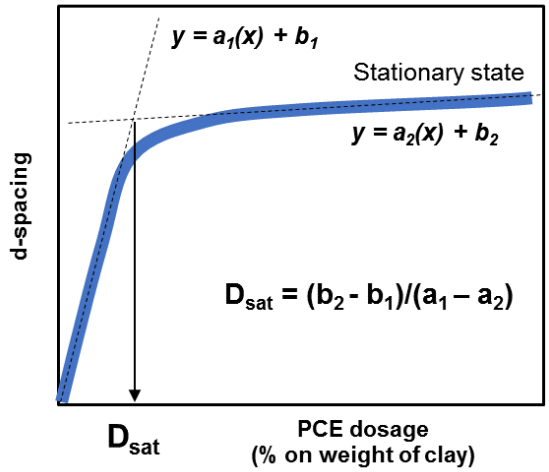

Figure 7. Methodology employed for the calculation of D_{sat}

D_{sat} – saturation dosage from *in situ* XRPD	M-Na7	M-Na18	M-Ca6
Per weight unit (as % PCE on weight of clay)	16.3	13.1	2.6
Per surface unit (as mg PCE/m^2 clay)	3.26	3.59	0.47

Table 7. Calculated saturation dosages, as per weight unit and surface unit of clay

From the values of D_{sat} presented in Table 7, it can be noted that at equivalent clay surface, M-Na18 demands the highest amount of PCE to be saturated by side chain intercalation despite having lower layer charge than M-Na7. Meanwhile M-Na7 demands higher dosage than M-Na18 for weight of clay.

Therefore, once the influence of the specific clay surface is removed, it is observed that, in addition to the layer charge, other clay properties must be influencing the demand of PCE to saturate the interlaminar space.

The relationship between D_{sat} – saturation dosages found (expressed per surface unit of clay, as mg/m^2) and the properties of the MNT clay samples used is shown in Figure 8(a). Additionally, Figure 8(b) displays the best correlation found between the maximum interlayer d-spacing recorded at the stationary phase (stationary d-spacing) and the properties of the clays used.

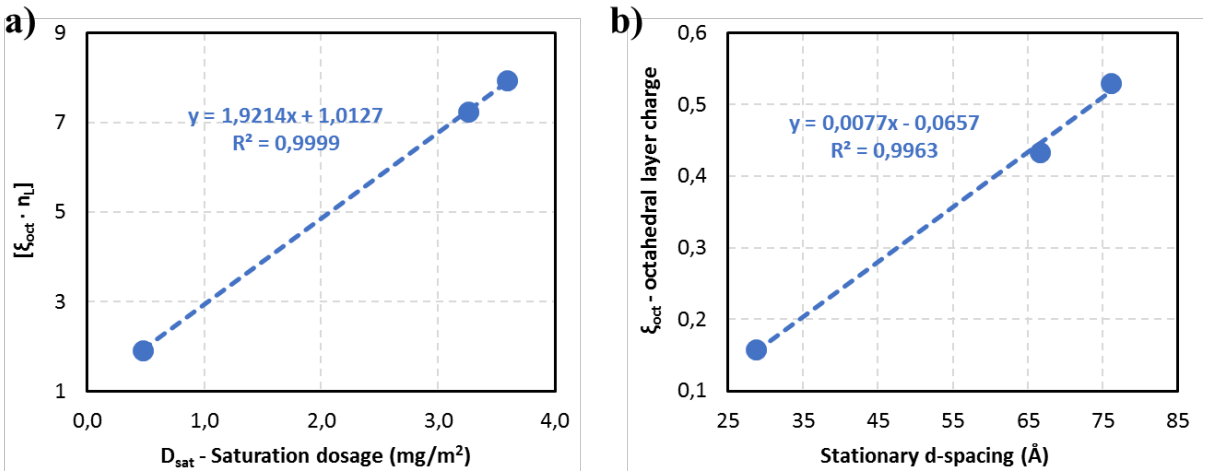

Figure 8. Relationship between clay properties of MNT samples used and; a) D_{sat} as per mg/m^2; b) stationary d-spacing

Figure 8(a) shows that D_{sat}, expressed as per surface unit of clay, linearly correlates with the expression [$y= \xi_{oct} \cdot n_L$]. From this observation, it is deduced that D_{sat} – saturation dosage

increases as the octahedral layer charge increases, and as the number of stacked plates per clay particle increases.

This relationship is coherent with the fact that intercalation occurs through the edge accesses of the interlaminar spaces, located in the lateral surface of the clay particle [13]. Therefore, from the clay perspective, the affinity for intercalation can be understood from the point that the octahedral layer charge ξ_{oct} is the driving force promoting the intercalation while the number of stacked plates n_L is the limiting parameter since it defines the number of available accesses in the clay particle by which the intercalation begins.

Conversely than for D_{sat}, the relationship shown in Figure 8(b) indicates that the stationary d-spacing increases solely as the octahedral layer charge ξ_{oct} increases, in agreement with [30,31], thus being independent of the number of plates and of the morphology of the clay particle.

5.3 Sorption isotherms of PCE polymer on MNT clays

The sorption isotherms of PCE polymer on each MNT clay sample are presented in Figure 9(a). Figure 9(b) shows how the named D_{sorp} dosage is estimated from the sorption isotherms. D_{sorp} is associated to the saturation of the clay particle by PCE sorption, including PCE absorbed by intercalation and PCE adsorbed on the clay surface. The values obtained for D_{sorp} are presented in Table 8.

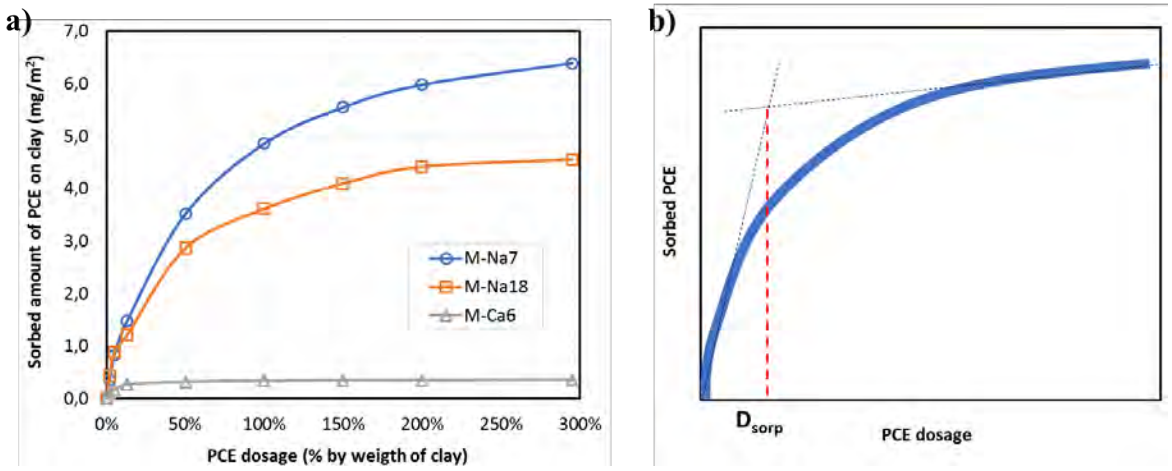

Figure 9. a) Sorption isotherms of PCE polymer on MNT clays; b) methodology employed for the calculation of D_{sorp}

D_{sorp} – saturation dosage from sorption isotherms	M-Na7	M-Na18	M-Ca6
Per weight unit (as % PCE on weight of clay)	49.6	53.6	5.9
Per surface unit (as mg PCE/m^2 clay)	10.02	10.84	1.18

Table 8. Calculated values for D_{sorp} from sorption isotherms

Figure 9(a) and Table 8 denote relevant differences in the progression of the net sorption of PCE within the used MNT clays, especially for M-Ca6, which requires much lower dosage (close to 10 times) than M-Na18 and M-Na7 to be saturated by PCE. M-Na18 is the clay showing the highest value of D_{sorp} despite having lower layer charge than M-Na7, meanwhile the net sorbed amount of PCE per m^2 of clay at saturation is higher for M-Na7 than for M-Na18.

Figure 10(a) shows the relationship between the clay properties and D_{sorp}. Figure 10(b) shows the relationship for the difference (D_{sorp} - D_{sat}) and Figure 10(c) for the maximum amount of sorbed PCE at the stationary phase, assumed as the net sorption measured at 295% dosage.

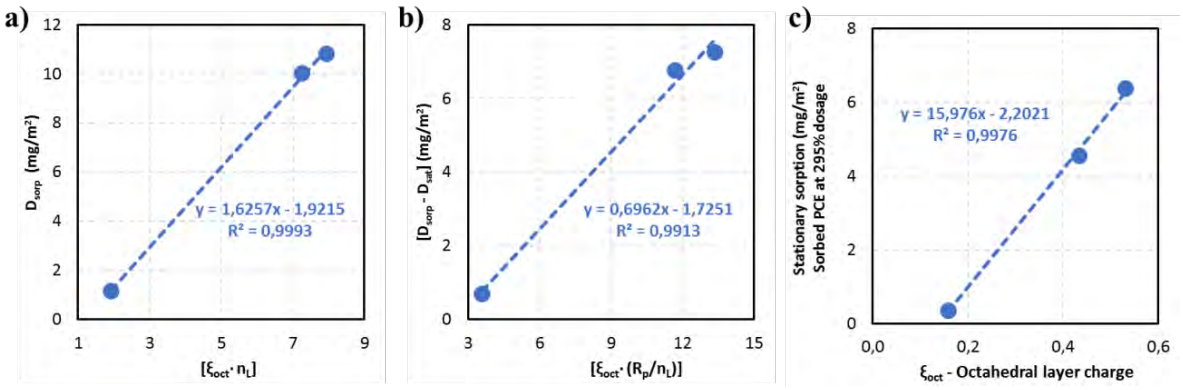

Figure 10. Relationship between clay properties and; a) D_{sorp}; b) [D_{sorp} - D_{sat}]; c) Stationary sorption of PCE at 295% dosage

In the same way than for D_{sat}, D_{sorp} increases as the octahedral layer charge and the number of stacked plates per particle increase. This is expected because D_{sorp} includes both absorption and adsorption processes. Nevertheless, since [D_{sorp} - D_{sat}] > D_{sat}, it cannot be assumed that the absorption of PCE is the main driver defining D_{sorp} values. Other phenomenon such as clay exfoliation are likely influencing on D_{sorp}. This proposal is consistent with the ratio [(D_{sorp} - D_{sat}) / D_{sat}] found for each clay sample, being 2.1 for M-Na7, 2.0 for M-Na18 and 1.5 for M-Ca6. This gradation of values is aligned with the expected tendency to exfoliate for each clay sample, since it increases as the layer charge and the number of plates per particle increase [32,34,35].

Therefore, the difference [D_{sorp} - D_{sat}] can be interpreted as the amount of PCE polymer needed to saturate the exposed basal planes of the clay, including the original basal surface of the pristine particle but also the new basal surface appearing by exfoliation. As observed in Figure 10(b), [D_{sorp} - D_{sat}] increases as the octahedral layer charge and the aspect ratio R_p increases, while [D_{sorp} - D_{sat}] decreases as the number of stacked plates (so the particle thickness) increases.

Thus, in addition to the adsorption capacity of the basal surface defined by the octahedral layer charge, this relationship highlights the relevance of the particle morphology in the saturation of the basal planes by adsorption of PCE. Finally, Figure 10(c) indicates that the maximum sorption capacity of each clay sample is defined solely by the octahedral layer charge, being independent of the particle morphology as it happens with the stationary d-spacing.

The interpretation of the relationships found for D_{sat}, D_{sorp}, the stationary d-spacing and the maximum PCE net sorption suggest that the morphology of the clay particle is relevant in the intercalation process only when the PCE/clay ratio (expressed as mg of PCE per m^2 of clay) is low, thus when the PCE is in stoichiometric limiting conditions.

Conversely, when the PCE/clay ratio increases, the relevance of the particle morphology is being reduced to the point that at high PCE/clay ratio (when PCE is in stoichiometric excess in relation to the total clay surface available) the interaction process seems to be controlled exclusively by the octahedral layer charge. This is a major conclusion since it seems to indicate that the key-parameters controlling the interaction process between PCE polymers and MNT clays varies as the PCE/MNT ratio evolves.

5.4 Fluidity loss behaviour of cement pastes containing MNT clays and water reducer admixtures

The reduction of paste flow promoted by the addition of different amounts of clay samples in cement pastes with w/c ratio of 0.26 containing water-reducer polymers is presented in Figure 11 and 12. The dosage used of PCE is 0.3% bwc to obtain an initial paste flow of 154 mm in the reference paste when no clay is added. For BNS water reducer, the dosage used is 1.2% bwc, which is the corresponding one to obtain an equivalent paste flow.

Figure 11(a,b) shows the paste flow results after mixing for the cement pastes produced with 1.2% bwc of BNS, expressing the clay content as per % bwc and as per m^2 of clay per gram of cement, respectively. Additionally, Figure 12(a,b) presents the same study but for the cement pastes produced with 0.3% bwc of PCE polymer.

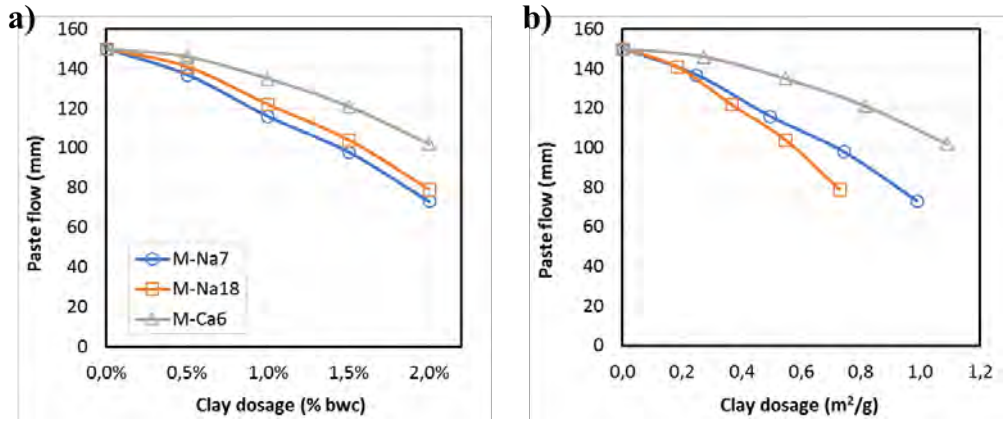

Figure 11. Paste flow evolution of cement pastes with 1.2% bwc of BNS and different amounts of MNT clays; a) clay dosage expressed as per % bwc; b) clay dosage expressed as per m^2/g of cement

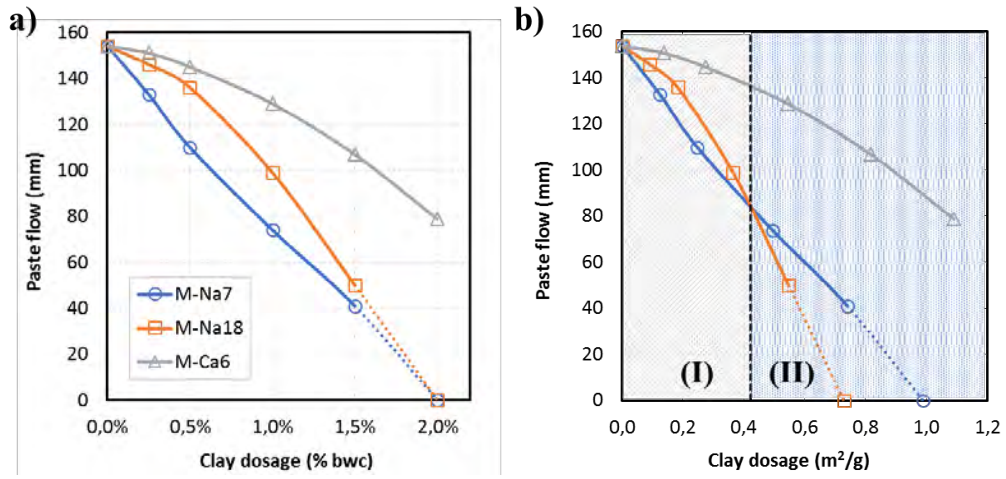

Figure 12. Paste flow evolution of cement pastes with 0.3% bwc of PCE and different amounts of MNT clays; a) clay dosage expressed as per % bwc; b) clay dosage expressed as per m^2/g of cement

For the BNS water reducer presented in Figure 11, the interference of the MNT clays in the fluidity behaviour of cement pastes is exclusively based on the adsorption of polymer on the external clay surface, both edge and basal surface. Therefore, from the paste flow evolution displayed in Figure 11(b), where the clay content is expressed as per m^2 of clay per gram of cement, it is possible to conclude that the higher the ratio between basal surface and edge surface, the higher the fluidity loss observed. It aims to propose that MNT clay particles with large aspect ratio, thus with large basal planes available for adsorption, generate higher impact in the fluidity reduction of cement pastes when non-intercalable water reducer admixtures such as BNS polymers are used.

The paste flow loss of cement pastes with MNT clays and PCE polymer presented in Figure 12 confirms that the impact in the reduction of fluidity is much more pronounced than for the pastes produced with BNS. It is especially evident for the high charged MNT clay samples M-Na7 and M-Na18, meanwhile M-Ca6 shows a profile of fluidity loss comparable to that the observed for BNS addition.

In the region (I) from Figure 12(b), at low dosage of MNT clay, the PCE/clay ratio is high. In this region it can be observed that M-Na7 clay (being the clay with the highest octahedral layer charge) produces faster fluidity loss than M-Na18 at equivalent clay surface added. But this behaviour is reverted in region (II), at higher clay concentration thus when PCE/clay ratio is low, observing that for the same clay surface added, M-Na18 (being the clay with the highest aspect ratio) produces the highest fluidity loss.

These results of fluidity loss are consistent with the hypothesis previously formulated: the availability of basal surface as consequence of the morphology of the clay particle is determinant at low PCE/clay ratio, but at high PCE/clay ratio the layer charge is the most determinant parameter driving the interaction process.

6. CONCLUSIONS

The influence of the properties of MNT clays in the intercalation behaviour of PCE polymers is proven. This fact is already well known confirmed by the experimental evidences of paste flow loss and sorption rates. Nevertheless, by tracking the interlaminar d-spacing using *in-situ* XRPD analysis performed on fresh, unaltered clay pastes, the influence of the clay properties in the intercalation process are also reflected by the expansion profile of the clay. It is a relevant insight since it allows to meet agreement between the expansion of the clay by d-spacing measurements and the experimental results of paste flow and sorption rate, which is not met with the d-spacing results obtained by XRPD analysis performed on separated and dried clay pastes (showing almost same d-spacing values always compressed between 18-21 Å despite using clays of different properties and diverse dosages of PCE polymers that generates clear differences in sorption and fluidity results).

The octahedral layer charge induced by aliovalent isomorphic substitution is identified as the most relevant clay property controlling the intercalation process. Nevertheless, the importance of the key-parameters controlling the interaction process change as the PCE/clay ratio (and mg/m^2 of clay) evolves. At low PCE/clay ratios, the interaction between PCE and MNT clay is controlled by the morphology of the clay particle and by the octahedral layer charge,

having both similar relevance. Conversely, at high PCE/clay ratios, there is almost no influence of the particle morphology, being the octahedral layer charge the clay property controlling the interaction. Therefore, it brings an additional complexity for the design of PCE polymers with improved clay tolerance since the polymer uptake by MNT clays is influenced by the polymer structure of the PCE and by the layer charge and the morphology of the clay particle at the same time, but also by the dosage ratio between PCE polymer and MNT clay.

The conclusions exposed are extracted from the use of one specific PCE structure in combination with three different montmorillonites. Therefore, it is possible that the relationships found between the properties of clays and the intercalation behaviour may vary by using a PCE polymer of different polymeric structure.

Based on these findings, it is suggested that future works addressed to investigate superplasticizer/clay interactions includes a detailed description of the clay samples used for the proper interpretation of the experimental results, in the same way that it is done for the PCE structures, attending to their proven influence in the intercalation process.

Acknowledgments

Mr. Borralleras thanks all the support given by BASF Construction Chemicals to the development of this work. Dr. I. Segura is supported by the postdoctoral Torres Quevedo program of the Spanish Ministry of Science.

References

[1] V.A. Fernandes, P. Purnell, G.T. Still, T.H. Thomas, The effect of clay content in sands used for cementitious materials in developing countries, Cement and Concrete Research 37 (2007) 751-758.

[2] L. Lei, J. Plank, A study on the impact of different clay minerals on the dispersing force of conventional and modified vinyl ether based polycarboxylate superplasticizers, Cement and Concrete Research 60 (2014) 1-10.

[3] S. Qian, H. Jiang, B. Ding, Y. Wang, C. Zheng, Z. Guo, Synthesis and performance of polycarboxylate superplasticizer with clay-inerting and high slump retention capability, Materials Science and Engineering 182 (2017).

[4] M.J. Wilson, Sheet silicates: clay minerals, ISBN 978-1-86239-359-2, The Geological Society Publishing House, Second edition (2013).

[5] C. Sun, H. Zhou, X. Li, S. Wang, J. Xing, The clay-tolerance of amide-modified polycarboxylate superplasticizer and its performance with clay-bearing aggregates, Proceedings of International Conference on Materials, Environment and Biological Engineering (2015) 237-241.

[6] G. Chen, J. Lei, Y. Du, X. Du, X. Chen, A polycarboxylate as a superplasticizer for montmorillonite clay in cement: adsorption and tolerance studies, Arabian Journal of Chemistry 27 (2017) 12-21.

[7] X. Shu, Q. Ran, J. Liu, H. Zhao, Q. Zhang, X. Wang, Y. Yang, Tailoring the solution conformation of polycarboxylate superplasticizer toward the improvement of dispersing performance in cement paste, Construction and Building Materials 116 (2016) 289-298.

[8] L. Lei, J. Plank, Synthesis and properties of a vinyl ether-based polycarboxylate superplasticizer for concrete possessing clay tolerance, Industrial & Engineering Chemistry Research 53 (2014) 1048-1055.

[9] H. Tan, Xin Li, M. Liu, B. Ma, B. Gu, X. Li, Tolerance of cement for clay minerals: effect of side-chain density in polyethylene oxide (PEO) superplasticizers additives, Clay and Clay Minerals 64-6 (2016) 732-742.

[10] H. Tan, B. Gu, B. Ma, X. Li, C. Lin, Mechanism of intercalation of polycarboxylate superplasticizer into montmorillonite, Applied Clay Science 129 (2016) 40-46.

[11] S. Ng, J. Plank, Interaction mechanisms between Na-montmorillonite clay and MPEG-based polycarboxylate superplasticizers, Cement and Concrete Research 42 (2012) 847-854.

[12] P. Borralleras, I. Segura, M.A.G. Aranda, A. Aguado, Influence of experimental procedure on d-spacing measurement by XRD of montmorillonite clay pastes containing PCE based superplasticizer, Cement and Concrete Research 116 (2019) 266-272, https://doi.org/10.1016/j.cemconres.2018.11.015.

[13] P. Borralleras, I. Segura, M.A.G. Aranda, A. Aguado, Influence of the polymer structure of polycarboxylate-based superplasticizers on the intercalation behaviour in montmorillonite clays, Construction and Building Materials 220 (2019) 285-296, https://doi.org/10.1016/j.conbuildmat.2019.06.014.

[14] R. Ait-Akbour, P. Boustingorry, F. Leroux, F. Leising, C. Taviot-Guého, Adsorption of polycarboxylate poly(ehtylene glycol) (PCP) esters on montmorillonite (MNT): Effect of exchangeable cations (Na^+, Mg^{2+} and Ca^{2+}) and PCP molecular structure, Journal of Colloid and Interface Science 437 (2015) 227-234.

[15] R.T. Martin, Report of the clay mineral society nomeclature committee: revised classification of clay minerals, Clays and Clay Minerals 39 (1991) 333-335.

[16] I. Bibi, J. Icenhower, N. K. Naz, M. Shahid, S. Bashir, Clay Minerals: Structure, Chemistry, and Significance in Contaminated Environments and Geological CO2 Sequestration, Environmental Materials and Waste (2016) 543-567.

[17] A.T. Serstevens, P.G. Rouxhet, A.J. Herbillon, Alteration of mica surfaces by water and solutions, Clay Minerals 13 (1978) 401-410.

[18] T. Preocanin, A. Abdelmonem, G. Montavon, J. Luetzenkirchen, Charging behavior of clays and clay minerals in aqueous electrolyte solutions. Experimental methods for measuring the charge and interpreting the results – Clays, clay minerals and ceramic materials based on clay minerals, ISBN 978-953-51-2259-3 (2016).

[19] A.A. Jones, Charges on the surfaces of two chlorites, Clay Minerals 16 (1981) 347-359.

[20] M. Matusewicz, K. Pirkkalainen, J.P. Suuronen, A. Root, A. Muurinen, R. Serimaa, M. Olin, Microstrcutural investigation of calcium montmorillonite, Clay Minerals 48 (2013) 267-276.

[21] P.H. Nadeau, The physical dimensions of fundamental clay particles, Clay Minerals 20 (1985) 499-514.

[22] X. Liu, X. Lu, M. Sprik, J. Cheng, E.J. Meijer, R. Wang, Acidity of edge surface sites of montmorillonite and kaolinite, Geochimica et Cosmochinica Acta 117 (2013) 180-190.

[23] E. Tombácz, M. Szekeres, Surface charge heterogeneity of kaolinite in aqueous suspension in comparison with montmorillonite, Applied Clay Science 34 (2006) 105-124.

[24] H. Zhao, S. Bhattarcharjee, R. Chow, D. Wallace, J.H. Masliyah, Z. Xu, Probing surface charge potentials of clay basal planes and edges by direct force measurements, Langmuir 24 (2008) 12899-12910.

[25] M.J. Wilson, L. Wilson, I. Patey, The influence of individual clay minerals on formation damage of reservoir sandstones: acritical review with some new insigthts, Clay Minerals 49 (2014) 147-164.

[26] M. Alvarez-Silva, M. Mirnezami, A. Uribe-Salas, J.A. Finch, Point of zero charge, isoelectric point and aggregation of phyllosilicate minerals, Canadian Metallurgical Quarterly 49 (2010) 405-410.

[27] E. Tombácz, M. Szekeres, Colloidal behavior of aqueous montmorillonite suspensions: the specific role of pH in the presence of indifferent electrolytes, Applied Clay Science 27 (2004) 75-94.

[28] C. Tournassat, J. Davis, C. Chiaberge, S. Grangeon, I.C. Bourg, Modeling the acid-base properties of montmorillonite edge surfaces, Environmental Science 50 (2016) 13436-13445.

[29] A. Meunier, Why are clay minerals small?, Clay Minerals 41 (2006) 551-566.

[30] I. Barshad, Absorptive and swelling properties of clay-water system, Clays and Clay Technology 169 (1950) 70-77.

[31] A. Seppälä, E. Puhakka, M. Olin, Effect of layer charge on the crystalline swelling of Na^+, K^+ and Ca^{2+} montmorillonites: DFT and molecular dynamics studies, Clay Minerals 51 (2016) 197-211.

[32] A. Maes, M.S. Stul, A. Cremers, Layer charge-cation exchange capacity relationships in montmorillonite, Clays and Clay Minerals 27 (1979) 387-392.

[33] L. Ammann, Cation exchange and adsorption on clays and clay minerals, Doctoral dissertation, Christian-Albrechts University of Kiel (2003).

[34] T. Chen, Y. Yuan, Y. Zhao, F. Rao, S. Song, Effect of layer charges on exfoliation of montmorillonite in aqueous solutions, Colloids and Surfaces: Physicochemical and Engineering aspects 548 (2018) 92-95.

[35] X. Zhang, H. Yi, H. Bai, Y. Zhao, F. Min, S. Song, Correlation of montmorillonite exfoliation with interlayer cations in the preparation of two-dimensional nanosheets, RSC Advances 7 (2017) 41471-41478.

[36] J. Srodon, D.J. Morgan, E.V. Eslinger, D.D. Eberl, M.R. Karlinger, Chemistry of illite/smectite and end-member illite, Clays and Clay Minerals 34 (1986) 368-378.

[37] G.E. Christidis, D.D. Eberl, Determination of layer-charge characteristics of smectites, Clays and Clay Minerals 51 (2003) 644-655.

[38] C. Gay, E. Raphael, Comb-like polymers inside nanoscale pores, Advances in Colloid and Interface Science 94 (2001) 229-236.

[39] Y.H. Shen, Estimation of surface area of montmorillonite by ethylene oxide chain adsorption, Chemosphere 48 (2002) 1075-1079.

[40] A. Kahn, Studies on the size and shape of clay particles in aqueous suspension, Clays and Clay Minerals 6 (1959) 220-236.

[41] D.P. Veghte, M.A. Freedman, Facile method for determining the aspect ratios of mineral dust aerosol by electron microscopy, Aerosol Science and Technology 48 (2014) 715-724.

[42] C. Weber, M. Heuser, H. Stanjek, A collection of aspect ratios of common clay minerals determined from conductometric titrations, Clay Minerals 49 (2014) 495-498

[43] R. Tettenhorst, H.E. Roberson, X-Ray diffraction aspects of montmorillonite, American Mineralogist 58 (1973) 73-80.

[44] F. Macht, K.U. Totsche, K. Eusterhues, G. Pronk, Topografy and surface properties of clay minerals analyzed by atomic force, Proceedings of 19th World Congress of Soil Science (2010) 206-209.

[45] F. Macht, K. Eusterhues, G.J. Pronk, K.U. Totsche, Specific surface area of clay minerals: comparison between force microscopy measurements and bulk-N_2 gas (BET) and bulk-liquid (EGME) absorption methods, Applied Clay Science 53 (2011) 20-26.

[46] S. Hillier, Accurate quantitative analysis of clay and other minerals in sandstones by XRD: comparison of a Rietveld and a reference intensity ratio (RIR) method and the importance of sample preparation, Clay Minerals 35 (1999) 291-302.

[47] P. Borralleras, I. Segura, M.A.G. Aranda, A. Aguado, Absorption conformations in the intercalation process of polycarboxylate ether-based superplasticizers into montmorillonite clay, Construction and Building Materials (submitted)

[48] E.C. Jonas, R.M. Oliver, Size and shape of montmorillonite crystallites, Clay and Clay Minerals 15 (1967) 27-33.

[49] N. Güven, Smectites – Hydrous phyllosilicates, Reviews in Mineralogy 19 (1988) 497-560.

[50] R. F. Geise, The electrostatic interlayer forces of layer structure minerals, Clay and Clay Minerals 26 (1978) 51-57.

[51] H. Li, Y. Zhao, S. Song, Y. Hu, Y. Nahmad, Delamination of Na-montmorillonite particles in aqueous solutions and isopropanol under shear forces, Journal of Dispersion Science and Technology 38 (2017) 1117-1123.

[52] M.A. González-Ortega, S.H.P. Cavalaro, A. Aguado, Influence of barite aggregate friability on mixing process and mechanical properties of concrete, Construction and Building Materials 74 (2015) 169-175.

4.2. ACCEPTED ABSTRACTS

11th ACI/RILEM International Conference on Cementitious Materials and Alternative Binders for Sustainable Concrete to be held in Toulouse, France, June 29th to July 1st, 2020

CONFERENCE ABSTRACT I:

Title

Improved analytical methodology for measuring interlayer d-spacing of montmorillonite clays expanded by intercalation of PCE polymers

Authors

Pere Borralleras[1,*], Ignacio Segura[2], Miguel A. G. Aranda[3] and Antonio Aguado[4]

[1] *Technical and Marketing Manager Iberia, BASF Construction Chemicals (Barcelona, Spain)*
[2] *Smart Engineering Ltd, Department of Environmental and Civil Engineering, UPC - Universitat Politècnica de Catalunya (Barcelona, Spain)*
[3] *Scientific Director, ALBA Synchrotron (Barcelona, Spain)*
[4] *Professor, UPC - Universitat Politècnica de Catalunya, Department of Environmental and Civil Engineering (Barcelona, Spain)*

**Corresponding author: pere.borralleras@basf.com / +34-659-957-521*

Abstract

Clays contained in sands for concrete interfere in the performance of superplasticizers. It is especially problematic for the combination PCE polymers-montmorillonite clays because it almost totally inhibits the dispersion capacity of the superplasticizer.

This interference is promoted by the absorption of polymer into the interlaminar space of montmorillonites, producing clay expansion by intercalating PCE side chains. Interlayer d-spacing is traditionally measured by XRPD analysis on powder samples obtained from separated and dried clay pastes. Nevertheless, the results reported are in disagreement with the experimental results of fluidity and sorption and does not reproduce the impact from the influence of diverse polymeric structures and clay properties on the fluidity loss and dosage efficiency.

This paper presents and describes an improved analytical method for d-spacing measurements, based on *in-situ* XRPD analysis performed directly on fresh, unaltered clay pastes. This method reveals new scenarios for the understanding of the interaction process, reporting degrees of PCE intercalation and clay expansion 10 times larger than the deducted with the results from the traditional method. It also allows to identify the real influence of the structure and dosage of PCE and of clay properties, while proving new tools for the understanding of the intercalation mechanism.

CONFERENCE ABSTRACT II:

Title

Influence of the structure of PCE polymers and of the properties of montmorillonite clays in the intercalation mechanism producing fluidity loss of cementitious systems

Authors

Pere Borralleras[1,*], Ignacio Segura[2], Miguel A. G. Aranda[3] and Antonio Aguado[4]

[1] *Technical and Marketing Manager Iberia, BASF Construction Chemicals (Barcelona, Spain)*
[2] *Smart Engineering Ltd, Department of Environmental and Civil Engineering, UPC - Universitat Politècnica de Catalunya (Barcelona, Spain)*
[3] *Scientific Director, ALBA Synchrotron (Barcelona, Spain)*
[4] *Professor, UPC - Universitat Politècnica de Catalunya, Department of Environmental and Civil Engineering (Barcelona, Spain)*

**Corresponding author: pere.borralleras@basf.com / +34-659-957-521*

Abstract

Future availability of sands is a real threat for construction industry, thus a more efficient use of extracted resources is required. One relevant contribution is to avoid sand washing, but

this is not possible nowadays because clays interfere on superplasticizers performance and all the attempts to design high-range superplasticizers insensitive to clays have not reported robust, cost-effective and sustainable solutions to allow a more efficient use of natural sands.

This paper presents how the PCE polymeric structure and montmorillonite properties condition the intercalation mechanism and the interference on the dispersing capacity of PCE-based superplasticizers. It is supported by d-spacing measurements with *in-situ* XRPD analysis on fresh, unaltered pastes, since with XRPD analysis on dried pastes almost no d-spacing changes are observed when different PCEs are used.

It is revealed that the conformation of side chains and the anionic charge are the most important parameters of PCEs controlling the intercalation, while for montmorillonites they are the layer charge and the particle morphology. The intercalation profiles confirm that PCE/clay ratio and clay exfoliation are key-conditioners for the intercalation process, while meeting agreement between the experimental results of fluidity loss and sorption rates and the measurements of clay expansion from d_{001}.

CONFERENCE ABSTRACT III:

Title

Interpretation of the mechanism and key-parameters controlling the interaction between PCE based-superplasticizers and montmorillonite clays

Authors

Pere Borralleras[1,*], Ignacio Segura[2], Miguel A. G. Aranda[3] and Antonio Aguado[4]

[1] Technical and Marketing Manager Iberia, BASF Construction Chemicals (Barcelona, Spain)
[2] Smart Engineering Ltd, Department of Environmental and Civil Engineering, UPC - Universitat Politècnica de Catalunya (Barcelona, Spain)
[3] Scientific Director, ALBA Synchrotron (Barcelona, Spain)
[4] Professor, UPC - Universitat Politècnica de Catalunya, Department of Environmental and Civil Engineering (Barcelona, Spain)

**Corresponding author: pere.borralleras@basf.com / +34-659-957-521*

Abstract

From the understanding and interpretation of the real influence of PCE polymeric structures and of montmorillonite clay properties provided by *in-situ* XRPD analysis, and supported by additional experiments, an extended model for the interaction mechanism between PCE and montmorillonites is proposed, concluding that he intercalation is not based on a single side-chain monolayer model, as currently accepted, but on multiple layers arranged into de clay interlaminar space.

Three spatial arrangements (named as absorption conformations) for intercalating PCE side chains are recognized, as well as their consequences in the interference produced, meeting alignment with the observed results of fluidity loss in cement pastes. The mechanism proposed is consistent with the identified key-parameters of PCE and montmorillonites conditioning the conformation of absorption taken as well as their relative importance in controlling the interference process overall.

These new insights of the intercalation mechanism allow to predict the most sensitive PCE structures and the most problematic montmorillonites having the greatest interference in the fluidity behavior. They also contribute with further knowledge to support the design of clay-insensitive high-range superplasticizers to promote the sustainable future of aggregates industry by a more efficient use of natural resources with the use of unwashed sands.

Chapter 5
SPECIFIC CONCLUSIONS, GENERAL CONCLUSIONS AND FURTHER RESEARCH

The last chapter is structured in three parts. The first part includes the specific conclusions structured in the main areas of contribution, related to the specific objectives, and the new insights derived from the discussion are gradually introduced into the discussion. The second part exposes the general conclusions related to the main objective, extracted from the jointly interpretation of the specific conclusions. This part also includes a proposal for the interpretation of the intercalation mechanism, grounded by the new insights obtained. Finally, some suggestions for further research are presented, aiming to complement the contributions from this thesis and to extend the understanding of the interaction process.

Contents

5.1. SPECIFIC CONCLUSIONS

The specific conclusions are structured in the three main areas of contribution investigated, which conform the specific objectives described in Chapter 2 and covered by each of the Journal Papers written.

5.1.1. Improved analytical method for the d-spacing measurements on montmorillonite clays expanded by intercalation of PCE polymers

The accomplishment of *specific objective 1* is to propose an improved test methodology for the measurements of d-spacing enlargements by XRPD analysis of montmorillonite clays intercalating PCE side chains. This is considered a relevant contribution because it will extend the analytical possibilities to understand and interpret the interaction process, which is a basic need to support the development of clay-insensitive high-performance superplasticizers.

The assessment on the analytical method for d-spacing is the main topic of study in Journal Paper I (pages 24-47). In this way, a new-alternative method of analysis is proposed, so accomplishing the specific objective 1. This method is based on *in-situ* XRPD measurements directly performed in fresh, unaltered clay pastes, so avoiding any previous treatment of samples. The detailed information on the methodoly used for the measurement of d-spacing is described in the Journal Paper I, including the sample treatment and the experimental measurement conditions used.

The current, traditional testing procedure for d-spacing determination involves several sample treatments. The basic steps of this testing procedure are summarized [1-3]:

1- Preparation of clay pastes in synthetic cement pore solution containing PCE based water reducer admixture
2- Separation of the solid phase from the liquid phase of the clay paste, by filtration or centrifugation
3- Drying of the recovered solid phase at <80 ºC
4- XRPD analysis performed on dried clay powder

By executing the traditional methodology described, constant and invariable results of d-spacing are always obtained, being compressed between 18-21Å in all the cases despite using different clays and diverse types and dosages of PCE polymers. From these results, an intercalation model based on the intercalation of one single monolayer of PEG/PEO side chains

together with two water units is deducted [1-5], independently of the type of clay and of the type and dosage of PCE polymer.

In the investigation of the influence of the previous sample treatment performed it is observed that the separation method does not alters the lectures of d-spacing. However, it is confirmed that the drying process of clay pastes produced huge distortions in the net expansion of the clay by lowering the d-spacing results up to 18-21Å, suggesting that the drying process forces the partial release of intercalated side chains.

This conclusion is grounded by the experimental results obtained when XRPD analysis are performed directly on fresh, unaltered clay pastes (*in situ* XRPD analysis). Figure 5.1 summarizes the experimental results supporting these statements. Figure 5.1(a) compares the d-spacing results obtained with the traditional method on dried clay pastes by using two different separation methods. Figure 5.1(b) shows the results of d-spacing obtained by XRPD analysis performed on dried clay samples (according to the traditional methodology) in comparison to the results obtained by the new-improved methodology proposed based on *in-situ* XRPD analysis directly performed on fresh, unaltered clay pastes.

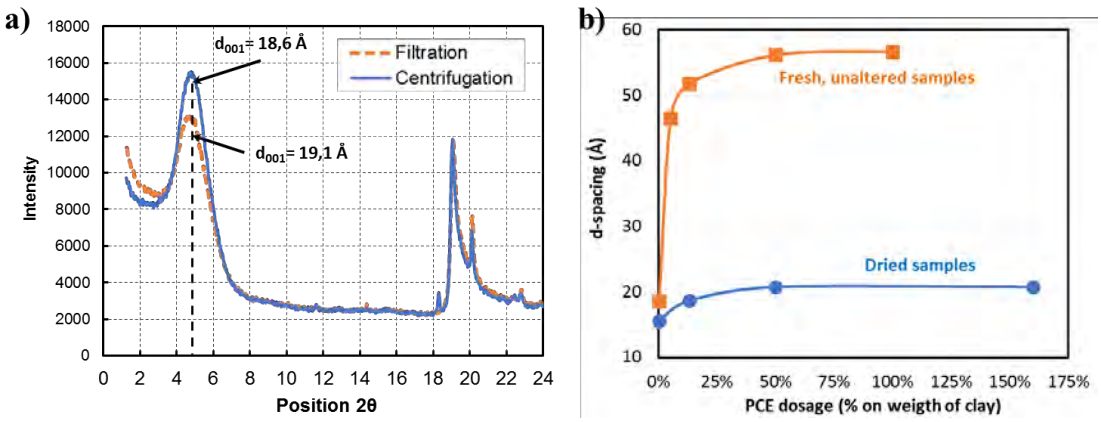

Figure 5.1. a) XRPD patterns and d-spacing of dried clay samples using two separation methods: filtration and centrifugation; b) Comparison of maximum d-spacing recorded at different PCE dosages between XRPD measurements on dried clay pastes according to the traditional method and *in-situ* XRPD measurements on fresh, unaltered clay pastes

As it is deducted from Figure 5.1(a), the separation method has no relevant influence in the d-spacing results obtained after drying the samples. Nevertheless, Figure 5.1(b) confirms that by avoiding the previous drying of clay pastes, *in-situ* XRPD analysis reveals that the net expansion of the clay measured raises up to 60Å, being up to three times larger than the measured with the traditional methodology.

In consequence, it can be affirmed that the d-spacing results obtained with the traditional analytical method are not representative of the real intercalation degree (n_{PEG}) produced in fresh state because most of the intercalated side chains are removed meanwhile water is evaporated during the drying process of the clay pastes, leaving only one single monolayer remaining inside the interlaminar space of the montmorillonite. Thus, it is denoting an intercalation model based on the multiple intercalation of side chains instead the monolayer model.

Another important featuring of the improved method is that it allows to identify how the d-spacing is increasing as the dosage of PCE increases. It is a relevant contribution since the variations in the dosage of PCE do not produce any significant change in the d-spacing recorded by the traditional method. The experimental results supporting this featuring are summarized in Figure 5.2, including the reproducibility and repeatability check by testing the same samples in two different laboratories using different diffractometers.

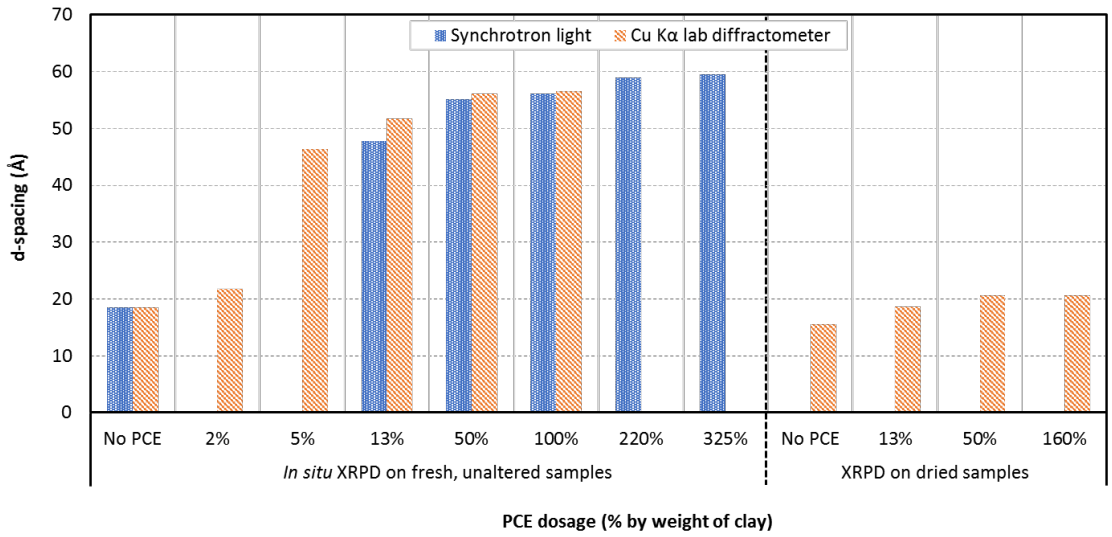

Figure 5.2. Comparison of the experimental results of d-spacing obtained on separated, dried clay pastes and on fresh, unaltered clay pastes by using diverse PCE dosages and performed in two laboratories using different diffractometers

The experimental results presented in Figure 5.2 reveal the real impact of the PCE dosage on the expansion profile of montmorillonites and confirms that the expansion of the clay increases as the dosage of PCE polymer increases. It can be observed that these results were reproduced by testing in two laboratories using diffractometers equipped with different X-ray source.

From the new insights previously described, it is very feasible to indicate that all the experimental results and conclusions from the previous studies using the traditional analytical

method must be questioned and the proposed relationships between clay interlayer d-spacing and clay properties and PCE polymeric structures shall be reviewed.

5.1.2. Identification of the influence of PCE polymeric structure on the intercalation behavior into montmorillonite clay and proposal of absorption conformations

The *specific objective 2* is structures in two sub-objectives, being the second consequent of the first. The *specific objective 2(a)* aims to understand how the different structures of PCE polymers influence on the intercalation process and, specifically, on the intercalation degree. Therefore, it is expected to identify which are the parts of the polymer controlling the intercalation behavior.

The influence of the polymeric structure on the d-spacing evolution is investigated in Journal Paper II (pages 24-47), concluding that the diverse structures of PCE polymers lead to relevant differences in the expansion profile of montmorillonite clays. It is deducted from the changes on d-spacing revealed by *in-situ* XRPD analysis performed on fresh, unaltered clay pastes. The experimental results of d-spacing displayed in Figure 5.3(a,b) support this statement, obtained by using four PCE polymers with different structure and at diverse dosages, performing the measurements with the traditional method on dried pastes and with the improved method based on *in-situ* XRPD analysis performed on fresh pastes, respectively.

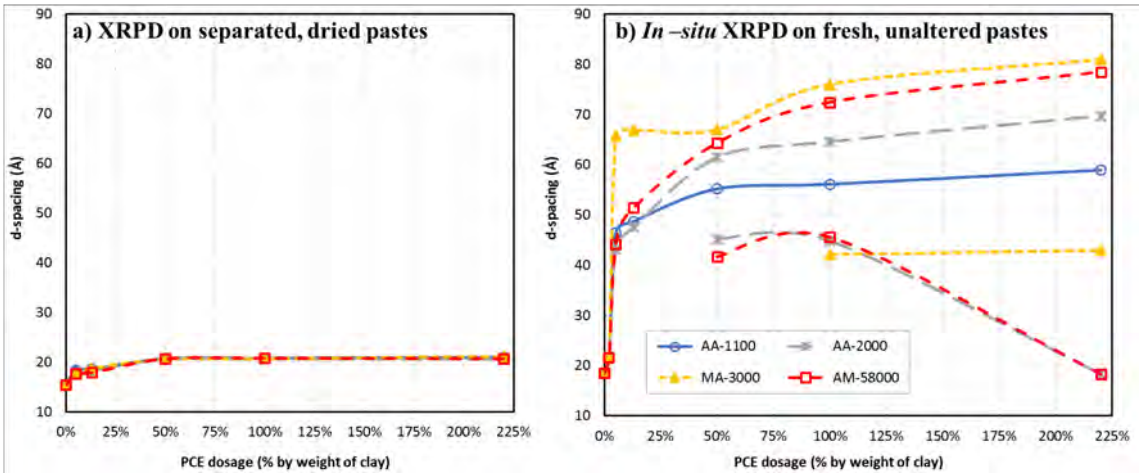

Figure 5.3. Experimental results of d-spacing obtained with different PCE polymers at diverse dosages by tested with; a) Traditional method on dried clay pastes; b) *In-situ* XRPD on fresh, unaltered clay pastes

The experimental results presented in Figure 5.3 obtained confirm that XRPD analysis performed on dried clay pastes do not show any difference in the d-spacing results between the different polymeric structures of PCEs and the dosage used. However, the improved method

based on *in-situ* XRPD analysis on fresh, unaltered clay pastes reveal significant differences in the expansion profile of the clay produced when different structures of PCE polymers and diverse dosages are used.

As described in Chapter 2, the proposal of an improved analytical method for d-spacing determination is motivated by the disagreements identified between the expansion profile of clays deducted from the traditional test method and the experimental results of fluidity loss and of sorption rate recorded on the same clay pastes. Therefore, to accomplish the specific objective 2, the experimental results of d-spacing obtained with the improved test method must to reproduce the fluidity and sorption behavior observed in clay pastes. In this respect, the dissertations included in Journal Paper II confirm that the alignment between all the experimental results is match, therefore, supporting the reliability of the new testing method proposed.

The XRD patterns obtained by *in-situ* XRPD analysis on fresh clay pastes also highlight the presence of new clay specimens released by exfoliation. This phenomenon is key to understand the relationship between sorption rates, fluidity loss and d-spacing results. The deducted roles for each of the structural parts of the PCE polymers conditioning the intercalation behavior are summarized:

- At low PCE/clay dosage ratio (dosage by weight), the degree of intercalation is controlled by the adsorption of PCE polymer, which increases as the PCE anionic charge increases. Polymers with higher anionic charge saturate the interlaminar space of the clay by intercalation of side chains at lower PCE/clay ratio. The specific dosage producing saturation is referred as D_{sat} - saturation dosage, which can be correlated with the anionic charge of the PCE.
- At high PCE/clay ratio, clay exfoliation is produced, releasing new-additional clay surface available for further PCE adsorption and forcing to a reorganization of the sorbed polymer (absorbed polymer by intercalation and adsorbed polymer on clay surface). The consequences of clay exfoliation allow to provide a reasonable explanation for the fluidity loss and for the sorption behavior observed to match with the expansion profiles of the clay.
- PCE polymers with high side chain density produces earlier and more severe exfoliation, in agreement with the increased fluidity loss and with the higher sorption rates observed for this particular PCE structures.
- The maximum d-spacing (stationary d-spacing) produced along the PCE dosage increases is limited by a stationary state, when the expansion profile of clay promoted by intercalation of polymer shows almost no further changes despite increasing the dosage of polymer. The stationary d-spacing is reached when PCE/clay ratio is the

highest and it is larger for PCE polymers having long side chains. Nevertheless, the stationary d-spacing is restricted by the own stability of the clay structure by producing exfoliation from a certain value of d-spacing.

Considering the current state of the art, the level of understanding obtained in regards of the influence of the structure of PCE polymers can be considered as a relevant contribution for the comprehension of the interaction process. Therefore, the *specific objective 2(a)* is accomplished, and at this point it is possible to approach the *specific objective 2(b)*. It is covered by Journal Paper III (pages 112-112), with the objective to propose the spatial arrangements taken by PCE polymers during the intercalation into the interlaminar space of montmorillonite clays. These arrangements are named as *absorption conformations* and the three models deducted are illustrated in Figure 5.4, including the most important key-parameters of polymer and clay controlling the conformation taken.

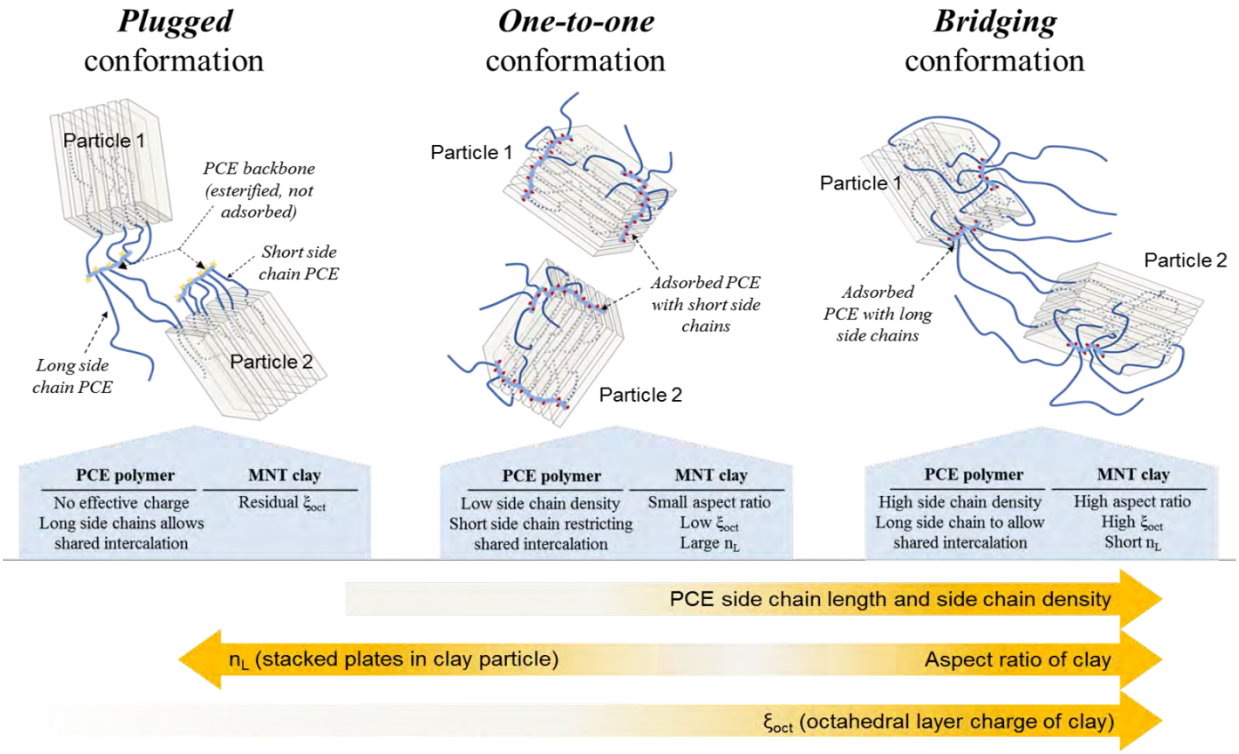

Figure 5.4. Absorption conformations for PCE polymers deducted and key-parameters of polymer and clay determining the conformation taken

The three models of the absorption conformations taken by the PCE polymer are named as *One-to-one* conformation, *Bridging* conformation and *Plugged* conformation. Nevertheless, despite three absorption conformations are deducted, in practical terms only the *One-to-one* and the *Bridging* conformations are feasible for PCE polymers with active anionic charge.

The *Plugged* conformation is the typical arrangement taken by linear polyglycols [6-9] intercalated and it is exclusively observed for PCE polymers with blocked anionic charge by esterification of the free carboxylate groups responsible for the adsorption of polymer in clay surface. Nevertheless, this absorption conformation proves the ability to intercalate side chains without requiring the previous adsorption of the polymer on the clay surface, overcoming all the expected steric and electrostatic hindrances.

From the perspective of polymeric structure, it is observed that PCE polymers with short side chains and low side chain density are prompt to *One-to-one* conformation. Same conformation is the proposed one for montmorillonites with low octahedral layer charge (ξ_{oct}), large number of stacked plates per particle (n_L) and small aspect ratio.

In the *One-to-one* conformation, the sorption of polymer is mainly located in the edge surface, thus easily allowing the absorption of side chains by intercalation. This is supported by the fact that when the *One-to-one* conformation is taken, D_{sat} (saturation dosage) is lower so the saturation of the interlaminar space is produced at lower dosage of PCE polymer.

Additionally, in this conformation each polymer unit interacts exclusively with one clay particle because PCE polymers having short side chains restricts the capacity to share intercalation of its side chains, since it would force the clay particles to be heavily compressed and it seems not possible due to the expected electrostatic repulsions between the negative charged surfaces of the clay particles.

Conversely, in the *Bridging* conformation one single unit of PCE polymer can interact with many clay particles simultaneously, by the shared intercalation of side chains with other clay particles different of the one where the polymer unit is adsorbed. Therefore, this absorption conformation is taken by PCE polymers having high side chain density and side chains of long length. The *Bridging* conformation is more prompt to be taken as the ξ_{oct} of the clay increases and for clay particles with high aspect ratio and short n_L.

This particular morphology of particles and the higher adsorption capacity of the basal surface promoted by the high ξ_{oct} of the clay displace the adsorption of polymer to the basal surface, thus restricting the amount of polymer units adsorbed in the edge surface easier to be intercalated.

Additionally, the *Bridging* conformation is related to high steric hindrance, generated by the bigger spatial arrangement of PCE polymers with long side chains and with high side chain density, but also by the narrow edge surface of the clay restricting the accessibility of the side chains for their intercalation into the interlaminar space of clay. These affirmations are aligned

with the observation by which when *Bridging* conformation is taken, D_{sat} (saturation dosage) increases so higher dosage of PCE polymer is required to saturate the interlaminar space of the clay.

The anionic charge of PCE is found not to be a relevant property determining the absorption conformation taken, since the *Plugged* conformation confirms that the intercalation process can proceed without the previous adsorption of PCE on clay surface. Nevertheless, it is identified that PCE anionic charge is a key-property of the PCE polymer controlling how the intercalation degree evolves among the dosage ratio PCE/clay increases, since the anionic charge defines the equilibrium between the amount of sorbed PCE interacting with the clay and the amount of non-sorbed PCE remaining free in solution, thus not interacting.

Therefore, since the higher the anionic charge the higher the sorbed amount of polymer, in the same absorption conformation taken, D_{sat} (saturation dosage) is lower for PCE polymers having higher anionic charge simply because there is more polymer interacting.

5.1.3. Identification of the influence of montmorillonite clay properties on the intercalation behavior of PCE polymers

In the same way than the specific objective 2 (focused on the influence of the structures of PCE polymers), the *specific objective 3* is set to assess on the impact of montmorillonite clay properties on the intercalation behavior. Therefore, this specific objective aims to clarify the discrepancies between the experimental results of fluidity loss and of sorption rates with the d-spacing measurement obtained with the traditional analytical method, being almost invariable despite using montmorillonite clays of different properties, in contrast with the clear differences observed in the fluidity and sorption behavior [4].

It is the main topic of study in the Journal Paper IV (pages 222-222). Here, from the determination of d-spacing by *in-situ* XRPD analysis performed on fresh, unaltered clay pastes, it is revealed that the properties of the clay have a huge impact on the evolution of the expansion of the clay and on the maximum expansion produced by the intercalation of PCE side chains.

Moreover, it is suggested that the tendency to exfoliate and the preferred intercalation degrees (n_{PEG}) are mainly defined and controlled by the clay properties and not by the structure of the PCE polymer. The experimental results supporting these conclusions are presented in Figure 5.5(a,b).

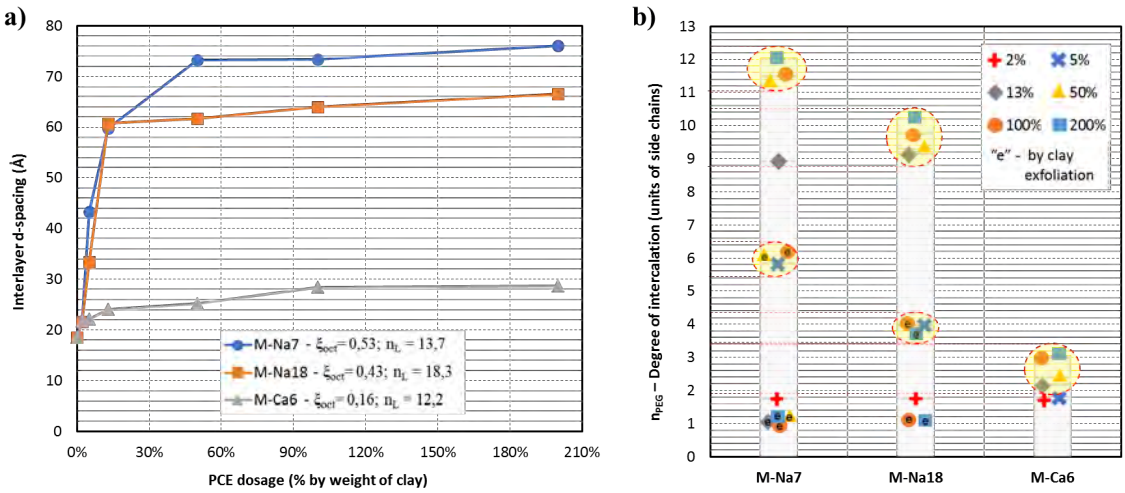

Figure 5.5. a) Experimental results of maximum d-spacing for different montmorillonites and at diverse dosages of PCE polymer; b) Intercalation degree (n_{PEG}) calculated for each clay and at each PCE dosage

Figure 5.5(a) collects the maximum d-spacing measured at different dosages of one single (same) PCE polymer with three montmorillonites owning significant differences in layer charge and in particle morphology. These results allow to deduct that montmorillonites with higher octahedral layer charge (ξ_{oct}) are able to intercalate bigger number of PCE side chains, thus producing larger expansions.

From the results presented in Figure 5.5(a), Figure 5.5(b) displays the corresponding intercalation degrees (n_{PEG}) calculated for each of the clays at the diverse PCE dosages tested. From this figure, two relevant conclusions can be extracted. Firstly, high charged clays experience delamination more easily and at lower dosage of PCE polymer, so more easily releasing new clay specimens with lower number of stacked plates from the delamination of the pristine particles. This observation is in agreement with the relationship presented by other studies [10,11] between the layer charge of clays and their absorptive properties [12-14] of linear polyglycols and also with the exfoliation behavior of montmorillonites induced by intercalation of polymers [15,16].

In Figure 5.5(b) it is observed that the intercalation degrees (n_{PEG}) of PCE side chains into the interlaminar space of the montmorillonite clays used are mainly concentrated at some specific and punctual levels, defined as *preferred intercalation degrees.* The preferred intercalation degrees are defined exclusively by the clay properties, while the PCE structure has not any influence. It is confirmed by the experimental results presented in the Journal Paper II (pages 333-333), covering the specific objective 2, in contrast with the results obtained when different montmorillonites are used, observing that for one specific clay, the same preferred

intercalation degrees are observed despite intercalating PCE polymers of different structure, but they show differences when different clays are tested with the same PCE polymer.

The key-properties of montmorillonite clays identified as the most influencing parameters controlling the intercalation behavior are summarized:

- At low PCE/clay dosage ratio (as per mg of PCE/m^2 of clay), the intercalation degree is controlled by both the morphology of the clay particle and the octahedral layer charge, having both the comparable influence.
- At high PCE/clay ratio, the intercalation is mainly controlled by the octahedral layer charge and almost no influence from the particle morphology is observed.

Comparing the relative influence of clay and PCE properties in the control of the intercalation mechanism, it is found that the properties of montmorillonite clays have a more important influence than the structure of PCE polymers on the definition of the absorption conformation taken and in the intercalation behavior overall. Nevertheless, in addition to the influence of all the direct properties of montmorillonite clays and of PCE polymers controlling the interaction process, the PCE/clay dosage ratio acts a modulating variable that enhances or restricts the influence of these parameters.

Finally, the d-spacing results recorded with the three different clays are found to be in agreement with both the experimental results of sorption and fluidity loss obtained with the respective clay pastes. Therefore, the existing disagreements in regards of the clay properties can be clarified, in the same way than those related to the structure of PCE polymers. Therefore, specific objective 4 is accomplished according to the expected outcome.

5.2. GENERAL CONCLUSIONS

The outcome of this thesis delivers two significant contributions to support the development of clay-insensitive high-performance water reducer for concrete.

The first relevant contribution is the development of an improved analytical method for d-spacing measurement of montmorillonite clays expanded by the intercalation of side chains of PCE polymers, reporting results which meet the required alignment with the experimental evidences observed when paste flow evolution and sorption rates are tested. A reliable testing method for clay expansion is a mandatory need since the results obtained with the traditional method are not representative of the real intercalation behavior.

The second relevant contribution, supported by the first one, is the clarification of the influence of the structure and dosage of PCE polymers and of the properties of montmorillonite clays in the intercalation process, as well as the absorption conformations taken, and the identification of the most critical variables controlling the mechanism of interaction responsible for the inhibition of the dispersing performance of PCE based superplasticizers.

Therefore, the new proposed testing methodology allows to discover a new scenario for the intercalation mechanism, while allow to stablish a logic relationship between the expansion profiles of montmorillonites and the fluidity loss and the sorption behavior, which is proven to be undoubtedly dependent on the structural properties of the PCE polymers and on the properties of montmorillonite clays but also controlled by the PCE/clay dosage ratio.

5.2.1. Relevant new insights to extend the understanding of the interaction process

From the jointly interpretation of the results collected in each of the experimental phases, some relevant new insights are obtained to extend the level of understanding for the better comprehension of the interaction mechanism between PCE based superplasticizers and montmorillonite clays by which the inhibition effect of the dispersing capacity of water-reducer admixtures is based.

- Efficiency of the dispersing capacity of PCE polymers by the shape of particles:

The positive generation of paste flow, thus the efficient dispersion of clay particles, recorded in clay pastes by progressive addition of PCE polymer is not observed until reaching the correspondent D_{sorp} dosage, which expresses the PCE threshold dosage by which the progressive evolution of sorbed polymer is stabilized. Since D_{sorp} is always higher than D_{sat}, the start of the efficient dispersion produced by the water-reducer is not exclusively determined by the saturation of the interlaminar space by intercalation of side chains.

Therefore, it leads to the conclusion that clay particles are not efficiently dispersed until the entire colloid surface is almost saturated by sorbed PCE polymer. This is the opposite behavior than observed in cement, by which the greatest increases of paste flow are produced meanwhile PCE polymers can be adsorbed on the surface of cement particles and no further dispersion is observed once the saturation by adsorption of polymer is reached despite increasing PCE dosage. Therefore, at equal exposed surface, clays demand higher amounts of polymer than cement to be dispersed, meaning that water-reducer polymers are less efficient to disperse lazy particles than to disperse particles with more spherical shape such as cement particles, apart from all the inhibition effects promoted by the absorption of polymer into the interlaminar space of clays.

- Variables involved in the mechanism of interaction promoting the fluidity loss and inter-relationships between themselves:

One relevant conclusion is that there is a large number of variables controlling the interaction process so defining the level of interference responsible for the fluidity loss overall. Equation [1] expresses in a simplified way how the fluidity loss (F_{loss}) experienced by a cementitious system containing montmorillonite clays and PCE polymers can be predicted:

$$F_{loss} = W + I = W + [\Sigma(I_{PCE}) + \Sigma(I_{MNT}) + R_{PCE/MNT}] \qquad \text{Equation [1]}$$

In Equation [1], two main variables controlling the fluidity loss are recognized. The first one (*W*) is referred to the own capacity of clays to capture water from the solution due to their intrinsic water demand to hydrate the exposed surface ionized and also due to the absorption of water by the accessible interlaminar space. Therefore, the variable *W* is an exclusive factor of the clay defined by its own properties [17-21], which is contributing to the fluidity loss independently of the usage of water-reducer admixtures.

The second variable (*I*) encompasses all the identified variables responsible of the inhibition of the dispersing capacity of the water-reducer polymers based on PCE. Thus, it is particularly referred to the loss of efficiency of PCE polymers when used as consequence of the interferences promoted by the clays.

Since *I* is including a group of different variables, it can be split in all the individual factors identified controlling the mechanism of interaction. This includes all the variables related to the PCE polymeric structure (I_{PCE}) and all the variables related to the clay properties (I_{MNT}), but also the confirmed influence of the dosage ratio between PCE polymer and clay surface ($R_{PCE/MNT}$).

Apart from the characteristics of montmorillonite clays and of PCE polymers, as well as of the dosage rates, it is expected that other variables play a relevant role in the definition of the fluidity loss behavior. Factors such as temperature, water-to-cement (mass) relationship and the type and the composition of the cement are expected to condition the impact on the fluidity behavior. In addition to the mentioned factors, other variables such as the shear stress generated during the mixing process as function of the mixing time and of the speed of the mixer are proven to promote the early delamination of exfoliable particles like clays [22].

Thus, from the simplified version of the equation defining the fluidity loss, there are two different processes/mechanisms involved. As described, the first one is directly related to the water demand of the raw clay and the second one is associated to the loss of dispersing capacity

of PCE polymer. However, at this point it must be considered how these groups of variables are inter-related within themselves and how these potential inter-relationships are impacting in the fluidity loss.

The simplest way is to consider that both mechanisms are independent, so without any mutual link within themselves and progressing without any inter-relationship. In this case, the variables *W* and *I* could be manager in an isolated way. Another possibility is to assume that the two mechanisms are progressing by following a competitive model, by which the major influence of one of the processes implies the lower influence of the other. This is the behavior observed in the mechanism produced by the non-swelling clays interfering on the dispersing capacity of water-reducers [23].

The inter-relationships between the two mechanisms controlling the fluidity loss for cementitious systems containing water-reducer superplasticizers based on PCE polymers and non-swelling clays is represented in Figure 5.6.

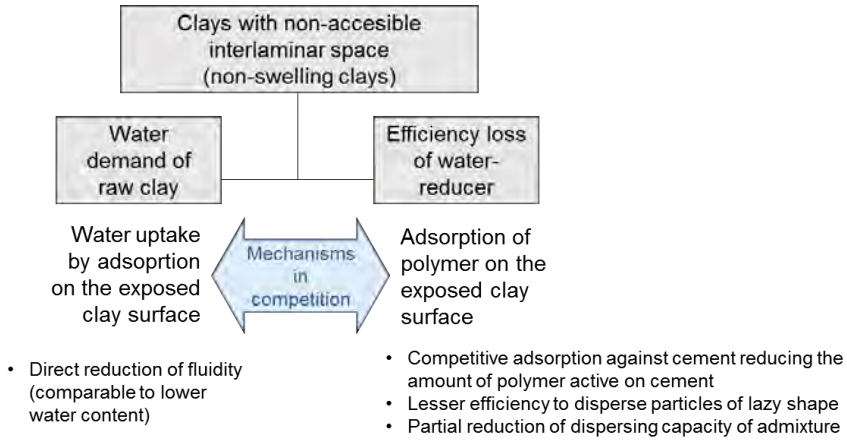

Figure 5.6. Schematic representation of the inter-relationships between the mechanisms promoting the fluidity loss for non-swelling clays without accessible interlaminar space

The mechanism of interference promoted by the non-swelling clays is exclusively based on the adsorption of polymer and/or water on the exposed surface of clay. Therefore, since water and admixture are adsorbed on the same active locations of the clay colloid surface, there is a competition for adsorption between both, where the higher adsorption of water means the lower adsorption of polymer [23]. In this case, the differences on the affinity for adsorption between the PCE polymer and the water molecules will determine the magnitude of the interference on the fluidity behaviour.

For the case of the swelling clays such as montmorillonites, the fluidity curves of clay pastes obtained by the progressive addition of PCE polymer (in Journal Paper III and IV) show that, at the first additions of PCE (at low PCE/clay ratio), the effect produced in the fluidity of the clay paste is flocculation but not dispersion, as initially expected. The initial suppression of fluidity is observed until reaching the correspondent D_{sat} dosage, thus meanwhile there is absorption of polymer by intercalation of side chains.

This phenomenon is explained by the further increase of water absorption into the interlaminar space promoted by the progressive increase of the amount of PCE side chains intercalated (according to the H_2O-PEO layer model of intercalation). It suggests that the direct water uptake by the raw clay and the loss of efficiency of the water-reducer (both controlling the fluidity loss) are retro-feeding processes and not competitive or independent.

All the inter-relationships deducted between the processes controlling the fluidity loss experienced when swelling clays and PCE polymers are used are presented un Figure 5.7.

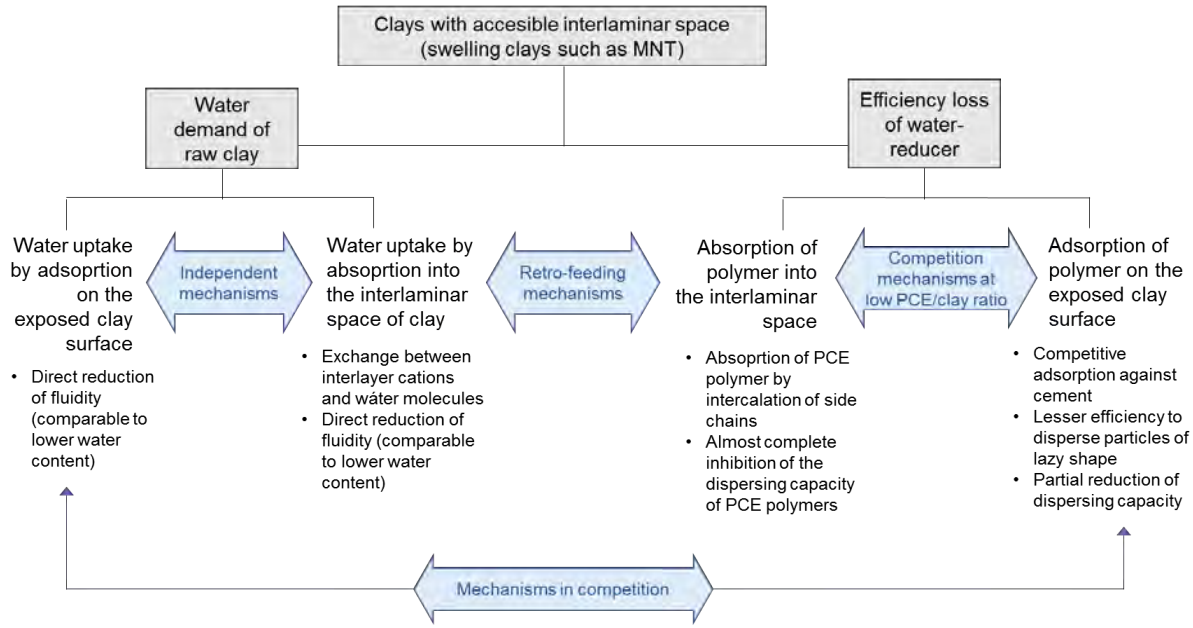

Figure 5.7. Schematic representation of the inter-relationships between the mechanisms promoting the fluidity loss for swelling clays with accessible interlaminar space such as montmorillonites

Therefore, according to the scheme presented in Figure 5.7, when the relative contribution of the variable *I* (exclusive of the PCE polymer) increases its influence, the relative influence of the other variable *W* controlling the fluidity loss increases simultaneously, despite being associated to the raw clay exclusively, because it is itself promoted by the increase of the variable *I*.

This hypothesis is consistent with the huge differences of fluidity loss observed between montmorillonite clays and the non-swelling clays, being far higher with montmorillonites, and provides a reasonable explanation for the initial flocculation observed in clay pastes when low PCE/clay dosage ratio are used. In these terms, the experimental results show that montmorillonites with higher octahedral layer charge generates a more pronounced flocculation effect, so aligned with the hypothesis proposed.

- Outlook for the development of clay-insensitive high-range water reducers:

Once all the process controlling parameters of montmorillonite clays and of PCE polymers are identified, it can be stated that there is a very large number of variables to be managed to design efficient, robust and cost-effective high-range water reducer/superplasticizer admixtures insensitive to clays.

In addition to the direct influencing factors related to the materials, it must be added all the inter-relationships between themselves, such as how the dosage ratio modulates their relative importance in the control of the interaction, and also the inter-dependences within all the processes modulating the impact on the fluidity loss generated.

All this huge complexity is suggesting that the development of reliable solutions to efficiently overcome the problematic generated by absorptive clays contaminating sands is really a very ambitious objective, being almost impossible to be achieved just by trial and error approaches. This is especially relevant considering that the level of improvement to be achieved must be enough to allow to avoid sand washing, since it is the process most damaging the efficient use of natural resources and the CO_2 footprint, while implying the generation of solid wastes, the additional consumption of water and energy and forcing to assume additional costs for both the sand manufacturers and the concrete producers.

This conclusion allows to understand why any of the diverse potential solutions investigated [3,24-26], including the design of new polymeric structures and the use of sacrificial agents, are not delivering promising results with enough robustness, efficiency (considering the clay tolerance improvement while keeping the same water reduction capacity of PCE polymers at the same time) and cost-effectiveness according to the expectations.

Therefore, this scenario of huge complexity is suggesting that the expected objective cannot be achieved without a deeper understanding of the interaction process. Moreover, it must be probably accepted that generic solutions (in terms of polymeric structures or formulated superplasticizers with sacrificial agents) able to efficiently perform in a wide range of situations is an unrealistic goal at short and mid-term. In consequence, customized designs of

superplasticizer admixtures adapted to the specific particularities of a reduced group of casuistries must be taken in consideration for the successful design of high-range superplasticizers with improved tolerance to clays.

- Suggestions to be considered in future research publications of this topic:

As mentioned previously, the complete understanding of the interaction process by which montmorillonite clays interference on the fluidity of cementitious systems still requires a lot of research to finally develop effective and efficient solutions to mitigate the harmful effects caused by montmorillonite clays.

However, since it is proved that both the characteristics of PCE polymers and of the montmorillonite clays condition the intercalation behavior, it is suggested that in the future works addressed to investigate this topic, a detailed description of the PCE polymers but of the clay samples used (normally missed) must be reported for the accurate interpretation of the experimental results.

From the identification of the most influencing properties of PCE polymers and montmorillonite clays in the interaction process, and as part of the outcome of this thesis under the scope of the investigation program, Table 5.1 proposes the basic properties for both the PCE polymer and the clay suggested to be included in the future research publications for a better interpretation of the experimental results.

PCE polymer	Montmorillonite clay
Anionic charge (by titration with KOH or with cationic polyelectrolyte)	Oxide and mineral composition (or directly layer charges)
Side chain length	Specific surface area (BET)
Grafting ratio (or directly side chain density)	Aspect ratio and number stacked plates per particle (theorical calculation from S_{BET} and D_{50})

Table 5.1. Summary of key-parameters of montmorillonite clay properties and of structure of PCE polymers influencing on the critical factors determining the intercalation behavior

5.2.2. Review of the interpretation of the intercalation mechanism

Since the general objective of this thesis is to extend the understanding of the interaction mechanism between PCE-based superplasticizer and montmorillonite clays, its accomplishment implies a review of the interpretation of this process in order to propose an updated model of the intercalation mechanism based on the new insights collected.

Therefore, from the jointly interpretation of all the investigated topics, it is feasible to propose an extended model of the intercalation mechanism.

- Review of the intercalation model:

In regards of the intercalation degree, the results of d-spacing obtained by using *in-situ* XRPD analysis on fresh, unaltered clay pastes confirms that the multiple intercalation of side chains takes place, defining a *multilayer model* of intercalation, while rejects the *monolayer model*. Therefore, the model based on the intercalation of one monolayer of side chains surrounded by two water layers is upgraded to a multilayer model where many side chains can be intercalated, replicating the repetitive unit of H_2O-PEO layers ($L_{H2O\text{-}PEO}$) and ended by a coordination water layer. The multilayer intercalation mechanism is illustrated in Figure 5.8.

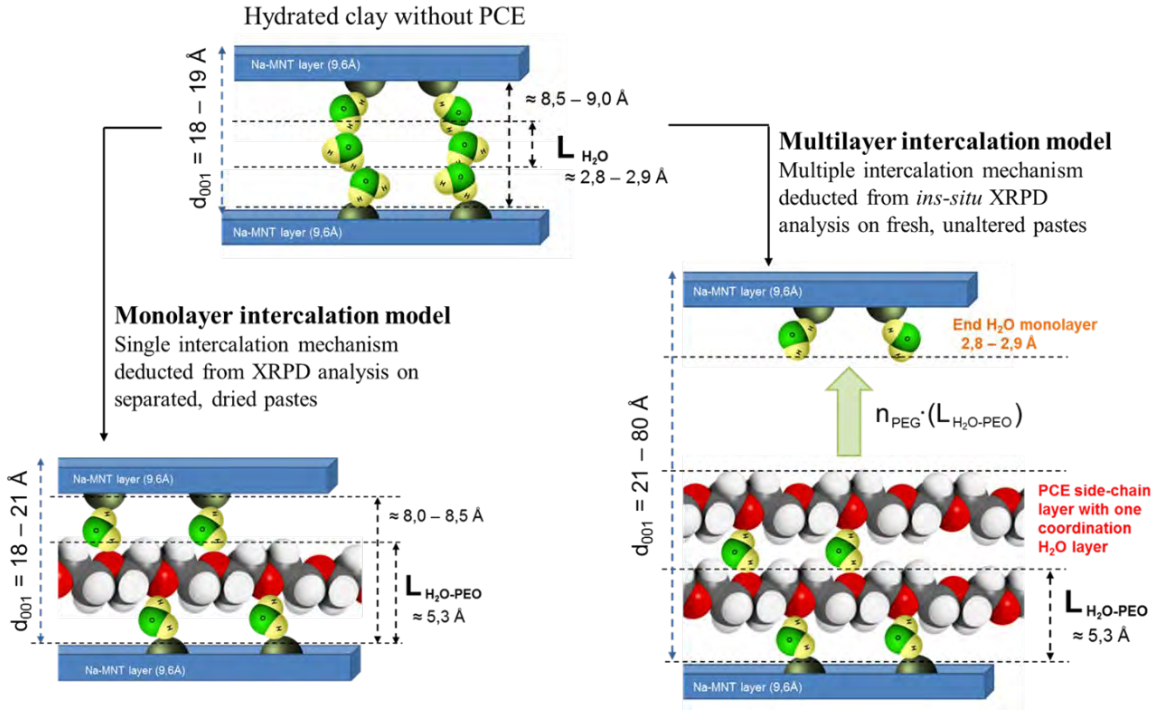

Figure 5.8. Model for the multilayer intercalation mechanism of PCE side chains into montmorillonite clay compared to the monolayer model deducted from the traditional analytical method

One can observe in Figure 5.8 that the multiple intercalation model is not invalidating the monolayer mechanism proposed in [1,2,4] (by which only one side chain is intercalated together with two coordination water layers) and simply means and extension of this interaction model. In fact, the assumed molecular interactions and the spatial arrangements taken are the same as than the proposed by the aforementioned authors (intercalation of side chains arranged in a planar zig-zag arrangement surrounded by coordination water molecules stablishing

hydrogen-bridge bonds between the oxygen atoms of the PEO sequences and the hydrogen atoms of the water molecules), but extending the single monolayer model of intercalation to a multiple intercalation model of side chain (multilayer), by which many layers of PCE side chains can be absorbed at the same time into the interlaminar space of montmorillonite clay.

However, it is very likely that the ideal planar arrangement of the intercalated PCE side chains proposed in the monolayer model suffers noticeable spatial distortions in the multilayer model due to the far larger number of intercalated side chains, the re-organization of the interlayer cations and the turbostratic distortions between the stacked clay plates produced by the high levels of expansion recorded.

According to the multiple (multilayer) intercalation mechanism proposed and represented in Figure 5.8, it is deducted that the number of PCE side chains intercalated (n_{PEG}) and the number of intercalated layers of water for coordination (n_{H2O}) always stays on the rule by which ($n_{H2O} = n_{PEG} + 1$). Therefore, since the number of intercalated side chains (n_{PEG}) increases as the dosage of PCE polymer increases until reaching a stationary d-spacing, the intercalation phenomenon itself is promoting the further absorption of water.

This deduction is consistent with the proposed retro-feeding character between the water uptake mechanism of the clay itself and the intercalation mechanism exclusive of the PCE polymer, so allowing to stablish a logical correlation between the expansion profiles of the clay and the fluidity behavior measured in fresh pastes.

The maximum values of stationary d-spacing measured are observed when clays with high octahedral layer charge and PCE polymers having long side chains are used, reporting net enlargement values of the interlaminar space close to 70Å, thus meaning an intercalation degree (n_{PEG}) of 13 side chains intercalated simultaneously into each interlaminar space of the montmorillonite particle together with the corresponding water layers of coordination absorbed (being $n_{H2O}= 14$ for $n_{PEG}= 13$). These results are noticeably far from the typical net enlargements reported by the traditional method, being close to 8-10 Å and constant, so associated to an invariable intercalation degree of $n_{PEG}= 1$ and $n_{H2O}= 2$.

Nevertheless, it is proven that the increase of the intercalation degree does not evolves progressively with the dosage increase of PCE polymer. It is observed that some n_{PEG} levels are more frequent, being replicated even at different dosages of PCE, while some others are not observed at any dosage. These most observed n_{PEG} levels are named as *preferred intercalation degrees*, which are the same when testing with different PCE polymers with the same clay but variable for each clay when different clays are tested with the same PCE. Therefore, due to this observation, it is considered that the preferred intercalation degrees mean an own attribute of

each clay, so being exclusively defined by its properties while remaining unmoved when the characteristics of the PCE polymer are changed. In any case, the proven existence of the preferred intercalation degrees indicates that the intercalation process is not linear-dependent neither exponential-dependent with the dosage of PCE, and at the same time it is evidencing that these are defined by some parameters exclusive of each clay.

The parameters of clays defining the preferred intercalation degrees remain unknown since they are not in the scope of this investigation. However, they undoubtably mean a critical aspect to be clarified by future investigations for the optimal understanding of the interaction mechanism between montmorillonite clays and PCE based superplasticizers.

- Steps of the interaction mechanism controlled by the PCE/clay dosage ratio:

Since it is confirmed that the PCE/clay dosage ratio has a direct influence on the interaction between PCE polymer and montmorillonite clays, a synthetized scheme proposing the steps of the mechanism as the PCE/clay dosage ratio increases is presented in Figure 5.9.

Five relevant locations as per PCE/clay dosage rate are highlighted since at these points, some relevant changes in the progression of the mechanism are observed. These characteristic dosages are D_{sat} (when saturation of the interlaminar space is reached), D_{sorp} (when sorption of polymer is stabilized), the PCE/clay ratio when first evidences of clay exfoliation are observed and the respective dosages by which the stationary d-spacing and the stationary sorption is reached.

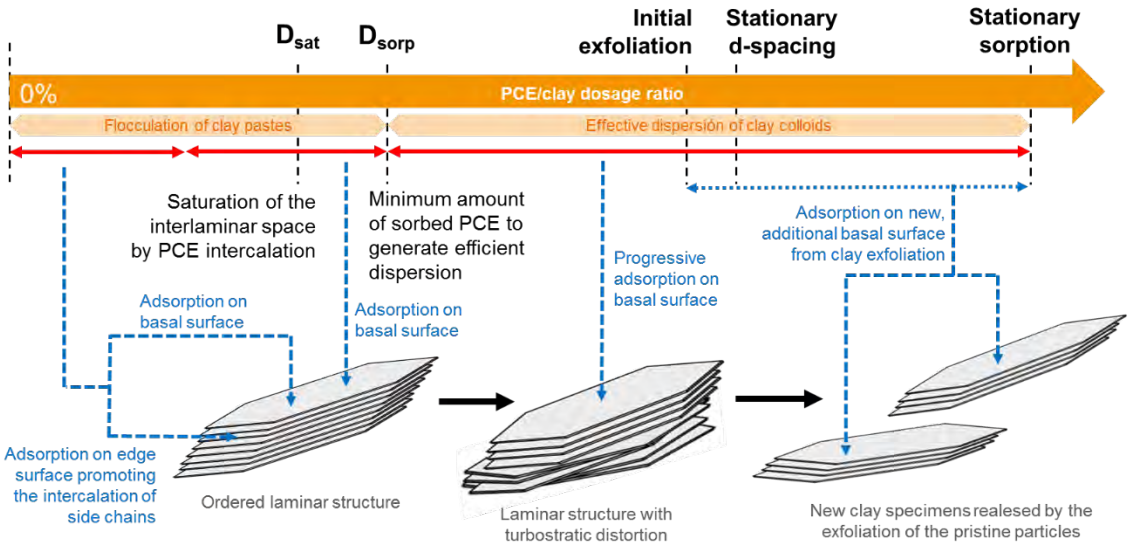

Figure 5.9. Synthetized scheme of the intercalation mechanism steps proposed as the PCE/clay dosage ratio increases

The major intercalation is produced at the first additions of PCE polymer. It is mainly controlled by the amount of PCE adsorbed on the edge surface of the clay and, for PCE polymers having long side chains, also by the polymer units adsorbed on the basal surface, but in a lesser influence.

The absorption of polymer by intercalation progresses until D_{sat} – saturation dosage is reached, and from this point upwards, almost no further side chains are intercalated so meaning the starting point of the stationary phase. D_{sat} – saturation dosage is defined by the PCE anionic charge and by the octahedral layer charge of the clay and by the number of stacked plates per clay particle.

In between D_{sat} and D_{sorp}, it is assumed that only the basal surface is further adsorbing PCE polymer, until being almost saturated. This assumption is supported by the fact that the edge surface is almost already saturated when D_{sat} is reached. And since D_{sorp} reflects the PCE/clay dosage ratio when the clay paste starts to gain positive fluidity by further addition of PCE polymer, this point can be associated to the minimum amount of PCE adsorbed on the basal surface needed to generate the efficient dispersion of the clay colloids.

The absorption conformation taken defines the dosage gap in between D_{sat} and D_{sorp}. In the *Bridging* conformation typical of PCE polymers having long side chains, it is observed that the total sorption rate progresses faster than the intercalation degree. It is grounded by shared intercalation of the side chains of the polymer units adsorbed on the basal surface with other neighboring clay particles. Therefore, the intercalation degree evolves smoothly and progressively with the increases of PCE dosage, resulting in higher saturation dosages (D_{sat}) closer to D_{sorp} since there is some polymer fraction already adsorbed on the basal surface. Thus, in the *Brinding* conformation the dosage gap between D_{sat} and D_{sorp} tends to be smaller than in the *One-to-one* conformation.

For PCE polymers having short side chains the expected absorption conformation is the *One-to-one* arrangement. In this conformation, the intercalation degree and the polymer sorption progress simultaneously because the major fraction of polymer is adsorbed on the edge surface. It means that almost all polymer sorbed is intercalated. In addition, the intercalation of polymer is concentrated in the same clay particle where the polymers units are adsorbed because short side chains do not allow the shared intercalation. Thus, the *One-to-one* conformation promotes larger expansions of the clay than the *Brinding* conformation at the same PCE dosage and progresses in a more sudden way resulting in lower saturation dosages (D_{sat}). Nevertheless, since there is almost no adsorption of PCE on the basal surface when D_{sat} is reached, in general the dosage gap between D_{sat} and D_{sorp} tends to be larger in the *One-to-one* conformation.

According to the previous reasoning, when the *Bridging* conformation is adopted it is expected that clay particles with high intercalation degrees coexist with particles with lower intercalation degrees as consequence of the more random process. Conversely, for the *One-to-one* conformation, most of the clay particles would have similar, homogeneous degree of intercalation.

Apart from the influence of the absorption conformations taken, almost all the intercalation phenomenon is produced when the PCE/clay dosage ratio is below D_{sat}. In this range of PCE/clay ratios, the key factor controlling the degree of intercalation is the balance between the net amount of PCE polymer adsorbed on the edge surface of the clay particle, which produces immediate intercalation of side chains, and the fraction of polymer adsorbed on basal surface, which can generate intercalation only in some specific circumstances. The balance between the polymer fraction adsorbed on each of the clay surfaces is controlled by the octahedral layer charge and by the morphology of the clay particle.

Figure 5.10 illustrates how the clay properties defines the balance between PCE polymer adsorbed on edge surface and PCE polymer adsorbed on basal surface when PCE/clay dosage ratio is below D_{sat}. And in particular for the adsorbed polymer on the basal surface of the clay, Figure 5.10 also shows how only the PCE polymers having long side chains are able to produce intercalation in this punctual situation.

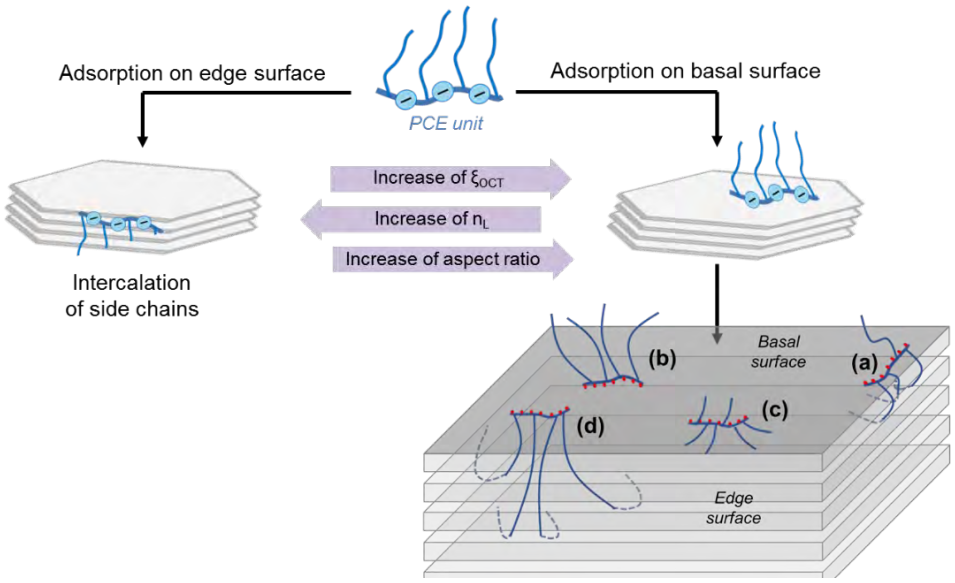

Figure 5.10. Clay properties controlling the adsorption on edge surface and on basal surface of clay and structural factors of PCE polymers determining the intercalation of the polymer units adsorbed on basal surface

As Figure 5.10 presents, for montmorillonite clays with lower octahedral layer charge and with particle shape of small aspect ratio and larger number of stacked plates the adsorption of PCE polymer is mainly produced on the edge surface, allowing the intercalation to progress easily. This is the typical situation where the polymer is adapting the *One-to-one* absorption conformation.

Conversely, montmorillonite clays of opposite properties will be more prompt to partially displace the adsorption of PCE polymer on the basal surface, thus competing against the adsorption of polymer on the edge surface.

In this situation, the factors determining if the polymer units adsorbed on the basal surface can be intercalated are the specific location of adsorption and the length of side chains of the PCE polymer, since it depends on the distance to be covered by the side chains between the location of adsorption and the closest interlaminar space opening.

PCE units adsorbed on the basal surface but closer to the edge borders (situation (a) in Figure 5.10) can be easily intercalated because the rotation of the side chains allows to cover the short distance from the basal location to the nearest opening of the interlaminar space.

Conversely, PCE units adsorbed in the most inner locations of the basal surface (situation (b) in Figure 5.10) can hardly be intercalated regardless of the length of the side chains, since the distance from the adsorption location to the nearest accessible interlaminar space is too long.

The factors determining the specific locations of adsorption of the PCE polymers on the basal planes of montmorillonite clays have not been deeply investigated, but the behavior observed suggests that the steric hindrance produced by the PCE polymers (determined by the side chain density) plays a relevant role on it.

For the PCE units adsorbed on the intermedium locations of the basal planes, Figure 5.10 also illustrates when the polymer can be intercalated. In this situation, it is observed that the length of the PCE side chains is the key-factor determining if the intercalation is produced or not. For PCE polymers having short side chains (situation (c) in Figure 5.8), the nearest interlaminar space cannot be reached and therefore, no intercalation will be produced.

Conversely, for PCE polymers having long side chains, the intercalation is produced if the side chain length is large enough to cover the distance between the adsorption location and the nearest interlaminar space (situation (d) in Figure 5.8).

Under this specific circumstance, PCE polymers based on short side chains are intercalated by adopting the *One*-to-*one* absorption conformation, and for polymers based on long side chains, the longer length allows the side chains to be intercalated by some neighboring clay particles by adopting the *Bridging* absorption conformation, especially when PCE polymers combines long side chains and high side chain density.

Moving back to the steps of the mechanism illustrated in the previous Figure 5.9, from D_{sorp} upwards almost no further changes in the expansion of the clay are observed despite increasing the PCE/clay dosage ratio. At this point, stationary d-spacing (maximum expansion of the clay) is almost reached, and the exfoliation of the clay particle is taking the control of the interaction process.

Meanwhile the clay is delaminating, the sorption rate still progresses due to the surface adsorption on the new additional basal surface released by the progressive exfoliation, producing changes in the progression of the fluidity curves of the clay pastes by increasing the dosage of PCE.

As it is deducted from the small changes of d-spacing observed at high dosage of PCE polymer, some re-arrangement of the intercalated units of polymer is forced by the exfoliation of clay, but having minor impacts on the expansion profile.

- Summary of key-properties of materials controlling the steps of the interaction mechanism:

The jointly interpretation of the specific conclusions suggests that is possible to characterize the overall interaction process just from the values of a few *particular dosage ratios* (D) where some of the steps of the process are experienced. Therefore, the expected magnitude of the impact on the fluidity loss could be predicted or estimated from the values of these particular dosage ratios.

The most important particular dosage ratios (D) deducted are displayed in Table 5.2, including the step of the mechanism reflected by each of them and the experimental criteria used for their identification, as well as the expected influence on the level of interference generated on the fluidity behavior promoting the slump loss.

Finally, Table 5.3 summarizes the key-properties of PCE polymers and montmorillonite clays identified as the most relevant properties conditioning the punctual values of each of the particular dosage ratios (D).

Particular dosage ratio (D)	Reflected step of the mechanism	Experimental criteria for identification	Expected impact on the fluidity loss
D_{sat}	Saturation of the interlaminar space by side chain intercalation	Stabilization of initial d-spacing incremental (saturation dosage)	Higher as D_{sat} increases
D_{sorp}	Saturation of basal surface by polymer adsorption	Stabilization of initial sorption rate incremental	Higher as D_{sorp} increases
$[D_{sat} - D_{sorp}]$	Early balance between adsorption on edge surface and basal surface	--- (calculated)	Higher as $[D_{sat} - D_{sorp}]$ increases
D_{exf}	Initial exfoliation of clay induced by intercalation of polymer	Change of the slope (positive) in the fluidity curves of clay pastes	Higher as D_{exf} decreases
$D_{d\text{-}max}$	Maximum expansion affordable by the pristine clay particle	Stationary d-spacing (maximum d-spacing measured)	Higher as $D_{d\text{-}max}$ increases
$D_{sorp\text{-}max}$	Complete saturation of all clay surface by adsorption (including delamination)	Stationary sorption (maximum sorption rate measured)	Higher as $D_{sorp\text{-}max}$ increases

Table 5.2. Particular dosage ratios (D) controlling the interaction process and their expected impact on the fluidity loss

Particular dosage ratio (D)	Montmorillonite clay properties	PCE polymer structure
D_{sat}	Higher as ξ_{oct} and n_L increase	Higher as side chain density and side chain length increase but lowers as anionic charge increases
D_{sorp}	Higher as ξ_{oct}, n_L and aspect ratio increase	Higher as side chain density and side chain length but lowers as anionic charge increases
$[D_{sat} - D_{sorp}]$	Higher as ξ_{oct} and n_L increase Lower as aspect ratio increase	Higher as side chain density and side chain length increase
D_{exf}	Lower as ξ_{oct} and n_L increase (estimated trend)	Lower as side chain density and side chain length increase
$D_{d\text{-}max}$	Higher as ξ_{oct} increases	Higher as side chain length increases
$D_{sorp\text{-}max}$	Higher as ξ_{oct} and n_L increase (estimated trend)	Higher as side chain length increases

Table 5.3. Summary of the key-parameters of montmorillonite clay properties and of the structure of PCE polymers controlling the values of the particular dosage ratios (D)

Therefore, from the relationships summarized in Table 5.2 and 5.3, it is feasible to conclude that the highest magnitude of interference on the fluidity behavior of cementitious systems containing PCE based superplasticizers and montmorillonite clays would be caused by combining montmorillonites having higher octahedral layer charge and larger number of stacked plates per particle together with PCE polymers having higher side chain density and, especially, longer side chains.

Conversely, in the combination between clays with reduced octahedral layer charge and PCE polymers with higher anionic charge, shorter side chains and lower side chain density, the interference in the fluidity behavior would be of lower magnitude, so generating a more moderate fluidity loss.

From the interpretation of all the influencing factors, and considering that there is no chance for choosing the type of clay to work with (since the properties of the clay are given according to the type of sand used), the recommended best practices for the selection of the PCE polymer used is to use PCE polymers having short side chains and high anionic charge in order to minimize the non-desired interferences in the fluidity of fresh concrete.

5.3. SUGGESTIONS FOR FURTHER RESEARCH

Attending to the limitations of the research program executed in this thesis, some suggestions for further research are proposed with the aim to validate and complement the interpretations and the conclusions proposed.

The first (and most important) suggestion for further research is addressed to validate all the hypothesis proposed in this thesis, by testing under different experimental conditions and observing if the same results are reproduced. It is key to finally confirm the models exposed in this thesis in regards of the multilayer intercalation mechanism of PCE polymers into the interlaminar space of montmorillonite clays.

Taking into consideration all the variables not studied in this investigation, additional suggestions for further research can be proposed. For example, the influence of the molecular weight of PCE polymers has not been evaluated, and it is expected to be another parameter conditioning the interaction process, so the impacts on the fluidity loss. It is expected that the molecular weight can modulate the balance between the polymer adsorbed on the basal surface and on the edge surface of clay. Therefore, due to the potential restrictions by steric hindrance

related to the size of the polymer), the molecular weight of the PCE polymer can directly influence on the values of D_{sat} and on the sorption profile, thus on the values of D_{sorp}.

Another suggestion for further research focused in the role of the structure of PCE polymers is the evaluation of the influence of the backbone composition. All the PCE polymers used in this investigation do not contain non-ionic groups in the backbone for the control of the adsorption affinity. Therefore, since it has been confirmed that the surface adsorption is promoting the intercalation of polymer (despite not being a mandatory condition), it would be interesting to investigate how the controlled adsorption of PCE polymers impacts on the overall intercalation behavior.

The assessment on the influence of the mixing process is considered as another variable to be understood. It is based on the proven influence of the clay exfoliation in the process and, since this property of clays is affected by some mechanical aspects such as the shear forces, the influence of the mixing speed and the mixing time should be clarified to support the role of clay exfoliation in the impact on the fluidity behavior. In the same way, the identification of the influence of other variables ignored in this investigation such as the type of cement, water-to-cement ratio and temperature would be of interest.

Finally, complementary research to further extend the understanding of the interaction mechanism between PCE based superplasticizers and montmorillonite clays are needed. In particular, the investigations addressed to understand how the preferred intercalation degrees are stablished and which are the clay properties determining their values is of high interest for the development of efficient clay-insensitive superplasticizers. This assessment could be carried out by theoretical studies using molecular dynamics simulations, in the same way that it is already done for simulating the water absorption behavior of montmorillonite clays [18], since it seems evident that the preferred intercalations degrees must be associated to mathematic minimum points in the level of energy Gibbs (G) or enthalpy (H) at these specific distances of expansion.

REFERENCES

[1] H. Tan, B. Gu, B. Ma, X. Li, C. Lin, Mechanism of intercalation of polycarboxylate superplasticizer into montmorillonite, Applied Clay Science 129 (2016) 40-46.

[2] S. Ng, J. Plank, Interaction mechanisms between Na-montmorillonite clay and MPEG-based polycarboxylate superplasticizers, Cement and Concrete Research 42 (2012) 847-854.

[3] L. Lei, J. Plank, A concept for a polycarboxylate superplasticizer possessing enhanced clay tolerance, Cement and Concrete Research 42 (2012) 1299-1306.

[4] R. Ait-Akbour, P. Boustingorry, F. Leroux, F. Leising, C. Taviot-Guého, Adsorption of polycarboxylate poly(ehtylene glycol) (PCP) esters on montmorillonite (MNT): Effect of exchangeable cations (Na+, Mg2+ and Ca2+) and PCP molecular structure, Journal of Colloid and Interface Science 437 (2015) 227-234.

[5] L. Lei, J. Plank, A study on the impact of different clay minerals on the dispersing force of conventional and modified vinyl ether based polycarboxylate superplasticizers, Cement and Concrete Research 60 (2014) 1-10.

[6] R.L. Parfitt, D.J. Greenland, Adsorption of water by montmorillonite-poly(ethylene glycol) adsorption products, Clay Minerals 8 (1970) 317-324.

[7] S. Zhu, H. Peng, J. Chen, H. Li, Y. Cao, Y. Yang, Z. Feng, Intercalation behavior of poly(ethylene glycol) in organically modified montmorillonite, Applied Surface Science 276 (2013) 502-511.

[8] R.W.A. Franco, C.A. Brasil, G.L. Mantovani, E.R. de Azevedo, T.J. Bonagamba, Molecular dynamics of poly(ethylene glycol) intercalated in clay, studied using13C solid-state NMR, Materials 6 (2013) 47-64.

[9] M.X. Reinholdt, R.J. Kirkpatrick, T.J. Pinnavala, Montmorillonite-poly(ethylene glycol) nanocomposites: interlayer alkali metal behavior, The Journal of Physical Chemistry 109 (2005) 16296-16303.

[10] A. Kobayashi, M. Kawaguchi, T. Kato, A. Takahashi, Intercalation adsorption of poly(ethylene oxide) into montmorillonite, Kyoto University – Bulletin of the Institute for Chemical Research 66 (1989) 176-183.

[11] J. Bujdak, E. Hackett, E.P. Giannelis, Effect of layer charge on the intercalation of polyethylene oxide in layered silicates: implications on nanocomposite polymer electrolytes, Chemistry of Materials 12 (2000) 2168-2174.

[12] A. Seppala, E. Puhakka, M Olin, Effect of layer charge on the crystalline swelling of Na+, K+ and Ca2+ montmorillonites: DFT and molecular dynamics studies, Clay Minerals 51 (2016) 197-211.

[13] A. Maes, M.S. Stul, A. Cremers, Layer charge-cation exchange capacity relationships in montmorillonite, Clays and Clay Minerals 27 (1979) 387-392.

[14] L. Ammann, Cation exchange and adsorption on clays and clay minerals, Doctoral dissertation, Christian-Albrechts University of Kiel (2003).

[15] T. Chen, Y. Yuan, Y. Zhao, F. Rao, S. Song, Effect of layer charges on exfoliation of montmorillonite in aqueous solutions, Colloids and Surfaces: Physicochemical and Engineering aspects 548 (2018) 92-95.

[16] H. Li, Y. Zhao, S. Song, Y. Hu, Y. Nahmad, Delamination of Na-montmorillonite particles in aqueous solutions and isopropanol under shear forces, Journal of Dispersion Science and Technology 38 (2017) 1117-1123.

[17] I. Barshad, Absorptive and swelling properties of clay-water system, Clays and Clay Technology 169 (1950) 70-77.

[18] W.A. White, E. Pichler, Water-sorption characteristics of clay minerals, Division of the Illinois state geological survey, Circular 266 (1959).

[19] A. Maes, M.S. Stul, A. Cremers, Layer charge-cation exchange capacity relationships in montmorillonite, Clays and Clay Minerals 27 (1979) 387-392.

[20] A. Seppala, E. Puhakka, M Olin, Effect of layer charge on the crystalline swelling of Na+, K+ and Ca2+ montmorillonites: DFT and molecular dynamics studies, Clay Minerals 51 (2016) 197-211.

[21] L. Ammann, Cation exchange and adsorption of clays and clay minerals, Doctoral dissertation, Christian-Albrechts University of Kiel (2003).

[22] M.A. González-Ortega, S.H.P. Cavalaro, A. Aguado, Influence of barite aggregate friability on mixing process and mechanical properties of concrete, Construction and Building Materials 74 (2015) 169-175.

[23] P. Borralleras, Arenas con arcillas y sus problemáticas en la producción de hormigón. Interferencia con los aditivos superplastificanes basados en PCE, Proceedings of the V Congreso Nacional de Áridos - Spain (2018), Area A, 49-70.

[24] G. Xing, W. Wang, J. Xu, Grafting tertiary amine groups into the molecular structures of polycarboxylate superplasticizers lowers their clay sensitivity, RSC Advances 6 (2016) 106921-106927.

[25] C. Sun, H. Zhou, X. Li, S. Wang, J. Xing, The clay-tolerance of amide-modified polycarboxylate superplasticizers and its performance with clay-bearing aggregates, MEBE - International Conference on Materials, Environment and Biological Engineering (2015) 237-241.

[26] A. Jeknavorian, E. Koehler, Use of chemical admixtures to modify rheological behavious of cementitious systems containing manufactured aggregates, Proceedings of the International Concrete Sustainability Conference, Qatar (2011).

[27] H. Tan, F. Zou, B. Ma, Y. Guo, Effect of competitive adsoprtion between sodium gluconate and polybarboxylate superplasticizer on rheology of cement paste, Construction and Building Materials 144 (2017) 338-346.

[28] M. Szczerba, Z. Klapyta, A. Kalinichez, Ethylene glycol intercalation in smectites, Applied Clay Science 91-92 (2014) 87-97.